SCHOOL OF PHYSICAL SCIENCES

NATIONAL INSTITUTE OF SCIENCE EDUCATION AND RESEARCH

Masters' Thesis Project:

PARTICLE PRODUCTION IN HIGH ENERGY COLLISIONS:

Made by:
AMAN DIMRI
5^{th} Year Integrated MSc.

Under The Supervision Of
Prof. BEDANGADAS MOHANTY

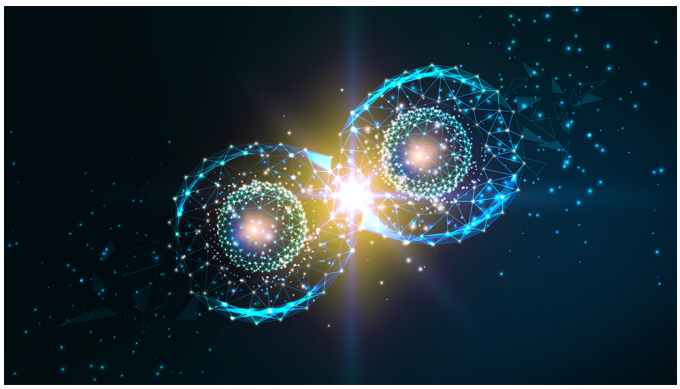

Acknowledgements

I would like to take this opportunity to express my gratitude and sincere thanks to Prof. Bedangadas Mohanty who offered me the chance to work on this wonderful project, for the time and effort he spent in ensuring smooth conduction of such incredible learning experience and guiding me through all the fundamentals. I am greatly obliged to Bedanga Sir for investing his time and being incredibly patient with me throughout the duration of this project. He has been a great mentor and a father like figure to me. It was an honor to work and learn from a person of his capabilities.

I would also like to thank Dr. Ashutosh Dash for helping and guiding me during the course of the project. I am thankful to him for having long discussions with me to make sure that I actually understand the research material (especially the hydro-simulation part). His suggestions and comments have been an invaluable asset in the making of this thesis.

I would like to acknowledge the unmatched help and support provided by Mr. Dukhishyam Mallick during this project. I am thankful to him for taking keen interest in my project, having interesting discussions, reviewing all my data/figures and giving valuable comments and suggestions for my presentations.

I would like to express my sincere gratitude to Dr. Varchaswi KS Kashyap and Mr. Debasish Mallick for their advice, support and assistance throughout this project. I would like to extend my thanks to all the members of Bedanga Sirs' group who were always there to help me during the frustrating moments of this project.

A special thanks goes to my friend Mr Pratyush Kumar Das who helped me with the coding aspect of this thesis' work. His help was invaluable in organizing the vast amounts of data and figures which form an integral part of this thesis.

Finally, I would like to thank my parents Mr Pradeep Chandra Dimri and Mrs Neelam Dimri alongwith with my baby sister Ms. Anushka Dimri for their unconditional love and support.

Contents

1 Abstract

The first few sections of this project revolves around solving the ideal Bose and Fermi gases under a variety of conditions using statistical mechanics. This is followed by introducing non-ideality into the system by allowing the constituents of the Bose/Fermi gases to have finite size. A direct evaluation of the integrals in canonical ensemble lead to the famous classical and quantum cluster expansions. We then proceed to solve the same problem using the mean-field approach (van der waals' excluded volume approach) which allowed us to formulate an equation of state for real gases on nuclear scale. Using a similar approach attractive interactions are also included into the formulation. Now all the relevant formulations (ideal gas, van der waals' EV and van der waals' EV+attractive interactions) are applied to the Hadron Resonance Gas (HRG) model which gives a statistical description of hadrons. The Grand Canonical Ensemble is used to compute the pressure, energy density, entropy density and number density. All the approaches have been compared to the lattice QCD data of Wuppertal-Budapest for 0 chemical potential. Using the ideal gas formulation in THERMUS model (GCE ensemble), we have computed the chemical freeze out parameters at a variety of collision energies and centralities. This is followed by simulating particle production in Au-Au collision for center of mass energy of 7.7 GeV and comparing the yields obtained through AMPT model with that of the STAR experiment. The project is ended by studying the concept of "Flow" in relativistic high energy collisions. This section tries to answer whether harmonic flow coefficients can be used as possible signatures of QGP. Using the AMPT and hydro simulations, it is observed that a large elliptic flow is a good indication for the formation of QGP like medium. Further, it is found that the presence of NCQ scaling of elliptic flow and a modified NCQ scaling of triangular flow is characteristic of the formation of QGP like medium during the evolution of the system produced in HIC.

1.1 Abbreviations Used

GCE: Grand Canonical Ensemble HRG: Hadron Resonance Gas EV: Excluded Volume
HI: High Energy HIC: High Energy Collisions QGP: Quark Gluon Plasma
SM: String Melting QCD: Quantum Chromodynamics EOS: Equation Of State
NR: Non-Relativistic UR: Ultra Relativistic CE: Canonical Ensemble

Chapter 1: Basics Of Particle Physics

2 Classification Of Sub-Atomic Particles

The sections below discuss some of the possible classifications of the sub-atomic particles. The groupings have been done while explicitly keeping the field of particle physics at the back of the mind. However, some of the classifying criterion is quite general and can be easily applied to other fields of physics. The section below discuss the classifications of only particles. After reading the definitions one can easily extend these definitions to anti-particles (some of them directly while some of them with a bit tweaking to maintain the visual symmetry with particles).

2.1 On The Basis Of Spin

This is an independent and complete classification of particles. This classification is based on one of the most important theorems' available to physicists, **The Spin Statistics Theorem** which says:

- Half-integer spin particles are subjected to Fermi-Dirac statistics. This implies that the wavefunction of such particles gains a '-' sign (can be thought as rotation by π in the space of fields) under exchange symmetry. The consequence of this fact is that each quantum state can be occupied by at most 1 such particle. These particles are termed as **fermions**. eg: $e^{\pm}$, $\mu^{\pm}$, all the quarks etc.
- Integer spin particles are subjected to Bose-Einstein statistics. This implies that wavefunction is symmetric under exchange symmetry which translates to the fact that each quantum state can be occupied by any any number of such particles. These particles are termed as **bosons**. eg: nucleus of C-12, nucleus of He, photon etc.

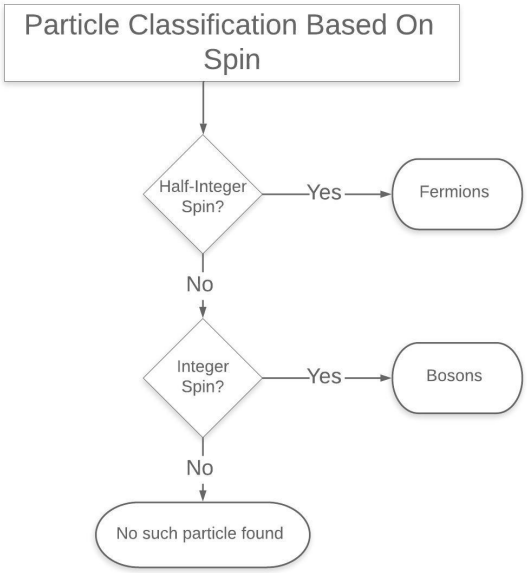

Figure 1: Flowchart For Classification Based On Spin

2.2 On the Basis Of Internal Composition

The particles can be divided into two categories via this decomposition:

1. Elementary Particles: The sub-atomic particles which have no known substructure or equivalently are not composed of any other sub-atomic particle is called an elementary particles in particles physics. for eg: $e^{\pm}$, $\mu^{\pm}$, all the quarks etc.

2. Composite Particles: All the sub-atomic particles which are composed of some other elementary particles are called composite particles. For eg: proton, neutron, pion etc.

This is again a complete and independent classification of particles. A particle being elementary or composite has nothing to do with the fact whether it is a fermion or a boson. For eg: quark is a fundamental particle whereas proton is a composite one, however, both are fermions.

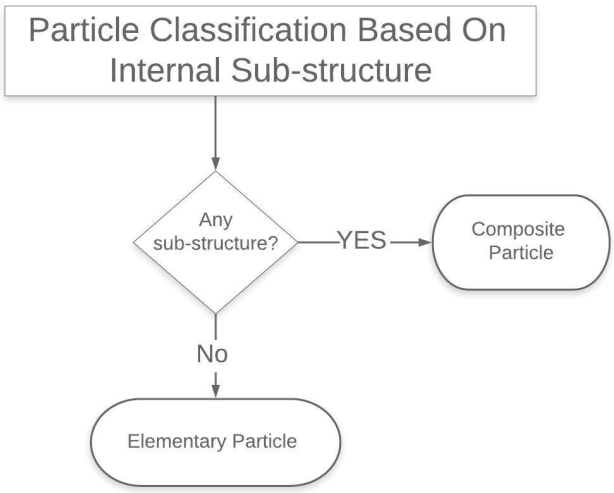

Figure 2: Flowchart For Classification Based On Composition

2.3 On the Basis Of Fundamental Interactions

This classification is not as strong as the previous ones but is quite useful. This method takes advantage of the fact that there are only four fundamental forces in nature and groups particles on the basis of their affinity and interaction towards these force fields. Broadly this classification categorises the whole particle family into two main parts (and a singleton!):

- Gauge Bosons: These elementary particles are also known as **force carriers** or **messenger particles**. The terminology arose because the known gauge bosons are vector particles corresponding the smallest quanta of some force field and when exchanged between particles give rise to forces between those two particles. Up until now, four gauge bosons are known to exist. We have photon for the EM field, gluon for the Strong field and $W^{\pm}$ & Z bosons for weak field. Some believe gravitons as the force carriers for the gravitational field, however, they are yet to be discovered.

- Fundamental Scalar Boson: This is just a fancy name for Higgs boson. The reason that higgs is given a category of its own is because it is fundamentally a unique particle. Higgs boson can be though of as mediator of the higgs field hence it is definitely not a matter particles. However, it is also not a gauge boson as higgs field is not really a force field. Further each gauge boson corresponds to a gauge field which arises due to some local internal symmetry while higgs boson corresponds to a gauge field which is responsible for breaking of aforementioned local internal symmetries. Thus, higgs is awarded a unique status among the elementary particles.

- Matter Particles: All the remaining particles fall into this category. The matter particles are further differentiated into two classes:

  - If the matter particles are unable to interact via the strong force then they are labeled as leptons.
  - If the matter particles can interact via the strong forces then they are further divided into two groups:
    * If the matter particles are elementary then they are termed as quarks.
    * If the matter particles are composite then they are termed as hadrons. Hadrons are defined to be a sub-atomic composite particles made up of two or more quarks(anti-quarks) held together in a stable configuration by the strong force. The strong force is quite special due to which only certain configurations of fundamental particles are allowed to come together and form a composite particle . Hence it makes sense to further classify hadrons as:
      · If the composite particles have the substructure qqq (3 quarks bound together), then they are called baryons.
      · If the composite particles possess the structure $q\bar{q}$ (quark-antiquark pair) then they are called mesons.
      · If the composite particles contain the sub-structure gg (two gluons bound together), then they are termed as gluionos. They are yet to be discovered, but they are a definite theoretical possibility and I would like to include them here.

    Sometimes one might come across the term Exotic Baryons. These are a type of hadrons having a half-integer spin but possess a different quark structure/content than the conventional hadrons (qqq or $q\bar{q}$). An example of exotic baryon is the penta-quark which has $qqqq\bar{q}$ as its quark configuration.

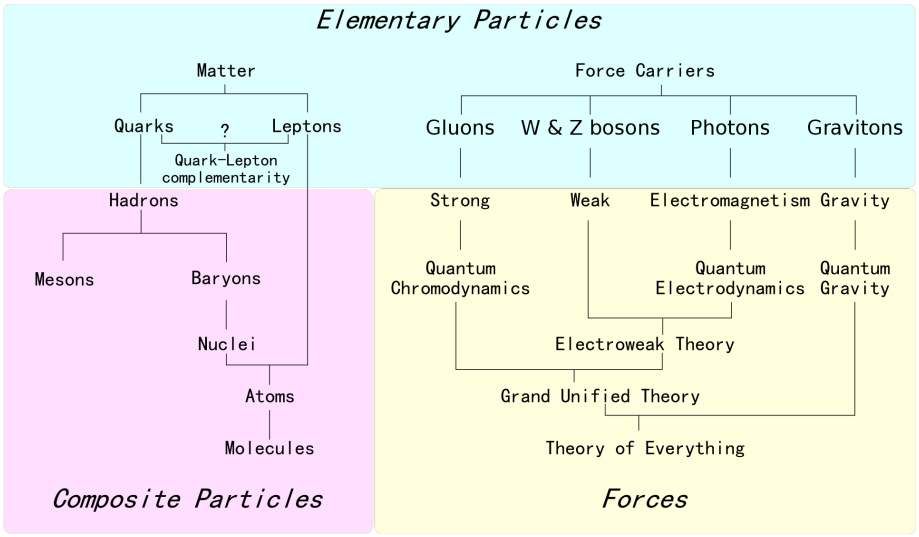

Figure 3: Classification Based On The Basis Of Fundamental Forces[1]

2.4 Classification Of Leptons

Now that we have an idea of what leptons are, we can dive deeper into this territory. Leptons are also characterised by flavours which form the basis of this classification. The lepton family has 3 known flavours which are electron, muon and tau flavours. Corresponding to each flavour we define a generation consisting of the particle and its neutrino along with a lepton flavour quantum number (which is assigned 1 for particles and -1 for anti-particles if they belong to that flavour otherwise 0). Within a generation , the particle can be differentiated from the its neutrino by noticing that the particle must be charged while its neutrino is neutral and the particle is infinitely heavier than its neutrino. The importance of this classification is the fact that in nearly all reactions concerning leptons, the lepton flavour quantum number is conserved. Hence, from the muon generation if you only have a muon in the reactant then the product must also contain a muon or its neutrino.

LEPTON CLASSIFICATION

	l	Q	L_e	L_μ	L_τ
First generation	e	−1	1	0	0
	ν_e	0	1	0	0
Second generation	μ	−1	0	1	0
	ν_μ	0	0	1	0
Third generation	τ	−1	0	0	1
	ν_τ	0	0	0	1

Figure 4: The 3 Generation Of Leptons[2]

In the recent years, lepton number violation have been found (eg: neutrino oscillation). However,

they are extremely rare and lepton flavour number conservation is still considered as quite a good law. Nevertheless, this weakens the above classification of leptons as a good classification.

2.5 Classification Of Quarks

This is the classification of one of the sub-categories of the material particles, quarks from section 2.3 . Quarks were categorised as the elementary particles that were capable of interacting via the strong force. Quarks, like leptons can be also be divided into 3 generations. The basis for this classification of quarks is isospin symmetry which is quite different from why we set the leptons into generations. So the basic question to ask is what is isospin symmetry for quarks? The answer being that if the quarks are only allowed to interact via the strong force then the pair of quarks which are indistinguishable from each other have an isospin symmetry and hence fall into the same generation. A simpler version would be that the pair of quarks which are isospin symmetric cannot be distinguished via the strong force. (Technically isospin symmetry is not an exact symmetry. The masses of the quarks in the same generation are not exactly equal and hence if one could devise a precise enough experiment, one would be able to distinguish between the quarks of the same generation even by only using the strong force.) Just like the leptons, the members of the of the same generation can be distinguished by their interaction with the EM field.

QUARK CLASSIFICATION

	q	Q	D	U	S	C	B	T
First generation	d	$-\frac{1}{3}$	−1	0	0	0	0	0
	u	$\frac{2}{3}$	0	1	0	0	0	0
Second generation	s	$-\frac{1}{3}$	0	0	−1	0	0	0
	c	$\frac{2}{3}$	0	0	0	1	0	0
Third generation	b	$-\frac{1}{3}$	0	0	0	0	−1	0
	t	$\frac{2}{3}$	0	0	0	0	0	1

Figure 5: Complete classification Of Quarks[2]

Another independent way of classifying quarks is to group them with flavours. Unfortunately, if we try this then each of the 6 elementary quark is to given its own flavour along with a quantum number (upness,downness, charmness, strangeness,topness and bottomness) which is conserved during a strong interaction. This can also been in figure 5.

2.6 Classification Of Elementary Particles

The classifications used for elementary particles in section 2.3-2.5 can be combined to get most famous chart available to all particle physicists. The chart is divided into two halves with the left side being given to material particles and the right to the force carriers and higgs boson. The left part is again divided into two parts. The top part is assigned to quarks divided into 3 pairs via generations. Within each generation the positively charged quark is kept above the negatively charged quark. The bottom part is assigned to leptons again arranged like quarks into 3 generations with the positively charged

lepton kept above the neutral one. The chart is extremely important as it clearly classifies each known elementary particle of the standard model.

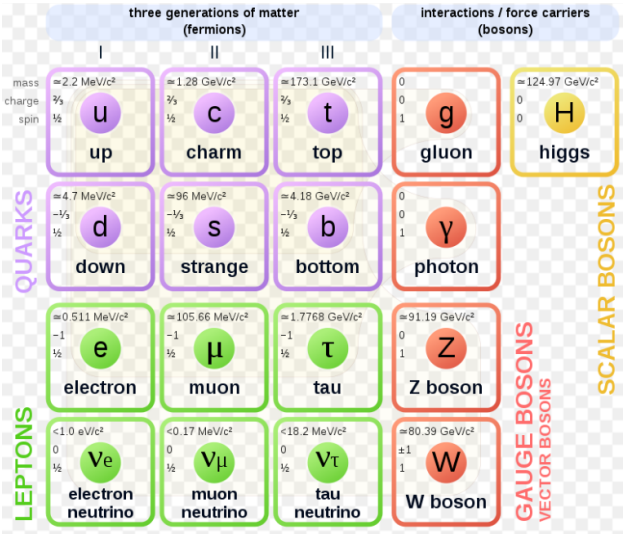

Figure 6: Standard Model Of Elementary Particles[3]

2.7 On The Basis Of Life-Time Of Particles

This is not an exact classification and only applies to material particles (generally to leptons and hadrons). I am going to provide the general rule of thumb I have empirically deduced from their usage and known examples. The basis of this classification is life time of particles combined with the general experimental techniques used to observe them.

- Stable Particles: All the particles that do not decay spontaneously when they are in free state are termed as stable particles. eg: proton, electron etc.
- Unstable Particles: All the particles which possess the ability to spontaneously decay are termed as unstable particles. eg: neutron,muon etc. Unstable particles can be further categorised into the following sub-categories:
  - Long-Lived Particles: These particles live long enough so that they can be detected by making them leave trails in some medium (bubble chambers, cloud chambers, spark chambers). It has been seen that a particle whose proper mean life time exceeds 10^{-11} s and is traveling almost with the speed of light leaves a reasonable track in the detector. This can be though of as a strict upper cut as particles in this domain generally do travel with the speed of light. eg: muon (2.2 μs)
  - Short-Lived Particles: These particles do not live long enough to leave a track and hence are generally observed as resonances peak in the production cross section or the decay modes of some particle. By rule of thumb their mean lifetime is less than 10^{-11} s. eg: π^0 (8.4 * 10^{-17} s).

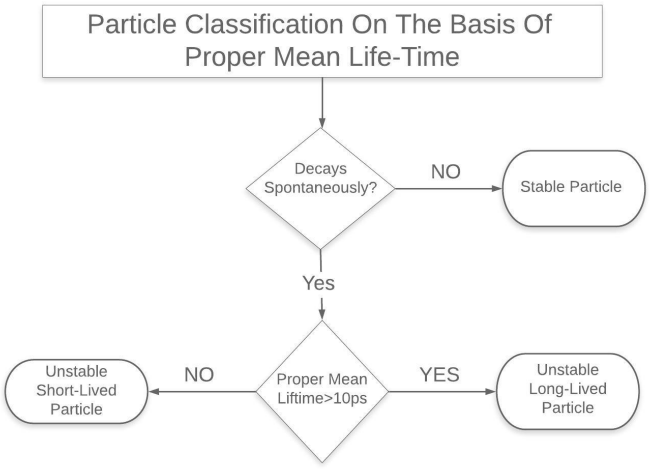

Figure 7: Flowchart For Classification Based On Life-Time

Note that this terminology of short and long lived is not strictly used but a generally true. A very famous example of its violation is the following example. The neutral kaon is thought of as a superposition of a short-lived (K_S) and a long-lived (K_L) component. For $K_S, \tau_S = 8.9 * 10^{-11}\ s \approx 10^{-10}\ s$ and for $K_L, \tau_L = 5.2 * 10^{-8}\ s$ which by my above definition should both be classified as long-lived particles. However, the reason for this terminology is that when we set to detect these components using neutral kaon, K_L on average decays much farther (in the detector chamber) and much later when compared to K_S. This is why I really don't like this classification but it is quite widely used to group particles coming out of high energy collisions.

2.8 As Excitations Of Some Other Elementary Particles[4]

This classification is independent of anything I have discussed earlier. This is not a widely used classification but I have included it here because the reasoning behind this grouping is quite interesting. The idea of this classification is to group particles by their stable end products of decay. If we think carefully, almost all of the sub-atomic particles are generally created by collisions of stable sub-atomic particles. These unstable particles live for some time and again decay back to the stable sub-atomic particles. If we consider the collision as some form of interaction with some generalized gravitational field then this process looks a lot similar to the interaction of electron of an atom with a photon field. To draw a better parallel first consider the electron of an atom to be in ground state, interacts with the photon field and goes to the excited state and finally falls back to the ground state after emitting photon.
Extending the same concept to our situation, the stable sub-atomic particles can be thought of as ground state of some new elementary particles in the generalised gravitational field. Any other particle can be thought of as excitations of the ground states of these new elementary particles. Thus, this classification basically reduces any particle to an allowed energy level in the generalized gravitational field. As with de-excitations, the new fundamental particles can directly go to the ground state or first go to a lower excited state and then to the ground state. This way of thinking elegantly explains

the presence of various decay modes for a particle in contemporary physics.
Logic dictates, that The number of new elementary particles should be equal to the number of stable sub-atomic particles. Indeed in the abstract the authors talk about four elementary classes: each giving electron, proton, photon and neutrino as its ground state. The authors do not discuss how different generations of neutrinos fit into this picture by arguing that not much is known about them. Hence in entirety they define three elementary particles: electrons (leptons), protons (baryons) and photons (bosons). The excited states are given by:

- Excited states of electrons are: muons, charged pions, charged kaons, τ, D and other leptons and charged mesons.
- Excited states of protons are: Λ, Σ, Δ, Ξ and other baryons.
- Excited states of photons are: uncharged pions, neutral kaons and neutral mesons.

Further the quarks are not even considered to be particles but simply the projections of the 4-D nuclear space onto the 3-D gravitational field space.

Figure 8: Allowed Electron Levels In Generalized Gravitational Field[4]

Chapter 2: Statistical Mechanics Of Ideal Fermi Gas

3 Solving The Ideal Fermi Gas

In this section, I will try to compute the pressure, chemical potential and other thermodynamic properties of a system of N (macroscopically large number) particles confines in a box (cube) of volume V at a certain temperature T. The setup screams of the Grand canonical ensemble of statistical mechanics. Further, the system will be composed only of identical relativistic fermions which would be following the Fermi-Dirac distribution. The system composed of only identical relativistic bosons can also be equivalently solved by replacing the Fermi-Dirac distribution with the Bose-Einstein distribution. It will also be assumed that there is no inter-particle potential. Basically fermions are free inside the box but they have to obey the Pauli's exclusion principle.

3.1 Quantum Particle In A Box

The potential for particle in a box with parameter l given by

$$V(x,y,z) = \begin{cases} 0 & if\ 0 \leq x,y,z \leq l \\ \infty & otherwise \end{cases} \tag{3.1.1}$$

This leads to the condition that the wave function must vanish at the boundary points (strict boundary conditions). The Schrodinger equation reads:

$$i\hbar\frac{\partial\psi}{\partial t} = \hat{H}\psi$$

where symbols have the usual meaning. The hamiltonian operator is given as: $\hat{H} = \frac{\hat{p}^2}{2m} = -\frac{\vec{\nabla}^2}{2m}$ in the position basis. A variable separable solution is assumed for the schrodinger equation namely,

$$\psi(\vec{r},t) = r_x(x)r_y(y)r_z(z)T(t) = T(t)\prod_{i=x,y,z} r_i(i)$$

The above equation solves for $\mathrm{T(t)} = e^{-\frac{iEt}{\hbar}}$. This leads to the following form of equation for each r_i wrt to i (i=$\{$x,y,z$\}$):

$$\frac{\partial^2 r_i}{\partial i^2} = \omega^2 r_i$$

The above system of equations can be easily solved. After applying the boundary condition (wave function must vanish at the end points of the box) and normalizing it, we have

$$\psi(\vec{r},t) = \psi(x,y,z,t) = \sqrt{\frac{8}{l^3}} sin\left(\frac{n_x\pi x}{l}\right) sin\left(\frac{n_y\pi y}{l}\right) sin\left(\frac{n_z\pi z}{l}\right) e^{-\frac{iEt}{\hbar}} \tag{3.1.2}$$

$$\text{with eigenenergies:} \quad E_{n_xn_yn_z} = \frac{\pi^2\hbar^2}{2ml^2}\left(n_x^2+n_y^2+n_z^2\right) \tag{3.1.3}$$

The states are both orthonormal and complete which is given as:

$$\int d^3\vec{r}\ \psi^*_{n_xn_yn_z}(\vec{r})\ \psi_{m_xm_ym_z}(\vec{r}) = \delta_{n_xm_x}\delta_{n_ym_y}\delta_{n_zm_z} \tag{3.1.4}$$

$$\sum_{n_xn_yn_z} \psi^*_{n_xn_yn_z}(\vec{r})\ \psi_{n_xn_yn_z}(\vec{p}) = \delta^3(\vec{r}-\vec{p}) \tag{3.1.5}$$

Here δ^3 is the dirac-delta function in three dimensions and $\delta_{n_xm_x}$ represents the Kronecker delta function.

3.2 Basic Tools Required To Solve The Problem

3.2.1 Concept Of Density Of States

Before defining the concept of density of states, let us first define the following quantity:

$$N(E) = \sum_{n_x n_y n_z} \Theta(E - E_{n_x n_y n_z})$$

Here, Θ denotes the Heavy-side step function. This function calculates the number of available states with energy $\leq$ E. Define density of states as $\rho(E)$ which denotes the instantaneous number of states available at energy E:

$$\rho(E) = \frac{dN}{dE} = \sum_{n_x n_y n_z} \delta(E - E_{n_x n_y n_z}) \tag{3.2.1}$$

The derivative of step function is the dirac-delta function. This is not immediately visible as they strictly are not functions but distributions. However, they can be viewed as the limiting sequence of the following real functions. This representation of the delta function is also known as Lorentzian Representation wherein this relationship is easier to view.

$$\theta(x) = \lim_{h \to 0} \frac{1}{\pi} \left[tan^{-1} \left(\frac{x}{h} \right) - \frac{1}{2} \right]$$

$$\delta(x) = \lim_{h \to 0} \frac{1}{\pi} \left[\frac{h}{x^2 + h^2} \right]$$

Note that both N(E) and $\rho(E)$ can only take integer values and hence are really not differentiable. However for macroscopically large N (and hence E), these functions can be very well approximated by some other continuously differentiable function which will be actually used to perform the calculations. Since we are solving the fermion system for a box, it will be quite useful to compute these quantities for this case. To compute the number of states, we are going to use equation 3.1.3.
Clearly at an energy E, N(E) = # states contained within the sphere of radius, r = $\sqrt{\frac{2ml^2E}{\pi^2\hbar^2}}$ in the $n_x n_y n_z$ space. Further each available states occupies unit volume in this space. Hence

$$N_{pb}(E) = \left(\frac{1}{8} \right) \frac{4\pi}{3} \left[\frac{2ml^2E}{\pi^2\hbar^2} \right]^{\frac{3}{2}} = \frac{V}{6\pi^2\hbar^3} \left[2mE \right]^{\frac{3}{2}} \tag{3.2.2}$$

Here $V = l^3$ which is the volume of the box and the factor of 1/8 is because we only consider states in the positive octant of the $n_x n_y n_z$ space. The reason for this is 3.1.2. Replacing $n_x \to -n_x$ does nothing except introduce a negative sign in the wavefunction which is not really a new state for the N particle fermion system as we have already imposed the permutation symmetry by introducing the Fermi-Dirac statistics at the beginning of the problem. Now

$$\rho_{pb}(E) = \frac{V}{4\pi^2\hbar^3} (2m)^{\frac{3}{2}} \sqrt{E} \propto \sqrt{E} \tag{3.2.3}$$

Hence in three spatial dimensions, the density of states is proportional to $\sqrt{E}$. Often a variable k is introduced. Generally, $\mathrm{k} \equiv \frac{p}{\hbar} = \frac{\sqrt{2mE}}{\hbar}$. In terms of this new variable:

$$\rho_{pb}(k) \equiv \frac{dN}{dk} = \rho_{pb}(E)\frac{dE}{dk} = \frac{4\pi k^2 V}{2\pi^3} \tag{3.2.4}$$

The above equation suggests a generalization: $dN = \frac{d^3x\ d^3k}{(2\pi)^3} = \frac{d^3x\ d^3p}{(2\pi\hbar)^3}$. The generalization makes sense on a lot of grounds. Firstly it makes N dimensionless and hence now it properly represents numbers. Secondly the volume element is phase space volume element with a measure of $1/h^3$ which basically says that there is 1 available state per h^3 unit volume of phase space which makes us remember the uncertainty relation.

3.2.2 Attacking The Problem Via Grand Canonical Ensemble (GCE)[5]

The construction of the problem might make one think that canonical ensemble is best to tackle this problem. That would have been true if the particles were not obeying the Pauli's exclusion principle. Due to this, there is an extra density function (Fermi-Dirac distribution) related to phase space volume in the canonical ensemble. To see how the Fermi-Dirac statistics naturally emerge one must take a dive into the grand canonical ensemble.
Define the GCE partition function

$$\mathcal{Z} = \sum_N \sum_\nu e^{\frac{\mu N - E_\nu}{kT}}$$

Here symbols have their usual meaning. The summand can be thought of as the relative probability of finding the system with N particles and an energy E_ν. In our case there are no interactions between the fermions and hence the whole quantum system can be completely defined by the occupation number of the quantum particles in each available quantum state. A system with N particles with occupation number n_j for quantum level j can be completely described as:

$$N = \sum_j n_j$$

$$E = \sum_j n_j\ E_j$$

As our system in hand decomposes so beautifully, each quantum level can be thought of as an independent system parameterized by the occupation number. The GCE for our system simply becomes the Cartesian product of all the independent systems. Mathematically the following function is the generating function for GCE partition function of our system:

$$\mathcal{Z} = \prod_j \left(\sum_{n_j} e^{n_j \frac{\mu - E_j}{kT}} \right) \tag{3.2.5}$$

As fermions can only have 0 or 1 as their occupation number, we have:

$$\mathcal{Z} = \prod_j Z_j = \prod_j \left(1\ +\ e^{\frac{\mu - E_j}{kT}} \right) \tag{3.2.6}$$

To connect to thermodynamics one defines the GCE potential function as:

$$\Omega = -kTln\mathcal{Z} \quad (3.2.7)$$

$$\Omega = \sum_j \Omega_j = -kT \sum_j ln\left(1 + e^{\frac{\mu - E_j}{kT}}\right) = kT \sum_j ln\left(1 - \frac{1}{1 + e^{\frac{E_j - \mu}{kT}}}\right) = kT \sum_j ln\left(1 - f(E_j)\right) \quad (3.2.8)$$

$$f(E_j) = \frac{1}{1 + e^{\frac{E_j - \mu}{kT}}} \quad (3.2.9)$$

It can be argued that the GCE potential function is the Legendre transform of the Helmholtz energy (potential function of the canonical ensemble) wrt the variables N and μ. Hence

$$\Omega(V, T, \mu) = A(V, T, N) - \mu N$$

where A(V,T,N) is the Helmholtz energy of the system. The advantage of doing this is in GCE is that we can finally connect to macroscopic thermodynamic parameter via the following relation:

$$d\Omega = \ -PdV \ - TdS \ - Nd\mu \quad (3.2.10)$$

Thus, the ensemble average for the number of particles is by:

$$\bar{N} = -\left(\frac{\partial \Omega}{\partial \mu}\right)_{V,T} \quad (3.2.11)$$

$$\bar{N} = \sum_j \frac{e^{\frac{\mu - E_j}{kT}}}{1 + e^{\frac{\mu = E_j}{kT}}} = \sum_j f(E_j) \quad (3.2.12)$$

Doing a similar calculation for the ensemble average energy (internal energy) on simplifying gives:

$$U \equiv \sum_N e^{\mu N} \sum_\nu E_\nu \ e^{\frac{-E_\nu}{kT}}$$

$$U = \sum_j E_j f(E_j) \quad (3.2.13)$$

Hence the final form of basic thermodynamic quantities becomes the sum of some function of E_j over all possible values of E_j. As the number of particles becomes macroscopically large, the discrete energy spectrum mimics a continuous energy spectrum. In that case the sum can be replaced with an integral. To find the thermodynamic parameters in the continuous case one can make the following transformation:

$$\sum_j h(E_j) \Longrightarrow \int_0^\infty dE \ \rho(E) \ h(E) \quad (3.2.14)$$

$\rho(E)$ is the density of states which is given bu 3.2.3 for our problem.

3.3 Solution At Zero Temperature, T=0

At 0 temperature, the second law of thermodynamics forces the system to go to the ground state and the system of N fermions will occupy all single particle levels upto some maximum energy, E_f called fermi energy. This suggests the fermi-distribution function to be:

$$f(E) = \begin{cases} 1 & if\ E\ <\ E_f \\ 0 & if\ E\ >\ E_f \end{cases} \tag{3.3.1}$$

Introduce fermi momentum as the momentum corresponding to the fermi energy, i.e. $p_f = \sqrt{2mE_f} = \hbar k_f$. The two can be instantly related using:

$$dN = g\frac{d^3x\ d^3k}{(2\pi)^3} = \frac{d^3x\ d^3p}{(2\pi\hbar)^3}.$$

The MCE definitions are easier and smoother to use for T=0 case. The above equation introduces 'g' as the degeneracy factor which is 2s+1 for a particle of spin s. Hence 2 for fermion.

$$N = Vg\int_0^{p_f} \frac{4\pi p^2}{(2\pi\hbar)^3}dp = \frac{gp_f^3}{6\pi^2\hbar^3}V = \frac{gp_f^3}{6\pi^2\hbar^3}V \tag{3.3.2}$$

$$n = \frac{N}{V} = \frac{gp_f^3}{6\pi^2\hbar^3} \tag{3.3.3}$$

$$\frac{dN}{dp_f} = \frac{gp_f^2}{2\pi^2\hbar^3}V \tag{3.3.4}$$

Here, n is the number density. Now differentiating 4.1.3 on both sides

$$dn = \frac{gp_f^2}{2\pi^2\hbar^3}dp_f = \frac{1}{V}dN + \left(-\frac{N}{V^2}\right)dV$$

Hence the partial derivatives can be read of as:

$$\frac{\partial p_f}{\partial N} = \frac{2\pi^2\hbar^3}{gp_f^2}\frac{1}{V} \tag{3.3.5}$$

$$\frac{\partial p_f}{\partial V} = -\frac{2\pi^2\hbar^3}{gp_f^2}\frac{N}{V^2} \tag{3.3.6}$$

3.3.1 Extremely Relativistic Case: E=$|\vec{p}c|$

The calculation of internal energy U is again done using the MCE analysis:

$$U = \int EdN = \int_0^{p_f} E(p)\ \frac{dN}{dp}dp$$

The above equation solves to give:

$$U = \frac{gcp_f^4}{8\pi^2\hbar^3}V \tag{3.3.7}$$

$$u = \frac{U}{V} = \frac{gcp_f^4}{8\pi^2\hbar^3} \tag{3.3.8}$$

The chemical potential can be computed as:

$$\mu = \frac{\partial U}{\partial N} = cp_f = E_f \tag{3.3.9}$$

This indeed looks like the correct answer as in the limit $T \to 0$ and $\mu = E_f$, the distribution function f(E) as defined by 3.2.9 mimics the function 4.1.1. The pressure can be computed using:

$$P = -\frac{\partial U}{\partial V} = \frac{\frac{\partial U}{\partial p_f}}{\frac{\partial V}{\partial p_f}} = \frac{u}{3} \tag{3.3.10}$$

Another thing which is useful to calculate the Inverse compressibility(dP/dn) and adiabatic(γ) index defined as:

$$\frac{dP}{dn} = \frac{1}{3}\frac{du}{dn} = \frac{p_f}{3} \tag{3.3.11}$$

$$\gamma = \frac{n}{P}\frac{dP}{dn} = \frac{4}{3} \tag{3.3.12}$$

Since the adiabatic index is a constant, the above differential equation can be integrated to give the equation of state as

$$P\left(\frac{V}{N}\right)^{\frac{4}{3}} = constant \tag{3.3.13}$$

The entropy of the system can be computed using the MCE definition of the entropy. The degeneracy of the ground state is upper bounded by the density of states at $E = E_f$. Hence:

$$S = kln(\rho(E_f)) = k\ ln\left(\frac{gV}{2\pi^2\hbar^3}E_F^2\right) \tag{3.3.14}$$

This is simply an O(log N) term which can be neglected for all macroscopical purposes. The entropy per molecule is $S_f \propto \frac{log(N)}{N}$ which goes to 0 as N $\longrightarrow$ 0. Hence we have completely solved the free fermi gas at 0 temperature for extremely relativistic case. All the macroscopic parameters are defined via the equations 4.1.2 - 4.1.13.
Now it's time to plot some graphs. In each case, I will try to keep the leading coefficient of the dependent variable to be 1. This is equivalent to resizing (contracting or expanding) the y-axis which would affect the absolute values of the function but wont change the nature of the graph. I am doing this because I am only interested in the nature of graph and not the absolute value of the functions. The constants are really daunting to keep in the equation and it's just easier to set them to 1.

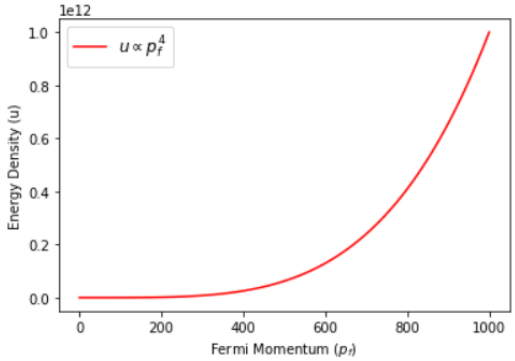

(a) Graph of Energy density vs Fermi Momentum

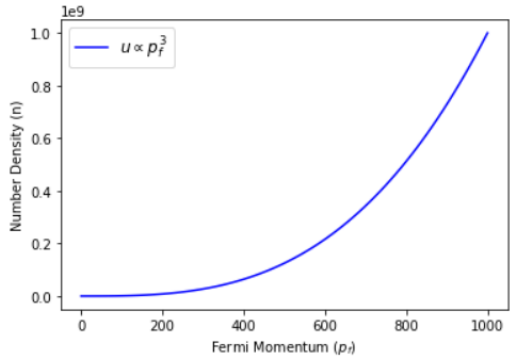

(b) Graph of Number density vs Fermi Momentum

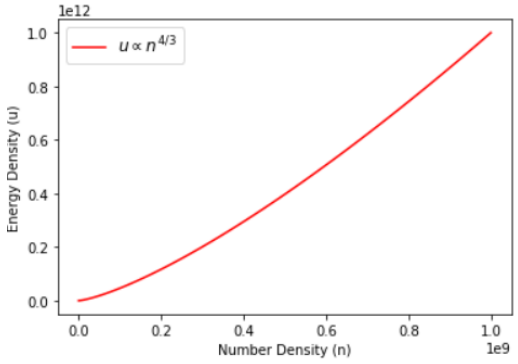

(c) Graph of Energy density vs Number density

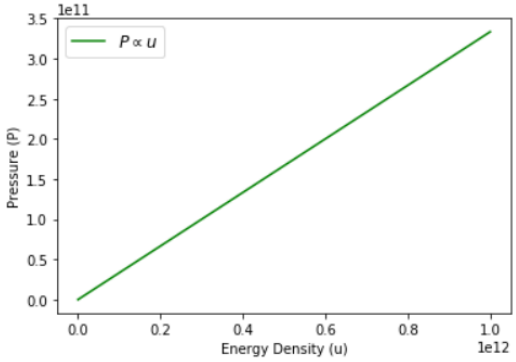

(d) Graph of Pressure vs Energy density

Figure 9: Graphs Of Some Important Parameters For A Highly Relativistic Fermi Gas At T=0

3.3.2 General Relativistic Case: E=$\sqrt{\vec{p}^2c^2 + m^2c^4}$

For convenience, I am going to work in the natural units $\hbar = c = 1$ The calculation of internal energy U is again done using the GCE analysis:

$$U = \int EdN = \int_0^{p_f} E(p)\ \frac{dN}{dp}dp = \int_0^{p_f} \sqrt{p^2+m^2}\ \frac{gp^2}{2\pi^2}V dp = \frac{gV}{2\pi^2}\int_0^{p_f} \sqrt{p^2+m^2}\ p^2\ dp$$

$$\int\ p^2\ \sqrt{p^2+m^2}\ dp = \frac{1}{8}\left[(2p^2+m^2)p\sqrt{p^2+m^2} - m^4 ln\left(p+\sqrt{p^2+m^2}\right)\right] + C$$

The above solution can be made to look better by making the substitution: $x = \frac{p}{m}$

$$\int\ p^2\ \sqrt{p^2+m^2}\ dp = f\left(x=\frac{p}{m}\right) + C = \frac{m^4}{8}\left[(2x^2+1)x\sqrt{x^2+1} - ln\left(x+\sqrt{1+x^2}\right)\right] + C \tag{3.3.15}$$

This gives the following equations:

$$U = \frac{gVm^4}{2\pi^2} f(x_f) \tag{3.3.16}$$

$$u = \frac{U}{V} = \frac{gm^4}{2\pi^2} f(x_f) \tag{3.3.17}$$

The chemical potential can be computed as:

$$\mu = \frac{\partial U}{\partial N} = \frac{\frac{\partial U}{\partial p_f}}{\frac{\partial N}{\partial p_f}} = \sqrt{p_f^2 + m^2} = E_f \tag{3.3.18}$$

This indeed looks like the correct answer as in the limit $T \to 0$ and $\mu = E_f$, the distribution function f(E) as defined by 3.2.9 mimics the function 4.1.1. The pressure can be computed using:

$$P = -\frac{\partial U}{\partial V} = \frac{\frac{\partial U}{\partial p_f}}{\frac{\partial V}{\partial p_f}} = \frac{gm^4}{6\pi^2} x_f^3 \sqrt{1 + x_f^2} - \frac{gm^4}{2\pi^2} f(x_f) \tag{3.3.19}$$

$$P = \frac{gm^4}{48} \left[(2x_f^2 - 3) x_f \sqrt{1 + x_f^2} + 3\ ln\left(x_f + \sqrt{1 + x_f^2} \right) \right] \tag{3.3.20}$$

Another thing which is useful to calculate the Inverse compressibility(dP/dn) and adiabatic(γ) index defined as:

$$\frac{dP}{dn} = \frac{\frac{dP}{dp_f}}{\frac{dn}{dp_f}} = \frac{1}{3} \frac{p_f^2}{\sqrt{m^2 + p_f^2}} \tag{3.3.21}$$

$$\gamma = \frac{n}{P} \frac{dP}{dn} = \frac{n}{3P} \frac{p_f^2}{\sqrt{m^2 + p_f^2}} \tag{3.3.22}$$

The inverse compressibility factor gives both the non-relativistic case, i.e. $\left(\frac{dP}{dn}\right)_{p \ll m} = \frac{p_f^2}{3m}$ and the ultra relativistic case, i.e. $\left(\frac{dP}{dn}\right)_{m \ll p} = \frac{p_f}{3}$. Thus, the adiabatic index also varies from $5/3 \to 4/3$ as p_f varies from $0 \to \infty$.

The entropy of the system can again be computed using the MCE definition and will be exactly equal to the expression given by 4.1.14. Hence:

$$S = kln(\rho(E_f)) = k\ ln\left(\frac{gV}{2\pi^2 \hbar^3} E_f \sqrt{E_f^2 - m^2} \right) \tag{3.3.23}$$

All the same arguments follow as before.Now it's time to plot some graphs. In each case, I will try to keep the leading coefficient of the dependent variable to be 1. This is equivalent to resizing (contracting or expanding) the y-axis which would affect the absolute values of the function but wont change the nature of the graph. I am doing this because I am only interested in the nature of graph and not the absolute value of the functions. Further the particle will be assumed to have unit mass unless explicitly stated otherwise.

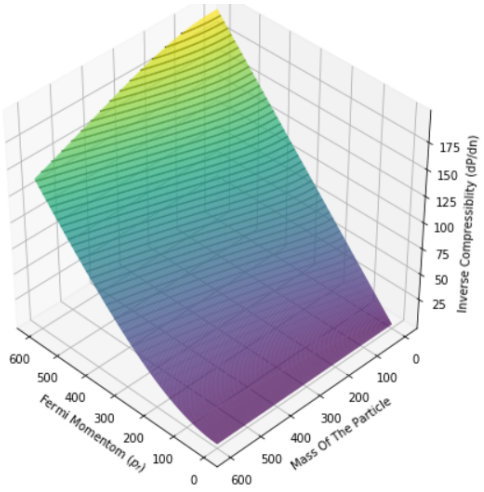

(a) Plot For Variation Of Inverse Compressibility

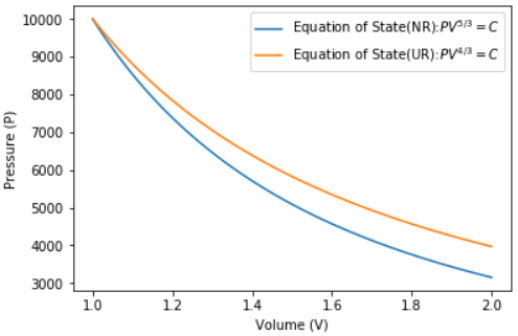

(b) Variation Of Pressure and Volume (fixed N) For A Non-Relativistic (NR,red) And Ultra-Relativistic(UR,blue) Free Fermi gas

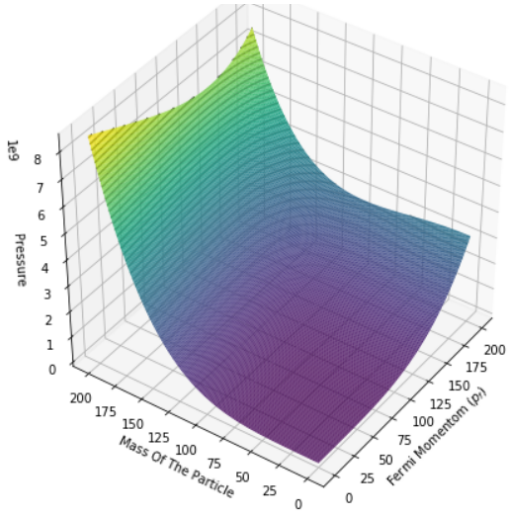

(c) Plot For Variation Of Pressure

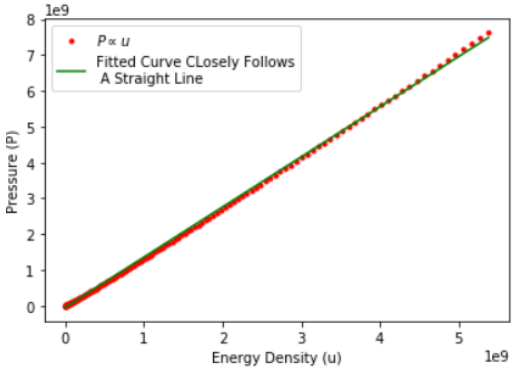

(d) Graph of Pressure vs Energy density

Figure 10: Plots Depicting Relation Between Some Parameters For A General Relativistic Fermi Gas At T=0

The plots from fig 10(a),10(b) suggest that the relativistic fermi gas is much more compressible than the non-relativistic counterpart provided other conditions remain the same. As expected dP/dn is linear all throughout the contour which is close to m=0 ($m \ll P_f$) region. However the m=600 contour, the increase first looks like a polynomial one (basically quadratic as $p_f \to 0$ in this region) and later becomes close to linear ($p_f \equiv m$ region). Pressure (fig 10(c)) has a polynomial growth in all the regions, however the degree of that polynomial seems to change uniformly throughout the graph. The one thing one can easily notice is that in the NR region ($p_f \to 0$ contour) the growth is much higher than the UR region ($m \to 0$), Although both look like polynomial growth but the degree of the polynomial higher in the NR case.

3.3.3 Non Relativistic Case (NR): E=$\frac{p^2}{2m}$

It is quite simple to reproduce the calculations of section 4.2.1 for this case. I will not reproduce these calculations but simply state the final solutions.

$$U = \frac{gcp_f^5}{20m\pi^2\hbar^3}V \tag{3.3.24}$$

$$u = \frac{U}{V} = \frac{gp_f^5}{20m\pi^2\hbar^3} \tag{3.3.25}$$

$$\mu = \frac{\partial U}{\partial N} = \frac{p_f^2}{2m} = E_f \tag{3.3.26}$$

$$P = -\frac{\partial U}{\partial V} = \frac{\frac{\partial U}{\partial p_f}}{\frac{\partial V}{\partial p_f}} = \frac{2u}{3} \tag{3.3.27}$$

$$\frac{dP}{dn} = \frac{1}{3}\frac{du}{dn} = \frac{2\mu}{3} = \frac{p_f^2}{3m} \tag{3.3.28}$$

$$\gamma = \frac{n}{P}\frac{dP}{dn} = \frac{5}{3} \tag{3.3.29}$$

$$P\left(\frac{V}{N}\right)^{\frac{5}{3}} = constant \tag{3.3.30}$$

$$S = kln(\rho(E_f)) = k\ ln\left(\frac{gV}{4\pi^2\hbar^3}(2m)^{\frac{3}{2}}\sqrt{E_f}\right) = k\ ln\left(\frac{gmV}{2\pi^2\hbar^3}p_f\right) \tag{3.3.31}$$

Note that p_f denotes the fermi momentum which has the relation to the upper energy bound as $E_f = \frac{p_f^2}{2m}$.

3.4 Solution At $T \neq 0$:Finite Temperature Effects

Using 3.2.14, we write the continuous version for all the thermodynamic parameters as:

$$\bar{N} = \int_0^\infty dE\ \rho(E)\ f(E) \tag{3.4.1}$$

$$U = \int_0^\infty dE\ E\ \rho(E)\ f(E) \tag{3.4.2}$$

$$\Omega = kT\int_0^\infty dE\ \rho(E)\ ln(1 - f(E)) \tag{3.4.3}$$

Here $\rho(E)$ is the density of states and f(E) is Fermi-Dirac distribution as defined by 3.2.3 and 3.2.9 respectively. The equation of state is quite easy to find in the GCE and can be calculated using the formula:

$$\frac{PV}{kT} = ln\mathcal{Z} = -\Omega \tag{3.4.4}$$

The above integrals are incredibly complex and cannot really be solved. They can be decomposed into some type of L functions but they are another class of unsolvable analytic number theory problems.

So, what can we really do. Well, we approximate. The previous section completely solves for T=0 and we will use those results to approximate near this region and finally argue when and where this approximation is decent.

3.4.1 Scheme For Low Temperature Expansion Of The Fermi-Integrals

The motivation for this scheme is the observation that the boundary term produced by doing integration by parts vanishes if f(E) is chosen to be the function to be differentiated. Hence our aim is to solve the integrals of the type:

$$I = \int_0^\infty dE\ h(E)\ f'(E)$$

Since, this is a low temperature expansion, we want our answer of the integral to be in some form of power series of T. Now the fermi-distribution at T=0 is simply f(E)=$\Theta(\mu - E_f)$, where $\Theta(x)$ is the step function. The derivative of this distribution is f'(E)=$-\delta(\mu - E_f)$. Now at finite temperatures close to 0, the derivative of the fermi distribution varies violently around the chemical potential (mimicking the delta function) and dies quickly. Hence the above type of integrals become easier to approximate when h(E) is a normal smooth continuous function. Integrals like I, can be approximated solely by the values of the function h(E) and its' derivatives computed near the region E=μ. The idea is to replace f'(E) with the delta function and its' derivatives. Keeping our observations in mind, the following form is quite apt:

$$f'(E) = -\delta(\mu - E) + \sum_{n=1}^{\infty} a_n\ (kT)^n\ \delta^n(\mu - E) \tag{3.4.5}$$

Here δ^n is the n-th derivative of the delta function. The following property which can be easily proved by integration by parts was the reason for such an expansion:

$$\int_0^\infty\ dx f(x)\delta^n(x) =\ (-1)^n f^n(0) = (-1)^n \left(\frac{d^n f}{dx}\right)_{x=0}$$

Another way to compute f'(E) is to directly use the definition 3.2.9 and differentiate it. The result is:

$$f'(E) = -\frac{1}{kT}\frac{e^{\frac{E-\mu}{kT}}}{[1+e^{\frac{E-\mu}{kT}}]^2} \tag{3.4.6}$$

The constants a_n can be calculated using:

$$a_n = \frac{1}{n!(kT)^n}\int_0^\infty dE\ f'(E)\ (\mu - E)^n \tag{3.4.7}$$

Now consider the following integral with O being an odd function in the variable (t=E-μ). Our function f'(E) is an even function in the variable (t=E-μ). Consider the following integral:

$$\int_0^{i\infty}\ dE\ f'(E)O(E) = \int_0^{2\mu}\ dE\ f'(E)O(E) + \int_{2\mu}^{\infty}\ dE\ f'(E)O(E)$$

Due to the odd-even symmetry about $E = \mu$, the first integral vanishes, Further:

$$\int_{2\mu}^{\infty} dE\ f'(E)O(E) \approx e^{\mu/kT} \int_{2\mu}^{\infty} dE\ \frac{1}{kT} e^{-E/kT} \approx e^{-\mu/kT} \to 0$$

Hence if $e^{-\mu/kT}$ is small enough to be ignored then $a_{2k+1} = 0$. All odd terms are essentially zero. Generally this is a valid approximation and works quite well in the region we are trying to produce a scheme. Now computing the remaining coefficients (here n is even):

$$a_n = -\frac{1}{n!(kT)^n} \int_0^{\infty} dE\ \frac{1}{kT} \frac{e^{\frac{E-\mu}{kT}}}{[1+e^{\frac{E-\mu}{kT}}]^2}\ (\mu - E)^n$$

Make the following substitution, x$\equiv \frac{E-\mu}{kT}$

$$a_n = -\frac{1}{n!} \int_{-\mu/kT}^{\infty} dx\ \frac{x^n e^x}{[1+e^x]^2}$$

Again via the same sorcery as before, we can make an insignificant error of $e^{-\mu/kT}$ to send the lower limit to $-\infty$. Since the integral is even in x (n is even), and making the substitution $x \to -x$,hence:

$$a_n = -\frac{2}{n!} \int_0^{\infty} dx\ \frac{x^n e^{-x}}{[1+e^{-x}]^2}$$

Expanding $\frac{1}{[1+e^{-x}]^2}$ into its' power series to get:

$$a_n = -\frac{2}{n!} \int_0^{\infty} dx\ \sum_{\alpha=1}^{\infty} (-1)^{\alpha+1} \alpha x^n e^{-\alpha x}$$

Using Dominated Convergence Theorem to interchange the order of sum and the integral

$$a_n = -\frac{2}{n!} \sum_{\alpha=1}^{\infty} (-1)^{\alpha+1} \alpha \int_0^{\infty} dx\ x^n e^{-\alpha x}$$

Now make the substitution for the integral u$\equiv \alpha x$ to get:

$$a_n = -\frac{2}{n!} \sum_{\alpha=1}^{\infty} (-1)^{\alpha+1} \frac{1}{\alpha^n} \int_0^{\infty} du\ u^n e^{-u}$$

Recognize the integral to be the generalized factorial function $\Gamma(n) = n!$ for integers. This solves to give:

$$a_n = -2 \sum_{\alpha=1}^{\infty} (-1)^{\alpha+1} \frac{1}{\alpha^n}$$

This looks like the Riemann-Zeta function with alternating signs. This can be easily computed in terms of the Riemann-Zeta function as:

$$a_n = -2\left(1 - 2^{1-n}\right)\zeta(n)$$

Our approxillator scheme is now ready. The definition is given by 4.2.5 and the coefficients are given by:

$$a_n = \begin{cases} -2\left(1-2^{1-n}\right)\zeta(n) & if\ n \cong 0\ mod(2) \\ 0 & if\ n \cong 1\ mod(2) \end{cases} \tag{3.4.8}$$

Lets finally comment on the validity of this approximation scheme. The approximation is good iff the errors are small. Mathematically:

$$0 \leq e^{-\mu/kT} \lll 1$$

Now define $\mu \equiv E_f \equiv kT_f$ as the corresponding energy or associated temperature where the probability of finding the fermion is 1/2. For the approximation to work well the equation becomes:

$$\frac{T_f}{T} \ggg 1 \implies T_f \ggg T \tag{3.4.9}$$

3.4.2 Deriving The Thermodynamics Using The Low Temperature Expansion(NR)

Let us compute average particle number using 4.2.1. Applying integration by parts:

$$\bar{N} = [f(E)N(E)]_0^\infty - \int_0^\infty dE\ N(E)f'(E)$$

The boundary term simply vanishes. Now using our previous scheme upto first non trivial term (n=2), $a_2 = -\frac{\pi^2}{6}$ gives

$$\bar{N} \approx N(\mu) + \frac{\pi^2 k^2 T^2}{6} N''(\mu) \tag{3.4.10}$$

Now using 3.2.2-3.2.4, relate:

$$N(\mu) = \frac{gV}{6\pi^2}(2m\mu)^{3/2} \tag{3.4.11}$$

$$N''(\mu) = \frac{d^2N}{d\mu^2} = \frac{gV}{8\pi^2}(2m)^{3/2}\frac{1}{\sqrt{\mu}} \tag{3.4.12}$$

$$\bar{N} \approx \sqrt{2m}\frac{mgV}{3\pi^2}\left(\mu^{3/2} + \frac{\pi^2 k^2 T^2}{8}\frac{1}{\sqrt{\mu}}\right) \tag{3.4.13}$$

The relation 4.2.12 can be inverted by expanding μ as a power series in T and comparing the coefficients of T on both sides. Since we only introduced the first term from our approxillator, it makes sense to expand only upto T^2 to get:

$$\mu(T) \approx \mu(0) - \frac{\pi^2 k^2 T^2}{12}\frac{1}{\mu(0)} \tag{3.4.14}$$

$$\mu(0) \equiv kT_f \equiv E_f = \frac{1}{2m}\left(\frac{6\pi^2\bar{N}}{gV}\right)^{2/3} \tag{3.4.15}$$

The energy E_f is now the energy where the probability of finding the fermion is 1/2.
Now let us determine the internal energy using 4.2.2. Before starting that calculation define:

$$\beta(E) = E\rho(E) = \frac{V}{4\pi^2}(2mE)^{3/2}$$

$$\beta_1(E) = \int dE\ \beta(E) = \frac{gV}{10\pi^2}(2m)^{3/2}E^{5/2} \tag{3.4.16}$$

Now:

$$U = [f(E)\beta_1(E)]_0^\infty - \int_0^\infty dE\ \beta_1(E)f'(E)$$

The boundary term simply vanishes. Now using our previous scheme upto first non trivial term (n=2), $a_2 = -\frac{\pi^2}{6}$ gives

$$U \approx \beta_1(\mu) + \frac{\pi^2k^2T^2}{6}\beta_1''(\mu) \tag{3.4.17}$$

Now using using our approxillator scheme, relate:

$$\beta_1(\mu) = \frac{gV}{10\pi^2}(2m)^{3/2}\mu^{5/2} \tag{3.4.18}$$

$$\beta_1''(\mu) = \frac{d^2\beta_1}{d\mu^2} = \frac{gV}{10\pi^2}(2m)^{3/2}\frac{15\sqrt{\mu}}{4} \tag{3.4.19}$$

$$U \approx (2m)^{3/2}\frac{gV}{4\pi^2}\left[\frac{2}{5}\mu^{5/2} + \frac{\pi^2k^2T^2}{4}\sqrt{\mu}\right] \tag{3.4.20}$$

Now use 4.2.13 to expand μ as a power series in T and ignore $O(T^3)$ and higher terms. Now the expression becomes:

$$U = (2m)^{3/2}\frac{gV}{4\pi^2}\left[\frac{2}{5}[\mu(0)]^{5/2} + \frac{\pi^2k^2T^2}{6}\sqrt{\mu(0)}\right] \tag{3.4.21}$$

To compute the entropy, we first calculate the specific heat at constant volume:

$$C_V = \left(\frac{\partial U}{\partial T}\right)_{\bar{N},V} = (2m)^{3/2}\frac{gV}{4\pi^2}\sqrt{\mu(0)}\frac{\pi^2k^2T}{3}$$

Using 4.2.14, this can be reduces to a more known form:

$$C_V = \frac{\bar{N}\pi^2k^2}{2}\frac{T}{\mu(0)} = \frac{\bar{N}\pi^2k}{2}\frac{T}{T_f} \tag{3.4.22}$$

Now the entropy can be calculated easily. Note that T_f is a constant at a process where Q=$C_V dT$ as both $\bar{N} and V$ are conserved during the process. Hence

$$S = \int_0^T \frac{C_V}{T}dT \tag{3.4.23}$$

$$S = \frac{\bar{N}\pi^2k}{2}\frac{T}{T_f} \tag{3.4.24}$$

Note unlike the classical limit, the specific heat goes to 0 as $T \to 0$. Finally, lets calculate the pressure in the low temperature expansion. For this we need to compute the GCE potential function first.

$$\Omega = -kT \int_0^\infty dE\ \rho(E)\ ln(1 + e^{\frac{\mu - E}{kT}})$$

Performing integration by parts and realizing that the boundary terms vanish we have:

$$\Omega = -\int_0^\infty dE\ N(E)\ f(E)$$

Applying integration by parts again to get:

$$\Omega = \int_0^\infty dE\ \beta_2(E)\ f'(E) \tag{3.4.25}$$

Where

$$\beta_2(E) = \int dE\ N(E) = \frac{gV}{15\pi^2}(2m)^{3/2}E^{5/2}$$

Now:

$$-\Omega \approx \beta_2(\mu) + \frac{\pi^2 k^2 T^2}{6}\beta_2''(\mu) \tag{3.4.26}$$

Now using using our approxillator scheme, relate:

$$\beta_2(\mu) = \frac{gV}{15\pi^2}(2m)^{3/2}\mu^{5/2} \tag{3.4.27}$$

$$\beta_2''(\mu) = \frac{d^2\beta_2}{d\mu^2} = \frac{gV}{15\pi^2}(2m)^{3/2}\frac{15\sqrt{\mu}}{4} \tag{3.4.28}$$

$$-\Omega \approx (2m)^{3/2}\frac{gV}{15\pi^2}\left[\mu^{5/2} + \frac{15\pi^2 k^2 T^2}{24}\sqrt{\mu}\right] \tag{3.4.29}$$

Now use 4.2.13 to expand μ as a power series in T and ignore $O(T^3)$ and higher terms. Now the expression becomes:

$$-\Omega = (2m)^{3/2}\frac{gV}{15\pi^2}\left[[\mu(0)]^{5/2} + \frac{5}{12}\pi^2 k^2 T^2\sqrt{\mu(0)}\right] \tag{3.4.30}$$

Rearranging, to get to a familiar form:

$$-\Omega = (2m)^{3/2}\frac{gV}{15\pi^2}[\mu(0)]^{5/2}\left[1 + \frac{5}{12}\pi^2 k^2 T^2\frac{1}{[\mu(0)]^2}\right] = \left\{\frac{2}{3}\frac{gp_f^5}{20\pi^2 m}\right\}V\left[1 + \frac{5}{12}\pi^2 k^2 T^2\frac{1}{E_f^2}\right]$$

Recognizing that the first term in the { } brackets is simply the pressure exerted by the NR Fermi gas at T=0. Making this final substitution gives:

$$-\Omega = P_0 V\left[1 + \frac{5}{12}\pi^2 k^2 T^2\frac{1}{E_f^2}\right] \tag{3.4.31}$$

Using the equation 4.2.4 to finally get the pressure:

$$P = P_0 V\left[1 + \frac{5}{12}\pi^2 k^2 T^2\frac{1}{E_f^2}\right] \tag{3.4.32}$$

All the above formulae reduce to the ones obtained in section 4.1.3 as T$\to$ 0.

3.4.3 Deriving The Thermodynamics Using The Low Temperature Expansion(UR)

The only difference in this section will be the fact that we will use the highly relativistic formula for the energy and then redo the calculations. I will be using the natural units ($\hbar = c = 1$). Hence:

$$Non - Relativistic\ Regime \rightarrow Ultra\ Relativistic\ Regime$$

$$p_f = \sqrt{2mE_f} \rightarrow p_f = E_f \tag{3.4.33}$$

Since the calculations are simple reproductions of section 4.2.2, hence I will skip a few steps this time around. The major difference is the functional form of density of the density of states. In section 4.2.2 it was given by equation 3.2.3. However this time around it is given by 4.1.4 as

$$\frac{dN}{dE} = \frac{gV}{2\pi^2}E^2 \tag{3.4.34}$$

The number density is given by:

$$\bar{N} \approx N(\mu) + \frac{\pi^2 k^2 T^2}{6} N''(\mu) \tag{3.4.35}$$

Now using equation 4.2.35, relate:

$$N(\mu) = \frac{gV}{6\pi^2}\mu^3 \tag{3.4.36}$$

$$N''(\mu) = \frac{d^2N}{d\mu^2} = \frac{gV}{6\pi^2}6\mu \tag{3.4.37}$$

$$\bar{N} = \frac{gV}{6\pi^2}\left(\mu^3 + \pi^2 k^2 T^2 \mu\right) = \frac{gV}{6\pi^2}\mu^3\left(1 + \frac{\pi^2 k^2 T^2}{\mu^2}\right) = N_0\left(1 + \frac{\pi^2 k^2 T^2}{E_f^2}\right) \tag{3.4.38}$$

The factor N_0 is exactly equal to the number of particles at T=0 with fermi energy E_f. The relation 4.2.12 can be inverted by expanding μ as a power series in T and comparing the coefficients of T on both sides. Since we only introduced the first term from our approxillator, it makes sense to expand only upto T^2 to get:

$$\mu(0) \equiv kT_f \equiv E_f = \left(\frac{6\pi^2\bar{N}}{gV}\right)^{1/3} \tag{3.4.39}$$

$$\mu(T) \approx \mu(0) - \frac{\pi^2 k^2 T^2}{3}\frac{1}{\mu(0)} = E_f\left[1 - \frac{\pi^2 k^2 T^2}{3E_f^2}\right] \tag{3.4.40}$$

The energy E_f is now the energy where the probability of finding the fermion is 1/2.
The calculation of internal energy leads to:

$$U = [f(E)\beta_1(E)]_0^\infty - \int_0^\infty dE\ \beta_1(E)f'(E)$$

The boundary term simply vanishes. Now using our previous scheme upto first non trivial term (n=2), $a_2 = -\frac{\pi^2}{6}$ gives

$$U \approx \beta_1(\mu) + \frac{\pi^2 k^2 T^2}{6}\beta_1''(\mu) \tag{3.4.41}$$

Now using using our approxillator scheme, relate:

$$\beta_1(\mu) = \frac{gV}{8\pi^2}(2m)\mu^4 \tag{3.4.42}$$

$$\beta_1''(\mu) = \frac{d^2\beta_1}{d\mu^2} = \frac{gV}{8\pi^2}12\mu^2 \tag{3.4.43}$$

$$U \approx \frac{gV}{8\pi^2}\left[\mu^4 + 2\pi^2 k^2 T^2 \mu^2\right] \tag{3.4.44}$$

Now use 4.2.39 to expand μ as a power series in T and ignore $O(T^3)$ and higher terms. Now the expression becomes:

$$U = \frac{gV}{8\pi^2}\left[[\mu(0)]^4 + \frac{2\pi^2 k^2 T^2}{3}[\mu(0)]^2\right] = \frac{gV}{8\pi^2}E_f^4\left[1 + \frac{2\pi^2 k^2 T^2}{3E_f^2}\right] = U_0\left[1 + \frac{2\pi^2 k^2 T^2}{3E_f^2}\right] \tag{3.4.45}$$

The preceding factor is exactly equal to the energy computed at T=0 To compute the entropy, we first calculate the specific heat at constant volume:

$$C_V = \left(\frac{\partial U}{\partial T}\right)_{\bar{N},V} = \frac{gV\mu(0)^3}{6\pi^2}\frac{\pi^2 k^2 T}{3\mu}$$

$$C_V = \bar{N}\pi^2 k\frac{T}{T_f} \tag{3.4.46}$$

The specific heat in the UR region is double than that of the NR region. Now the entropy can be calculated easily. Note that T_f is a constant at a process where Q=$C_V dT$ as both $\bar{N}$ *and* V are conserved during the process. Hence

$$S = \int_0^T \frac{C_V}{T}dT \tag{3.4.47}$$

$$S = \bar{N}\pi^2 k\frac{T}{T_f} \tag{3.4.48}$$

The GCE potential function is given by:

$$\Omega = \int_0^\infty dE\ \beta_2(E)\ f'(E) \tag{3.4.49}$$

Now:

$$-\Omega \approx \beta_2(\mu) + \frac{\pi^2 k^2 T^2}{6}\beta_2''(\mu) \tag{3.4.50}$$

Now using using our approxillator scheme, relate:

$$\beta_2(\mu) = \frac{gV}{24\pi^2}\mu^4 \tag{3.4.51}$$

$$\beta_2''(\mu) = \frac{d^2\beta_2}{d\mu^2} = \frac{gV}{24\pi^2}12\mu^2 \tag{3.4.52}$$

$$-\Omega \approx \frac{gV}{24\pi^2}\left[\mu^4 + 2\pi^2k^2T^2\mu^2\right] \tag{3.4.53}$$

Now use 4.2.39 to expand μ as a power series in T and ignore $O(T^3)$ and higher terms. Now the expression becomes:

$$-\Omega = \frac{gV}{24\pi^2}\left[[\mu(0)]^4 + \frac{2}{3}\pi^2k^2T^2[\mu(0)]^2\right] \tag{3.4.54}$$

This can be re-arranged to get:

$$-\Omega = P_0\left[1 + \frac{2}{3}\frac{\pi^2k^2T^2}{E_f^2}\right] \tag{3.4.55}$$

$$P_0 = \frac{1}{3}\frac{gV}{8\pi^2}E_f^4 \tag{3.4.56}$$

Note that P_0 is the same pressure as exerted in the UR case at T=0. Now the pressure is given by:

$$P = P_0\left[1 + \frac{2}{3}\frac{\pi^2k^2T^2}{E_f^2}\right] \tag{3.4.57}$$

3.4.4 Analysis Of The Results Obtained

The NR and UR analysis covers the extreme ends of the relation of energy with mass and momentum. If we closely look at our equations (this is much more apparent in the UR results), we find that upto the lowest vanishing order of the power series expansion in temperature all computed thermodynamic quantities have the following relation for relative error in both the extremes:

$$\frac{\Delta Q}{Q_0} = \alpha \left(\frac{T}{T_f}\right)^2 \tag{3.4.58}$$

Here $\alpha \in [1, 10]$ and hence is an O(1) constant and Q is some thermodynamic quantity. This formula should work well even in the general relativistic region as in physics the values of any thermodynamic function smoothly varies as we go from NR to UR region wherein this formula is valid. The important thing to notice is that the growth is quadratic.

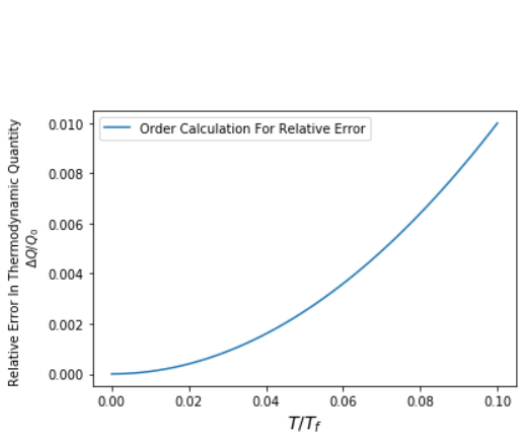

(a) Quadratic Variation In Relative Error

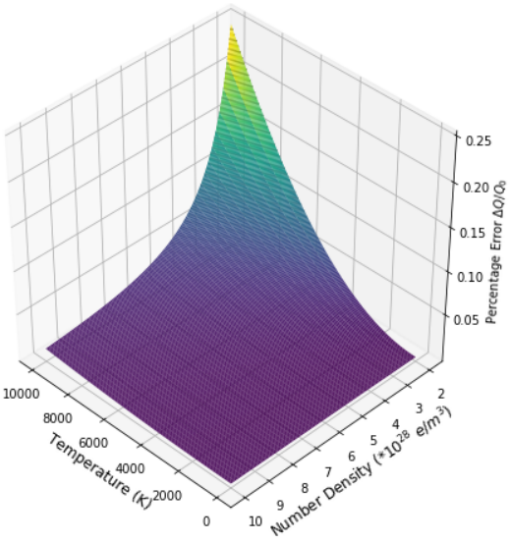

(b) Plot For Electrons In Metals

Figure 11: Temperature Range In Which Our Scheme Works

Graph 11(a) suggests that if 1% is an acceptable error then we stretch our approxillator scheme to roughly $t/t_f \to .1$. To put into perspective what this actually means, we have plotted 11(b). This plot is for electrons in metals. The fermi temperature is connected with the number density which is why we have set it as a parameter. Typical densities of electrons in metals vary from 2-10 * $10^{28}/m^3$ which correspond to a fermi temperature of 1-10 *10^5 K. As we can see that percentage error is 0.25% even at 2000^0K for the metal with lower electron density. This is well beyond the room temperature. Of course this assumes that the metal retains its form at the temperature else there will be serious density fluctuations. Although, it might not look like that but we have developed a good scheme to approximate the basic thermodynamic functions.

Chapter 3: Statistical Mechanics Of Ideal Bose Gas

4 Solving The Ideal Bose Gas

Unfortunately, this section will be quite similar to my previous one. The major difference would be that I would be trying to solve the system of bosons. I will try to compute the pressure, chemical potential and other thermodynamic properties of a system of N (macroscopically large number) particles confines in a box (cube) of volume V at a certain temperature T with **periodic boundary conditions**. I will mainly be using the Canonical or the Grand Canonical Ensemble to solve the problem. The system is composed of bosons and hence will be following a Bose distribution and the aim of this exercise is to solve the free boson gas for various cases and interpret the results.
This section is mainly divided into two parts: one to solve the highly relativistic limit (massless limit) in terms of known massless bosons. I have used photons in a black body and phonons in solids to show the massless limit behaviour of the ideal bose gas. The second part solves heavy bosons in the classical/non-relativistic limit. I have not solved the general relativistic version as it is a repetition of the classical limit with a more complex formula for the energy-momentum relation and is computationally tedious.

4.1 Quantum Particle In A Box

The solution for particle in a cubical box with length parameter L given by:

$$\Psi(x,y,z,t) = \mathcal{N} e^{xk_x + yk_y + zk_z - \omega t} \tag{4.1.1}$$

Here, $\mathcal{N}$ is the normalization constant. The periodic boundary conditions reads:

$$\Psi(x,y,z,t) = \Psi(x+L,y,z,t) = \Psi(x,y+L,z,t) = \Psi(x,y,z+L,t) \tag{4.1.2}$$

This leads to the following solution:

$$k_i = \frac{2\pi}{L} n_i \quad where\ i \in \{x,y,z\}\ and\ n_i \in \mathbb{Z} \tag{4.1.3}$$

Here all values of n_i lead to new solution.This happens because the repeated boundary conditions allow the presence of waves moving in both forward and backward directions with respect to an axis which is in contrast with the strict box boundary conditions where only the standing waves survived. In shorthand, the above equation is written in vector form as:

$$\vec{k} = \frac{2\pi}{L}\vec{n} \tag{4.1.4}$$

Here $\vec{k} - k_x\hat{i} + k_y\hat{j} + k_z\hat{k}$ and $\vec{n} - n_x\hat{i} + n_y\hat{j} + n_z\hat{k}$. Equation 3.1.4 suggests that in the k-space each allowed state has a volume of $\frac{(2\pi)^3}{V}$ with V being the volume of the cubical box. In contrast with the strict boundary conditions, each allowed state has twice the volume. The states are both orthonormal and complete which is given as:

$$\int d^3\vec{r}\ \psi^*_{n_x n_y n_z}(\vec{r})\ \psi_{m_x m_y m_z}(\vec{r}) = \delta_{n_x m_x}\delta_{n_y m_y}\delta_{n_z m_z} \tag{4.1.5}$$

$$\sum_{n_x n_y n_z} \psi^*_{n_x n_y n_z}(\vec{r})\ \psi_{n_x n_y n_z}(\vec{p}) = \delta^3(\vec{r} - \vec{p}) \tag{4.1.6}$$

Here δ^3 is the dirac-delta function in three dimensions and $\delta_{n_x m_x}$ represents the Kronecker delta function.

4.2 Basic Tools Required To Solve The Problem

4.2.1 Concept Of Density Of States

The concept remains the same as in the previous draft, however a will be showing a second method to compute density of states which is often more useful. To jog up the memory, here are the relevant definitions. Before defining the concept of density of states, let us first define the following quantity:

$$N(E) = \sum_{n_x n_y n_z} \Theta(E - E_{n_x n_y n_z})$$

Here, Θ denotes the step function. This function N(E) calculates the number of available states with energy $\leq$ E. Define density of states as $\rho(E)$ which denotes the instantaneous number of states available at energy E:

$$\rho(E) = \frac{dN}{dE} = \sum_{n_x n_y n_z} \delta(E - E_{n_x n_y n_z}) \tag{4.2.1}$$

The derivative of step function is the dirac-delta function. Now, let us begin to compute this important parameter for our periodic boundary conditions. The total number of available states (N) in the k space within appropriate boundaries are:

$$N = \sum_{\vec{k}} \tag{4.2.2}$$

Now using 3.1.4, if $V \to \infty$ then essentially we have a continuum of states in the k-space. Hence within a k-space volume of $dk_x dk_y dk_z$ we have:

$$N = \sum_{\vec{k}} \to \frac{V}{(2\pi)^3} \int dk_x dk_y dk_z$$

Now we just have to integrate over the volume contained within the appropriate boundary. Switching over to polar coordinates (boundary is generally spherical due to symmetry of the problem and solution) we have:

$$N = \frac{4\pi V}{(2\pi)^3} \int k^2 dk \ = \int \left[\frac{V}{(2\pi)^3} 4\pi k^2 \frac{dk}{dE} \right] dE$$

Compare this to the well-known formula:

$$N = \int \left[\frac{dN}{dE} \right] dE$$

And voila we get the formula for density of states as:

$$\frac{dN}{dE} = \frac{V}{(2\pi)^3} 4\pi k^2 \frac{dk}{dE} \tag{4.2.3}$$

Of course, the relation between k and E will depend on the nature of the problem (eg:Non-Relativistic, Ultra-Relativistic etc) and hence would finally affect the expression for the density of states. The only assumption made during this process is that $E = E(|\vec{k}|)$=E(k). This is quite a reasonable assumption since we will be working with systems which are isotropic in space (the system has no preferred sense of direction).

4.2.2 Attacking The Problem Via Grand Canonical Ensemble (GCE)

In this section, we will be deriving the Bose distribution which is simply the average occupation number of a particular quantum state for free bosons energy spectrum. All the other formulae will follow the fermion case with fermi distribution being replaced by bose distribution (See my May draft for more details). In the non-interacting case each individual quantum state can be labeled by $(\vec{k}, s)$ denoting quantum numbers for momentum and spin respectively. Each micro-state can be described as a collection of all occupation numbers $\{n_{\vec{k},s} = 0, 1, 2...\} \equiv \{n_{\vec{k},s}\}$ A system with N particles with occupation number $n_{\vec{k},s}$ for quantum level $(\vec{k}, s)$ can be completely described as:

$$N_{\{\vec{k},s\}} = \sum_{\vec{k},s} n_{\vec{k},s}$$

$$E_{\{\vec{k},s\}} = \sum_{\vec{k},s} n_{\vec{k},s}\ \epsilon_{\vec{k},s}$$

Using the above decomposition the partition function in the GCE for bosons can be derived using the following generating function:

$$\mathcal{Z} = \prod_{\vec{k},s} \left(\sum_{n_{\vec{k},s}=0}^{\infty} e^{n_{\vec{k},s} \frac{\mu - \epsilon_{\vec{k},s}}{kT}} \right) \tag{4.2.4}$$

Since bosons can have any occupation number in each state, Thus, the sum goes to infinity. 3.2.4 can be reduced to:

$$\mathcal{Z} = \prod_{\vec{k},s} \left(\frac{1}{1 - e^{-\beta(\epsilon_{\vec{k},s} - \mu)}} \right) \tag{4.2.5}$$

$$log(\mathcal{Z}) = -\sum_{\vec{k},s}\ log(1 - e^{-\beta(\epsilon_{\vec{k},s} - \mu)}) \tag{4.2.6}$$

Here $\beta = 1/(kT)$. Formula 3.2.5 is conditioned upon the fact:

$$\epsilon_{\vec{k},s} - \mu \geq 0 \quad \forall\ \vec{k} \Longrightarrow \mu \leq 0 \quad (\because \epsilon_{gs} = 0) \tag{4.2.7}$$

The ensemble average occupation number for a state labeled by $(\vec{p}, s')$ is:

$$\langle \vec{p}, s' \rangle = \frac{1}{\mathcal{Z}} \sum_{N=0}^{\infty} \sum_{\{\vec{k},s\}}^{\sum_{\{\vec{k},s\}} n_{\vec{k},s} = N} n_{\vec{p},s'} e^{\sum_{\vec{k},s} -\beta(\epsilon_{\vec{k},s} - \mu)}$$

$$= -\frac{1}{\beta} \frac{\partial}{\partial \epsilon_{\vec{p},s'}} log(\mathcal{Z})$$

Now, all that is left is to substitute to get the famous bose distribution:

$$\langle \vec{k}, s \rangle = \frac{1}{e^{\beta(\epsilon_{\vec{k},s} - \mu)} - 1} \tag{4.2.8}$$

4.3 Photons

Problem Setup - Consider EM radiation enclosed within a cavity of volume V and an equilibrium temperature T. The cavity is assumed to be sufficiently large so that the equilibrium thermodynamic properties are independent of the nature of the nature of the wall and other boundary conditions. Of as explained earlier, we always presume repeated boundary conditions.
The quantum theory of radiation says that a photon corresponding to a plane-wave of electromagnetic radiation with electric field vector **E(r,t)**

$$\mathbf{E}(\mathbf{r},t) = \epsilon e^{i(\mathbf{k}\cdot\mathbf{r}-\omega t)} \tag{4.3.1}$$

has a frequency ω with the following properties:

$$Energy = \hbar\omega \tag{4.3.2}$$

$$Momentum = \hbar\mathbf{k}, \quad |\mathbf{k}| = \frac{\omega}{c} \tag{4.3.3}$$

$$Polarization\ vector = \epsilon, \quad |\epsilon| = 1, \quad \mathbf{k}\cdot\epsilon = 0 \tag{4.3.4}$$

Here c is the speed of light. The polarization vector (ϵ) has only two degrees of freedom due to the Maxwell equation for divergence of electric field. This is reflected in the fact that photon must always move with a constant speed of 'c'. The energy for a state of EM field having $n_{\mathbf{k},\epsilon}$ photons of momentum vector $\mathbf{k}$ and polarization vector ϵ is:

$$\begin{aligned} E\left\{n_{\mathbf{k},\epsilon}\right\} &= \sum_{\mathbf{k},\epsilon} \hbar\omega n_{\mathbf{k},\epsilon} \\ \omega &= c|\mathbf{k}| \\ n_{\mathbf{k},\epsilon} &= 0, 1, 2, \ldots \end{aligned} \tag{4.3.5}$$

Since atoms at the boundary can emit/absorb photons freely, the total number of photons is not a conserved quantity. Hence the number of photons is indefinite which is equivalent to the statement that chemical potential μ=0 for photons. Hence the partition function of the CE and the GCE will be the same. The CE partition function is given as:

$$Q = \sum_{\{n_{\mathbf{k},\epsilon}\}} e^{-\beta E\{n_{\mathbf{k},\epsilon}\}} \tag{4.3.6}$$

This can be solved as:

$$Q = \sum_{\left\{n_{\mathbf{k},\epsilon}\right\}} \exp\left(-\beta \sum_{\mathbf{k},\epsilon} \hbar\omega n_{\mathbf{k},\epsilon}\right) = \prod_{\mathbf{k},\epsilon} \sum_{n=0}^{\infty} e^{-\beta\hbar\omega n} = \prod_{\mathbf{k},\epsilon} \frac{1}{1-e^{-\beta\hbar\omega}} \tag{4.3.7}$$

$$\log Q = -\sum_{\mathbf{k},\epsilon} \log\left(1-e^{-\beta\hbar\omega}\right) = -2\sum_{\mathbf{k}} \log\left(1-e^{-\beta\hbar\omega}\right) \tag{4.3.8}$$

Here the factor of 2 comes from summing up the ϵ variable (each polarization provided 2 degrees of freedom). The average occupation number for photons of momentum $\mathbf{k}$, independent of polarization is:

$$\langle n_{\mathbf{k}} \rangle = -\frac{1}{\beta} \frac{\partial}{\partial(\hbar\omega)} \log Q = \frac{2}{e^{\beta\hbar\omega} - 1} \tag{4.3.9}$$

After 4.3.8, the job of calculating thermodynamic parameters becomes mechanical. The internal energy is given by:

$$U = -\frac{\partial}{\partial\beta} \log Q = \sum_{\mathbf{k}} \hbar\omega \langle n_{\mathbf{k}} \rangle \tag{4.3.10}$$

The pressure can be calculated by using the formula:

$$P = \frac{1}{\beta} \frac{\partial}{\partial V} \log Q(V, \beta)$$

The formula of log Q as given by 4.3.8 is not in the correct form to take the partial derivative with respect to V. Hence, we must first change it into appropriate form. This can be done using 4.3.5 and 4.3.4 to arrive at:

$$\log Q = -2 \sum_{\mathbf{n}} \log \left(1 - e^{-\beta\hbar c 2\pi |\mathbf{n}| V^{-1/3}} \right)$$

Now, the pressure of the system can be computed and it comes out to be:

$$P = \frac{1}{3V} \sum_{\mathbf{k}} \hbar\omega_{\mathbf{k}} \langle n_{\mathbf{k}} \rangle \tag{4.3.11}$$

Combining 4.3.11 and 4.3.10, we get the equation of state:

$$PV = \frac{1}{3} U \tag{4.3.12}$$

Now this is an excellent opportunity to derive the Stephan-Boltzmann law and the Wien's displacement Law for black bodies. To arrive to these classical laws we must first take the $V \to \infty$ limit to change the sum into the integrals. Using:

$$As\ V \to \infty \quad \sum_{\mathbf{k}} \to \int_0^\infty \frac{V}{(2\pi)^3} 4\pi k^2 dk$$

and equations 4.3.5, 4.3.8 and 4.3.9, we now arrive at the integral version of U:

$$U = \frac{2V}{(2\pi)^3} \int_0^\infty dk 4\pi k^2 \frac{\hbar c k}{e^{\beta\hbar c k} - 1} = \frac{V\hbar}{\pi^2 c^3} \int_0^\infty d\omega \frac{\omega^3}{e^{\beta\hbar\omega} - 1} \tag{4.3.13}$$

Using 4.3.13, define the internal energy per unit volume:

$$\frac{U}{V} = \int_0^\infty d\omega\ u(\omega, T) \tag{4.3.14}$$

$$u(\omega, T) = \frac{\hbar}{\pi^2 c^3} \frac{\omega^3}{e^{\beta\hbar\omega} - 1} \tag{4.3.15}$$

The above equations can be solved (see Appendix A1 for explicit solution) to give the internal energy per unit volume and specific heat per unit volume:

$$\frac{U}{V} = \frac{\pi^2}{15}\frac{(kT)^4}{(\hbar c)^3} \tag{4.3.16}$$

$$c_V = \frac{4\pi^2 k^4 T^3}{15(\hbar c)^3} \tag{4.3.17}$$

Equation 4.3.15 might trouble you as the specific heat per unit volume blows up at temperature goes to infinity. This is however not a problem as in addition to indefinite number of photons we have also allowed for all possible photon modes (frequencies). As $T \to \infty$, the average occupation number in each mode becomes finite and in some sense the ensemble average for number of photons blows up to infinity. Looking at 4.3.15 and carefully understanding the description of the problem solved, one can loosely argue the number of available modes to photon at any temperature T is O(T^3).
Now assume that the black body is allowed to interact with the surroundings through an exit window. The intensity of the radiation in form of photons with frequency ω is:

$$I(\omega, T) = c\int u(\omega, T)\cos\theta\frac{d\Omega}{4\pi} = \frac{cu(\omega, T)}{4\pi}\int_0^{2\pi}\int_{\pi/2}^{0}[-cos(\theta)]\ d(-cos(\theta))\ d\phi = \frac{c}{4}u(\omega, T) \tag{4.3.18}$$

The intensity of radiation radiated by a black body at temperature T can be found using:

$$I(T) = \int_0^\infty d\omega\ I(\omega, T) = \sigma T^4$$
$$\sigma = \frac{\pi^2 k^4}{60\hbar^3 c^3} \tag{4.3.19}$$

Equation 4.3.19 (See Appendix A1 for solution) gives the famous Stephan-Boltzmann Law. The peak of the I(ω,T) at a certain temperature T can be found by setting the partial derivative with $\omega \to 0$. Using: 4.3.18 and 4.3.15 we have:

$$\frac{\partial I(\omega, T)}{\partial\omega} = \frac{\hbar}{4\pi^2 c^2}\frac{1}{(e^{\beta\hbar\omega})^2}\omega^2\left[e^{\beta\hbar\omega}(\beta\hbar\omega - 3) + 3\right] \tag{4.3.20}$$

$$\frac{\partial I(\omega, T)}{\partial\omega} = 0 \implies e^{\beta\hbar\omega}(\beta\hbar\omega - 3) + 3 = 0 \tag{4.3.21}$$

Equation 4.3.21 can be solved (See Appendix A2 for solution) to give

$$\beta\hbar\omega = 2.82144 = Constant \tag{4.3.22}$$

The above equation can be written in terms of wavelength of radiation λ and temperature T as:

$$\lambda T = C' = \frac{h}{2.82144 * k_B} = Constant \tag{4.3.23}$$

$$\lambda \propto \frac{1}{T} \tag{4.3.24}$$

Equation 4.3.24 gives the famous Wien's displacement law. It says that the peak intensity of radiation by a black body changes as its temperature changes and the wavelengths corresponding to those peaks is inversely proportional to the temperature. The graph in Figure 12 shows this explicitly:

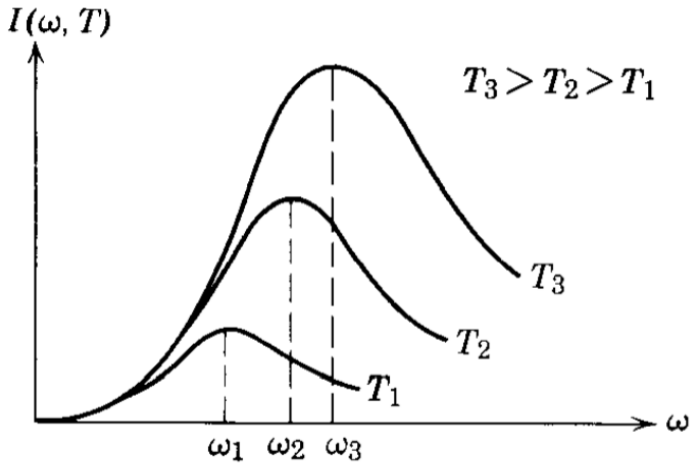

Figure 12: (1)The area under the curve $\propto T^4$ by Stephan-Boltzmann Law and (2)The peak shifts towards higher frequency or lower wavelength with increasing temperature by Wien's Displacement Law[5]

4.4 Phonons In Solids

Problem Setup: For low-lying excitations in the solids (no anharmonic terms in the hamiltonian), the Hamiltonian can be expresses as a sum of simple harmonic oscillators with frequency ω where each frequency corresponds to a normal mode of lattice oscillation. Assuming, the number of atoms to be N in the lattice; the maximum number of available modes is 3N.
In quantum theory every single of these normal modes give rise to a quanta called phonon. At low temperatures, the quantum state of the lattice can expressed by enumerating all the phonons present in the lattice. A small change of perspective and the statement becomes that at low temperatures a solid can be thought of as a gas of non-interacting phonons. A phonon with a characteristic frequency ω has the following properties:

$$Energy = \hbar\omega \tag{4.4.1}$$

$$Momentum = \hbar\mathbf{k}, \quad |\mathbf{k}| = \frac{\omega}{c} \tag{4.4.2}$$

Here c is the speed of the sound wave propagating in solid and not the speed of light. Although phonons are massless, they are not bounded to move with a particular velocity, c. This is further reflected in the polarization vector which has 3 degrees of freedom for phonons (unlike photon which had only 2) Thus, possessing both transverse and longitudinal modes of oscillation. To make the problem easier, we assume an isotropic medium which means that the speed 'c' of sound wave is independent of the polarization vector. A single phonon of frequency ω corresponds to pressure wave, generally called a sound wave of the form:

$$\mathbf{P}(\mathbf{r}, \mathbf{t}) = \epsilon e^{i(\mathbf{k}\cdot\mathbf{r} - \omega t)} \tag{4.4.3}$$

Here ϵ is the polarization vector. Since any allowed mode may occupy number of quanta, the Bose statistics is followed by the bosons. Further the atoms of the lattice can freely absorb or emit phonons. Hence we don't have any conservation of number of phonons equivalently, the chemical potential is 0 ($\mu = 0$). However, the maximum number of allowed modes in 3N with N being the number of atoms in the lattice.

Now, we cam begin to work on our problem. Before starting it, let us first find the transformation for going from discrete sums to continuous integrals for phonons. To develop this scheme we will be using the Debye model where one considers the solid to be an elastic continuum of volume V. The frequencies are then taken to be the lowest 3N normal frequencies of the system. The boundary conditions here are again the periodic boundary conditions.

$$\sum_{\mathbf{k},\epsilon} = 3\sum_{\mathbf{k}} \rightarrow \frac{3V}{(2\pi)^3}\int 4\pi k^2 \; dk$$

$$\implies \int \left[\frac{3V}{(2\pi)^3} 4\pi k^2 \; \frac{dk}{d\omega}\right] \; d\omega = \int f(\omega) \; d\omega$$

Now, we can define the density of modes using 4.4.2 as:

$$f(\omega)d\omega = V\frac{3\omega^2}{2\pi^2 c^3}d\omega \tag{4.4.4}$$

The cut-off frequency can be computed using the fact that only the lowest 3N modes are available:

$$\int_0^{\omega_m} f(\omega) \; d\omega = 3N = \sum_{w_i=1}^{3N} \tag{4.4.5}$$

Equation 4.4.5 gives the formulation for conversion from the discrete to the continuous limit. This solves to give the cut-off frequency ω_m and the wavelength corresponding to it as:

$$\omega_m = c\left(\frac{6\pi^2 N}{V}\right)^{1/3} \tag{4.4.6}$$

$$\lambda_{\cdot} = \frac{2\pi c}{\omega_m} = \left(\frac{4\pi V}{3N}\right)^{1/3} \approx inter - particle \; distance \tag{4.4.7}$$

Equation 4.4.6 makes a lot of sense as it suggests the displacements of the order of inter-particle distance produces sound waves in the lattice. Finally, we can really begin to solve. Consider the energy of a lattice state consisting of n_i phonons of the i^{th} type.

$$E\left\{n_i\right\} = \sum_{i=1}^{3N} n_i \hbar\omega_i \tag{4.4.8}$$

The CE partition function is:

$$Q = \sum_{\{n_i\}} e^{-\beta E\{n_t\}} = \prod_{i=1}^{3N} \frac{1}{1 - e^{-\beta\hbar\omega_t}} \tag{4.4.9}$$

$$\log Q = -\sum_{i=1}^{3N} \log\left(1 - e^{-\beta\hbar\omega_t}\right) \tag{4.4.10}$$

The average occupation number for each state is (same logic as for photons):

$$\langle n_i \rangle = -\frac{1}{\beta}\frac{\partial}{\partial(\hbar\omega_i)}\log Q = \frac{1}{e^{\beta\hbar\omega_i}-1} \tag{4.4.11}$$

As expected, this is the Bose statistics. The internal energy can be computed as:

$$U = -\frac{\partial}{\partial\beta}\log Q = \sum_{i=1}^{3N}\hbar\omega_i\langle n_i\rangle = \sum_{i=1}^{3N}\frac{\hbar\omega_i}{e^{\beta\hbar\omega_i}-1} \tag{4.4.12}$$

Going to the continuous limit and solving the continuous version of 4.4.12 (See Appendix B1 for solution), to get:

$$\frac{U}{N} = 3kTD(T_D/T) = \begin{cases} 3kT\left(1-\frac{3}{8}\frac{T_D}{T}+\cdots\right) & (T \gg T_D) \\ 3kT\left[\frac{\pi^4}{5}\left(\frac{T}{T_D}\right)^3 + O\left(e^{-T_D/T}\right)\right] & (T \ll T_D) \end{cases} \tag{4.4.13}$$

Here D(x) is the Debye function and T_D is the Debye Temperature defined as:

$$D(x) \equiv \frac{3}{x^3}\int_0^x dt\frac{t^3}{e^t-1} \tag{4.4.14}$$

$$T_D = \frac{\hbar\omega_m}{k} \tag{4.4.15}$$

Equation 4.4.13 can be used to compute the specific heat for the solid (See Appendix B2 for calculation). The high and low temperature limits wrt Debye temperature come out to be:

$$C_V = \begin{cases} 3Nk\left[1-\frac{1}{20}\left(\frac{T_D}{T}\right)^2+\cdots\right] & (T \gg T_D) \\ \frac{12Nk\pi^4}{5}\left(\frac{T}{T_D}\right)^3 + O\left(e^{-T_D/T}\right) & (T \ll T_D) \end{cases} \tag{4.4.16}$$

Equation 4.4.16 is one of the greatest achievements of quantum mechanics for condensed matter physics. The equation predicts that the specific heat goes to 0 as $\sim T^3$ thus, verifying the third law of thermodynamics. Further the high temperature limit gives the famous Dulon-Petit Law, $C_V = 3Nk$. Note that our model is only valid until anharmonic terms can be ignored from the Hamiltonian. Once they can no longer no ignored, from a quantum point of view the phonons become interacting and our analysis breaks down.
Still 4.4.16 is a beautiful equation which can be much more appreciated from the following graph:
The pressure calculation is exactly same to that of the photon case and will not be repeated here. The equation of state is again $PV = U/3$ which can be used to compute the pressure of the system.

4.5 Study Of Non-Relativistic Massive Bosons

The Model - Consider a gas of N non-interacting, non-relativistic massive bosons of mass m within a cubical box of volume V=L^3. The Hamiltonian and the energy spectrum is is:

$$\hat{H} = \frac{\hat{\mathbf{p}}^2}{2m} = -\frac{\hbar^2}{2m}\left[\frac{\partial^2}{\partial x^2}+\frac{\partial^2}{\partial y^2}+\frac{\partial^2}{\partial z^2}\right] \tag{4.5.1}$$

$$\epsilon_{k,s} = \epsilon_k = \frac{\hbar^2k^2}{2m} \tag{4.5.2}$$

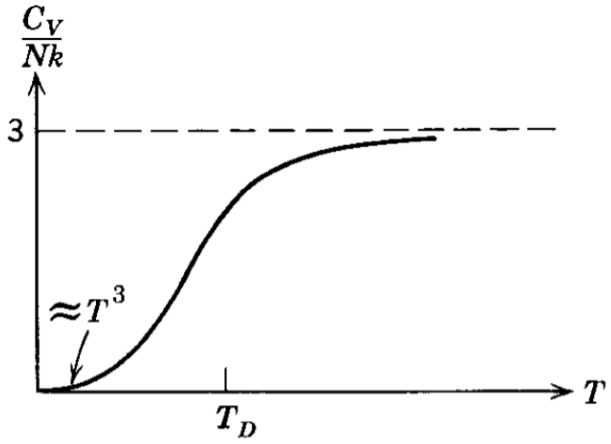

Figure 13: The Graph For Specific Heat Of Solids Via Debye Scheme[5]

The states are indexed by the quantum numbers for the momentum ($p = \hbar k$) and spin. Since there is no magnetic field, the energy states are spin degenerate. Before starting the problem, lets find the formula for transformation between the discrete and continuous limits as $V \to \infty$.

$$\sum_{\vec{k},s} \to g \sum_{\vec{k}} \to \frac{gV}{(2\pi)^3} \int 4\pi k^2 \, dk \to \int \left[\frac{gV}{(2\pi)^3} 4\pi k^2 \, \frac{dk}{d\epsilon} \right] d\epsilon$$

Using 4.5.2, we finally have:

$$\sum_{\vec{k},s} \to \int \left[\frac{gV}{4\pi^2} \left(\frac{2m}{\hbar^2} \right)^{3/2} \sqrt{\epsilon} \right] d\epsilon \tag{4.5.3}$$

Using the formulae derived in section 3.2.3 and equation 4.3.3 we have the following formulae in the continuous limit:

$$\log \mathcal{Z} = -V \frac{g}{4\pi^2} \left(\frac{2m}{\hbar^2} \right)^{\frac{3}{2}} \int_0^\infty d\epsilon \sqrt{\epsilon} \log \left(1 - e^{-\beta(\epsilon - \mu)} \right) \tag{4.5.4}$$

The ensemble average for number of particles and internal energy is:

$$\langle N \rangle = V \frac{g}{4\pi^2} \left(\frac{2m}{\hbar^2} \right)^{\frac{3}{2}} \int_0^\infty d\epsilon \sqrt{\epsilon} \frac{1}{e^{\beta(\epsilon_{\vec{k}} - \mu)} - 1} \tag{4.5.5}$$

$$U = V \frac{g}{4\pi^2} \left(\frac{2m}{\hbar^2} \right)^{\frac{3}{2}} \int_0^\infty d\epsilon \; \epsilon^{\frac{3}{2}} \frac{1}{e^{\beta(\epsilon_{\vec{k}} - \mu)} - 1} \tag{4.5.6}$$

The pressure can be computed using $P = \frac{1}{\beta} \frac{\partial \log \mathcal{Z}}{\partial V}$ to get:

$$P = -kT \frac{g}{4\pi^2} \left(\frac{2m}{\hbar^2} \right)^{\frac{3}{2}} \int_0^\infty d\epsilon \sqrt{\epsilon} \log \left(1 - e^{-\beta(\epsilon - \mu)} \right) \tag{4.5.7}$$

Using integration by parts, we have:

$$P = \frac{2}{3}\frac{g}{4\pi^2}\left(\frac{2m}{\hbar^2}\right)^{\frac{3}{2}}\int_0^\infty d\epsilon\ \epsilon^{\frac{3}{2}}\frac{1}{e^{\beta(\epsilon_{\vec{k}}-\mu)}-1} = \frac{2}{3}\frac{U}{V} \tag{4.5.8}$$

This also gives the equation of state $PV = \frac{2}{3}U$.All the above integrals depend on the general integral of the type:

$$I_\nu(\beta,\beta\mu) = \int_0^\infty d\epsilon\frac{\epsilon^\nu}{e^{\beta(\epsilon-\mu)}-1} = \frac{\Gamma(\nu+1)}{\beta^{\nu+1}}g_{\nu+1}(z) \tag{4.5.9}$$

$$g_\nu(x) = \sum_{k=1}^{\infty}\frac{x^k}{k^\nu} \tag{4.5.10}$$

$$z = e^{\beta\mu} \tag{4.5.11}$$

To see, how the integral was solved See Appendix C1. In the newer notation, the formulae looks cleaner:

$$n = \frac{\langle N\rangle}{V} = \frac{g}{4\pi^2}\left(\frac{2m}{\hbar^2}\right)^{\frac{3}{2}}\frac{\Gamma\left(\frac{3}{2}\right)}{\beta^{\frac{3}{2}}}g_{\frac{3}{2}}(z) \tag{4.5.12}$$

$$u = \frac{U}{V} = \frac{g}{4\pi^2}\left(\frac{2m}{\hbar^2}\right)^{\frac{3}{2}}\frac{\Gamma\left(\frac{5}{2}\right)}{\beta^{\frac{5}{2}}}g_{\frac{5}{2}}(z) \tag{4.5.13}$$

4.5.1 The High Temperature Limit

Being a physicist has some great perks. We can approximate without any remorse and this is what we will use to solve the high temperature limit and then examine the validity of that limit. The high temperature limit is classical. This is realized in the following way:

$$z = e^{\beta\mu} \ll 1 \qquad as\ T \to \infty$$

This can be used to approximate the Bose integral using the above criterion in the following manner:

$$I_\nu(\beta,\beta\mu) = \int_0^\infty d\epsilon\frac{\epsilon^\nu}{e^{\beta(\epsilon-\mu)}-1} \approx \int_0^\infty d\epsilon\epsilon^\nu e^{-\beta(\epsilon-\mu)} = \frac{\Gamma(\nu+1)}{\beta^{\nu+1}}e^{\beta\mu} \tag{4.5.14}$$

Refer to Appendix C1 for the solution of the integral. Equation 4.5.14 is the approximated version of the Drichlet-Reimann function defined in 4.5.10 where only first terms of the expansion are considered. This actually allows us to solve equations for n and U exactly to give:

$$n = \frac{g}{4\pi^2}\left(\frac{2m}{\hbar^2}\right)^{\frac{3}{2}}\frac{\Gamma\left(\frac{3}{2}\right)}{\beta^{\frac{3}{2}}}e^{\beta\mu} = \frac{g}{\lambda^3}e^{\beta\mu} \tag{4.5.15}$$

$$\frac{1}{\lambda} = \sqrt{\frac{2\pi mkT}{h^2}} \tag{4.5.16}$$

$$U = V\frac{g}{4\pi^2}\left(\frac{2m}{\hbar^2}\right)^{\frac{3}{2}}\frac{\Gamma\left(\frac{5}{2}\right)}{\beta^{\frac{5}{2}}}e^{\beta\mu} = \frac{3}{2\beta}Vn = \frac{3}{2}\langle N\rangle kT \tag{4.5.17}$$

Equation 4.5.16 is also consistent with the law of equi-partition of energy. We had only 3 degrees of freedom in the Hamiltonian which corresponded to 3 translational degree of freedom in space. Equation 4.5.15 can be easily inverted to solve for the chemical potential to get:

$$\mu = -kT \log\left(\frac{gV}{\langle N\rangle}\left(\frac{2\pi mkT}{h^2}\right)^{\frac{3}{2}}\right) \tag{4.5.18}$$

The pressure of the gas can be computed using the equation of state.

$$PV = \frac{2}{3}U = \langle N\rangle kT \tag{4.5.19}$$

All the relations from 4.5.15-4.5.19 are classical relations holding for both the fermi and bose gases. The reason behind this is that the bose distribution and the fermi-distribution match each other in the high temperature limit. This is encoded in the following relation and is the reason why we don't have any sense of bosons and fermions at the classical level.

$$\frac{1}{e^{\beta(\epsilon-\mu)}+1} \approx \frac{1}{e^{\beta(\epsilon-\mu)}-1} \approx e^{-\beta(\epsilon-\mu)} \ll 1 \quad as\ T \to \infty \tag{4.5.20}$$

Now let's check the validity of the approximation made. The approximation fails if:

$$z = \frac{n\lambda^3}{g} \sim 1 \to n = \frac{g}{\lambda^3} = g\left(\frac{2m\pi k_B T_D}{h^2}\right)^{\frac{3}{2}}$$

This leads to:

$$k_B T_D = \frac{h^2}{2m\pi}\left(\frac{n}{g}\right)^{\frac{2}{3}} \tag{4.5.21}$$

Hence our approximation works iff $T>T_D$. Further, equation 4.5.21 is ridiculously close (just off by a constant factor) for the definition of the fermi-temperature for a fermi gas which was arrived using the perturbation theory (Equation 3.4.15). I believe that this is quite a self-consistent achievement.

4.5.2 The Low-Temperature Limit

The low temperature limit for bosons is much more interesting than fermions. As $T \to 0$ the fugacity $z \to 1$ which leads to a unique situation. If you look at the integral versions of the thermodynamic parameter, you quickly realize that the contribution of ground state is being ignored since it is a boundary point for the integral. The unique situation that arises due to $z \to 1$ is that finite fraction of molecules are found in the ground state whose contribution we are ignoring. Hence, to solve the low temperature limit we separate the ground state contribution during the discrete version and then move to the continuous limit. This leads to the following equations:

$$\frac{P}{kT} = -\frac{4g\pi}{h^3}\int_0^\infty dpp^2 \log\left(1 - ze^{-\beta p^2/2m}\right) - \frac{g}{V}\log(1-z) \tag{4.5.22}$$

$$\frac{1}{v} = \frac{\langle N\rangle}{V} = \frac{4g\pi}{h^3}\int_0^\infty dpp^2 \frac{1}{z^{-1}e^{\beta p^2/2m}-1} + \frac{g}{V}\frac{z}{1-z} \tag{4.5.23}$$

Here p is the momentum variable ($\hbar k$). Solving the Bose integrals (using Appendix C1) we have:

$$\frac{P}{kT} = \frac{g}{\lambda^3} g_{5/2}(z) - \frac{1}{V}\log(1-z) \tag{4.5.24}$$

$$\frac{1}{v} = \frac{g}{\lambda^3} g_{3/2}(z) + \frac{g}{V}\frac{z}{1-z} \tag{4.5.25}$$

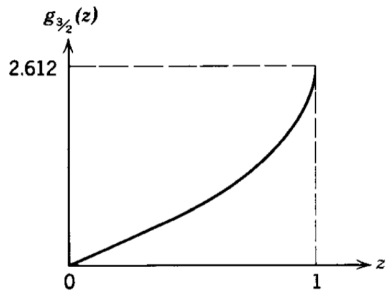

Figure 14: The Graph of $g_{3/2}(z) \in [0,1]$ in the relevant region[5]

Here λ and the function $g_\nu(x)$ is defined by equations 4.5.16 and 4.3.10 respectively. The above analysis suggests that the group state average occupation number is $\langle n_0 \rangle = \frac{gz}{1-z}$. To understand bosons, we must first understand the Drichlet-Reimann function corresponding to equation 4.5.25, $g_{3/2}(z)$. Since for bosons $z \in [0,1]$, we only consider this interval. Luckily for us these functions are studied in mathematics extensively. First, let's look at the graph of $g_{3/2}(z)$. The graph is monotonically increasing in the required regions and converges on both the boundary points.
From 4.5.25 and figure 14. we realize that:

$$\frac{\lambda^3 \langle n_0 \rangle}{gV} = \frac{\lambda^3}{gv} - g_{3/2}(z)$$

Hence $\langle n_0 \rangle$ is finite (due to particle number conservation) when:

$$\frac{\lambda^3}{gv} > g_{3/2}(1) = \zeta(3/2) \tag{4.5.26}$$

The relation 4.5.26 describes a region in the P-V-T space separating the two thermodynamic phases, one with $\vec{p} = 0$ and the other $\vec{p} \neq 0$. The $\vec{p} = 0$ region is called the condensation region separated from the other region by the surface $\frac{\lambda^3}{gv} = g_{3/2}(1)$.
Now let's define some parameters. For a given specific volume, define the specific temperature as:

$$kT_c = \frac{2\pi\hbar^2/m}{\left[v g_{3/2}(1)\right]^{2/3}} \tag{4.5.27}$$

Also for a given isotherm at temperature T, define a critical volume:

$$v_c = \frac{\lambda^3}{g_{3/2}(1)} \tag{4.5.28}$$

Thus, the condensation region lies within $T < T_c$ or $v < v_c$. Hence, in the contnuous limit we have the following solution for fugacity:

$$z = \begin{cases} 1 & \left(\frac{\lambda^3}{gv} \geq g_{3/2}(1)\right) \\ \text{the root of } g_{3/2}(z) = \lambda^3/gv & \left(\frac{\lambda^3}{gv} \leq g_{3/2}(1)\right) \end{cases} \tag{4.5.29}$$

Now let's look at the expression of $\langle n_0 \rangle$ using the equations 4.5.23 and 4.5.27 for $T < T_c$.

$$N = \langle n_0 \rangle + g\left(\frac{2\pi m k_B T}{h^2}\right)^{\frac{3}{2}} \zeta\left(\frac{3}{2}\right)$$

$$N = g\left(\frac{2\pi m k_B T_c}{h^2}\right)^{\frac{3}{2}} \zeta\left(\frac{3}{2}\right)$$

$$\langle n_0 \rangle = N\left[1 - \left(\frac{T}{T_c}\right)^{\frac{3}{2}}\right]$$

The second equation is by definition of the critical temperature. Hence:

$$\frac{\langle n_0 \rangle}{N} = \begin{cases} 0 & \left(\frac{\lambda^3}{gv} \leq g_{3/2}(1)\right) \\ 1 - \left(\frac{T}{T_c}\right)^{3/2} = 1 - \frac{v}{v_c} & \left(\frac{\lambda^3}{gv} \geq g_{3/2}(1)\right) \end{cases} \tag{4.5.30}$$

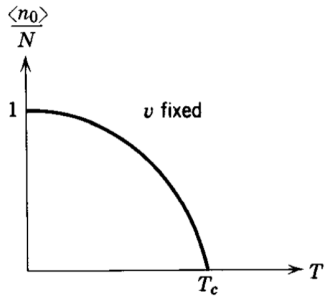

Figure 15: Average Occupation Number of Bosons In Ground State[5]

This phenomenon is called the Bose-Einstein condensation wherein at low temperatures (T< T_c) the bose gas particles are divided into two phases, a finite fraction occupying the ground state and the rest spread thinly over the remaining levels. Now let's look at whats happens to other thermodynamic parameters.
First let's take a looks at energy.

$$E = \sum_{\{\vec{k},s\}} \epsilon_{\vec{k}} n_{\vec{k},s} = \sum_{\{\vec{k}\neq 0,s\}} \epsilon_{\vec{k}} n_{\vec{k},s} \tag{4.5.31}$$

Since, the ground state energy is 0, it does not contribute to the internal energy. Hence the form of internal energy remains the same. Now lets look at what happens to pressure. The ground state term

added to pressure is $\frac{\log(1-\mathcal{Z})}{V}$. From previous analysis we know:

$$\lim_{V\to\infty, z\to 1} \frac{z}{V(z-1)} = finite$$
$$\implies (z-1) \propto \frac{1}{V}$$

$$\implies \lim_{V\to\infty} \frac{\log(1-\ddagger)}{V} \propto \lim_{V\to\infty} \frac{1}{V\log(V)} \to 0 \tag{4.5.32}$$

Hence there is no change in pressure. This is to be expected as ground state particles don't have any momentum and hence cannot collide with the walls of the container to exert pressure. Hence the equation of state remains same $PV = \frac{2}{3}U$ and is valid along everywhere. By the same logic the entropy and specific heat formula is also not affected. Following through the mathematics, we have:

$$\frac{P}{kT} = \begin{cases} \frac{1}{\lambda^3} g_{5/2}(z) & (v > v_c) \\ \frac{1}{\lambda^3} g_{5/2}(1) & (v < v_c) \end{cases} \tag{4.5.33}$$

$$\frac{U}{N} = \frac{3}{2} Pv = \begin{cases} \frac{3}{2}\frac{kTv}{\lambda^3} g_{5/2}(z) & (v > v_c) \\ \frac{3}{2}\frac{kTv}{\lambda^3} g_{5/2}(1) & (v < v_c) \end{cases} \tag{4.5.34}$$

$$\frac{S}{Nk} = \begin{cases} \frac{5}{2}\frac{v}{\lambda^3} g_{5/2}(z) - \log z & (v > v_c) \\ \frac{5}{2}\frac{v}{\lambda^3} g_{5/2}(1) & (v < v_c) \end{cases} \tag{4.5.35}$$

$$\frac{C_V}{Nk} = \begin{cases} \frac{15}{4}\frac{v}{\lambda^3} g_{5/2}(z) - \frac{9}{4}\frac{g_{3/2}(z)}{g_{1/2}(z)} & (v > v_c) \\ \frac{15}{4}\frac{v}{\lambda^3} g_{5/2}(1) & (v < v_c) \end{cases} \tag{4.5.36}$$

The equations 4.5.35 and 4.5.36 show consistency with the third law of thermodynamics. Both the specific heat and entropy goes to 0 as $T \to 0$. Further we observe that as $T \to 0$, $C_v \propto T^{3/2}$ which is in contrast to the massless limit where $C_v \propto T^3$. The reason for this difference is quite simple and comes from the fact that the energy relation in the former was $\epsilon = \frac{p^2}{2m}$ and in the latter was $\epsilon = pc$.

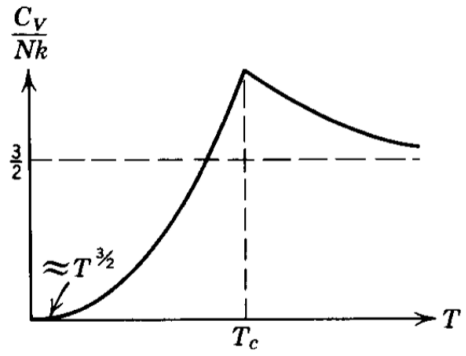

Figure 16: Graph Of Specific Heat For Bosons[5]

Note that this analysis can be easily extended to the general relativistic version. However, one should use the true invariant: |#(Particles)-#(Anti-Particles)| to allow for particle pair production. Other

than this, the formula for conversion from to discrete to the relativistic limit will get changed (basically more complicated) but nonetheless, similar analysis as above can give a good closed form for the various thermodynamic formulae. If we use the highly relativistic version of the formula, we obtain the same form for density of states as obtained for photons and phonons which has solved already.

4.5.3 Bose-Einstein Condensation As Self-Consistent First Order Phase Transition

If we look at the P-v-T diagram for the ideal bose gas, it turns out that the equality in equation 4.3.26 defines a sub-space corresponding to a transition region. On one side of the transition region we have the so called gas-phase ($\langle n_0 \rangle / V \to 0$) and the condensed phase ($\langle n_0 \rangle / V \to 0$). On the transition region, we have a mixture of these two thermodynamic phases. Using equations 4.5.33 and 4.5.27 one can find the critical line for isotherms (P-v diagrams) and P-T diagrams to get:

$$For\ P - v\ diagram : Pv^{5/3} = \frac{2\pi\hbar^2}{m} \frac{g_{5/2}(1)}{\left[g_{3/2}(1)\right]^{5/3}} \tag{4.5.37}$$

$$For\ P - T\ diagram : P = \left(\frac{m}{2\pi\hbar^2}\right)^{3/2} g_{5/2}(1)(kT)^{5/2} \tag{4.5.38}$$

All this information is explicit from the graph for ideal bose gas, Figure 6. Now consider the isotherm for the ideal bose gas with a decreasing v. As soon as the isotherm cuts the critical line, v_c is obtained and both phases can coexist. Going further below gives a straight line acting as the transition region between the two phases for temperature T and critical volume v_c. Consider the transition line at which the following equilibrium process happens:

$$Bosons\ (condensed) \rightleftharpoons Bosons\ (gas)$$

The vapour equilibrium pressure can be computed using the equation of state as:

$$P_0(T) = \frac{kT}{\lambda^3} g_{5/2}(1) \tag{4.5.39}$$

$$\frac{dP_0(T)}{dT} = \frac{5}{2}\frac{k g_{5/2}(1)}{\lambda^3} = \frac{1}{T v_c}\left[\frac{5}{2} kT \frac{g_{5/2}(1)}{g_{3/2}(1)}\right] \tag{4.5.40}$$

Taking this to be the first order phase transition we match equation 4.5.40 with the famous Clayperon equation (see Appendix C2) identify Latent heat of transition per particle (L_p) as:

$$L_p = \frac{5}{2} kT\ \frac{g_{5/2}(1)}{g_{3/2}(1)} \tag{4.5.41}$$

However, the Latent heat per particle can also be computed from the change in specific entropy at the critical line of the P-v diagram. For Bose-Einstein condensation to be a self-consistent first order transition, both methods should give the same result. Let's quickly check that. At any temperature, the total entropy of bose gas is only due to liquid phase and condensed phase has 0 entropy ($S \to 0$

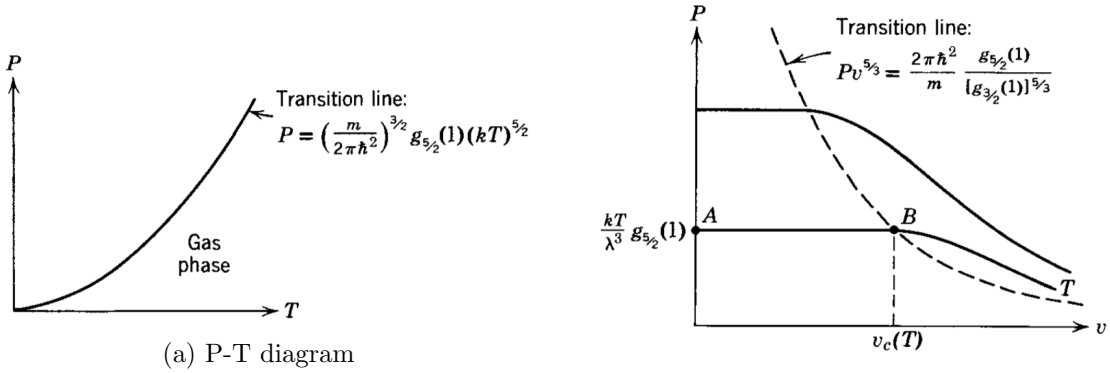

(a) P-T diagram

(b) P-v diagram

Figure 17: Graphs For Ideal Bose Gas[1]

as $T \to 0$). Using 4.5.35 and 4.5.28, the difference in specific entropy of the thermodynamic phases at the critical line is:

$$\Delta s = s_{gp} - s_{cp} = s = \frac{g_{5/2}(1)}{g_{3/2}(1)} \frac{5}{2} k \tag{4.5.42}$$

$$L_p = T\Delta s = \frac{5}{2} kT \, \frac{g_{5/2}(1)}{g_{3/2}(1)} \tag{4.5.43}$$

Equation 4.5.43 and 4.5.41 make the first order phase transition interpretation as a self-consistent one.

Chapter 4: Approximation Schemes To Handle Non-Ideal Gases

5 Development Of Approximation Schemes

In the previous sections, the integration of the spatial coordinates in the phase space was trivial, giving out a factor of the volume of the system. However doing this we made a fatal flaw and assumed that two particles can occupy the same position in space. This was essentially the assumption about the constituent particles of the system being point particles without any sub-structure. This assumption however naive gives some quite powerful results. However now, we wish to introduce the finite size of the particles and see how that changes the equation of state and other parameters of the system. In the following sections, we will build some machinery to deal with central potentials which can be used to incorporate finite size of the particles by taking a hard-sphere potential. The general Hamiltonian we are interested to solve has the form:

$$\mathscr{H} = \sum_{i=1}^{N} \frac{p_i^2}{2m} + \sum_{i<j} V_{ij}^P \tag{5.0.1}$$

$$V_{ij}^P \equiv V^P(|r_i - r_j|) \tag{5.0.2}$$

$$f_{ij} \equiv e^{-\beta V_{ij}^P} - 1 \tag{5.0.3}$$

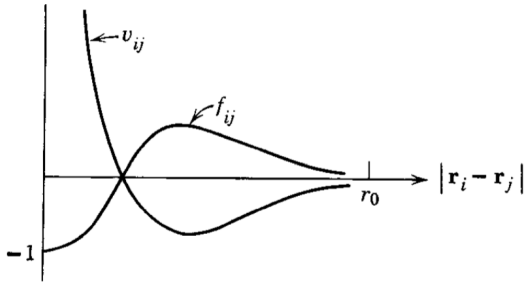

Figure 18: General Forms Of V_{ij}^P and f_{ij} [5]

As we will further see that the integrals obtained in the position portion of the phase space are almost impossible to solve analytically. Hence like a good physicist we do the only thing we can do, we approximate. The general parameter of the perturbation series will be the density of the system ρ and the equation of state obtained will be called the Virial Equation Of State. Our aim will be compute the first non-trivial coefficient of this perturbation series which is the Second-Virial Coefficient (as we shall see later) leading to an effective solution for a dilute gas composed of finite size particles. The Virial equation of state is defined to be :

$$\frac{Pv}{kT} = \sum_{l=1}^{\infty} a_l(T) \left(\frac{\lambda^3}{v}\right)^{l-1} \tag{5.0.4}$$

Here $v = 1/\rho$, a_l is the l^{th} Virial Coefficient, P is pressure, k is Boltzmann constant, T is temperature and λ is the thermal wavelength ($1/\lambda^3$ is solution to the momentum integral of phase space in 3-D). Further $\rho = N/V$ where N is the number of particles and V is the volume occupied by the system. The machinery here will be based upon both classical and quantum considerations. Further I will solve

in the non-relativistic limit because the calculations are actually analytical for most part and doesn't require as much use of numerical integrations for the solving the momentum part of the integral. However the generalization to the relativistic limits is quite trivial and can be easily implemented once we understand the job of each variable in the classical limit.

5.1 Classical Cluster Expansion

The CE partition function is:

$$Q_N(V,T) = \frac{1}{N!h^{3N}} \int d^{3N}p d^{3N}r \exp\left(-\beta \sum_i \frac{p_i^2}{2m} - \beta \sum_{i<j} V_{ij}^P\right)$$
$$= \frac{1}{\lambda^{3N} N!} \int d^{3N}r \exp\left(-\beta \sum_{i<j} V_{ij}^P\right)$$

Here we have integrated out the momentum part of the phase space integral to give the factor of $1/\lambda^3 N$. For our non-relativistic Hamiltonian, $\lambda = \sqrt{\frac{2\pi\hbar^2}{mkT}}$. The left over integral over the spatial coordinates is called the "Configuration Integral" and is denoted by $Z_N(V,T)$. In this notation, we have the CE and GCE partition functions as:

$$Q_N(V,T) = \frac{1}{N!\lambda^{3N}} Z_N(V,T) \tag{5.1.1}$$

$$\mathcal{Q}(z,V,T) = \sum_{N=0}^{\infty} \left(\frac{z}{\lambda^3}\right)^N \frac{Z_N(V,T)}{N!} \tag{5.1.2}$$

My previous two reports focused on how to compute the momentum integral and in this one we will develop methods to compute the configuration integral. Using 5.0.3:

$$Z_N(V,T) = \int d^3r_1 \cdot \cdots \cdot d^3r_N \prod_{i<j} (1 + f_{ij})$$

Expanding the product we have the configuration integral as:

$$Z_N(V,T) = \int d^3r_1 \cdots d^3r_N \left[1 + (f_{12} + f_{13} + \cdots) + (f_{12}f_{13} + f_{12}f_{14} + \cdots) + \cdots \cdots\right] \tag{5.1.3}$$

The expansion in 5.1.3 gives a cluster expansion of the configuration integral. It is because of this and the fact that we are treating the system classically that we call this approximation method the Classical Cluster expansion. This expansion as of now looks quite ridiculous but can be easily converted to an analogous graph theory problem where it is much easier to understand.

5.1.1 Attacking The Problem Using Graph Theory

The idea behind this transformation is to easily manipulate and enumerate each and every term of the expansion in 5.1.3 and hope that some sort of structure comes out from it.[1] The transformation

[1] The substructure here is that only connected graphs matter.

is done in the following manner. Consider, each of the N particles as vertices of an N vertex graph with any number of undirected edges between the vertices. Suppose in a graph G(N,E), distinct pair of vertices are connected by the edges labeled by $\alpha, \beta, \gamma, \cdots, \delta$ then this graph G corresponds to the following term of the configuration integral:

$$\int d^3r_1 \cdots d^3r_N \; f_\alpha \; f_\beta \; f_\gamma \; \cdots \; f_\delta \tag{5.1.4}$$

Some basic properties of these graphs are mentioned in a pictorial fashion in Figure 19. The most important property is the fact that any generic graph can be decomposed into some smaller connected graphs. This property arises because the integration variables are independent of each other and only connected by the functions 'f' which correspond to edges of the connected graph. In this notation:

$$Z_N(V,T) = (Sum\ Of\ All\ distinct\ N-particle\ graphs) \tag{5.1.5}$$

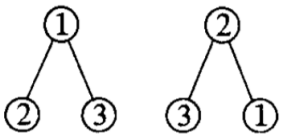

(a) Two Distinct Graphs for N=3

(b) Two Identical Graphs for N=3

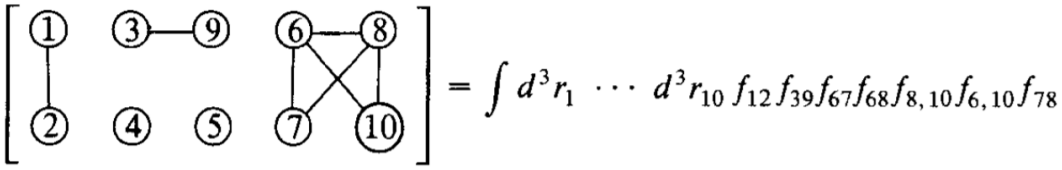

(c) Pictorial Representation Of One Of the terms in the Configuration Integral for N=10

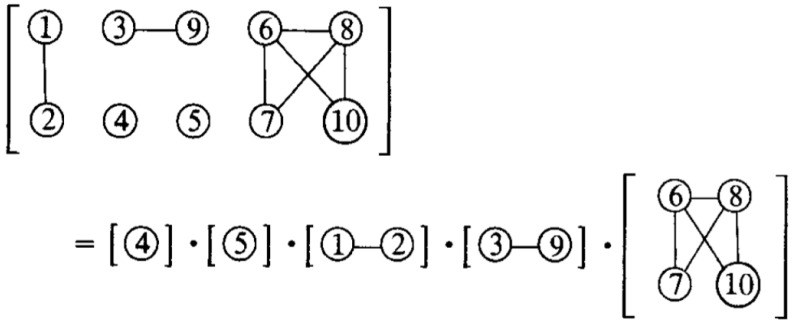

(d) Decomposition Of A Generic Graph into Smaller Connected components

Figure 19: Basic Properties Of The N-Particle Graphs [1]

Now that we are armed with this powerful tool, it is time to define a cluster integral. Since only connected graphs matter, we define an l-cluster to be a l-particle connected graph. For eg: In figure 19(c), is a product of '2' 1-cluster, '2' 2-cluster and '1' 4-cluster. In this notation define the cluster

integral as:

$$b_l(V,T) = \frac{1}{l!\lambda^{3l-3}V}(Sum\ over\ all\ l-clusters) \tag{5.1.6}$$

The normalization factor is chosen such that:

1. $b_l(V,T)$ is dimensionless.
2. $\bar{b} = \lim_{V\to\infty} b_l(V,T)$. This happens because the function 'f' is of finite range and hence in an l-cluster, the integration only gives a factor of V (which is usually over the center of mass of the combined system).

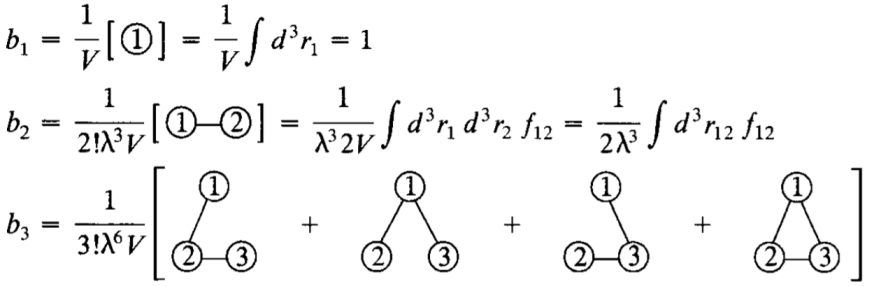

Figure 20: Some Examples Of Cluster Integrals [5]

The decomposition property allows us to write any generic N-particle graph into a number of smaller clusters out of which m_l are l- clusters leading to the constraining equation:

$$\sum_{l=1}^{N} m_l l = N \tag{5.1.7}$$

Hence each N- particle graph can be mapped onto an 'l' dimensional vector with l^{th} entry being m_l. However, this is not an injective mapping. Given a vector containing the set of $\{m_l\}$ values satisfying the 5.1.7 constraint, a unique N-particle graph cannot be recovered due to the following reasons:

- There are multiple ways of forming a single l-cluster. (See b_3 in Fig 20)
- There are multiple ways of enumerating which particles belong to which cluster.

Hence set of $\{m_l\}$ values satisfying the 5.1.7 constraint gives a collection of graphs. Let the sum of the contributions of all these graphs be denoted by $S(\{m_l\})$. In this notation:

$$Z_N = \sum_{\{m_l\}} S(\{m_l\}) \tag{5.1.8}$$

Using the Generating function method, we can $S(\{m_l\})$ as:
The expansion of $S(\{m_l\})$ has the following properties:

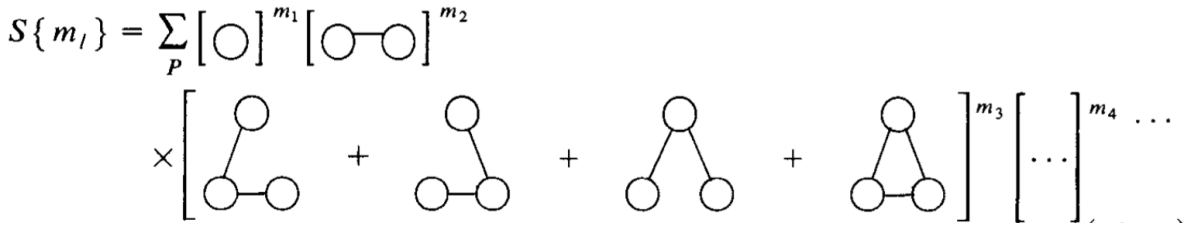

1. Each bracket is a sum over all possible l-clusters.
2. If all the brackets are expanded using the multinomial theorem then the summand itself will contain a large number of terms wherein each term will contain N-empty circles pointing to a N-particle graph which is free to be enumerated.
3. The summation is over all **distinct ways of numbering** these circles from 1 to N.

Now here comes the real trick to compute $S(\{m_l\})$. Looking at the expansion of $S(\{m_l\})$, one observes that that each term in summand has the same value. Hence the sum is simply the number of distinct permutations times the value of any term in the sum. The value of each summand is same because each graph simply represents an integral whose value is independent of the fact how those circles are enumerated. The number of distinct permutations can be found by noticing:

- There are m_l l clusters and a permutation among them does not lead to a new graph.
- Within each l-cluster, a permutation of the l-particles enumeration does not lead to a new graph.

Hence:

$$S(\{m_l\}) = \frac{N!}{[(1!)^{m_1}(2!)^{m_2}(3!)^{m_3}\cdots][m_1!m_2!m_3!\cdots]} \times (1!Vb_1)^{m_1}(2!Vb_2)^{m_2}(3!Vb_3)^{m_3}\cdots$$

$$S\{m_l\} = N!\prod_{l=1}^{N}\frac{\left(V\lambda^{3l-3}b_l\right)^{m_l}}{m_l!} = N!\lambda^{3N}\prod_{l=1}^{N}\frac{1}{m_l!}\left(\frac{V}{\lambda^3}b_l\right)^{m} \tag{5.1.9}$$

Using 5.1.9 and 5.1.8, one can effectively compute the configuration integral and hence the CE and GCE partition functions. The computation of GCE partition function is shown below. Using 5.1.2 and the fact that: $\sum_{N=0}^{\infty}\sum_{\{m_l\}} \equiv \sum_{m_1=0}^{\infty}\sum_{m_2=0}^{\infty}\cdots\cdots$ Here $\{m_l\}$ denotes a restricted sum following the 5.1.7 constraint. However when this constraint is allowed to vary over all possible particle numbers, it changes to an unrestricted sum with the parameters varying independently with each other. Thus

$$\mathcal{Q}(z,V,T) = \sum_{m_1=0}^{\infty}\sum_{m_2=0}^{\infty}\cdots\left[\frac{1}{m_1!}\left(\frac{V}{\lambda^3}zb_1\right)^{m_1}\frac{1}{m_2!}\left(\frac{V}{\lambda^3}z^2b_2\right)^{m_2}\cdots\right]$$
$$= \prod_{l=1}^{\infty} exp\left(\frac{V}{\lambda^3}z^lb_l\right)$$

$$\frac{1}{V}\log\left[\mathscr{Q}(z,V,T)\right] = \frac{1}{\lambda^3}\sum_{l=1}^{\infty} z^l b_l \tag{5.1.10}$$

Now, we already have the GCE machinery to compute the useful functions. the equation of state obtained via 5.1.10 is called the cluster expansion for the equation of state. In parametric form it is given by:

$$\begin{cases} \frac{P}{kT} = \frac{1}{\lambda^3}\sum\limits_{l=1}^{\infty} b_l z^l \\ \\ \frac{1}{v} = \frac{1}{\lambda^3}\sum\limits_{l=1}^{\infty} l b_l z^l \end{cases} \tag{5.1.11}$$

Now if we consider the dilute gas system, we can expand the pressure in terms of a perturbation series of density $\rho = 1/\nu = N/V$. However in this limit the equation of state becomes:

$$\begin{cases} \frac{P}{kT} = \frac{1}{\lambda^3}\sum\limits_{l=1}^{\infty} \bar{b}_l z^l \\ \\ \frac{1}{v} = \frac{1}{\lambda^3}\sum\limits_{l=1}^{\infty} l\bar{b}_l z^l \end{cases} \tag{5.1.12}$$

where $\bar{b} = \lim\limits_{V\to\infty} b_l$ which is a well defined quantity as explained at 5.1.6. Only the dilute gas systems can be terminated upto second order in perturbation series to get any useful results. Using the Virial equation of state 5.0.4, the equation of state for dilute gas systems 5.1.12 and terminating the series at the first non-trivial term (the second Virial coefficient), we arrive at the Van der waals' equation of state for real gases containing on the repulsive potential term (see Appendix D1):

$$P(V - NB_2) = NkT \tag{5.1.13}$$

$$\begin{aligned} B_2(T) &= -\frac{1}{2V}\iint f_{12}d\vec{r}_1 d\vec{r}_2 = -\frac{1}{2V}\iint f_{12}d\vec{r}_1 d\vec{r}_{12} \\ &= -\frac{1}{2}\int_0^{\infty}\int_0^{\pi}\int_0^{2\pi} dr d\theta d\phi r^2 \sin\theta f_{12} = -2\pi\int_0^{\infty} f_{12} r^2 dr \end{aligned} \tag{5.1.14}$$

5.1.2 Second- Virial coefficients For Some Useful Potentials

- Hard-Sphere Potential: The potential is given by:

$$\begin{aligned} u(r) &= \begin{cases} \infty & \text{for } r < \sigma \\ 0 & \text{for } r > \sigma \end{cases} \\ e^{-\beta u(r)} &= \begin{cases} 0 & \text{for } r < \sigma \\ 1 & \text{for } r > \sigma \end{cases} \end{aligned} \tag{5.1.15}$$

  Using the appropriate relations we have:

$$B_2 = 2\pi\int_0^{\infty} \left[1 - exp(-\beta u(r))r^2 dr\right]$$

$$B_2 = 2\pi\left[\int_0^{\sigma}\left(1 - \exp(-\beta u(r))r^2 dr + \int_{\sigma}^{\infty}\left(1 - \exp(-\beta u(r))r^2 dr\right]\right.$$

$$B_2 = 2\pi\left(\left[\frac{r^3}{3}\right]_0^{\sigma} + 0\right) = \frac{2\pi\sigma^3}{3} = 4\times\left[\frac{4\pi}{3}\left(\frac{\sigma}{2}\right)^3\right] \tag{5.1.16}$$

This is simply four times the total volume occupied by each molecule (σ acts like the molecule diameter). This is exactly the excluded volume per molecule given that only two-particle collision processes occur in the system.

- Square-Well Potential: The potential is given by:

$$\begin{aligned} u(r) &= \begin{cases} \infty & \text{for } r<\sigma \\ -\epsilon & \text{for } \sigma<r<\lambda\sigma \\ 0 & \text{for } r>\lambda\sigma \end{cases} \\ e^{-\beta u(r)} &= \begin{cases} 0 & \text{for } r<\sigma \\ e^{\beta\epsilon} & \text{for } \sigma<r<\lambda\sigma \\ 1 & \text{for } r>\lambda\sigma \end{cases} \end{aligned} \tag{5.1.17}$$

Using the appropriate relations we have:

$$\begin{aligned} B_2(T) &= 2\pi\left[\int_0^{\sigma} r^2dr + \int_{\sigma}^{\lambda\sigma}\left(1-e^{\beta\epsilon}\right)r^2dr + 0\right] \\ &= 2\pi\left[\frac{\sigma^3}{3} + \left(1-e^{\beta\epsilon}\right)\int_{\sigma}^{\lambda\sigma} r^2dr\right] \\ &= \frac{2\pi\sigma^3}{3}\left[1+\left(1-e^{\beta\epsilon}\right)\left(\lambda^3-1\right)\right] \end{aligned} \tag{5.1.18}$$

Hence, one can always compute the integrals for any general central potential. It might sometimes be too difficult to calculate the expression analytically but numerically, it can always be done which makes the classical cluster expansion quite a powerful tool.

5.1.3 Variation In Number And Energy Density In Imperfect Gas When Compared To Ideal Gas

The number density $\mathscr{N}$ and the energy density $\mathscr{U}$ can be computed using the following formulae of the GCE:

$$\begin{aligned} \mathscr{N} &= z\frac{\partial\left(\frac{1}{V}log\mathscr{Q}(z,V,\beta)\right)}{\partial z} \\ \mathscr{U} &= -\frac{\partial\left(\frac{1}{V}log\mathscr{Q}(z,V,\beta)\right)}{\partial\beta} \end{aligned}$$

From now, the superscript (0) will be used for ideal gas. For the ideal gas we have $\bar{b}_1^{(0)} = 1$ and $\bar{b}_{l>1}^{(0)} = 0$. For the imperfect gas we have a hard sphere potential of radius 'a' and an expansion only upto the first non-trivial term which is the second cluster coefficient. Hence $\bar{b}_1 = 1$, $\bar{b}_2 = -B_2/\lambda^3$ and $\bar{b}_{l>2} = 0$. Here B_2 is defined via 5.1.16. Using 5.1.10 and substituting this back into theformulae, we

have:

$$\mathscr{N} - \mathscr{N}^{(0)} = -\frac{2z^2 B_2}{\lambda^6} = \frac{z^2}{\lambda^6} \times \frac{4\pi a^3}{3} \qquad \mathscr{N} - \mathscr{N}^{(0)} \propto -a^3 T^3 e^{\frac{2\mu}{kT}} \tag{5.1.19}$$

$$\mathscr{U} - \mathscr{U}^{(0)} = -\frac{3z^2 B_2}{\beta\lambda^6} = \frac{z^2}{\beta\lambda^6} \times 2\pi a^3 \qquad \mathscr{U} - \mathscr{U}^{(0)} \propto -a^3 T^4 e^{\frac{2\mu}{kT}} \tag{5.1.20}$$

The results are within our expectation. The difference between the imperfect gas and ideal gas comes up in the form of an extra term depending on the second cluster coefficient which in turn depends on the cube of the hard sphere parameter 'a'. The ratio of the difference of energy density to number density is proportional to T which is within our expectations due to the formula for equation of state for the ideal gas, $PV = NkT \propto U$.

5.2 Quantum Cluster Expansion

Consider N identical particles in an enclosed volume V. Let the Hamiltonian now be an operator $\mathscr{H}$ instead of a number. In the coordinate representation, we have for the momentum operator:

$$\mathscr{H} = \sum_{i=1}^{N} \frac{\hat{p_i}^2}{2m} + \sum_{i<j} \hat{V}_{ij}^P$$

$$\langle x_i|\hat{p}|x_j\rangle = p_i \delta(x_i - x_j) = -i\hbar\nabla_i \delta(x_i - x_j)$$

Using the above expression and inserting two identities in position space representation we have:

$$Q_N(V,T) = \mathrm{Tr}\, e^{-\beta H} = \int d^{3N} r \sum_{\alpha} \Psi_\alpha^*(1,\ldots,N) e^{-\beta\mathscr{X}} \Psi_\alpha(1,\ldots,N)$$

Here $\{\Psi\}$ are a complete set of orthonormal wave-functions depending upon $(r_1, r_2, \cdots, r_N)$ which is written in shorthand form as $(1, 2, \cdots, N)$. Defining:

$$W_N(1,\ldots,N) \equiv N!\lambda^{3N} \sum \Psi_\alpha^*(1,\ldots,N) e^{-\beta\mathscr{H}} \Psi_\alpha(1,\ldots,N) \tag{5.2.1}$$

$$Q_N(V,T) = \frac{1}{\lambda^{3N} N!} \int d^{3N} r W_N(1,2,\cdots,N) \tag{5.2.2}$$

Here again the factor of $1/\lambda^{3N}$ comes out by integrating put the momentum part of the phase space integrals. Some important properties of $W_N(1,2,\cdots,N)$ are (see Appendix D2):

1. $W_1(1) = 1$
2. $W_N(1,2,\cdots,N)$ is a symmetric function of its arguments.
3. $W_N(1,2,\cdots,N)$ is invariant under unitary transformations.
4. Suppose that the molecules could be divided into two groups, say α (with m molecules) and β (with N-m molecules) with the property that:

$$|r_i - r_j| >> r_0 \; and \; |r_i - r_j| >> \lambda. \; Then$$

$$W_N(r_1, r_2, ..., r_N) \approx W_\alpha(r_{1,\alpha}, \cdots, r_{m,\alpha}) W_\alpha(r_{1,\beta}, \cdots, r_{N-m,\beta})$$

Here r_0 and λ are the two length scales available to the problem which are the mean free path and the thermal wavelength respectively.

Consider the case for N=2. Property 4 suggests that if we write: $W_2(1,2) = W_1(1)W_!(2) + U_2(1,2)$. Then as $|r_1 - r_2| \to \infty$ then $U_2(1,2) \to \infty$. Hence $U_2(1,2)$ should act like the quantum analogue to the classical 2-cluster. Now, we proceed systematically to produce a scheme to recover the equation of $U_l(1,2,\cdots,l)$ from $W_l(1,2,\cdots,l)$.[2]

$$\begin{aligned} W_1(1) =& U_1(1) = 1 \\ W_2(1,2) =& U_1(1)U_1(2) + U_2(1,2) \\ W_3(1,2,3) =& U_1(1)U_1(2)U_1(3) + U_1(1)U_2(2,3) \\ &+ U_1(2)U_2(3,1) + U_1(3)U_2(1,2) + U_3(1,2,3) \\ &\cdots \end{aligned}$$

Repeating the recursion, the N^{th} equation will look like:

$$W_N(1,\ldots,N) = \sum_{\{m_l\}} \sum_P \underbrace{[U_1()\cdots U_1()]}_{m_1 \text{ factors}} \underbrace{[U_2(,)\cdots U_2(,)]}_{m_2 \text{ factors}} \cdots \underbrace{[U_N(,\cdots,)]}_{m_N \text{ factors}} \tag{5.2.3}$$

$$\sum_{l=1}^{N} l m_l = N \tag{5.2.4}$$

$\sum_P$ is sum over all distinct permutations.

Now, the above equations look awfully close to the classical equations obtained earlier however we arrived them from a completely quantum mechanical point of view. Using the above system of equations to recursively solve for $U_l(1,2,\cdots,l)$. The first two are:

$$\begin{aligned} U_1(1) &= W_1(1) = 1 \\ U_2(1,2) &= W_2(1,2) - W_1(1)W_1(2) \end{aligned} \tag{5.2.5}$$

Now we are ready to define the l-cluster integral in the quantum cluster expansion as:

$$b_1(V,T) \equiv \frac{1}{l!\lambda^{3l-3}V} \int d^3r_1 \cdots d^3r_l U_l(1,\ldots,l) b_1(V,T) \equiv \frac{1}{l!\lambda^{3l-3}V} \int d^3r_1 \cdots d^3r_l U_l(1,\ldots,l) \tag{5.2.6}$$

Some properties of the quantum cluster integral b_l are:

- b_l is dimensionless.
- $\bar{b}_l(V,T) = \lim_{V\to\infty} b_l(V,T)$ is a well-defined quantity. The reason for this is property 4 of $W_N(1,2,\cdots,N)$. Due to that $U_l(1,2,\cdots,N) \to 0$ as soon as the distance between any two of its arguments become much larger than the prescribed length scale of the problem. Hence each cluster integral is at max has a direct proportionality with V.

[2]This systematic expansion was initially developed by Kahn and Uhlenbeck

Now, we are ready to compute the CE and GCE partition functions. The technique used is same as that in the classical case.

$$\begin{aligned}
&\int d^{3N}rW(1,\ldots,N)\\
&= \sum_{\{m_1\}} \tfrac{N!}{[(1!)^{m_1}(2!)^{m_2}\cdots](m_1!m_2!\cdots)} \quad \times \int d^{3N}r\left[(U_1\cdots U_1)\,(U_2\cdots U_2)\cdots\right]\\
&= N!\sum_{\{m_1\}} \tfrac{1}{m_1!}\left[\tfrac{1}{1!}\int d^3r_1U_1(1)\right]^{m_1}\tfrac{1}{m_2!}\left[\tfrac{1}{2!}\int d^3r_1d^3r_2U_2(1,2)\right]^{m_2}\ldots\\
&= N!\sum_{\{m_l\}}\prod_{l=1}^{N}\frac{\left(V\lambda^{3l-3}b_l\right)^{m_l}}{m_l!}\\
&= N!\lambda^{3N}\sum_{\{m_l\}}\prod_{l=1}^{N}\tfrac{1}{m_l!}\left(\tfrac{V}{\lambda^3}b_l\right)^{m_l}
\end{aligned}$$

$$Q_N(V,T) = \sum_{\{m_l\}}\prod_{l=1}^{N}\frac{1}{m_l!}\left(\frac{V}{\lambda^3}b_l\right)^{m_l} \tag{5.2.7}$$

$$\frac{1}{V}\log\left[\mathscr{Q}(z,V,T)\right] = \frac{1}{\lambda^3}\sum_{l=1}^{\infty}z^lb_l \tag{5.2.8}$$

In the $V\to\infty$, $b_l(V,T)\to\bar{b}_l(V,T)$ and hence, subsequently we get an expansion in terms of perturbation series of density for pressure and other relevant thermodynamic quantities of the system. From the analysis of equation of states of ideal Bose and Ideal Fermi gases in the previous reports we have:

$$b_l^{(0)} = \begin{cases} l^{-5/2} & \text{(ideal Bose gas)}\\ (-1)^{l+1}l^{-5/2} & \text{(ideal Fermi gas)}\end{cases} \tag{5.2.9}$$

Equation 5.2.8 and 5.2.9 combined gives back the Reimann-Drichlet functions obtained in the equation of state of ideal Bose/Fermi gases. The superscript 0 is to signify that the system under consideration is ideal. An important distinction from classical gases is the observation that even for quantum ideal gases, the higher order cluster integrals and hence subsequently the virial coefficients are non-zero. This is something that just cannot happen in the classical case.

5.3 Second-Virial Coefficient For Radial Potential In Quantum Expansion

To find the second virial coefficient in quantum expansion, we require the knowledge of $W_2(1,2)$ which is the property of a two body Hamiltonian. Hence our general N-body problem reduces to a 2-body problem. Let the Hamiltonian be (non-relativistic as it is easier to manipulate):

$$\mathscr{H} = \frac{-\hbar^2}{2m}\left(\nabla_1^2+\nabla_2^2\right)+\nu(|\vec{r}_1-\vec{r}_2|)$$
$$\mathscr{H}\Psi_\alpha(1,2) = E_\alpha\Psi_\alpha$$

Now make the following substitutions:

$$\vec{R} = \frac{1}{2}\left(\vec{r}_1+\vec{r}_2\right) \qquad \vec{r} = \vec{r}_2-\vec{r}_1$$

Our Hamiltonian now becomes:

$$\mathscr{H} = -\left(\frac{\hbar^2}{4m}\nabla_R^2 + \frac{\hbar^2}{m}\nabla_r^2\right) + \nu(|\vec{r}|)$$

Applying separation of variables and solving we have:

$$\begin{aligned} \Psi_\alpha(1,2) &= \frac{1}{\sqrt{V}} e^{i\vec{P}\cdot\vec{R}}\psi_n(\vec{r}) \\ E_\alpha &= \frac{P^2}{4m} + \epsilon_n, \quad \alpha \equiv \ (\vec{P}, n) \ \text{ independent set of quantum numbers} \end{aligned} \tag{5.3.1}$$

$$\left[-\frac{\hbar^2}{m}\nabla^2 + v(r)\right]\psi_n(\vec{r}) = \epsilon_n\psi_n(\vec{r}) \tag{5.3.2}$$

$$\text{With the normalization condition: } \int d^3r|\psi_n(\vec{r})|^2 = 1 \tag{5.3.3}$$

Now:

$$W_2(1,2) = 2\lambda^6 \sum_\alpha |\Psi_\alpha(1,2)|^2 e^{-\beta E\alpha} = \frac{2\lambda^6}{V}\sum_{\vec{P}}\sum_n |\psi_n(\vec{r})|^2 e^{-\beta P^2/4m} e^{-\beta\epsilon_n}$$

As $V \to \infty$, $\frac{1}{V}\sum\limits_P$ can be transformed to an integral (as I have done many times in the previous reports) and solved (using a simple substitution it becomes the integral for the Γ function) as:

$$\frac{1}{V}\sum_{\vec{P}} e^{-\beta P^2/4m} = \frac{4\pi}{h^3}\int_0^\infty dP P^2 e^{-\beta P^2/4m} = \frac{2^{3/2}}{\lambda^3}$$

Combining everything we have:

$$W_2(1,2) = 2^{5/2}\lambda^3 \sum_n |\psi_n(\vec{r})|^2 e^{-\beta\epsilon_n} \tag{5.3.4}$$

Repeating the calculation for the ideal gas (representing all parameters of the ideal gas with (0) in superscript):

$$W_2^{(0)}(1,2) = 2^{5/2}\lambda^3 \sum_n \left|\psi_n^{(0)}(\vec{r})\right|^2 e^{-\beta\epsilon_n^{(0)}}$$

The second virial can now be calculated as:

$$\begin{aligned} \bar{b}_2 &= \frac{1}{2\lambda^3 V}\int d^3r_1 d^3r_2 U_2(1,2) = \frac{1}{2\lambda^3 V}\int d^3R d^3r\,[W_2(1,2) - 1] \\ \bar{b}_2 - \bar{b}_2^{(0)} &= \frac{1}{2\lambda^3 V}\int d^3R d^3r\left[W_2(1,2) - W_2^{(0)}(1,2)\right] \\ &= 2\sqrt{2}\int d^3r \sum_n \left[|\psi_n(\vec{r})|^2 e^{-\beta\epsilon_n} - \left|\psi_n^{(0)}(\vec{r})\right|^2 e^{-\beta\epsilon_n^{(0)}}\right] \end{aligned}$$

$$\bar{b}_2 - \bar{b}_2^{(0)} = 2\sqrt{2}\sum_n \left(e^{-\beta\epsilon_n} - e^{-\beta\epsilon_n^{(0)}}\right) \tag{5.3.5}$$

$\bar{b}_2^{(0)}$ has already been calculated in 5.2.9. To further solve 5.3.5, we first need to understand the energy spectrum of both the ideal and the interacting two-body system.

- For the ideal system, the energy eigenvalues form a continuum in the dilute gas limit. The eigenvalues are labeled by quantum number 'k' which has the physical interpretation of being the relative wave-number for the ideal system.

$$\epsilon_n^{(0)} = \frac{\hbar^2 k^2}{2m}$$

- For the interacting system, we have two different types of energy states. First is a discrete set of values of energy, labeled by B. These denote the bound states of two-body Hamiltonian. Then, there is again a continuum of states labeled by the relative wave number 'k' for the interacting system.

$$\epsilon_n = \begin{cases} \epsilon_B & \text{For Bound States} \\ \frac{\hbar^2 k^2}{2m} & \text{For Continuum States} \end{cases}$$

Now, let $g(k)$ *and* $g^{(0)}(k)$ be the density of states for the interacting and the ideal system respectively. Then, in the most general case, we have:

$$\bar{b}_2 - \bar{b}_2^{(0)} = 2^{3/2}\left\{\sum_B e^{-\beta\epsilon_B} + \int_0^\infty dk\left[g(k) - g^{(0)}(k)\right]e^{-\beta\hbar^2k^2/m}\right\} \tag{5.3.6}$$

Even the factor of $2^{3/2}$ has a physical interpretation and is recognized as $\left[\frac{\lambda}{\lambda_{CM}}\right]^{3/2}$ with λ and λ_{CM} being the thermal wavelength of individual system and the center of mass of the 2-particle system respectively. Now all that is left is to compute the difference in the density of states of the interacting and the ideal system.

5.3.1 Machinery To Calculate The Difference In Density Of States: $g(k) - g^{(0)}(k)$

To compute the density of states, we first take the help of equation 5.3.2 to account for the quantum statistics of the Bose and Fermi gases. This equation looks very close to the hydrogen atom equation and for a central potential, it will be solved in exactly the same way. The solution will look like:

$$\Psi_{klm}(\vec{r}) = A_{klm} Y_l^m(\theta, \phi) \frac{u_{kl}(r)}{r} = A_{klm} Y_l^m(\theta, \phi) j_l(kr) \tag{5.3.7}$$

The $Y_l^m(\theta, \phi)$ *and* $j_l(kr)$ are the spherical harmonics and the Bessel functions of order l respectively. Bessel functions for an integer order l, follow the property:

$$j_l(-kr) = (-1)^l j_l(kr)$$

The above property combined with the completely symmetric and anti-symmetric nature of the Bose and Fermi gases respectively leads to:

$$l = \begin{cases} 0, 2, 4, \cdots & \text{For Bosons} \\ 1, 3, 5, \cdots & \text{For Fermions} \end{cases} \tag{5.3.8}$$

The square integratibility of the wavefunction sets the boundary conditions to be: $u_{kl}(R) = u_{kl}^{(0)}(R) = 0$ with $R \to \infty$ at the end of the computation. Under the assumption that the perturbing potential is confined in a short-range, the process can be treated as a scattering process. As the particle goes far away from the effect of the potential, it again acts like a free particle. The only change in the wavefunction of the perturbed particle is the introduction of a phase shift from the ideal case. Using the partial-wave phase shift analysis we have:

$$u_{kl}(r) \overline{_{r\to\infty}} \sin\left[kr + \tfrac{l\pi}{2} + \eta_l(k)\right]$$

$$u_{kl}^{(0)}(r) \overline{_{r\to\infty}} \sin\left(kr + \tfrac{l\pi}{2}\right)$$

This asymptotic form defines the phase shift function $\eta_l(k)$ for the corresponding radial potential. The eigenvalues are determined using the boundary conditions as:

$$\begin{aligned} kR + \frac{l\pi}{2} + \eta_l(k) &= n\pi \quad \text{(Interacting system)} \\ kR + \frac{l\pi}{2} &= n\pi \quad \text{(Ideal system)} \end{aligned} \tag{5.3.9}$$

Some important properties of the eigenvalues are:

- Here n $\in$ W as the boundary condition in solved in the asymptotic when $r \to \infty$.
- The eigenvalue 'k' depends only on 'n' and 'l'.
- Each eigenvalue 'k' is 2l+1 fold degenerate as for a given 'l', Y_l^m has 'm' varying from $-l \to l$.

Now let the number of states between k *and* $k+dk$ for a given l be given by $g_l(k)dk$ and $g_l^{(0)}(k)dk$ for the interacting and the ideal system respectively. Using the last property of the energy eigenvalues listed earlier,we have:

$$\frac{g_l(k)dk}{2l+1} = 1$$
$$\frac{g_l^{(0)}(k)dk^{(0)}}{2l+1} = 1$$

Since 'l' is fixed the change dk must be produced by a change in 'n'. Since 'n' can only change by an integer value, a change of 1 unit in 'n' produces a change dk in k which can be related as:

$$Rdk + \frac{\partial n_l(k)}{\partial k}.dk = \pi$$
$$\implies dk = \frac{\pi}{R + \left[\frac{\partial n_l(k)}{\partial k}\right]}$$

Similarly for an ideal system:

$$dk^{(0)} = \frac{\pi}{R}$$

Substituting these back we have:

$$g_l(k) - g_l^{(0)}(k) = \frac{2l+1}{\pi}\frac{\partial \eta_l(k)}{\partial k}$$

Now, all that is left is to take sum over all valid valid values of 'l', leading to:

$$g(k) - g^{(0)}(k) = \frac{1}{\pi}\sum_l{}'(2l+1)\frac{\partial \eta_l(k)}{\partial k} \tag{5.3.10}$$

Here $\sum_l{}'$ is a restricted sum over the 'l' values following 5.3.8. Substituting everything back, we finally have the formula for the second virial coefficient for a finite-radial potential as:

$$b_2 - b_2^{(0)} = 2^{3/2}\left\{\sum_B e^{-\beta\epsilon_B} + \frac{1}{\pi}\int_0^\infty dk \sum_l{}'(2l+1)\frac{\partial \eta_l(k)}{\partial k}e^{-\beta\hbar^2k^2/m}\right\} \tag{5.3.11}$$

5.3.2 Variation In Number And Energy Density In Imperfect Gas When Compared To Ideal Gas

Again the formulae from section 5.1.3 remain valid for the computation of the number and energy density. However, this time around the cluster coefficients of ideal gases are non-trivial and are given by 5.2.9. Further, we shall assume only first order expansion in the second virial coefficient and

also assume that the imperfect gas sways away from the ideal gas only at the level of second cluster coefficient. Finally, the Bose and Fermi gases are considered to be spinless. Then:

$$\mathscr{N} - \mathscr{N}^{(0)} = \frac{z^2}{\lambda^3}(b_2 - b_2^{(0)}) \tag{5.3.12}$$

$$\mathscr{U} - \mathscr{U}^{(0)} = -\left[\left\{z^2(b_2 - b_2^{(0)})\right\}\frac{\partial}{\partial\beta}\left(\frac{1}{\lambda^3}\right) + \frac{z^2}{\lambda^3}\frac{\partial(b_2 - b_2^{(0)})}{\partial\beta}\right] \tag{5.3.13}$$

For Bosons, $(b_2 - b_2^{(0)}) = -\frac{2a}{\lambda}$ (see Appendix D3), hence:

$$\mathscr{N}_B - \mathscr{N}_B^{(0)} = -\frac{2z^2a}{\lambda^4} \qquad \mathscr{N}_B - \mathscr{N}_B^{(0)} \propto -aT^2e^{2\mu/kT} \tag{5.3.14}$$

$$\mathscr{U}_B - \mathscr{U}_B^{(0)} = -\frac{7}{2}\frac{z^2a}{\lambda^4\beta} \qquad \mathscr{U}_B - \mathscr{U}_B^{(0)} \propto -aT^3e^{2\mu/kT} \tag{5.3.15}$$

Unlike the classical gas the dependence on the hard sphere parameter for the difference in thermodynamic macroscopic variables is linear for the Imperfect Bose Gases. As expected both the number and the energy densities decrease at the same macroscopic state when compared to the ideal Bose Gas. The ratio of difference in energy to number density is again directly proportional to the temperature as in the classical case. All these results except the linear dependence are within our expectations.
For Fermions, $(b_2 - b_2^{(0)}) = -6\pi\left[\frac{a}{\lambda}\right]^3$ (see Appendix D3), hence:

$$\mathscr{N}_F - \mathscr{N}_F^{(0)} = -\frac{6\pi z^2a^3}{\lambda^6} \qquad \mathscr{N}_F - \mathscr{N}_F^{(0)} \propto -a^3T^3e^{2\mu/kT} \tag{5.3.16}$$

$$\mathscr{U}_F - \mathscr{U}_F^{(0)} = -\frac{18\pi z^2a^3}{\lambda^6\beta} \qquad \mathscr{U}_F - \mathscr{U}_F^{(0)} \propto -a^3T^4e^{2\mu/kT} \tag{5.3.17}$$

These results for the Fermi Gas match exactly with that obtained from the classical cluster expansion. The reason being that in both of these cases the difference in the second virial coefficients (upto first order in imperfect and ideal Fermi Gas) is proportional to $\frac{a^3}{\lambda^3}$. The results definitely make sense and all previous analysis passes through, however it is quite funny that Fermi gases are mimicking the classical gases in this context.

6 Imperfect Gases At Low Temperatures

The imperfect gas in our case has the following defining properties:

- It is a dilute system of particles that interact among themselves via a finite inter-particle potential. This potential has a finite range and the forces involved do not lead to any two-particle bound states.
- The diluteness of the gas allows us to treat the inter-particle interaction as a small perturbation to the ideal gas.
- Our system has two defining length scales, the thermal wavelength and the average inter-particle separation. For our imperfect gas these length scales are much greater than the range of inter-particle interaction.

The advantages of making the above approximations are:

- The quantum particle cannot be localised in its thermal wavelength (which is the analogue of de-Broglie wavelength to our problem). Thus, (by last defining property), the probability of finding a second particle within the range of interaction of another particle is non-existent.
- Therefore, the effective potential as seen by a particle is very small even though inter-particle potential may have large values. The exact details of the potential become irrelevant in the first order (as we shall see later) of perturbation as the particles only experiences an average effect of the potential.
- The gas is considered at low temperatures so that only low-lying energy levels (ground state and levels close to it) contribute to the problem. For this purpose, we introduce an effective Hamiltonian for the low-lying energy levels replacing the original Hamiltonian to compute the partition function and hence everything subsequently. This method was first introduced by Fermi and is called the **Method Of Pseudopotentials**[3]. This method aims to obtain the relevant energy levels of the system in terms of the scattering phase-shifts of the potential.

6.1 Machinery To Handle Quantum Gases

6.1.1 Handling The Hard-Sphere Potential

Consider the interacting potential of the following form:

$$V(|\vec{r}_1 - \vec{r}_2|) = \begin{cases} \infty & |\vec{r}_1 - \vec{r}_2| < a \\ 0 & |\vec{r}_1 - \vec{r}_2| > a \end{cases} \tag{6.1.1}$$

Using the analysis in section 2.3 and 2.3.2, we have the schrodinger equation applied to our potential in the coordinates of the center of mass of the system as:

$$\begin{aligned} \left(\nabla^2 + k^2\right)\psi(\vec{r}) &= 0 \quad (r > a) \\ \psi(\vec{r}) &= 0 \quad (r \leq a) \end{aligned} \tag{6.1.2}$$

$$\text{with} \qquad E(\vec{P}, \vec{r}) = \frac{P^2}{2M} + \frac{\hbar^2 k^2}{2\mu} \tag{6.1.3}$$

Here $\vec{r} = \vec{r}_2 - \vec{r}_1$, $\vec{P}$ is momentum vector for the COM of the system, M is the total mass and μ is the reduced mass. Equation 6.1.2 suggests that hard sphere potential just introduces an extra boundary condition to the relative wavefunction $\psi(\vec{r})$ at $|r| = a$ in addition to some other boundary condition as $r \to \infty$ which is irrelevant to our problem.
The radial solution to 6.1.2 for spherically symmetric waves (S-waves,l=0) at low energies ($k \to 0$) is:

$$\psi(r) = \begin{cases} \mathrm{C}\left(1 - \frac{a}{r}\right) & (r > a) \\ 0 & (r \leq a) \end{cases} \tag{6.1.4}$$

Now the idea of pseudopotentials is borrowed from electrostatics wherein the boundary condition provided by the metallic sphere is removed by positioning a series multipole sources at the center

[3] E. Fermi, Ricerca Sci., 7,13(1936)

of the origin so that the electrostatic potential as obtained in both cases matches exactly outside the sphere. In an analogous way, the method of pseudopotentials replaces the hard-sphere boundary condition on the relative wavefunction $\psi(\vec{r})$ with a series of sources at the origin producing scattered S,P,D, $\cdots$ waves (corresponding to l=0,1,2,$\cdots$). Having this in mind, define an extended wave-function which satisfies:

$$\left(\nabla^2 + k^2\right)\psi_{\text{ex}}(r) = 0 \quad (\text{ everywhere except at } r = 0)$$
$$\text{with the boundary condition:} \quad \psi_{\text{ex}}(a) = 0$$
$$\psi_{\text{ex}}(r) \underset{r\to 0}{\longrightarrow} \left(1 - \frac{a}{r}\right)\chi$$

Here χ is a constant that depends on the boundary conditions at r=∞. χ can also be expressed in a more convenient form:

$$\chi = \left[\frac{\partial}{\partial r}\left(r\psi_{\text{ex}}\right)\right]_{r=0}$$

To eliminate the boundary condition one simply extends the equation of $\psi_{ex}(r)$ to include the origin. This can be done by taking the limit as $r \to 0$.

$$\nabla^2\psi_{\text{ex}}(r) \underset{r\to 0}{\longrightarrow} 4\pi a\delta(\vec{r})\chi = 4\pi a\delta(\vec{r})\frac{\partial}{\partial r}\left(r\psi_{\text{ex}}\right) \tag{6.1.5}$$

In 3.1.5, one recognises $\delta(\vec{r}\frac{\partial}{\partial r}r)$ as the redefined Hamiltonian operator (for the potential energy) acting on extended wavefunction. This operator is the pseudopotential for our problem upto this point. By construction, $\psi_{ex}(r)$ has the satisfies the same equation and boundary condition as $\psi(r)$ for $|r| > a$ and $k \to 0$. Let's note a few properties of the pseudopotential we have obtained:

- Pseudopotential obtained via 6.1.5 is not the exact pseudopotential as it is only valid for $k \to 0$. However, in the low temperature approximation and first order analysis in parameter 'a', 6.1.5 is good enough.
- Technically we should be adding an infinite series of pseudopotentials to 6.1.5 representing the S,P,D,F... scattered waves. However, the l^{th} wave pseudopotential $\propto a^{2l+1}$ (related to the scattering phase shifts). Hence, they need not be taken into consideration at the lowest order of perturbation theory.
- Due to the presence of the delta function, the operator is only evaluated at r=0. The differential operator takes the values:
  - $\left[\frac{\partial}{\partial r}(r\psi_{ex}(r))\right]_{r=0} = 1$, if $\psi_{ex}(r)$ is well-behaved and normalized at r=0
  - $\left[\frac{\partial}{\partial r}(r\psi_{ex}(r))\right]_{r=0} = B$, if $\psi_{ex}(r) \underset{r\to 0}{\longrightarrow} \frac{A}{r} + B$

  Hence if the wavefunctions are well-behaved the differential operator can be replaced by unity.

6.1.2 Extending The Concept To A General Finite Potential

Let $\nu(r)$ be the general finite ranged potential in consideration. Then the differential equation of the relative wavefunction becomes:

$$\frac{\hbar^2}{2\mu}\left(\nabla^2 + k^2\right)\psi(\vec{r}) = v(r)\psi(\vec{r}) \tag{6.1.6}$$

Again at low temperatures and hence low energies only the S-waves are important. Further due to finite range of potential no bound states are possible for the 2-body system. Hence, we expect a sinusoidal solution for the wavefunction at $r = \infty$.

$$u''(r) + k^2 u(r) = \tfrac{\mu}{\hbar^2} v(r) u(r)$$
$$u(r) \equiv r\psi(r)$$
$$u(r) \underset{r\to\infty}{\longrightarrow} u_\infty(r)$$
$$u_\infty(r) \equiv r\psi_\infty(r) = \text{C}\ \ (\sin kr + \tan\eta_0 \cos kr)$$

By definition, η_0 is S-wave scattering phase shift. For $k \to 0$:

$$\psi_\infty(r) \underset{r\to 0}{\longrightarrow}\ \text{C'}\ \left(1 + \frac{\tan\eta_0}{kr}\right)$$

In general, the scattering phase shift is a function of relative wavenumber, 'k'. However for small k, there is an available expansion:

$$k\cot\eta_0 = -\frac{1}{a} + \frac{1}{2}k^2 r_0 + \cdots$$

Here 'a' is called the scattering length and 'r_0' the effective range of the potential. Considering only the first term of the expansion we have the shape independent approximation.

$$\frac{tan\eta_0}{k} \approx -a \tag{6.1.7}$$

Replacing this back into the asymptotic wavefunction solution, we have:

$$\psi_\infty(r) \underset{r\to 0}{\longrightarrow}\ \text{C'}\ \left(1 - \frac{a}{r}\right) \tag{6.1.8}$$

Equation 6.1.8 and $\psi_{ex}(r)$ for the hard sphere solution have the same form as $r \to 0$. Thus, all the hard-sphere analysis again goes through. Thus, any finite ranged potential at low energies can be equivalently replaced by a hard-sphere potential of some diameter 'a' characteristic to the potential at the first order analysis.

6.1.3 Extension To A N-Particle System

The previous analysis was for a 2-body system. However, the problems generally encountered are for a complicated N-body system. From previous analysis we can say that to our concern (first order analysis in parameter 'a') only the s-wave l body pseudopotentials have the chance to trigger

any effects. Further, at our level of analysis any general finite potential is equivalent to a hard-sphere potential (diameter 'a') in some 3N-dimensional configuration. Hence, without the loss of generalization consider the N-body problem with hard sphere interactions. The differential equation now required to be solved is:

$$\begin{gathered} -\frac{\hbar^2}{2m}\left(\nabla_1^2+\cdots+\nabla_N^2\right)\Psi=E\Psi \quad (|\vec{r}_i-\vec{r}_j|>a, \quad \text{for all } i\neq j) \\ \Psi=0 \quad (\text{otherwise}) \end{gathered} \tag{6.1.9}$$

6.1.9 provides another complex boundary condition for Ψ in a 3N-dimensional configuration space. Now, here comes the awesome trick. Like before we will introduce an extended wavefunction. Now consider a region $S_{12}: |r_1-r_2|=a$. For this region the 2-body analysis goes through (as we have nothing to do with other coordinates) and hence we get a 2-body pseudopotential corresponding to S_{12}. Hence for each S_{ij} **i<j** we have a corresponding 2-body pseudopotential.
However, the above analysis doesn't take into account the regions where say S_{12} *and* S_{13} intersect. This region is where 3 particles simultaneously collide. To incorporate this effect we need to include a 3-body S-wave pseudopotential. However it turns out that N-body S-wave pseudopotential $\propto a^{3N-5}$ (see Appendix E1). Thus only, 2-body pseudopotentials are of relevance in our analysis. Hence our effective Hamiltonian at low temperatures simply becomes (in accordance with 6.1.5):

$$\mathscr{H}=-\frac{\hbar^2}{2m}\left(\nabla_1^2+\cdots+\nabla_N^2\right)+\frac{4\pi a\hbar^2}{m}\sum_{i<j}\delta\left(\vec{r}_i-\vec{r}_j\right)\frac{\partial}{\partial r_{ij}}r_{ij} \tag{6.1.10}$$

Finally, we use another trick to make our life easier. This is based on the realization that if we treat the pseudopotentials only in first order of the perturbation theory then the differential operator only acts on the unperturbed wavefunctions (due to the presence of the factor of 'a' in the pseudopotential). Since the unperturbed wavefunctions are always well-behaved, we can replace the differential operator with unity to achieve the following reduced effective Hamiltonian:

$$\mathscr{H}_{eff}=-\frac{\hbar^2}{2m}\left(\nabla_1^2+\cdots+\nabla_N^2\right)+\frac{4\pi a\hbar^2}{m}\sum_{i<j}\delta\left(\vec{r}_i-\vec{r}_j\right) \tag{6.1.11}$$

Equation 6.1.11 is the culmination of an incredible number of approximations. Always keep in mind that 6.1.11 works only in the first order of perturbation theory in 'a'. For this the gas must be dilute and the length scale of the thermal wavelength and the inter-particle separation must be greater than any other length scale in the problem except for the container in which the system is bound. Further 6.1.11 works only where the momentum energy is close to 0 from the baseline state. In a real system this is realized at extremely temperatures where the particles can only get excited to those states from ground state which have vanishingly small momentum.

6.2 Imperfect Spinless Bose Gases At Low Temperatures

Now finally, the time has arrived to use the effective Hamiltonian for low temperature on quantum bose gases to see how the imperfect gas differs from its ideal counterpart. The energy eigenvalues as computed using 6.1.11 for the Bose gas comes out to be (see Appendix F2):

$$H_{eff} = H_0 + \frac{4\pi a\hbar^2}{m}\sum_{i<j}\delta\left(\vec{r}_i - \vec{r}_j\right) \tag{6.2.1}$$

$$E_n = \epsilon_n + \frac{4\pi a\hbar^2}{mV}\left(N^2 - \frac{1}{2}N - \frac{1}{2}\sum_{\vec{p}} n_p^2\right) \tag{6.2.2}$$

Here ϵ_n is the kinetic energy part obtained from the ideal Bose gas Hamiltonian. Now, if we assume that we are working when temperatures are so small that very very few particles are able to get excited from the ground state, then we can make another approximation to the energy spectrum of the imperfect Bose Gas by letting $\frac{1}{N} \to 0$ & $\frac{n_k}{N} \to 0$ for all $k \neq 0$:

$$E_n \approx \epsilon_n + N\left(\frac{\hbar}{m}\right)^2 4\pi a\rho\left[1 - \frac{1}{2}\left(\frac{n_0}{N}\right)^2\right] \tag{6.2.3}$$

Introducing the parameter $\xi \equiv \frac{n_0}{N}$ and $\lambda = \sqrt{\frac{2\pi\hbar^2}{mkT}}$, the non-relativistic thermal wavelength, the energy spectrum and hence the CE partition function becomes:

$$E_n = \epsilon_n + N\left(\frac{a\lambda^2}{\nu}\right)\left(2 - \xi^2\right)$$
$$\nu = \frac{V}{N}$$

$$Q_n = \sum_n e^{-\beta\epsilon_n} e^{-N\left(a\lambda^2/v\right)\left(2-\xi^2\right)} = Q_N^{(0)}\left\langle e^{-N\left(a\lambda^2/v\right)\left(2-\xi^2\right)}\right\rangle_0 \tag{6.2.4}$$

Here $Q_N^0 = \sum_n e^{-\beta\epsilon_n}$ and $\langle\rangle_0$ represents the thermodynamic ensemble average with respect to ideal Bose Gas. Now, we can use all the tools available to us from Statistical Mechanics to find the thermodynamic parameters. For instance the Helmholtz free energy of the particle is:

$$\frac{A}{N} = \frac{A^{(0)}}{N} - \frac{kT}{N}\log\left\langle e^{-N\left(a\lambda^2/v\right)(2-\xi)^2}\right\rangle_0$$

The superscript 0 is to denote the parameter for the ideal gas. Now using linearity of the expectation operator, $e^x \approx 1 + x$, $log(1 + x) \approx x$ and that the mean-square fluctuations for any observable at thermodynamic equilibrium are small ($\left\langle\xi^2\right\rangle_0 - \left(\langle\xi\rangle_0\right)^2 \approx 0$), we have:

$$\frac{A}{N} = \frac{A^{(0)}}{N} + \frac{\hbar^2}{m}\frac{4\pi a}{v}\left(1 - \frac{1}{2}\bar{\xi}^2\right) \tag{6.2.5}$$

$$\bar{\xi} \equiv \langle\xi\rangle_0 = \langle n_0/N\rangle_0 = \begin{cases} 0 & T > T_c, \nu > \nu_c \\ 1 - \left[\frac{T}{T_c}\right]^{3/2} = 1 - \frac{\nu}{\nu_c} & T < T_c, \nu < \nu_c \end{cases} \tag{6.2.6}$$

Equation 6.2.6 is the result of previous reports from analysis on Ideal Bose Gases. Now the pressure can be easily obtained using $P = -\frac{\partial(A/N)}{\partial\nu}$:

$$P = P^{(0)} + \frac{4\pi a\hbar^2}{m}\left[\frac{1}{v^2}\left(1 - \frac{1}{2}\bar{\xi}^2\right) + \frac{1}{v}\bar{\xi}\frac{\partial\bar{\xi}}{\partial v}\right]$$

Using 6.2.6 we finally have:

$$P = \begin{cases} P^{(0)} + \frac{4\pi a\hbar^2}{mv^2} & (v > v_c, T > T_c) \\ P^{(0)} + \frac{2\pi a\hbar^2}{m}\left(\frac{1}{v^2} + \frac{1}{v_c^2}\right) & (v < v_c, T < T_c) \end{cases} \tag{6.2.7}$$

Similarly, we can compute all other thermodynamic parameters upto first order in the perturbation series of hard sphere diameter 'a'. Here again P^0 is the pressure for the ideal Bose gas. The results 6.2.5 and 6.2.7 are extremely simple and within expectations. These predict that the hard sphere potential in the imperfect Bose gas at low temperatures acts as a perturbation to the ideal bose gas leading to a simple extra correction term in all of the thermodynamic parameters.

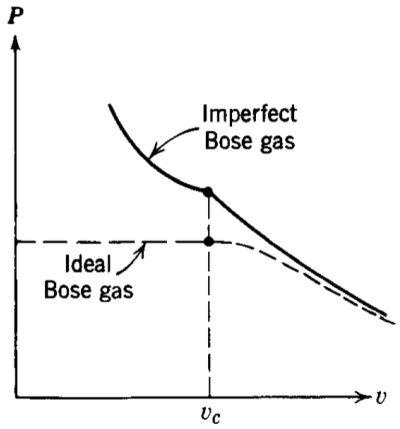

Figure 21: The Isotherms Of Ideal Vs Imperfect Bose Gas [5]

As expected the Pressure of Ideal and Imperfect Bose Gas seem to converge at $\nu = \infty$. There is one more interesting feature that pops out from these calculations that are in contradistinction to the ideal Bose gas. To see that, we first need to compute the internal energy for which we require the entropy. The entropy can be computed as S $= -\frac{\partial A}{\partial T}$. We then have:

$$S = S^{(0)} + N\frac{4\pi a\hbar^2}{m\nu}\left(\xi\frac{\partial\xi}{\partial T}\right) \tag{6.2.8}$$

Using 6.2.6, we finally have:

$$S = \begin{cases} S^{(0)} & (v > v_c, T > T_c) \\ S^{(0)} - N\frac{4\pi a\hbar^2}{m\nu}\left(1 - \left[\frac{T}{T_C}\right]^{3/2}\right)\left(\frac{3}{2}\frac{T^{1/2}}{T_C^{3/2}}\right) & (v < v_c, T < T_c) \end{cases} \tag{6.2.9}$$

Now, we are ready to compute the internal energy. This can be done by using the formula: U = A + TS. We then have:

$$U = \begin{cases} U^{(0)} + N\frac{4\pi a\hbar^2}{m\nu} & (v > v_c, T > T_c) \\ U^{(0)} + N\frac{4\pi a\hbar^2}{m\nu}\left[\left(1 - \frac{1}{2}\left\{1 - \left(\frac{T}{T_C}\right)^{3/2}\right\}^2\right) - \left(1 - \left[\frac{T}{T_C}\right]^{3/2}\right)\left(\frac{3}{2}\frac{T^{3/2}}{T_C^{3/2}}\right)\right] & (v < v_c, T < T_c) \end{cases} \tag{6.2.10}$$

Now, we see the magic. Let's calculate the change in specific heat across the transition line.

$$\begin{aligned} \frac{\Delta C_V}{Nk} &= \left|\frac{1}{Nk}\left[C_V(\text{at } T_C^+) - C_V(\text{at } T_C^-)\right]\right| \\ &= \left|\frac{1}{Nk}\left\{\left[\frac{\partial U}{\partial T}\right]_{T=T_C^+} - \left[\frac{\partial U}{\partial T}\right]_{T=T_C^-}\right\}\right| \end{aligned}$$

A simple calculation from 6.2.10 gives:

$$\frac{\Delta C_V}{Nk} = \frac{9a\pi\hbar^2}{mk\nu T_C} = \frac{9a}{2\lambda_C} g_{3/2}(1) \tag{6.2.11}$$

The second equality comes from the previous reports where all the appropriate functions are defined in detail.The beauty of 6.2.11 is that the change in specific heat as one crosses the transition point is non-zero. This is characteristic of a second-order phase transition phenomenon. Hence in our low temperature analysis, the Bose Einstein condensation appears to be a second order phase transition which is in contradistinction to the ideal bose gas where we showed that Bose-Einstein condensation is a self-consistent first order phase transition. The only difference till now in the imperfect gas is the introduction of finite size of the constituent particles. Note that the present model doesn't confirm that Bose-Einstein condensation is a second order phase transition but just says that it appears to be like a second order phase transition in the lowest order of the perturbation theory in the hard-sphere diameter 'a' (along with the length scale assumptions of thermal wavelength and inter-particle separation).

6.3 Imperfect Spin-1/2 Fermi Gas At Low Temperatures

In the last report we saw how spinless bosons behave under the Fermi's pseudopotential approximation. Now we will explore what happens to a spin-1/2 fermi gas under the same scheme. The energy eigenvalues as computed using 6.1.11 for the spin 1/2 Fermi gas comes out to be (see Appendix E3):

$$H_{eff} = H_0 + \frac{4\pi a\hbar^2}{m}\sum_{i<j}\delta\left(\vec{r}_i - \vec{r}_j\right) \tag{6.3.1}$$

$$E_n = \langle\Phi_n|H_{eff}|\Phi_n\rangle = \sum_{\vec{p}}(n_{p,+} + n_{p,-})\frac{|\vec{p}|^2}{2m} + \frac{4\pi a\hbar^2}{mV}\left(N_+N_-\right) = \epsilon_n + \frac{4\pi a\hbar^2}{mV}\left(N_+N_-\right) \tag{6.3.2}$$

Here $n_{p,\pm}$ is the number of particles with momentum p and in spin state $\pm 1/2$ sand N_+, N_- are the total number of particles in spin states $\pm 1/2$ respectively and ϵ_n denotes the ideal part. For a spin 1/2 in a canonical ensemble we have $N_+ + N_- = N$. Now define the canonical ensemble partition function for the imperfect fermi gas:

$$Q_n = \sum_n e^{-\beta\epsilon_n} \left[e^{-\frac{2a\lambda^2}{V}\left(NN_+ - N_+^2\right)} \right]$$

Here λ is the standard thermal de-Broglie wavelength. Just like the Boson case this can be re-written in terms of expectation values of ideal fermi gas as:

$$Q_N = Q_N^0 \left\langle e^{-\frac{2aN^2\lambda^2}{V}\left(\frac{N_+}{N} - \frac{N_+^2}{N^2}\right)} \right\rangle_0 \tag{6.3.3}$$

Here $Q_N^0 = \sum_n e^{-\beta\epsilon_n}$ and $\langle\rangle_0$ represents the thermodynamic ensemble average with respect to ideal Fermi Gas. Now, we can use all the tools available to us from Statistical Mechanics to find the thermodynamic parameters. For instance the Helmholtz free energy per particle of the system is:

$$A = A^0 + \log\left[\left\langle e^{-\frac{2aN^2\lambda^2}{V}\left(\frac{N_+}{N} - \frac{N_+^2}{N^2}\right)} \right\rangle_0 \right]$$

The superscript 0 is to denote the parameter for the ideal gas. Now using linearity of the expectation operator, $e^x \approx 1 + x$, $log(1 + x) \approx x$ and that the mean-square fluctuations for any observable at thermodynamic equilibrium are small $\left(\frac{1}{N^2}\left[\left\langle N_+^2\right\rangle_0 - \langle N_+\rangle_0^2\right] \approx 0\right)$, we have:

$$\frac{A}{N} = \frac{A^0}{N} + \frac{4\pi a\hbar^2}{m\nu}\left(\left\langle \frac{N_+}{N} \right\rangle_0 - \left\langle \frac{N_+^2}{N^2} \right\rangle_0\right) \tag{6.3.4}$$

Here $\nu = 1/\rho = V/N$. Note that since our Hamiltonian does not have a preference for any spin direction, we expect that at low temperatures $\langle N_+\rangle = \langle N_-\rangle = N/2$. Substituting this back in 6.3.4, we have:

$$\frac{A}{N} = \frac{A^0}{N} + \frac{3\pi a\hbar^2}{m\nu} \tag{6.3.5}$$

Hence the per particle Helmholtz free energy of the interacting system is simply related to that of the ideal system by an additive function of macroscopic parameters (V,N). The unexpected thing is that the correction term does not depend on T explicitly. However one needs to be careful while making such a statement as the whole approximation scheme is built around the low temperature approximation. Nevertheless, we move on to compute the macroscopic thermodynamic parameters of the system.
The pressure is simply: $-\frac{\partial A/N}{\partial \nu}$. This gives:

$$P = P^0 + \frac{3\pi a\hbar^2}{m\nu^2} \tag{6.3.6}$$

As expected the pressure exerted by the imperfect gas is more than that of the ideal gas. The entropy is given by: $S = -\frac{\partial A}{\partial T}$.This gives:

$$S = S^0 \tag{6.3.7}$$

This result is expected as the correction term has no explicit dependence on temperature. Now the internal energy is given by: $U = A + TS$. This gives:

$$U = U^0 + \frac{3N\pi a\hbar^2}{m\nu}$$

As expected the internal energy of the imperfect gas is more than that of the ideal gas. Finally the specific heat is given by: $c_V = \frac{\partial U}{\partial T}$. This gives:

$$C_V = C_V^0 \tag{6.3.8}$$

Again the specific heat doesn't change as the correction factor does not have an explicit temperature dependence.

Chapter 5: Mean-Field Approach To Handle Non-Ideal Gases

7 The Van-Der Waals Equation Of State

7.1 The Classical Derivation

Consider the Hamiltonian of the following form:

$$H = \sum_{i=1}^{N} \left(\frac{p_i^2}{2m} + U_{0i} \right) \tag{7.1.1}$$

Then the canonical ensemble partition function can be defined as:

$$Q_N(V,T) = \frac{1}{h^{3N} N!} \int \int d^3 r_1 \cdots d^3 r_n d^3 p_1 \cdots d^3 p_n e^{-\beta \sum_{i=1}^{N} (p_i^2/2m + U_{0,i})}$$

Making a simple change of variables: $r_2 \to r_1$, $p_2 \to p_1$ and $U_{02} \to U_{01}$ and realizing the indistinguishability of particles we have:

$$Q_N(V,T) = \frac{1}{N!} \left[\int \int e^{(p^2/2m + U_0)} \frac{d^3 r d^3 p}{h^3} \right]^N$$

where I have used the indistinguishability to completely remove the indices. Using the results of standard Gaussian integral, our partition function reduces to:

$$Q_N(V,T) = \frac{1}{N!} \left[\left(\frac{2\pi m}{\beta h^2} \right)^{3/2} \int e^{-\beta U_0} d^3 r \right]^N$$

The remaining configuration integral is solved by noting that due to finite size and subsequently strong repulsion of particles there are regions where $U_0 \to \infty$. Hence the integrand vanishes in these regions, This volume where the integrand vanishes is called the excluded volume V_0. In the remaining volume $V - V_{EX}$, we assume that U_0 varies slowly with respect to the inter-molecular separation. Thus, we replace the potential by a mean field value $\bar{U}_0$. Hence:

$$Q_N(V,T) \approx \frac{1}{N!} \left[\left(\frac{2\pi m}{\beta h^2} \right)^{3/2} (V - V_{EX}) e^{-\beta \bar{U}_0} \right]^N \tag{7.1.2}$$

Now, we estimate the values of $\bar{U}_0$ & V_0. The mean potential energy of the system is $\bar{E} = N\bar{U}_0$. Here we will be taking only binary collisions into consideration. Then the number of scattering interactions possible are: ${}^N C_2 \approx \frac{N(N-1)}{2} \approx N^2/2$ as $N \to \infty$. Let $\bar{u}$ be the average potential energy of this binary interaction. Then:

$$E \approx \frac{1}{2} N^2 \bar{u} \implies \frac{1}{2} N^2 \bar{u} = N\bar{U}_0$$
$$\implies \bar{U}_0 = \frac{1}{2} N \bar{u}$$

Now an estimation of the function $\bar{u}$ is required, Starting with the following simplistic assumption:

$$u(R) = \begin{cases} \infty & R<R\_0 \\ -u_0 \left(\frac{R_0}{R} \right)^\lambda & R>R\_0 \end{cases}$$

Here, of course $u_0>0$, $\lambda>0$. The most appropriate exponent usually is 6 (Appendix F1). The average interaction energy of the binary collisions can now be given as:

$$\begin{aligned}\bar{u} &= \int u(R)dP(R) \\ &= \int u(R)\frac{4\pi R^2}{V}dR \\ &= \left[-\frac{4\pi u_0}{V}\right]\int_{R_0}^{\infty}\left(\frac{R_0}{R}\right)^{\lambda}R^2dR\end{aligned}$$

The above integral converges only for $\lambda>3$. The mean interaction energy is given by:

$$\bar{U}_0 = -\alpha'\frac{N}{V}$$

$$\text{where } \alpha' = \left[\frac{2\pi u_0}{V}\right]\int_{R_0}^{\infty}\left(\frac{R_0}{R}\right)^{\lambda}R^2dR$$

The integral for the parameter α can be easily solved to get:

$$\alpha' = \left[\frac{2\pi u_0}{\lambda-3}\right]R_0^3 \qquad \text{where } \lambda \geq 4 \tag{7.1.3}$$

Now by nature of the potential, R_0 is the distance of closest approach or diameter of the particles of the system. Thus, due to the presence of 1 molecule in the system, other molecules now do not have access to a volume equivalent to the sphere of radius R_0. Hence the total excluded volume is roughly:

$$V_C = \frac{1}{2}N^2 \times \frac{4\pi}{3}R_0^3$$

But the total excluded volume is simply $V_{EX} = N \times V_0$ where V_0 is simply the excluded volume per particle. A simple comparison gives:

$$V_0 = b'N$$

$$\text{where } b' = \frac{2\pi}{3}R_0^3 = 4\left[\frac{4\pi}{3}\left(\frac{R_0}{2}\right)^3\right]$$

Hence:

$$b' = 4 \times \text{Volume of each particle} \tag{7.1.4}$$

Now, we are ready to write the canonical partition function. Substituting this back in 7.1.2, we have:

$$Q_N(V,T) \approx \frac{1}{N!}\left[\left(\frac{2\pi m}{\beta h^2}\right)^{3/2}(V-b'N)e^{-\beta\times-\alpha'\frac{N}{V}}\right]^N$$

Now pressure can be computed by using the formula: $P = \frac{1}{\beta}\frac{\partial \log(Q_N(V,T))}{\partial V}$. This gives:

$$P = \frac{1}{\beta}\left[\frac{N}{V-b'N} - \alpha'\frac{N^2\beta}{V^2}\right] \tag{7.1.5}$$

Rearranging this equation a bit to get:

$$(P + \alpha' n^2)(\nu - b') = kT$$
$$\text{where } n = \frac{N}{V} \text{ and } \nu = \frac{V}{N}$$

Now using the concept of molar volume: $V_\nu = \nu N_A$ (N_A is the Avagadro's number), we have the Van der waals equation of state in a much more familiar form from chemistry:

$$\left[P + \frac{a}{V_\nu^2}\right][V_\nu - b] = N_A kT = RT$$
$$\text{where } a = N_A^2 \alpha' \text{ and } b = N_A b'$$

7.2 Quantum Statistical Formulation Of Equation Of State For Real Gases On Nuclear Scale In GCE

The section below discusses the possible equation of states under the Van der waals' formalism in the cases where finite size (excluded volume effects) and attractive potential are considered within the system.

7.2.1 Effects Of Excluded Volume[7]

We are aware that the pressure of the system is related to the grand partition function $\mathscr{L}$ via the relation:

$$p(T, \mu) = \lim_{V \mapsto \infty} T \frac{\ln \mathscr{Z}(T, \mu, V)}{V} \tag{7.2.1}$$

Here μ is the chemical potential, V is the volume of the system in consideration and T is the temperature. The Grand partition function is defined using the canonical partition function as follows:

$$\mathscr{Z}(T, \mu, V) = \sum_{N=0}^{\infty} \mathrm{e}^{\mu N/T} Q(T, N, V) \tag{7.2.2}$$

Here Q is the canonical ensemble partition function. To introduce van der waals excluded volume effects, one needs to introduce an appropriate change in the canonical ensemble partition function. This is done by the following substitution:

$$Z^{\text{excl}}(T, N, V) = Z\left(T, N, V - v_0 N\right) \theta\left(V - v_0 N\right) \tag{7.2.3}$$

The excluded volume canonical partition function is quite simple to understand. It is simply the ideal gas partition function with the additional reasonable constraint that once a molecule occupies some volume in real space. the same volume is now unavailable for other molecules of the system. Thus, any additional molecule experiences the same system with a reduced volume. Here v_0 is the excluded volume per molecule and θ is the step function that makes sure that the total excluded volume does not exceed the volume of the system in consideration. The definition of θ function is given as follows:

$$\theta(x - x_0) = \begin{cases} 1 & x > x_0 \\ 0 & x < x_0 \end{cases}$$

This leads to the following formulation of the grand partition function:

$$\mathscr{Z}^{\text{excl}}(T,\mu,V) = \sum_{N=0}^{\infty} \mathrm{e}^{\mu N/T} Z\left(T,N,V-v_0N\right)\theta\left(V-v_0N\right) \tag{7.2.4}$$

Now here comes the great trick to solve 7.2.4. The idea is to take the Laplace transform to remove the complicated excluded volume dependence in the grand partition function. Taking the Laplace transform gives:

$$\begin{aligned}\hat{\mathscr{Z}}^{\text{excl}}\left(T,\mu,\xi\right) &\equiv \int_0^{\infty} \mathrm{d}V \mathrm{e}^{-\xi V}\,\mathscr{Z}^{\text{excl}}(T,\mu,V) \\ &= \int_0^{\infty} \mathrm{d}x\ \mathrm{e}^{-\xi x}\,\mathscr{Z}(T,\hat{\mu},x)\end{aligned} \tag{7.2.5}$$

Here $\hat{\mu} \equiv \mu - v_0 T\xi$. Equation 7.2.5 is obtained by taking the Laplace transform of 7.2.4 and then making the substitution $V \to x \Rightarrow x = V - v_0N$. Now the following property of Laplace transforms is the reason why we really did it. The pressure in GCE can be written as:

$$p^{\text{excl}}(T,\mu) \equiv \lim_{V\mapsto\infty} T\frac{\ln \mathscr{Z}^{\text{excl}}(T,\mu,V)}{V} = T\xi^*(T,\mu) \tag{7.2.6}$$

Here $\xi^*(T,\mu)$ is the extreme right singularity of $\hat{\mathscr{Z}}^{\text{excl}}$ in the variable ξ. For our function, there is only one singularity when the integral over x diverges in 7.2.5. Hence:

$$\xi^* = \lim_{x\mapsto\infty} \frac{\ln \mathscr{Z}(T,\tilde{\mu},x)}{x} \text{where} \quad \tilde{\mu} = \mu - v_0T\xi^* \tag{7.2.7}$$

Comparing 7.2.1 and 7.2.6, we have an implicit equation for pressure in the excluded volume model as:

$$p^{\text{excl}}(T,\mu) = p^{id}(T,\tilde{\mu}) \tag{7.2.8}$$

$$\text{where} \quad \tilde{\mu} = \mu - v_0 p^{\text{excl}}(T,\mu) \tag{7.2.9}$$

Now that we have a formulation for pressure, the other thermodynamic parameters can be easily computed as:

$$n_{\text{id}}^{\text{excl}}(T,\mu) \equiv \left(\frac{\partial p_{\text{id}}^{\text{exc}}}{\partial\mu}\right)_T = \frac{n_{\text{id}}(T,\tilde{\mu})}{1+v_0 n_{\text{id}}(T,\tilde{\mu})} \tag{7.2.10}$$

$$s_{\text{id}}^{\text{excl}}(T,\mu) \equiv \left(\frac{\partial p_{\text{id}}^{\text{excl}}}{\partial T}\right)_\mu = \frac{s_{\text{id}}(T,\tilde{\mu})}{1+v_0 n_{\text{id}}(T,\tilde{\mu})} \tag{7.2.11}$$

$$\varepsilon_{\text{id}}^{\text{excl}}(T,\mu) \equiv Ts_{\text{id}}^{\text{excl}} - p_{\text{id}}^{\text{excl}} + \mu n_{\text{id}}^{\text{excl}} = \frac{\varepsilon_{\text{id}}(T,\tilde{\mu})}{1+v_0 n_{\text{id}}(T,\tilde{\mu})} \tag{7.2.12}$$

The above formulae are only valid under first order approximation in the perturbation series of v_0 (Appendix F2). The above equations are quite easy to implement in a computer. First 7.2.8 is solved numerically and then 7.2.8-7.2.10 are used to compute all the basic macroscopic parameters of the

system.
A keen reader observes that the above formulation can be easily extended to a system of multi-particle species. Consider a system with 'k' different types of particles each being characterised by chemical potential μ_i and having an excluded volume of $v_0^{(i)}$. Then:

$$\begin{aligned} &p^{\text{excl}}\left(T,\mu_1,\ldots,\mu_k\right) = p\left(T,\tilde{\mu}_1,\ldots,\tilde{\mu}_k\right) \\ &\text{where} \\ &\tilde{\mu}_i = \mu_i - v_0^{(i)} p^{\text{exc}\,1}\left(T,\mu_1,\ldots,\mu_k\right), \quad i=1,\ldots,k \end{aligned} \tag{7.2.13}$$

Furthermore

$$n_i^{ex} = \left(\frac{\partial p^{excl}}{\partial \mu_i}\right)_T = \frac{n_i\left(T,\hat{\mu}_i\right)}{1+\sum\limits_k v_0^{(k)} n_k^{id}\left(T,\hat{\mu}_k\right)} \tag{7.2.14}$$

$$s_i^{excl} = \left(\frac{\partial p^{ex}}{\partial T}\right)_{\{\mu_i\}} = \frac{s_i^{id}\left(T,\hat{\mu}_i\right)}{1+\sum\limits_k v_0^{(k)} n_k^{id}\left(T,\hat{\mu}_k\right)} \tag{7.2.15}$$

$$\epsilon^{excl} = Ts - P + \sum_k \mu_i n_i = \frac{\sum\limits_i \epsilon_i^{id}\left(T,\hat{\mu}_i\right)}{1+\sum\limits_k v_{0k} n_k^{id}\left(T,\hat{\mu}_k\right)} \tag{7.2.16}$$

A similar formulation as above can be obtained by directly applying the mean field approach to the grand-partition function. Introducing excluded volume correction directly into the grand partition function (for a system with a single specie) we have:

$$\mathscr{Z}^{\text{excl}}(T,\mu,V) = \mathscr{Z}\left(T,\mu,V-v_0\bar{N}^{\text{excl}}\right) \tag{7.2.17}$$

Now we know that in GCE formulation:

$$P^{\text{excl}} = \frac{1}{\beta}\frac{\mathscr{Z}^{\text{excl}}(T,\mu,V)}{V}$$

$$\text{Using Taylor's Expansion } \rightarrow P^{\text{excl}} = \frac{1}{\beta}\left[\frac{\mathscr{L}(T,\mu,V)}{V} - \frac{v_0\bar{N}^{\text{excl}}}{V}\frac{\partial\mathscr{L}(T,\mu,V)}{\partial V}\right]$$

This finally gives:

$$P^{\text{excl}} = P_{id}(T,\mu)(1-v_0 n^{excl}(T,\mu)) \tag{7.2.18}$$

Now if $-v_0 n^{excl}(T,\mu) \ll 1$, 3.2.13 can be re-written by using the first order Taylor expansion as:

$$p^{\text{excl}}(T,\mu) \cong p_{id}\left(T,\mu - v_0 p(T,\mu)\right) = p_{id}(T,\tilde{\mu}) \tag{7.2.19}$$

Equation 7.2.17, under first order perturbation in v_0 can be re-written as:

$$P^{\text{excl}} = P_{id}(T,\mu)(1-v_0 n_{id}(T,\mu)) \tag{7.2.20}$$

Now all the other macroscopic parameters can be found using:

$$n_{\text{id}}^{\text{excl}}(T,\mu) \equiv \left(\frac{\partial p_{\text{id}}^{\text{exc}}}{\partial \mu}\right)_T$$
$$s_{\text{id}}^{\text{excl}}(T,\mu) \equiv \left(\frac{\partial p_{\text{id}}^{\text{excl}}}{\partial T}\right)_\mu$$
$$\varepsilon_{\text{id}}^{\text{excl}}(T,\mu) \equiv T s_{\text{id}}^{\text{excl}} - p_{\text{id}}^{\text{excl}} + \mu n_{\text{id}}^{\text{excl}}$$

Here the partial derivatives will be computed using equation 7.2.19. Of course, this formulation is going to follow the ideal gas much more closely as I have essentially removed the concept of shifted chemical potential and simply connected the excluded and ideal gas models with a small suppression factor. This will be shown in detail in the discussion of excluded gas model below.

For the van der waals' interaction the excluded volume per particle v_0 is estimated using the formula 7.1.4.

7.2.2 Excluded Volume Effects + Attractive Interactions[8]

Before inserting an ansatz form for the free energy of the system, let us look at the requirements that a quantum gas should satisfy considering the classical solution.

- If the parameters corresponding to the non-idealities ('a' for attractive interactions and 'b' for finite size) are 0, then the formulation should give solutions corresponding to an ideal quantum gas.
- In the thermodynamic region where quantum fluctuations can be ignored, the solutions should reduce to that of the classical case.
- The entropy should be non-negative and the formulation should follow the third law of thermodynamics i.e. Entropy $\to 0$ as $t \to 0$.

Considering this in mind, the following ansatz form of free energy in the canonical ensemble is introduced:

$$F(T,V,N) = F^{\text{id}}(T, Vf(\eta), N) + Nu(n) \tag{7.2.21}$$

Here $\eta = bn/4$, $n = N/V$, $F^{\text{id}}(T, Vf(\eta), N)$ gives the free energy of the corresponding ideal gas system and $u(n)$ gives the attractive potential in consideration of the system. Now by construction of 7.2.19, the first two points in the requirements are satisfied. The third point is also satisfied which can be seen by an explicit calculation of entropy as follows:

$$S(T,V,N) = -\left(\frac{\partial F}{\partial T}\right)_{V,N} = S^{\text{id}}(T, Vf(\eta), N) \tag{7.2.22}$$

The RHS of 7.2.20 follows the last requirement as quantum ideal gases do not violate the third law of thermodynamics. The remaining quantities can be calculated as:

$$\begin{aligned}
E(T,V,N) &= F - TS = E^{\mathrm{id}}(T, Vf(\eta), N) + Nu(n) \\
p(T,V,N) &= -\left(\frac{\partial F}{\partial V}\right)_{T,N} \\
&= p^{\mathrm{id}}(T, Vf(\eta), N)\left[f(\eta) - \eta f'(\eta)\right] + n^2 u'(n) \\
\mu(T,V,N) &= \left(\frac{\partial F}{\partial N}\right)_{T,V} \\
&= \mu^{\mathrm{id}}(T, Vf(\eta), N) - \frac{b}{4} f'(\eta) p^{\mathrm{id}}(T, Vf(\eta), N) \\
&\quad + u(n) + nu'(n)
\end{aligned}$$

Now in the thermodynamic limit, all the intensive parameters in the canonical ensemble depend only on the temperature (T) and number density (n). Hence, finally we have:

$$p(T,n) = p^{\mathrm{id}}_{\mathrm{CE}}\left(T, \frac{n}{f(\eta)}\right)\left[f(\eta) - \eta f'(\eta)\right] + n^2 u'(n) \tag{7.2.23}$$

$$s(T,n) = \frac{S}{V} = f(\eta) s^{\mathrm{id}}_{\mathrm{CE}}\left(T, \frac{n}{f(\eta)}\right) \tag{7.2.24}$$

$$\varepsilon(T,n) = \frac{E}{V} = f(\eta)\varepsilon^{\mathrm{id}}_{\mathrm{CE}}\left(T, \frac{n}{f(\eta)}\right) + nu(n) \tag{7.2.25}$$

$$\mu(T,n) = \mu^{\mathrm{id}}_{\mathrm{CE}}\left(T, \frac{n}{f(\eta)}\right) - \frac{b}{4} f'(\eta) p^{\mathrm{id}}_{\mathrm{CE}}\left(T, \frac{n}{f(\eta)}\right) + u(n) + nu'(n) \tag{7.2.26}$$

Here ^{id} denotes ideal gas and $_{CE}$ denotes the canonical ensemble. Now we use the thermodynamic equivalence of CE and GCE to transform the CE relations into the GCE ones. However before that, we introduce the following notation:

$$\begin{aligned}
p^* &= p^{\mathrm{id}}_{\mathrm{CE}}\left(T, \tfrac{n}{f(\eta)}\right), \quad n^* = n^{\mathrm{id}}_{\mathrm{CE}}\left(T, \tfrac{n}{f(\eta)}\right) \\
s^* &= s^{\mathrm{id}}_{\mathrm{CE}}\left(T, \tfrac{n}{f(\eta)}\right), \quad \mu^* = \mu^{\mathrm{id}}_{\mathrm{CE}}\left(T, \tfrac{n}{f(\eta)}\right)
\end{aligned} \tag{7.2.27}$$

Looking at the expression of μ^*, we identify the following as the number density of the ideal system:

$$\frac{n}{f(\eta)} = n^{\mathrm{id}}\left(T, \mu^*\right) \tag{7.2.28}$$

From 7.2.26, it follows that:

$$p^* = p^{\mathrm{id}}\left(T, \mu^*\right), \quad n^* = n^{\mathrm{id}}\left(T, \mu^*\right), \quad s^* = s^{\mathrm{id}}\left(T, \mu^*\right) \tag{7.2.29}$$

Now from 7.2.27 and 7.2.21-7.2.24, one finds that:

$$p(T,\mu) = \left[f(\eta) - \eta f'(\eta)\right] p^{id}\left(T, \mu^*\right) + n^2 u'(n) \tag{7.2.30}$$

$$s(T,\mu) = f(\eta) s^{id}\left(T, \mu^*\right) \tag{7.2.31}$$

$$\varepsilon(T,\mu) = f(\eta)\varepsilon^{id}\left(T, \mu^*\right) + nu(n) \tag{7.2.32}$$

$$n(T,\mu) = f(\eta) n^{id}\left(T, \mu^*\right) \tag{7.2.33}$$

In the above equations, it is implied that $n \equiv n(T,\mu)$. The value of shifted chemical potential $\mu^* = \mu^*(T,\mu)$ itself is calculated using the following implicit equation:

$$\mu = \mu^* - \frac{b}{4} f'(\eta) p^* + u(n) + n u'(n) \tag{7.2.34}$$

This completes the GCE analysis for a generalised system. These equations are difficult to solve analytically however a computer can easily solve it numerically. First 7.2.22 and 7.2.31 are used to solve for μ^* which is then used to compute $n(T,\mu)$. Finally 7.2.28-7.2.30 are used to compute the remaining quantities.
Finally for the van der waals' model we have the following substitutions for $f(\eta)$ and u(n):

$$f(\eta) = 1 - 4\eta \tag{7.2.35}$$

$$u(n) = -an \tag{7.2.36}$$

Substituting these back into 7.2.28-7.2.32, we have for a van der waals' model:

$$p^{int}(T,\mu) = p^{id}(T,\mu^*) - a(n^{int}(T,\mu))^2 \tag{7.2.37}$$

$$n^{int}(T,\mu) = \frac{n^{id}(T,\mu^*)}{1 + b n^{id}(T,\mu^*)} \tag{7.2.38}$$

$$\mu^* = \mu - b p^{id}(T,\mu^*) + 2a n^{int}(T,\mu) \tag{7.2.39}$$

$$s \equiv s(T,\mu) = (1 - b n^{id}(T,\mu^*)) s^{id}(T,\mu^*) \approx \frac{s^{id}(T,\mu^*)}{1 + b n^{id}(T,\mu^*)} \tag{7.2.40}$$

$$\varepsilon \equiv \varepsilon(T,\mu) = \frac{\varepsilon^{id}(T,\mu^*)}{1 + b n^{id}(T,\mu^*)} - a n^2 \tag{7.2.41}$$

Again equations 7.2.35-7.2.39, can be easily extended to a system containing many species. For a multi-particle system[9] of baryons(B) and anti-baryons ($\bar{B}$) (not interacting with each other), we

have:

$$p(T,\mu) = p_B(T,\mu) + p_{\bar{B}}(T,\mu) \tag{7.2.42}$$

$$p_{B(\bar{B})}(T,\mu) = \sum_{k\in B(\bar{B})} p_k^{id}\left(T,\mu_k^{B(\bar{B})*}\right) - an_{B(\bar{B})}^2 \tag{7.2.43}$$

$$\mu_k^{B(\bar{B})*} = \mu_k - bp_{B(\bar{B})} - abn_{B(\bar{B})}^2 + 2an_{B(\bar{B})} \tag{7.2.44}$$

$$n_{B(\bar{B})} = \frac{\sum\limits_{k\in B(\bar{B})} n_k^{id}\left(T,\mu_k^{B(\bar{B})*}\right)}{1 + b\sum\limits_{k\in B(\bar{B})} n_k^{id}\left(T,\mu_k^{B(\bar{B})*}\right)} \tag{7.2.45}$$

$$s_{B(\bar{B})} = \frac{\sum\limits_{k\in B(\bar{B})} s_k^{id}\left(T,\mu_k^{B(\bar{B})*}\right)}{1 + b\sum\limits_{k\in B(\bar{B})} n_k^{id}\left(T,\mu_k^{B(\bar{B})*}\right)} \tag{7.2.46}$$

$$\varepsilon_{B(\bar{B})} = \frac{\sum\limits_{k\in B(\bar{B})} \varepsilon_k^{id}\left(T,\mu_k^{B(\bar{B})*}\right)}{1 + b\sum\limits_{k\in B(\bar{B})} n_k^{id}\left(T,\mu_k^{B(\bar{B})*}\right)} - an_{B(\bar{B})}^2 \tag{7.2.47}$$

Chapter 6: Application To Hadron Resonance Gas

8 Application To Hadron Resonance Gas

The ideal hadron resonance gas in consideration contains all the Baryons and Mesons (which can be built using up,down and strange) available to us from the Particle Data Group. All particles here are considered to be stable and their decays are not included in this analysis. Further we are working at extremely high temperatures and hence particle production is a real possibility. Hence the choice of ensemble is the Grand Canonical Ensemble. For the time being the chemical potential includes only the baryonic chemical potential and hence what is conserved in our analysis is simply the Baryon number. I have parameterized the chemical potential as:

$$\mu = B \cdot \mu_B \tag{8.0.1}$$

where B=0/1 for mesons/baryons respectively. Further, I am using quantum statistics and hence baryons follow the fermionic while mesons follow the bosonic formulation in the Grand Canonical Ensemble.

8.1 Data Used

The data in consideration consists of two excel files containing information of all the stable Baryons and Mesons upto an invariant rest mass of 2500 MeV. Further, only those baryons and mesons are taken into consideration which can be constructed using the up,down and strange quarks. Both files contain 6 columns which represent the 'index no.', 'Baryon/Meson Name', 'Mass(MeV)', 'Degeneracy factor (2S+1)(2I+1)','Baryon Number (0 for Mesons and 1 for Baryons)' and 'Type Of Quantum particle (0 for Bosons and 1 for Fermions)'. There are 66 Mesons and 64 Baryons that satisfy our required criterion. All the data is taken from pdg (Particle Data Group). To access the excel files please click on the following hyperlink: Data For Hadron Resonance Gas.

8.2 The Ideal Hadron Resonance Gas

This section uses the ideal gas formalism defined in the previous reports. Before I start combining the data for all the particles present in our hadron gas, let us first look at the temperature dependence of the pressure variable on the invariant mass parameter of the individual hadron.

8.2.1 Looking For Temperature Dependence For Pressure Variable As A function Of Invariant Mass At 0 Chemical Potential

In the GCE, for an individual hadron having a degeneracy factor 'g', the formula for the pressure variable at 0 chemical potential reads:

$$p^{id}_{F/B} = \left(\frac{g}{2\pi^2\hbar^3}\right)\int_m^\infty \left(\frac{1}{3}\left(\varepsilon^2 - m^2\right)^{3/2}\right)\frac{1}{e^{\beta\varepsilon} \pm 1}d\epsilon \tag{8.2.1}$$

Here '+' sign is for fermions and '-' sign is for bosons. The idea is to generate a power law relation between the pressure and the temperature variable which looks like:

$$P \propto T^b \tag{8.2.2}$$

The idea is to characterize the formula for the variable 'b' in terms of the invariant mass of the hadron. The following fitting formula was used for this purpose:

$$b = Am^B + C \tag{8.2.3}$$

This formulation was implemented in python to generate the following results:

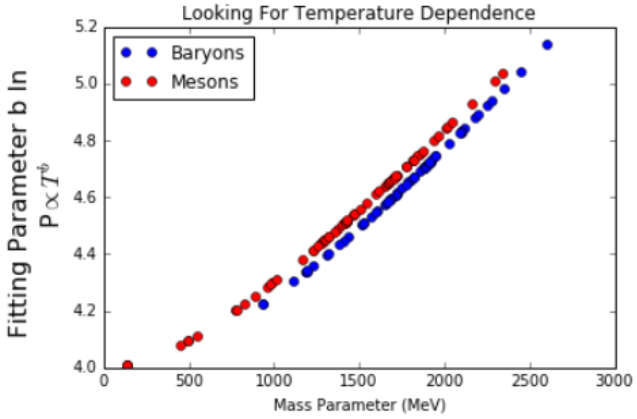

(a) Parameter 'b' As Function Of Mass For Bosons/Fermions

```
For A x**B + C, respective coefficients are:
[2.21125708e-05 1.38284527e+00 3.98183344e+00]
The error in the fits are:
[7.42820567e-06 4.21599675e-02 1.50049342e-02]
```

(b) Value Of Fit Parameters A,B,C in 4.2.3

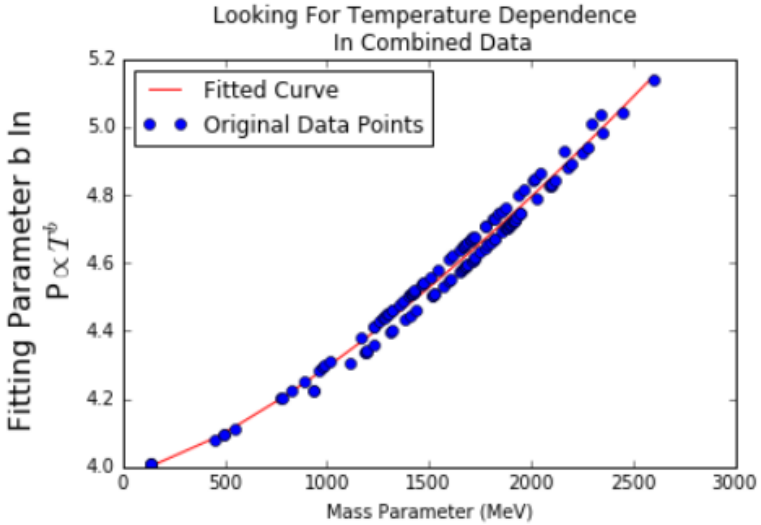

(c) Fitted Curve (Done After Combining Bosons And Meson Data)

Figure 22: Looking For Temperature Dependence For Pressure Variable As A function Of Invariant Mass At 0 Chemical Potential

As one can observe from part (b); the value of fit parameter A is quite small nearly nullifying the effect of mass parameter 'm'. The main contribution comes from the parameter 'C' which is roughly equal to 4 which is what we divide the pressure variable with to get the normalised (dimensionless) pressure.

8.2.2 Graphs For Ideal Hadron Resonance Gas

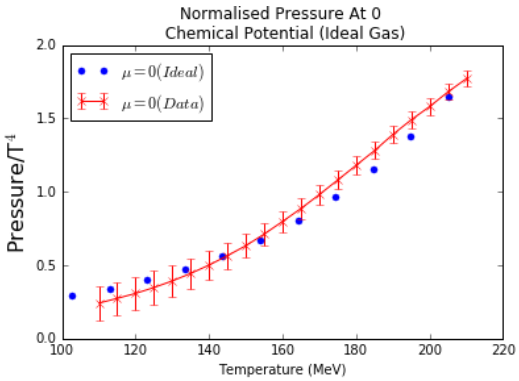

(a) Graph of Normalised Pressure vs Temperature

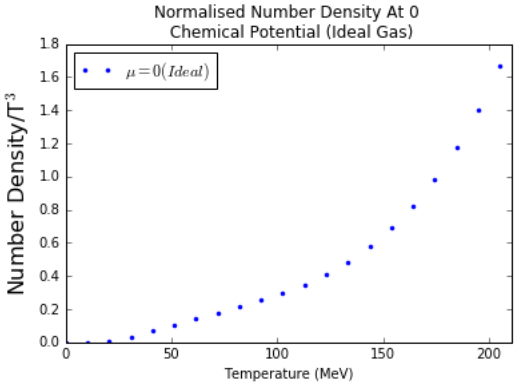

(b) Graph of Normalised Number Density vs Temperature

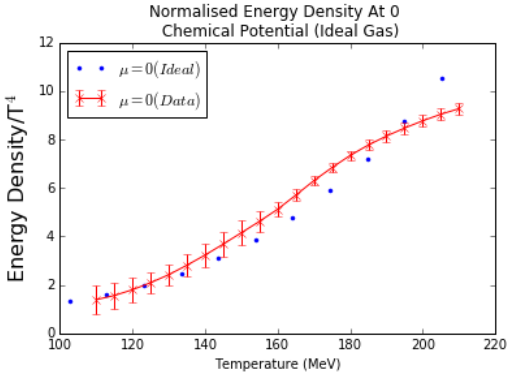

(c) Graph of Normalised Energy Density vs Temperature

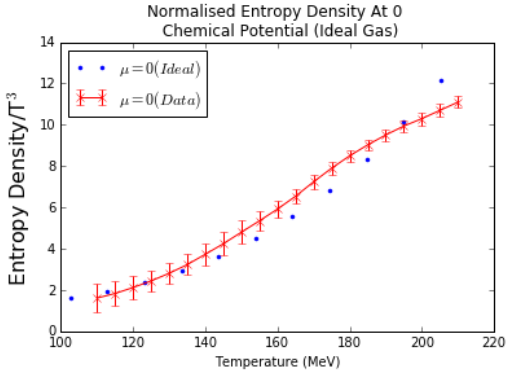

(d) Graph of Normalised Entropy Density vs Temperature

Figure 23: Graphs For A Relativistic Ideal Hadron Resonance Gas At 0 Chemical Potential

To view the non-normalised graphs and graphs for different values of the baryonic chemical potential coefficient μ_B, see (Appendix G1). **The data for 0 chemical potential has been obtained from reference [14] and represents the lattice QCD results of the Wuppertal-Budapest.**

8.3 Van Der Waals' Excluded Volume Model For Hadron Resonance Gas

This section has been divided into three parts: First where we have used the formulation as defined by 7.2.12-7.2.15, second where we have used the formalism as defined by 7.2.17-7.2.19 and third where we have compared the results for both the formulations. In this subsection, this is done only for 0 chemical potential. The computation is done for hard sphere radius of 0.1 fm. To view the same results for different values of the baryonic chemical potential coefficient μ_B, see (Appendix G2).

8.3.1 Part 1: Using Formalism As Defined In 7.2.12-7.2.15

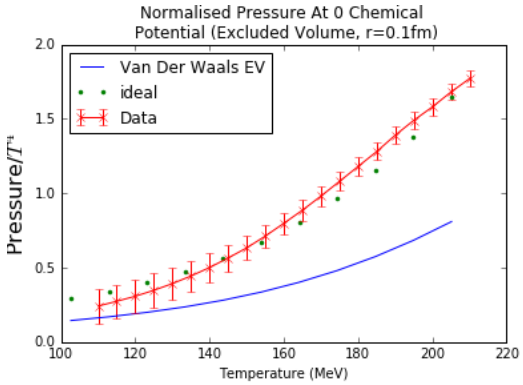

(a) Graph of Normalised Pressure vs Temperature

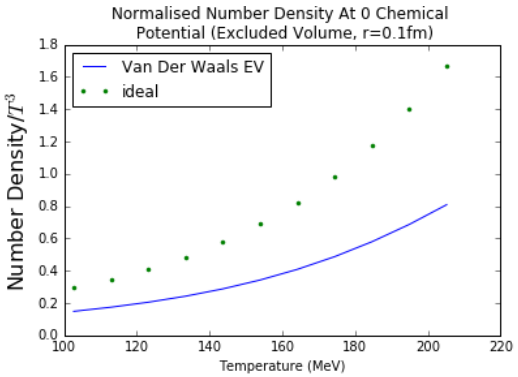

(b) Graph of Normalised Number Density vs Temperature

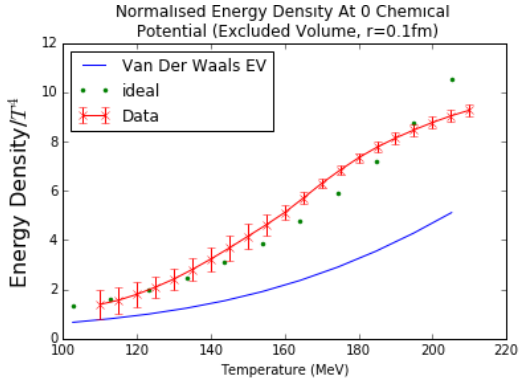

(c) Graph of Normalised Energy Density vs Temperature

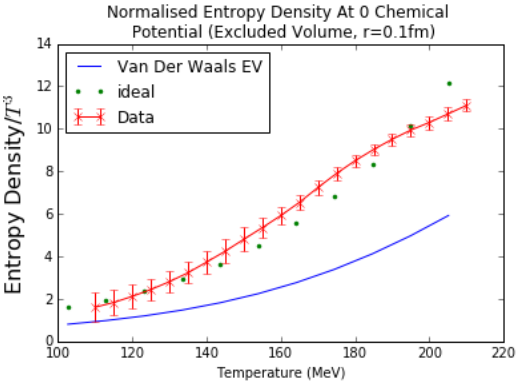

(d) Graph of Normalised Entropy Density vs Temperature

Figure 24: Graphs Of Some Important Parameters For A General Relativistic Van Der Waals'EV Hadron Resonance Gas At 0 Chemical Potential

At this point, it is instructive to check whether our formulation is thermodynamically consistent or not. This means that our macroscopic thermodynamics variables should indeed follow the first law of thermodynamics. By construction of the formalism, one can easily see that the equations are thermodynamically consistent. However, to be sure we compute energy density of the system in two different ways (LHS and RHS of 3.2.15) for 0 chemical potential and check if we are getting the same values of energy density. We plot the energy densities computed via two different ways against each other and check if the curve obtained can be fitted with a straight line. If the values are same then we should get the fit curve as a straight line with slope 1 and 0 y-intercept.
Performing the fit gave me the following results: As we can see from part (b) of the figure below, the fit slope is indeed 1. The y-intercept is quite close to 0, however there is a huge error in it. This implies that the values obtained through the two ways are not exactly equal everywhere. This can be traced back to rounding-off errors and errors while computing the integrals involved by the python

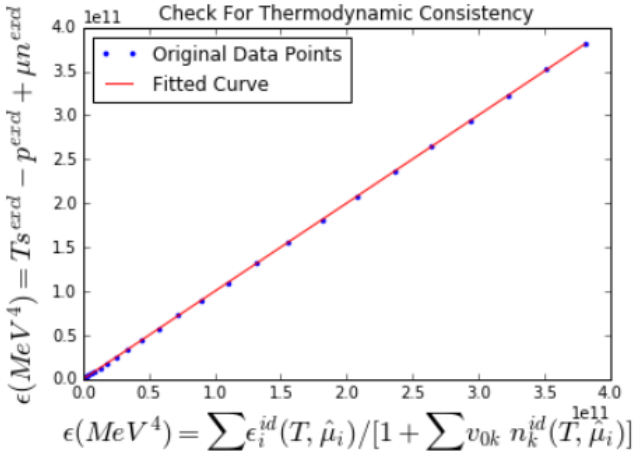

(a) Graph Of energy density computed two ways

```
For A*x + B, respective coefficients are:
[1.00000000e+00 7.81302034e-06]
The error in the fits are:
[2.12259098e-12 5.25649066e-01]
```

(b) Value Of Fit Parameters And Errors In Them

Figure 25: Check For Thermodynamic Consistency

compiler. Hence our formulation is thermodynamically consistent.

8.3.2 Part 2: Using Formalism As Defined In 7.2.17-7.2.19

From the graphs shown below, one can see that in this formulation the excluded volume model follows the ideal gas model much more closely. This is well within expectations as we removed most of the effects of the excluded volume model when we didn't write the equations in terms of the shifted chemical potential as in the previous case. The correction term introduced shows significant effect only at a high chemical potential and a temperature greater than that of 250 MeV.The main motive here is to understand that ones needs to be careful while inserting the equations into the computer. A small change in formalism can lead to very different results as we see here.

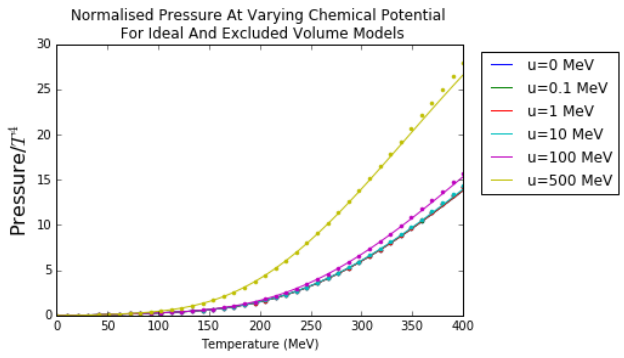

(a) Graph of Normalised Pressure vs Temperature

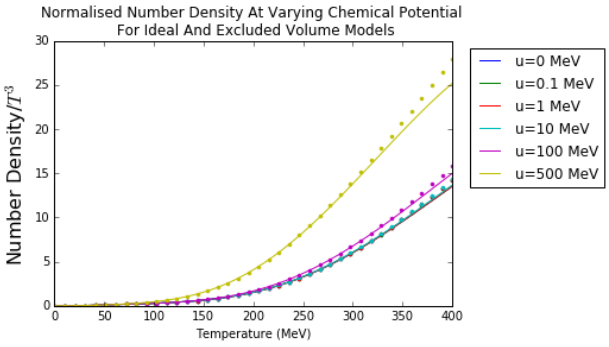

(b) Graph of Normalised Number Density vs Temperature

Figure 26: Normalised Graphs For Van Der Waals' EV Hadron Resonance Gas At Various Chemical Potential. Dots Represent Ideal Gas and Solid Line represents calculation done via Part 2 Formalism

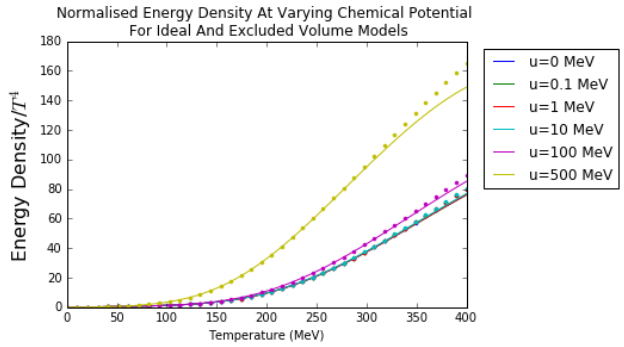

(a) Graph of Normalised Energy Density vs Temperature

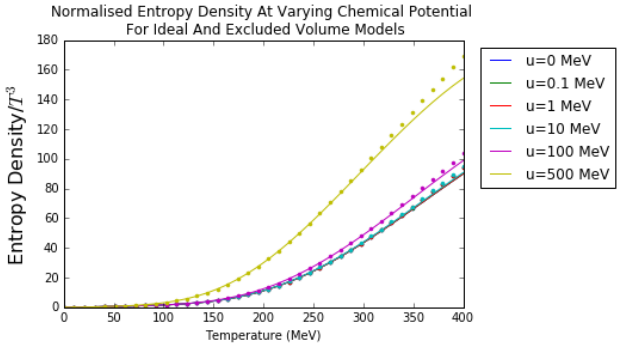

(b) Graph of Normalised Entropy Density vs Temperature

8.3.3 Comparing Results Of Part - I and II:

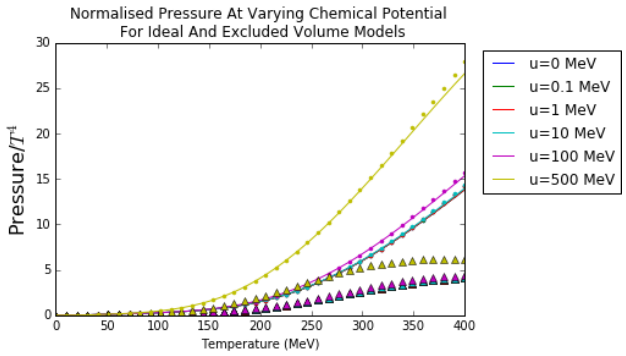

(a) Graph of Normalised Pressure vs Temperature

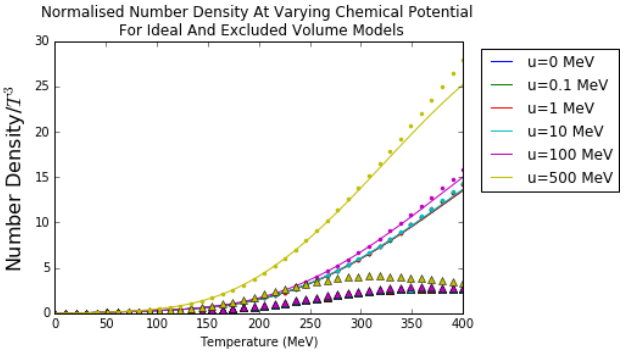

(b) Graph of Normalised Number Density vs Temperature

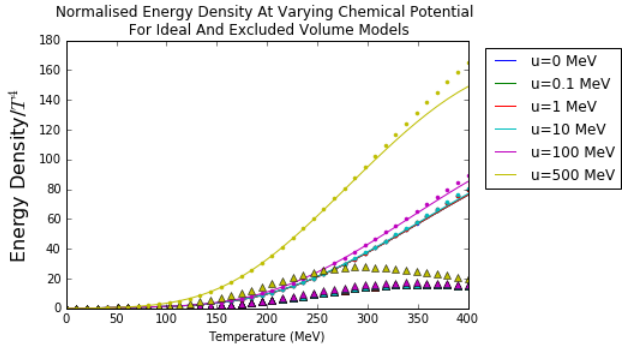

(c) Graph of Normalised Energy Density vs Temperature

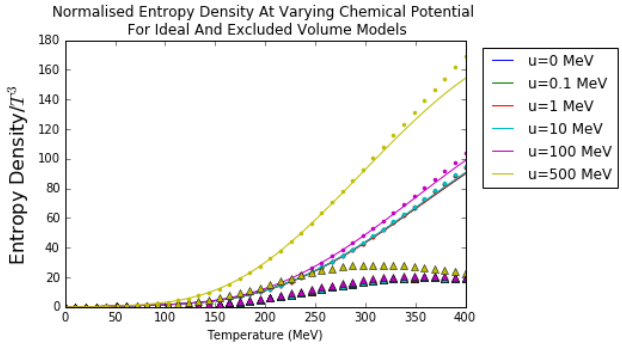

(d) Graph of Normalised Entropy Density vs Temperature

Figure 28: Comparing Normalised Graphs. Dots represent ideal gas while triangles and solid line represents calculation done via Part- I and II respectively

8.4 Interacting Van Der Waals' Hadron Resonance Gas

8.4.1 Mesons And Baryons Are Part Of The Same System

In this subsection, I have treated baryons and mesons on equal footing. They are the part of the same system and Meson-Baryon interactions exist in this system. These interactions are parameterised by the variable 'a' in the van der waals' equation of state and is same for Meson-Meson and Baryon-Baryon attractive interactions. Of course excluded volume effects are taken into consideration but it is assumed that all the particles occupy the same excluded eigenvolume (average excluded volume per particle). The values for the van der waals' parameters are chosen[8] to be: a = $329 MeV fm^3$ and b = $3.41 fm^3$ corresponding to a hard sphere radius of $0.59 fm$.

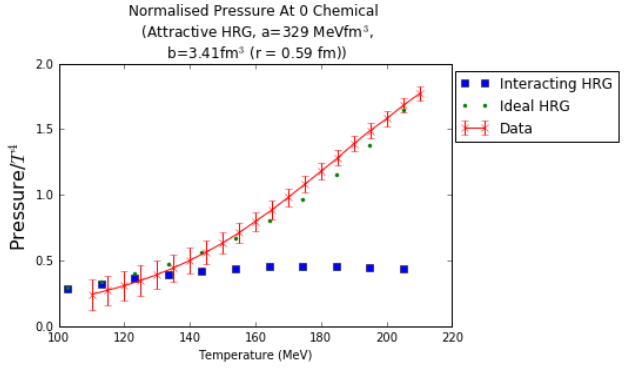

(a) Graph of Normalised Pressure vs Temperature

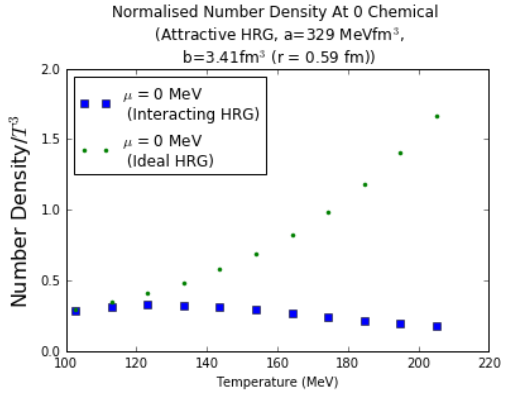

(b) Graph of Normalised Number Density vs Temperature

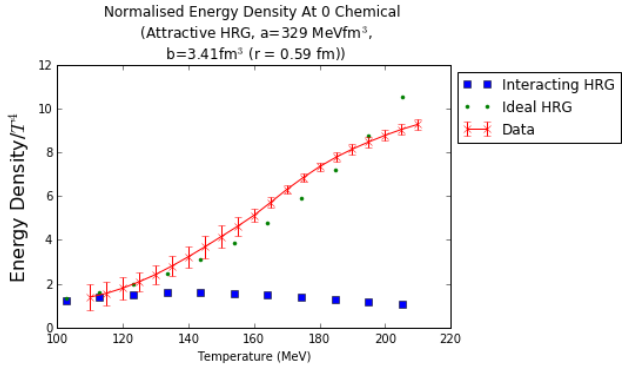

(c) Graph of Normalised Energy Density vs Temperature

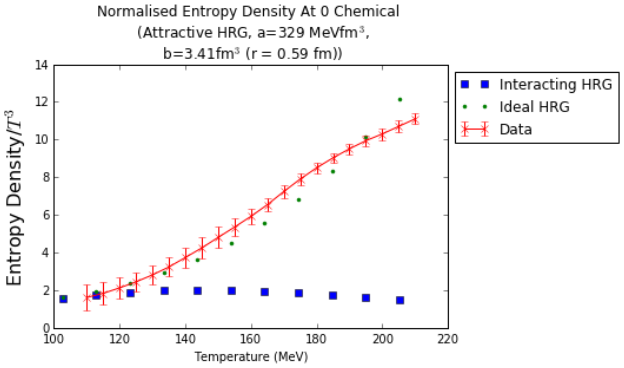

(d) Graph of Normalised Entropy Density vs Temperature

Figure 29: Normalised Graphs For Interacting Van Der Waals' HRG At 0 Chemical Potential

These graphs are plotted only for a temperature range of 0-200 MeV as beyond this the deviations from the ideal gas model are quite large. This happens because the system can no longer be described as a resonance hadron gas. For more information visit Appendix G3)

8.4.2 Mesons And Baryons Belong To Different Subsystems

In this subsection, Baryons and Mesons are considered to be a part of different subsystems and they are not interacting with each other. The Meson subsystem is assumed to be ideal while the Baryon subsystem includes the Van Der Waals' interactions. The parameters chosen for interacting part is same as that of the previous subsection.

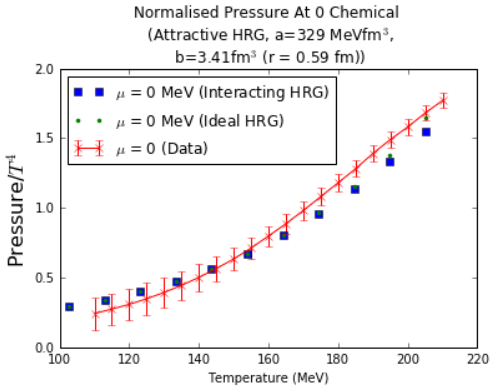

(a) Graph of Normalised Pressure vs Temperature

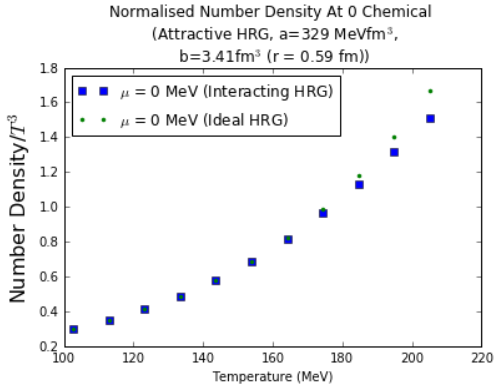

(b) Graph of Normalised Number Density vs Temperature

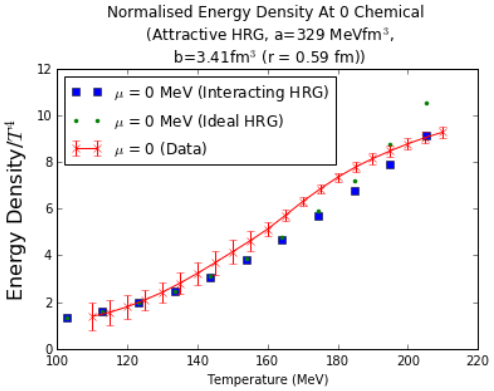

(c) Graph of Normalised Energy Density vs Temperature

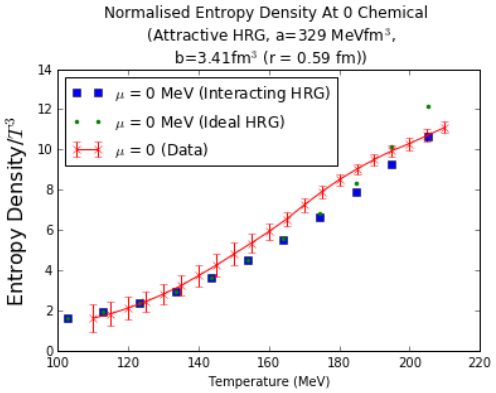

(d) Graph of Normalised Entropy Density vs Temperature

Figure 30: Normalised Graphs For Interacting Van Der Waals' HRG At 0 Chemical Potential. Here Mesons and Baryons belong to different sub-systems. Mesons are considered to be ideal while baryons are considered to a interacting Van Der Waals' subsystem.

As expected, this model follows the ideal gas much more closely than when both mesons and baryons were part of the same interacting system.

8.4.3 An Interesting Case

In reference 9, the authors have taken the value of van der waals' parameter a= 1250 MeV fm^3 and a hard sphere radius value of 0.7 fm. Even under my analysis (0 chemical potential), if the mesons and

baryons are allowed to be the part of the same system (like in 8.4.1), the shifted baryonic chemical potential for mesons at a temperature of 102.6 MeV goes as high as 138.9 Mev (Fig 31). This is clearly a problem since the invariant rest mass of the pion family is below (extremely close) to this value. Hence the Bose integrals will simply diverge in our original formulation. The way to get around such divergences is to assume that at higher temperatures, either the mesons follow the simple Boltzmann statistics or allow mesons and baryons to be a part of different subsystems (as proceeded in 8.4.2). The authors in reference proceed forward by using the latter technique.

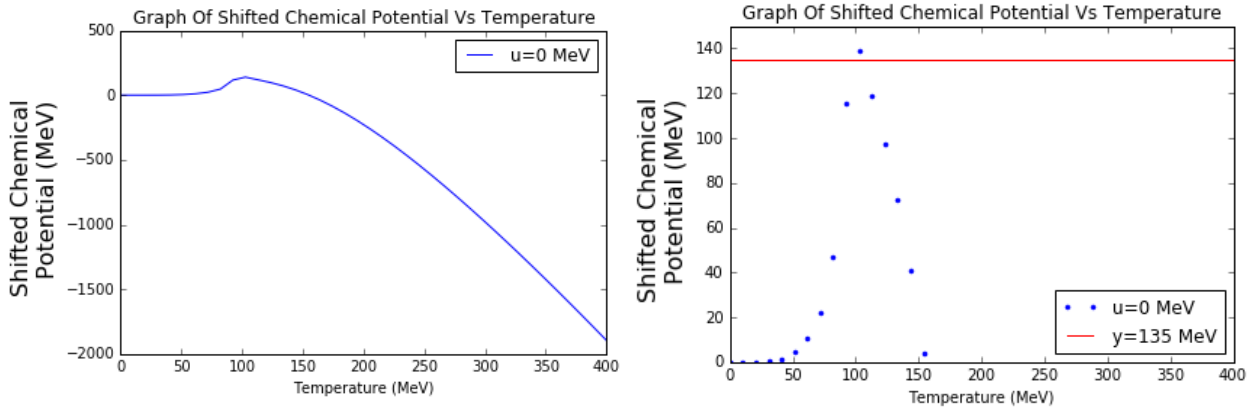

(a) Complete Graph

(b) Zoomed Version

Figure 31: Graphs Of Shifted Chemical Potential For Mesons And Baryons

8.5 Conclusions

- The ideal gas model for hadron resonance gas (0 chemical potential) is in quite good agreement with the lattice qcd data of Wuppertal-Budapest. The normalized pressure, energy density and entropy density are very well described by this model. Significant deviations start appearing for T $>$ 150 MeV.
- The Van der Waals' EV model (hard-sphere radius=0.1 fm) gives values for relevant normalised thermodynamic quantities, which are significantly lower than what is obtained from ideal HRG and the lattice qcd data.
- The case of interacting HRG is quite interesting. The analysis is done for van der waals' parameters a=329 MeVfm^3 and b=3.41 fm^3:
  - If mesons and baryons are kept on the same footing and are included as part of the same system then interacting HRG grossly underestimates the relevant thermodynamic parameters when compared to lattice data. This is quite expected since Van der Waals' EV model was already underestimating the parameters (and that too when the sphere radius was lower than what is taken for this case).

– Consider mesons and baryons to be the parts of different sub-systems. Further allowing mesons to be ideal while treating baryons using the interacting HRG formalism leads to excellent agreement with the lattice qcd data.

9 Particle Production In Relativistic Heavy Ion (Au-Au) Collisions

9.1 Extracting The Chemical Freeze-Out Parameters

9.1.1 Particle Yields For Normal Hadrons

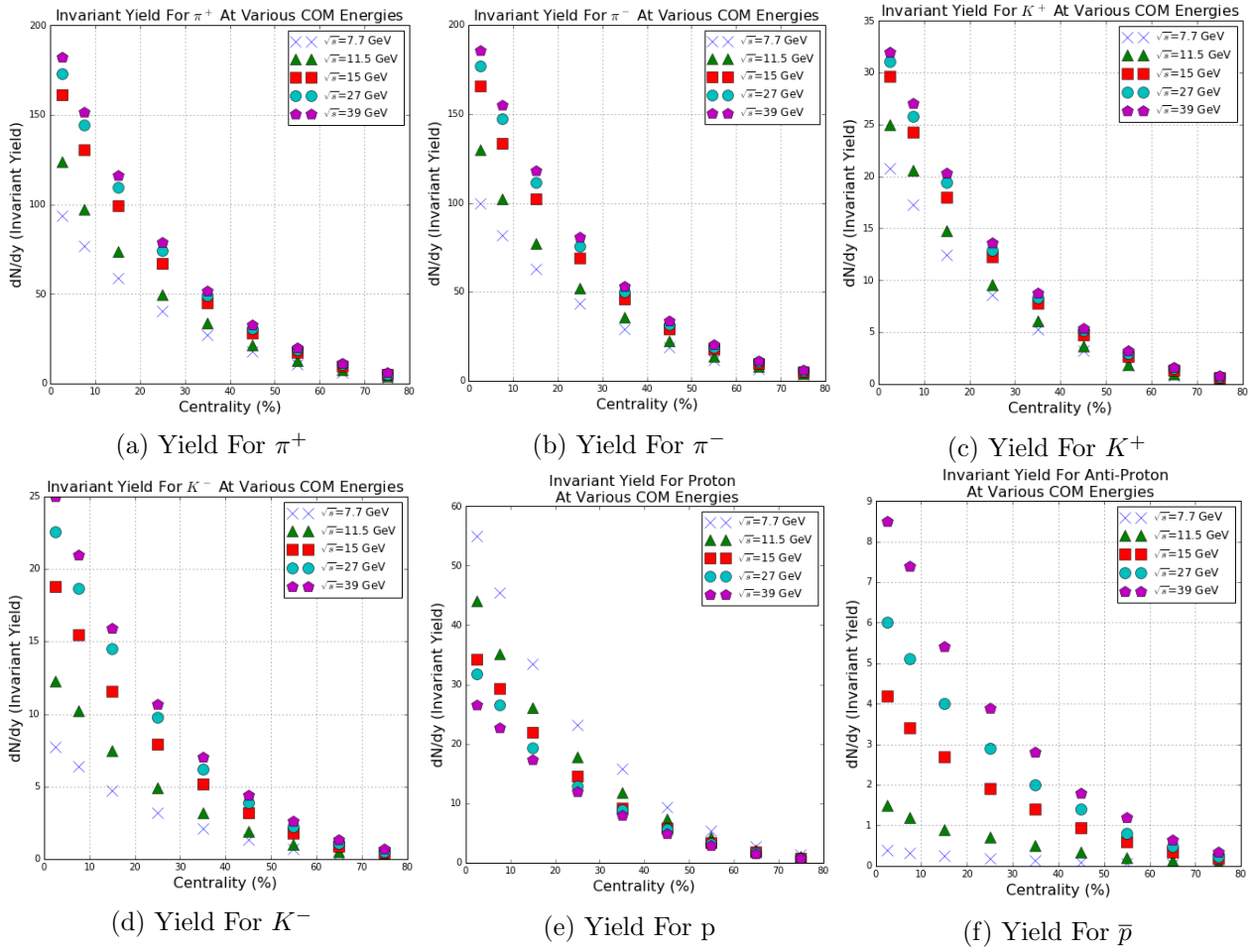

(a) Yield For π^+ (b) Yield For π^- (c) Yield For K^+

(d) Yield For K^- (e) Yield For p (f) Yield For $\overline{p}$

Figure 32: Graphs Of Particle Yields vs Collision Centrality

In this subsection we will be looking at the particle yields of $\pi^+, \pi^-, K^+, K^-, p$ and $\overline{p}$. I have drawn the graphs for particle yields as a function of collision centrality. In reference [10], the events have been divided into 9 centrality classes:classes: 0–5%, 5–10%, 10–20%, 20–30%, 30–40%, 40–50%, 50–60%, 60–70%, and 70–80%. In the following graphs each centrality class is represented by its center point. For eg: the centrality class 10-20 will be represented by the point 15 on the X-axis. The center of

mass energies that have been taken into consideration are 7.7 GeV, 11.5 GeV, 19.6 GeV, 27 GeV and 39 GeV. All the data presented in this section has been taken from reference 10 which itself is taken at the mid-rapidity range of $y =\mid 0.1 \mid$.
As expected, the particle yields for all particles (except proton) increase with increase in the center of mass energy of the collision. For protons, interestingly, the maximum yield is at the lowest energy of 7.7 GeV (suggesting highest baryon density at midrapidity for this energy). The main reason for this trend is that at lower energies, the hadrons maintain their identity throughout multiple collisions and hence partonic degrees of freedom are not as important. Thus, baryon density becomes quite high when collision energies are small ($0 \sim 30$ GeV). Further, lower collision centrality implies a head on collision, a higher production of particles and consequently higher particle yields.

9.1.2 Particle Yields For Strange Hadrons

In this subsection we will be looking at the particle yields of $K^0_S, \Lambda, \overline{\Lambda}, \Xi^-$ and $\overline{\Xi}^+$. I have drawn the graphs for particle yields as a function of collision centrality. In reference [10], the events have been

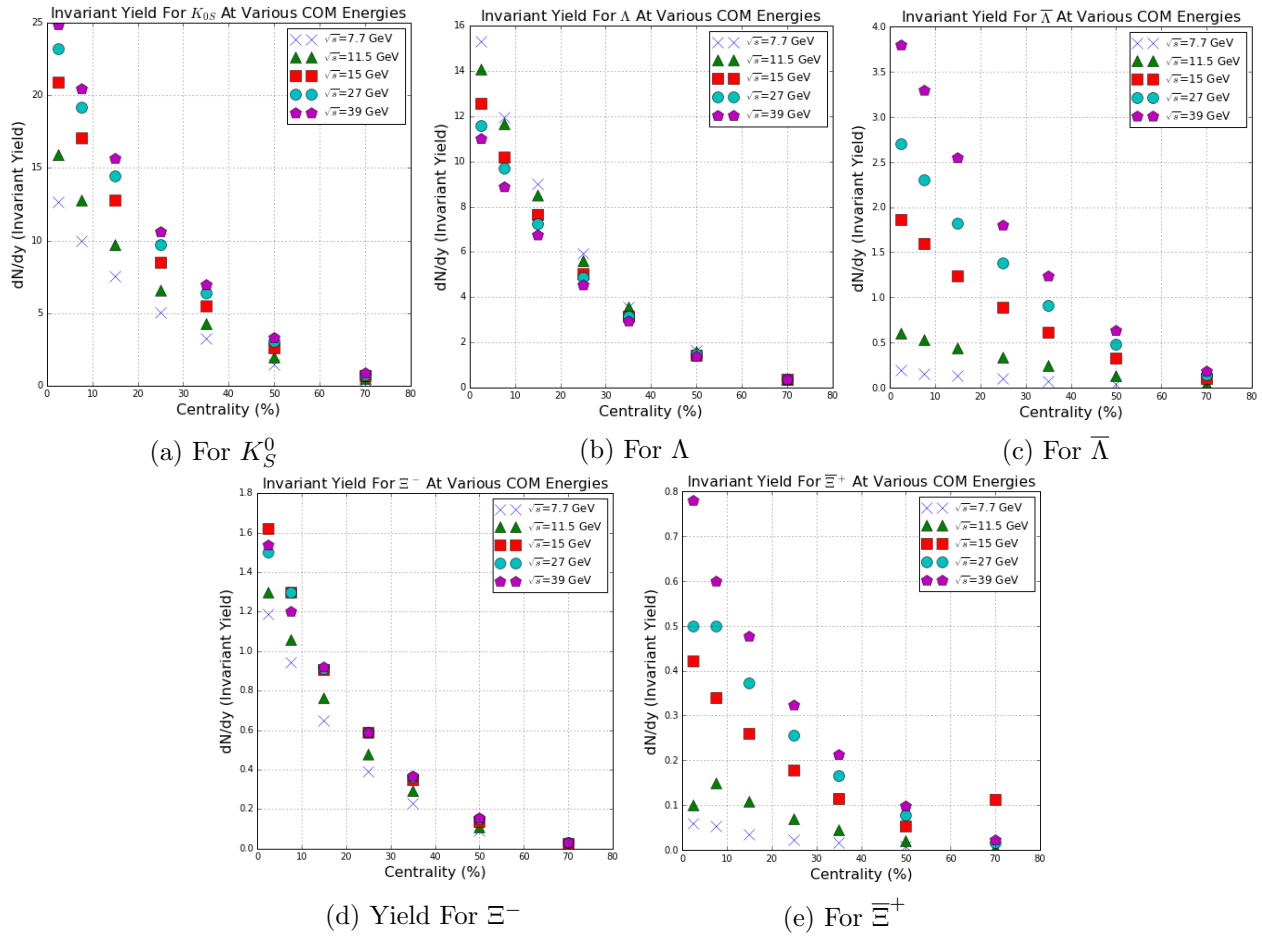

(a) For K^0_S (b) For Λ (c) For $\overline{\Lambda}$

(d) Yield For Ξ^- (e) For $\overline{\Xi}^+$

Figure 33: Graphs Of Particle Yields vs Collision Centrality For Strange Hadrons

divided into 7 centrality classes:classes: 0–5%, 5–10%, 10–20%, 20–30%, 30–40%, 40–60% and 60–80%. In the following graphs each centrality class is represented by its center point. For eg: the centrality class 10-20 will be represented by the point 15 on the X-axis. The center of mass energies that have been taken into consideration are 7.7 GeV, 11.5 GeV, 19.6 GeV, 27 GeV and 39 GeV. All the data presented in this section has been taken from reference 11 which itself is taken at the midrapidity range of $y =| 0.5 |$.

9.1.3 Chemical Freeze Out Parameters

The yields obtained from the previous two subsections are processed using THERMUS ("a package of C++ classes and functions allowing statistical-thermal model analyses of particle production in relativistic heavy-ion collisions"[12]) to give temperature (T_{ch}), baryonic (μ_B) and strange (μ_S) chemical potential, strange suppression factor (γ_S) and the radius of the thermal system.

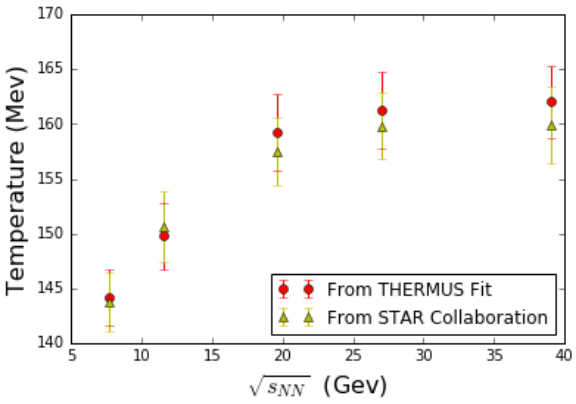

(a) Variation Of Temperature with COM energy

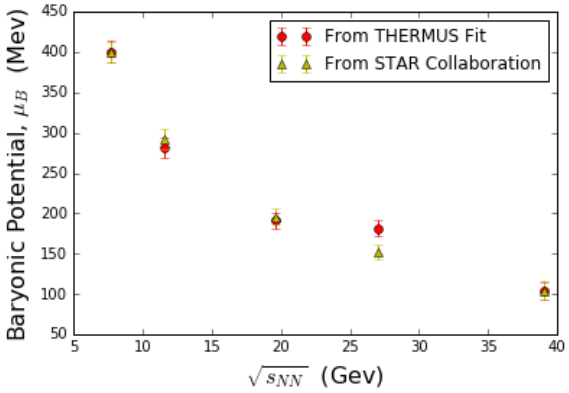

(b) Variation Of Baryonic chemical potential with COM energy

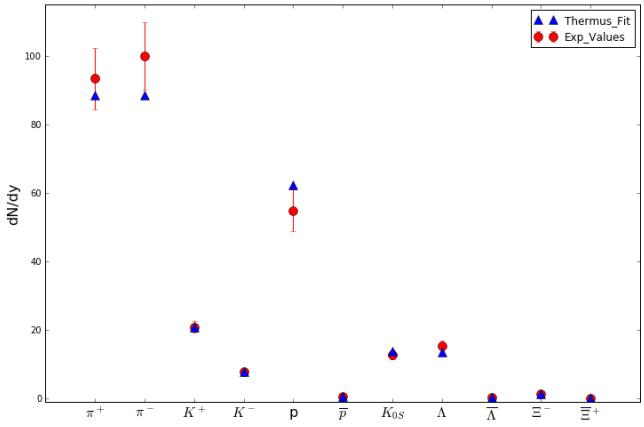

(c) Yield Comparison For Model and Experiment at $\sqrt{s_{NN}}$=7.7 GeV

Figure 34: For Most Central Collisions (0-5%)

The choice of ensemble for fitting is the Grand Canonical Ensemble (GCE). As expected as the

temperature of the thermal system increases with the increase in the center of mass energy. The chemical potentials decrease with increasing energies simply because pair production starts becoming the dominant mechanism for particle production. The anti-particle to particle ratio starts going towards 1 consequently sending the corresponding chemical potentials to 0. For all the energies the suppression factor is close to 1 in most central collisions.

Table 1: Extracted chemical freeze-out parameters for grand canonical ensemble

$\sqrt{s_{NN}}$(GeV)	Centrality(%)	T_{ch} (MeV)	μ_B (MeV)	μ_S (MeV)	γ_S	R (fm)	χ^2/ndf
7.7	0-5	144.2 ± 2.6	400.1 ± 13.8	89.3 ± 7.4	1.09 ± 0.06	5.63 ± 0.30	1.2
	5-10	144.6 ± 2.5	402.3 ± 14.1	91.7 ± 7.7	1.09 ± 0.06	5.22 ± 0.28	1.7
	10-20	144.8 ± 2.7	390.6 ± 13.9	86.7 ± 7.5	1.00 ± 0.05	4.86 ± 0.26	1.3
	20-30	143.5 ± 2.9	383.4 ± 14.3	84.9 ± 8.3	0.93 ± 0.05	4.46 ± 0.26	1.1
	30-40	147.4 ± 2.8	378.3 ± 14.9	87.7 ± 7.8	0.86 ± 0.04	4.03 ± 0.22	0.9
11.5	0-5	149.8 ± 3.0	281.4 ± 12.3	47.1 ± 7.2	0.90 ± 0.05	6.21 ± 0.33	1.5
	5-10	152.6 ± 3.3	286.8 ± 14.4	57.8 ± 10.4	0.97 ± 0.07	5.41 ± 0.34	1.6
	10-20	152.6 ± 3.3	288.1 ± 13.9	67.1 ± 7.8	1.03 ± 0.06	4.84 ± 0.29	1.6
	20-30	156.6 ± 3.4	280.5 ± 13.3	63.2 ± 7.6	0.92 ± 0.05	4.09 ± 0.24	1.3
	30-40	158.8 ± 3.6	270.7 ± 13.9	59.9 ± 8.1	0.85 ± 0.05	3.52 ± 0.21	1.3
19.6	0-5	159.2 ± 3.5	191.4 ± 13.3	41.6 ± 8.1	1.06 ± 0.06	5.73 ± 0.34	2.2
	5-10	160.6 ± 3.4	192.8 ± 13.0	42.6 ± 7.8	1.04 ± 0.06	5.28 ± 0.31	2.0
	10-20	166.8 ± 4.3	180.8 ± 13.7	39.8 ± 9.9	0.95 ± 0.07	4.40 ± 0.33	3.0
	20-30	162.0 ± 3.7	182.2 ± 13.5	41.8 ± 8.4	0.97 ± 0.06	4.21 ± 0.26	1.8
	30-40	162.7 ± 3.8	170.5 ± 13.0	38.9 ± 8.2	0.92 ± 0.05	3.67 ± 0.22	1.8
27	0-5	161.2 ± 3.5	181.7 ± 12.6	47.6 ± 7.7	1.07 ± 0.06	5.62 ± 0.33	4.2
	5-10	162.5 ± 3.5	151.1 ± 12.5	35.1 ± 7.9	1.10 ± 0.06	5.24 ± 0.31	1.4
	10-20	161.2 ± 3.4	141.1 ± 12.0	31.7 ± 7.9	1.03 ± 0.06	5.00 ± 0.29	2.1
	20-30	161.9 ± 3.4	135.9 ± 11.7	31.7 ± 7.6	1.01 ± 0.05	4.37 ± 0.25	2.2
	30-40	164.0 ± 3.7	138.8 ± 12.3	34.5 ± 8.0	0.96 ± 0.05	3.72 ± 0.22	1.8
39	0-5	162.0 ± 3.3	104.0 ± 11.1	22.8 ± 7.1	1.11 ± 0.06	5.79 ± 0.32	2.5
	5-10	162.7 ± 3.4	102.4 ± 11.2	22.6 ± 7.4	1.03 ± 0.06	5.52 ± 0.31	2.0
	10-20	163.1 ± 3.4	103.8 ± 11.5	24.6 ± 7.4	1.05 ± 0.06	4.98 ± 0.28	2.2
	20-30	164.0 ± 3.6	99.9 ± 11.7	24.3 ± 7.7	1.01 ± 0.06	4.37 ± 0.25	1.9
	30-40	165.3 ± 3.6	96.9 ± 11.4	24.5 ± 7.4	0.97 ± 0.05	3.76 ± 0.21	1.7

Finally, the radius of the system decreases from central to peripheral collisions. The table tabulated here is in fine agreement with the one tabulated in reference [10]. The parameters obtained here are close but not exact to what was obtained in [10]. The reason for this could be they that have included the contribution of Ω and $\overline{\Omega}$ baryons which is not done by me. (To see fit parameters without including strange baryons visit Appendix H1).

9.2 Constraining Particle Production Mechanism Using AMPT Model For $\sqrt{s_{NN}}$=7.7 GeV

9.2.1 AMPT Model

AMPT[14] stands for A Multi-Phase Transport model and is used to simulate the dynamics of a relativistic heavy-ion collision. It is a hybrid model and has 4 main components.

- Initial Condition: These are obtained using the HIJING (Heavy-Ion Jet Interaction Generator). Hard minijet partons are produced perturbatively if the transfer of momentum is greater than a threshold value else soft strings are produced. This threshold value is set to be 2 GeV/c for our simulation. In the default AMPT model the soft strings are retained while in string melting formalism they are completely converted into partons.

- Partonic Interactions: ZPC (Zhang's Parton Cascade) is used for this part. The differential parton-parton scattering cross section is given by: $\frac{d\sigma}{dt} \approx \frac{9\pi\alpha_s^2}{2(t-\mu^2)^2}$ Here t is the Mandelstam variable, α_s is the strong coupling constant, and μ is the Debye screening mass in partonic matter.

- Hadronization: For default model, partons stop interacting after they combine with their parent strings. Hadronization of this model takes place through Lund String Fragmentation model [14]. Here $\langle p_T^2 \rangle$ depends on the Lund-string fragmentation parameters (a,b) as: $\langle p_T^2 \rangle \propto \frac{1}{b(2+a)}$. In the string melting version, Hadronization takes place via a quark coalescence model. Here the nearest partons are combined together to form the quark-antiquark pair (mesons) or quark triplets (baryons).

- Hadronic interactions: These describe the dynamics of the hadronic matter as described by the ART (A relativistic Transport)[14] model. This model includes baryon-baryon,meson-meson, meson-baryon, elastic and inelastic scatterings.

In this section, we have used the following parameter values for both default and string melting version to try and simulate the particle production of Au-Au collisions at $\sqrt{s_{NN}} = 7.7GeV$. These parameters are supposed to be fine-tuned for this energy scale and were obtained from reference [13].

Table 2: Initial Values For Lund-String Fragmentation Parameters And Parton-scattering Cross section

Set	a	b (GeV^{-2})	α_S	μ (fm^{-1})	σ (Cross-Section in mb)
A	0.55	0.15	0.33	2.265	3
B	0.5	0.9	0.33	3.2	1.5
C	2.2	0.5	0.47	1.8	10

9.2.2 Results

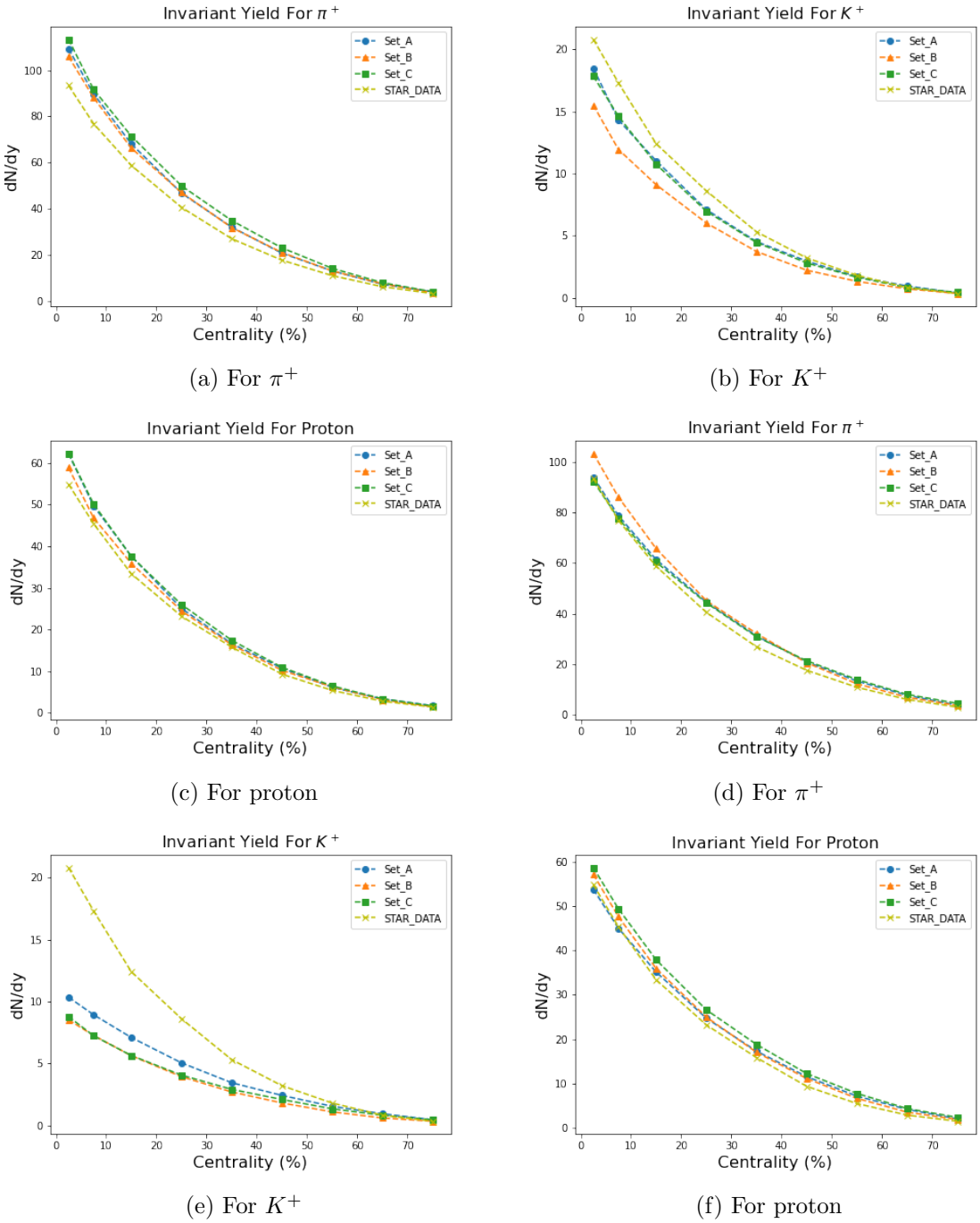

(a) For π^+ (b) For K^+

(c) For proton (d) For π^+

(e) For K^+ (f) For proton

Figure 35: Graphs Of Particle Yields vs Collision Centrality At Mid-rapidity ($y< \mid 0.1 \mid$) from AMPT default (a-c) and string melting (d-f) models

For each set A,B,C and each model (default and string melting), we have simulated 20,000 events. From the figure above we have the following observations:

- For π^+ - In the default model, set B seems to able to best describe the dn/dy graph. However even set B is consistently above the points obtained from data. The string melting model seems to much better describe the yield of pion. Again the parameters of set C in the string melting model best describe the pion yield plot.
- For K^+ - Both the default and string melting models (all three sets) consistently fail to mimic the kaon yield plot especially at centrality class 0-5%. None of the models seem to be able to properly describe the kaon yield plot. Hence AMPT model fails to describe the production of K^+ at 7.7 GeV center of mass energy.
- For proton - Both the default and the string melting models (all three sets) seem to be able to properly describe the proton yield curve. For the default model, the parameters of set B best describe the dN/dy graph of proton. In the string melting formalism, set B and set C describe the proton yield curve quite well with set B better explaining the central collision portion while set C is better explaining the peripheral collision part.
- Overall, it was observed that for the same set of parameters the yield obtained through the default model was a little higher than that obtained via the string melting model. It was also observed that generally the yields obtained through set A were highest followed by set C and set B for the default model.

To see the plots for the corresponding anti-particles visit Appendix H2.

Chapter 7:
Flow In Relativistic High Energy Collisions

10 Flow In Relativistic High Energy Collisions

Studies from the RHIC (Relativistic Heavy Ion Collider) suggests that the QGP matter formed due to the deconfinement of partonic degrees of freedom appear to be more like a liquid rather than a gas. This indicates that the particles produced in HIC tend to move collectively due to the variations of pressure across the the volume of the overlap region formed by the colliding nuclei. This phenomenon has been termed as **flow**[15] as this collective behavior is analogous to the properties of particles moving in a fluid. One of the basic problems is to discover the fundamental laws leading to this emergent behavior of produced particles.

10.1 Collision Geometry

For HIC, the number of nucleons is generally large. Hence, nucleus itself can be approximated by a round (spherical) shape as shown in the figure below. The impact parameter vector, $\tilde{\mathbf{b}}$ is defined along the line joining the centers of the two nuclei at the point of closest approach. It's magnitude is given by the closest distance of approach between the centers of the two nuclei. Due to the non-spherical shape of the overlapping region (which is generally observed to be dominated by elliptic flow), three different kinds of planes can be defined:

- Reaction Plane (RP) : This plane is defined by the vectors of the beam direction and the impact parameter.
- Participant Plane (PP): This plane is defined by the vectors of the beam direction and the average vector of the participants.
- Event Plane (EP): This plane is defined by the vectors of the beam direction and the average vector of the final particles detected

Clearly, in an experiment, one does not have access to the Reaction plane and the participant plane as they are defined in the initial stages of the HIC. However, we will be working with models and hence have access to both of these planes.

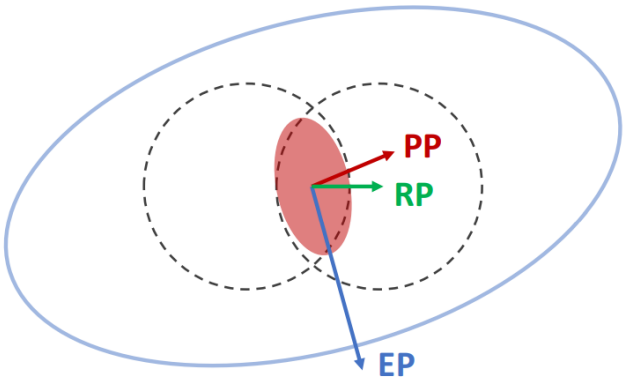

Figure 36: Reaction Plane (RP), Participant Plane (PP) and Event Plane (EP)[16]

10.2 Anisotropic Flow

Consider a non-central collision ($\tilde{\mathbf{b}} \neq 0$) as shown in the figure below. The overlap region formed the two colliding nuclei is non-spherical ("almond-like" shape is what people to call) within which nuclear matter can be roughly considered to be continuous. A keen eye directly notices that the average pressure gradient between the center of the overlap region and the surrounding vacuum is larger for the reaction plane (xz plane in the figure) when compared to the out of plane direction. This is because the overlapping region is thinner along the reaction plane.

We know that: $\vec{F} \propto \nabla P$. Hence forces are different along different directions in the overlapping

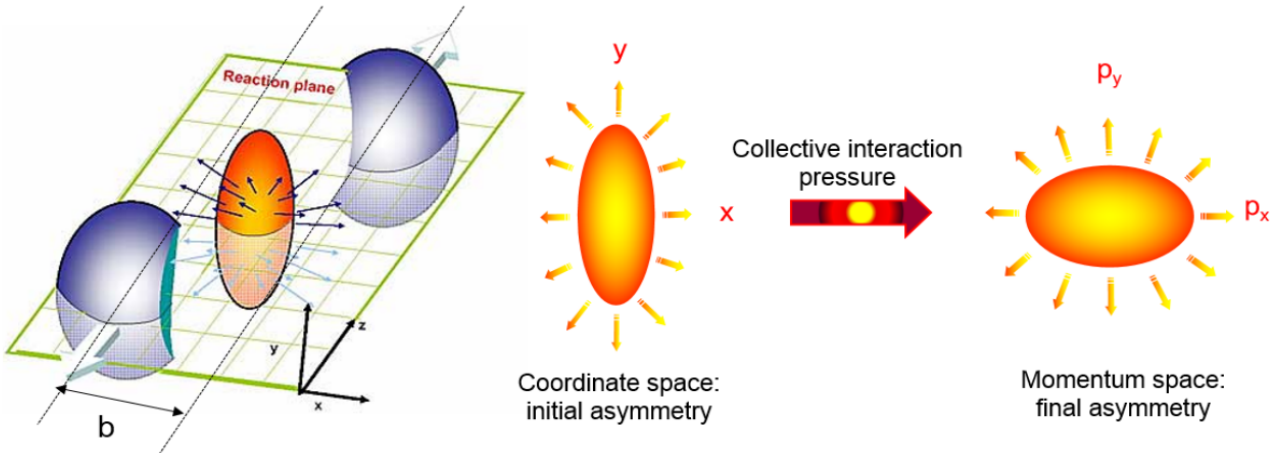

Figure 37: Left: Example Of A Non-Central Collision and Right: Initial spatial anisotropy translating into final momentum anisotropy of produced particles (https://cds.cern.ch/record/2634558/files/ATL-PHYS-SLIDE-2018-604.pdf)

region. Therefore, the particles emitted along the flow direction (xz plane in the figure) have a higher momenta when compared to the other directions leading to an anisotropy in the azimuthal momenta distribution of the produced particles. Further, it is not unreasonable to expect this momentum anisotropy is approximately proportional to the initial anisotropy in the collision geometry.

It was later realized that initial geometry fluctuates around the averaged elliptic shape. This happens due to random positions of the participant nucleons in the overlapping region on an event by event basis.This deformation can be cleverly quantified by a mode decomposition method with respect to the azimuthal anisotropy of the positions of the participant nucleons. It leads to the definition of dimensionless harmonic coefficients eccentricity as[15]:

$$\begin{aligned} \varepsilon_1 \equiv \epsilon_1 e^{i\phi_1} &= -\frac{\langle r^3 e^{i\phi}\rangle}{\langle r^3\rangle} \\ \varepsilon_n \equiv \epsilon_n e^{i\phi_n} &= -\frac{\langle r^n e^{in\phi}\rangle}{\langle r^n\rangle} \qquad (n>1) \end{aligned} \tag{10.2.1}$$

Here (r, ϕ) is relative to the center of mass coordinate system and the average is over all the participating nucleons.

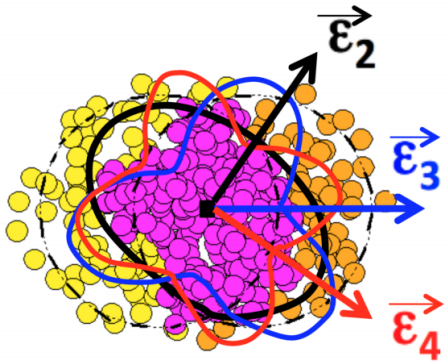

Figure 38: Initial spatial anisotropy (for n=2,3,4) from Monte-Carlo Glauber[15]

10.3 Harmonic Flow

The study of momentum anisotropy is of prime importance as not only is it related to the initial spatial anisotropy but also the medium properties of QGP. It is the latter observation which makes the harmonic flow coefficients a possible signature of QGP like behavior.
Let us formally try to quantify this momentum anisotropy. To do this, first define a coordinate system $(p_T, \phi, \eta/y)$. This is related to the cartesian momentum coordinate system $(p_x, p_y.p_z)$ as:

$$\begin{aligned} p_x &= p_T \cos\phi \\ p_y &= p_T \sin\phi \\ p_z &= \sqrt{p_T^2 + m^2}\sinh y \end{aligned} \tag{10.3.1}$$

$$\text{where the rapidity (y) is:} \qquad y = \frac{1}{2}\ln\frac{E+p_z}{E-p_z} \tag{10.3.2}$$

$$\text{the pseudorapidity } (\eta) \text{ is:} \qquad \eta = \frac{1}{2}\ln\frac{|\boldsymbol{p}|+p_z}{|\boldsymbol{p}|-p_z} = -\ln\tan\left(\frac{\theta}{2}\right) \tag{10.3.3}$$

where θ is the polar angle between $\boldsymbol{p}$ and beam axis (z). When particle mass becomes negligible, $E \approx p$, then $\eta \approx y$. For HIC, this this is generally true and hence both are interchangly used sometimes. Finally p_T is the transverse momentum and ϕ is the azimuthal angle.
Now we are ready to quantify the momentum anisotropy mathematically of the produced particles. Let us begin with the invariant yield of the produced particles:

$$E\frac{d^3N}{dp^3} = E\frac{d^3N}{dp_x dp_y dp_Z}$$

$$dy = \frac{dp_z}{E} \qquad dp_x dp_y = p_T dp_T d\phi$$

$$E\frac{d^3N}{dp^3} = \frac{d^3N}{p_T dp_T d\phi dy}$$

Now integrating out the ϕ variable (integration limits from 0 to ϕ), one realizes that that the obtained function is periodic in the variable ϕ with a period of 2π. Hence it can be decomposed using a Fourier

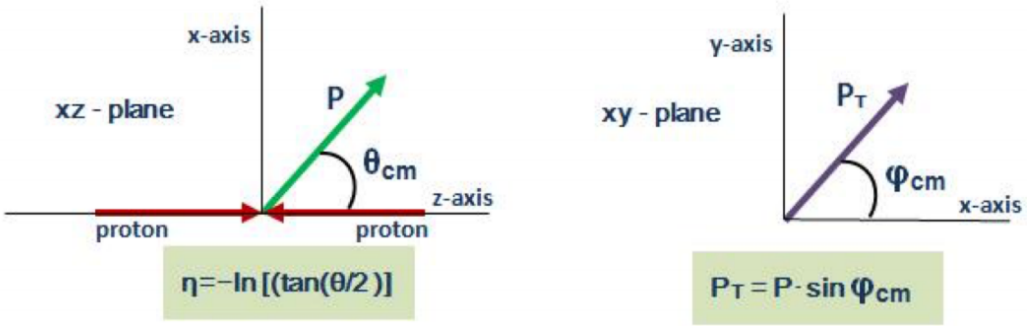

Figure 39: Schematic Of $(p_T, \phi, \eta/y)$ coordinate system[15]

decomposition to get:

$$E\frac{d^3N}{d^3p} = \frac{1}{2\pi}\frac{d^2N}{p_{\mathrm{T}}dp_{\mathrm{T}}dy}\left[1 + \sum_{n=1} 2v_n(p_T, y)\cos(n(\phi - \Psi_R))\right] \tag{10.3.4}$$

Here Ψ_R is the reaction plane angle with respect to the x-axis. Note that, flow is always computed with respect to a symmetry plane which is chosen to be the reaction plane in our case. The sine terms vanish in the Fourier expansion due to the reflection symmetry wrt to the reaction plane. This symmetry corresponds to the invariance of the invariant yield under the coordinate transformation: $(\phi - \Psi_R) \rightarrow -(\phi - \Psi_R)$. Physically, this can be understood in the following manner. Collision dynamics are completely constrained by the colliding beam directions and their distance of closest approach (governed by impact parameter). Since, reaction plane is defined by these two vectors, a person sitting on the reaction plane cannot differentiate between the collision dynamics if he looks out of/into the plane.
The Fourier coefficients v_n are called the as harmonic flow coefficients, The flow is usually dominated by the first few harmonics: directed flow (v_1), elliptic flow (v_2), triangular flow (v_3) and quadrangular flow (v_4). Here the v_n coefficients are functions of η *and* p_T and they are often referred to as differential flow.
The flow coefficients can be computed as:

$$\langle \cos n(\phi - \Psi_R)\rangle = \frac{\int_{-\pi}^{\pi} \cos n(\phi - \Psi_R) \quad E\frac{d^3N}{d^3p}d\phi}{\int E\frac{d^3N}{d^3p}d\phi}$$

$$\langle \cos n(\phi - \Psi_R)\rangle = \frac{\int_{-\pi}^{\pi} \cos n(\phi - \Psi_R)\left(1 + \sum\limits_{n=1}^{\infty} 2v_n \cos n(\phi - \Psi_R)\right)d\phi}{\int\left(1 + \sum\limits_{n=1}^{\infty} 2v_n \cos n(\phi - \Psi_R)\right)d\phi}$$

Now using the orthogonality relation of the Fourier decomposition:

$$\int_0^{2\pi} cos(m(\phi - \Psi_R))\ cos(n(\phi - \Psi_R))\ d\phi = \ \pi\delta_{mn}$$

This finally gives:

$$v_n = \langle cos(n(\phi - \Psi_R)) \tag{10.3.5}$$

10.3.1 Harmonic Flow Visualization

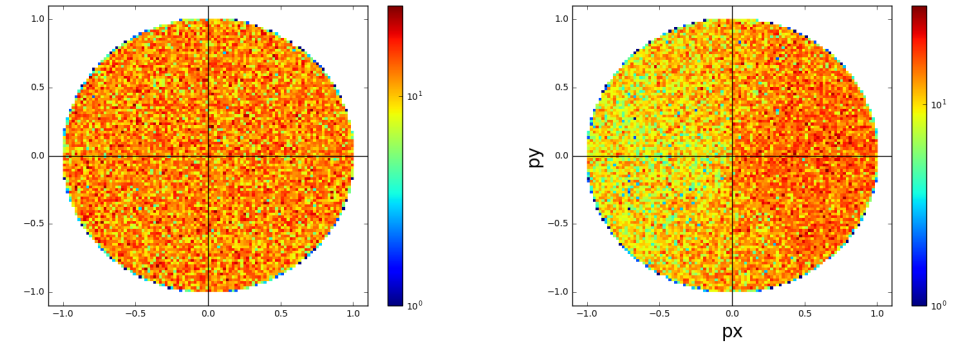

(a) No Flow (Uniform Distribution)

(b) Flow Dominated by v_1 (Directed Flow)

(c) Flow Dominated by v_2 (Positive Elliptic Flow coefficient)

(d) Flow Dominated by v_2 (Negative Elliptic Flow Coefficient)

(e) Flow Dominated by v_3 (Triangular Flow)

(f) Flow Dominated by v_4 (Quadrangular Flow)

Figure 40: Effect of dominant flow coefficients on momenta distribution

Before we move any further, it is instructive to see how various harmonic coefficients of equation 10.3.4

affects the final momenta distribution. In the plots drawn above, the impact parameter direction is chosen to be along the x-axis. This sets the reaction plane angle to 0. The momenta distribution (2-D histogram) in the transverse plane has been simulated keeping only the dominant flow term (non zero v_1 for directed flow, non zero v_2 for elliptic flow and so on). The flow coefficient is a small positive number unless stated otherwise. Finally for each plot, the distribution has been simulated for a region covered by unit circle centered at origin in the momentum space.
One observes that uniform distribution is the no flow condition. This makes sense as no flow implies no anisotropy in the distribution. For flow dominated by v_1, we observe that more number of particles flow along a particular direction (defined by impact parameter here). This justifies it's name of directed flow (sometimes also referred to as sideward flow). Moving onto flow dominated by v_2, we see an elliptic deformation in the distribution of momentum of particles justifying it's name of elliptic flow. When $v_2 > 0$, then the major axis of the deformed ellipse is along the impact parameter direction (x axis above). $v_2 < 0$, then the major axis of the deformed ellipse is perpendicular to the impact parameter direction. This is also know as squeeze-out flow. For flow dominated by v_3, we see that particles prefer to arrange themselves in a triangular type deformation in the momentum space. Finally, for flow dominated by v_4 we observe that particles in momentum space try to preferentially orient themselves into one of the smaller four rooms which seem to be separated by the diagonals of a large rectangle.

10.4 Hydrodynamic Framework

Every behavior of the strong interactions can technically be described by the beautiful QCD lagrangian density:

$$L = \bar{\psi_i} \left(i\gamma_\mu D^\mu_{ij} - m\delta_{ij} \right) \psi_j - \frac{1}{4} F_{\mu\nu\alpha} F^{\mu\nu\alpha} \tag{10.4.1}$$

where ψ_i is a quark field, γ_μ are Dirac matrices, D_μ is a covariant gauge derivative, m is a quark mass, δ is Kronecker delta and $F_{\mu\nu\alpha}$ is the field strength of the gluons corresponding to the color index α. In a perfect world, this lagrangian would have been exactly solvable. However, interesting properties such as running coupling, color confinement and self-interaction between gluons makes this impossible with our current knowledge of mathematics. So the solution is to use a hydrodynamic model to provide a phenomenological theory. Hydrodynamic models require two main conditions to work:

- the mean free path of the system is smaller than the size of the system. Mathematically,

$$\lambda_{mean free path} \ll L \text{ (Box Size)}$$

- The system must be in approximate local thermal equilibrium.

For a hydrodynamic simulation, we require three things. First an initial condition model, second the relevant hydrodynamic equations and third an algorithm for particle production.

10.4.1 Initial Conditions

The initial condition provides a description of the initial state geometry and fluctuations within it. The model which has been used in the hydro-simulator that I have been using is the Monte Carlo

Glauber. In this model each nucleon is treated as hard sphere and is distributed within the nucleus with a Wood-Saxon distribution. It is given by:

$$\rho(r) = \rho_0 \left[1 + exp\left(\frac{r-R}{a}\right)\right]^{-1} \tag{10.4.2}$$

where R corresponds to the classical radius of the nuclei given by $R_0 A^{1/3}$ and 'a' is called the skin depth. A nucleus-nucleus collision is considered to be a superposition of many nucleon nucleon collision. Fluctuation of initial geometry in each event arises from the random position of finite nucleons within the nucleus when sampled from the Wood-Saxon probability distribution.

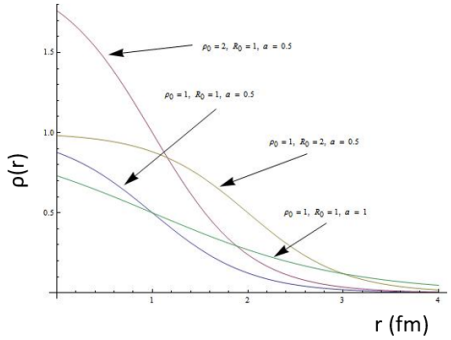

Figure 41: Wood-Saxon Distribution (From Google Images)

10.4.2 Relevant Hydrodynamic Equations

The equations of hydrodynamics are simply a set of conservation equations. For ideal hydrodynamics, the conservation laws are for the energy momentum tensor and the conserved charges of the system are:

$$\partial_\mu N_k^\mu = 0 \tag{10.4.3}$$

$$\partial_\mu T^{\mu\nu} = 0 \tag{10.4.4}$$

where $T^{\mu\nu}$ is the energy momentum tensor defined as a function of energy density ϵ, flow four-velocity u^{mu} and pressure P. N_k refers to the k^{th} conserved charge of the system. The system further satisfies another constraint given by the 2 law of thermodynamics. This says that the entropy of the universe must increase. However we demand a much stricter condition that individually the entropy of both the system and surrounding should increase. Mathematically, if S^μ is the entropy four current then:

$$\partial_\mu S^\mu \geq 0$$

with equality holding for the equilibrium condition.
A keen reader observes that we are still missing 1 equation to completely describe the system. The energy momentum tensor provides 4 equations which each conserved current equation gives one equation. This gives a total of 4+k equation (assuming k conserved charges). Now the number of independent parameters are 5+k. k for each conserved charge, 2 corresponding to energy and pressure while 3

corresponding to fluid four velocity ($u\mu u^\mu = 1$ decrease one free parameter). This extra equation is provided in the form of equation of state (EOS) and governs the pressure-energy relation of the system.

10.4.3 Algorithm Of Particle Production[17]

Once, the system has fully evolved using the hydrodynamic equations we require an algorithm to recover back the particle spectra. This is usually done using the Copper-Fyre freeze-out algorithm and is shortly discussed below:
. The Lorentz invariant momentum space distribution is given by:

$$E\frac{dN_i}{d^3p} = \frac{dN_i}{dyp_\perp dp_\perp d\varphi_p} = \frac{dN_i}{dym_\perp dm_\perp d\varphi_p} = \frac{1}{(2\pi)^3}\int_\Sigma p\cdot d^3\sigma_\mu(x) f_i(x,p) \tag{10.4.5}$$

where $p_\perp, m_\perp$ are transverse momenta and mass respectively, ϕ_p is the azimuthal angle, y is rapidity, σ is a 3-dimensional hypersurface, $d^3\sigma_\mu(x)$ is the normal vector to hypersurface at point x, N_i is the particle of type i and f_i is the distribution function. It can be derived [17] that two separate hypersurfaces Σ_1 and Σ_2 produce the same particle spectra if the distribution function evolves via a boltzmann equation with a collision kernel that preserves the corresponding particle number. The same momentum spectrum is reproduced iff $f_i(x)$ is a solution to the kernel corresponding to a collisionless Boltzmann equation. Hence to compute the momentum spectrum, surface Σ which corresponds to the detector is replaced by the surface Σ_F which is the earliest surface enclosing all scattering processes. This is why it is called the "surface of last scattering" or the "freeze-out surface". Now parameterize the 3-dimensional surface by local orthogonal coordinates (u,v,w). Then the normal $d^3\sigma_\mu(x)$ transforms into the new local system as:

$$d^3\sigma_\mu = -\epsilon_{\mu\nu\lambda\rho}\frac{\partial\sigma^\nu}{\partial u}\frac{\partial\sigma^\lambda}{\partial v}\frac{\partial\sigma^\rho}{\partial w}dudvdw \tag{10.4.6}$$

where $\epsilon_{\mu\nu\lambda\rho}$ corresponds to the four-dimensional completely antisymmetric levi-cevita symbol. Assuming longitudinal boost invariance, the freeze out surface can be parameterized by a longitudinal proper time $\tau_f(\mathbf{r}_\perp)$ as:

$$\Sigma^\mu_{\mathrm{f}}(\boldsymbol{r}_\perp,\eta) = (t_{\mathrm{f}}, x_{\mathrm{f}}, y_{\mathrm{f}}, z_{\mathrm{f}}) = (\tau_{\mathrm{f}}(\boldsymbol{r}_\perp)\cosh\eta, \boldsymbol{r}_\perp, \tau_{\mathrm{f}}(\boldsymbol{r}_\perp)\sinh\eta) \tag{10.4.7}$$

$$d^3\sigma_\mu = \left(\cosh\eta, -\frac{\partial\tau_{\mathrm{f}}}{\partial x}, -\frac{\partial\tau_{\mathrm{f}}}{\partial y}, -\sinh\eta\right)\tau_{\mathrm{f}}(\boldsymbol{r}_\perp)\,d^2r_\perp d\eta \tag{10.4.8}$$

$$p\cdot d^3\sigma(x) = (m_\perp\cosh(y-\eta) - \boldsymbol{p}_\perp\cdot\boldsymbol{\nabla}_\perp\tau_{\mathrm{f}}(\boldsymbol{r}_\perp))\,\tau_{\mathrm{f}}(\boldsymbol{r}_\perp)\,d^2r_\perp d\eta \tag{10.4.9}$$

with $\boldsymbol{\nabla}_\perp = (\partial_x, \partial_y)$, $\boldsymbol{r}_\perp$ is the transverse radius and η is the pseudorapidity. Now all that is left is to somehow find the phase-space distribution function on the freeze-out surface. For that assume that system in consideration expands extremely fast such that the mean free path increases rapidly. Thus, the transition from strong interacting hydrodynamic medium to an essentially free medium occurs in a very short interval. Now, one can safely assume that this time scale is not large enough to affect the macroscopic variables of the system. Hence, the distribution function on the freeze-out surface can be roughly approximated by its thermal equilibrium form. This is given by:

$$f_{i,\mathrm{eq}}(x,p) = \frac{g_i}{e^{[p\cdot u(x)-\mu_i(x)]/T(x)}\pm 1} = g_i\sum_{n=1}^{\infty}(\mp 1)^{n+1}e^{-n[p\cdot u(x)-\mu_i(x)]/T(x)} \tag{10.4.10}$$

This is the standard Bose/Fermi distribution function. This small derivation leads to the famous Cooper-Fyre freeze-out algorithm:

- Determine the freeze-out surface where the local thermal equilibrium just begins to break down.
- Use the local equilibrium distribution function as given by 10.4.10 in 10.4.5 to get the invariant yield.

11 Harmonic Flow Coefficients As QGP Signatures

One of the main objectives of HIC, is to probe the realm of QGP (Quark-Gluon Plasma) which is a de-confined state of quarks and gluons. Now, assume that you collided two heavy ions. How does one know that QGP like medium was actually formed during the evolution of the collision system? Hence, we need some kind of signature which can identify if QGP like medium was formed or not.
In this section, we will see if flow coefficients can be used as QGP signatures. The major focus will be on elliptic flow (which is the major deformation in the initial spatial anisotropy) along with a minor focus on triangular flow. This test will be done using the simulations produced from the AMPT (A Multi-Phase Transport) Model and hydrodynamic simulation of Au-Au collisions at $\sqrt{s_{NN}} = 200$ GeV.

11.1 Analysis Using The AMPT Model

The basics of the AMPT model has already been discussed in section 9.2. 20,000 events were simulated for both the default and string models. The initial values required to run the AMPT model is given in table 3.

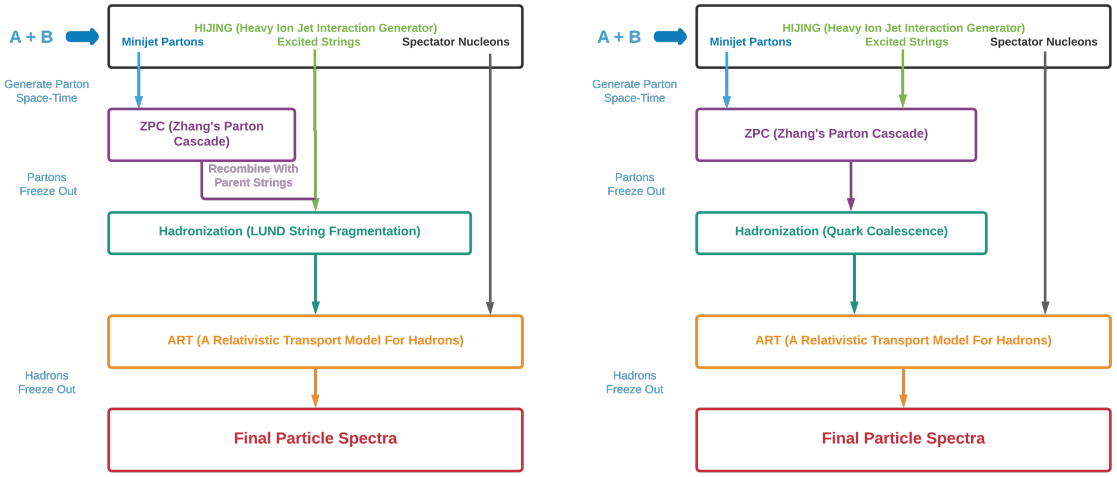

(a) Schematic for the Default Version (b) Schematic for the String Melting Version

Figure 42: Versions Of The AMPT Model

Table 3: Initial Values For Lund-String Fragmentation Parameters And Parton-scattering Cross section

a	b (GeV^{-2})	α_S	μ (fm^{-1})	σ (Cross-Section in mb)
2.2	0.5	0.47	1.8	10

These set of values is the same as set C used in section 9.2 for constraining particle production of Au-Au collisions at $\sqrt{s_{NN}} = 7.7$ GeV. This set was used as it gave the correct magnitude for the coefficient of elliptic flow in the string melting version when compared to the data available from the STAR collaboration.
To test v_2/v_3 as possible qgp signatures, we need to produce two different scenarios and compare their performances keeping all other parameters fixed. This is done by:

- Scenario 1- NO QGP like medium is produced. This scenario is simulated using the default version of the AMPT model. The process of hadronization in this version follows the LUND string fragmentation model. This model incorporates color strings between partons which then later on fragments successively into final state hadrons. The major thing to notice is that partons are never actually free and exist in a color singlet form by always remaining in a bound state. see the figure below for more clarity. Hence, default version is a good candidate to simulate this scenario.

- Scenario 2- QGP like medium IS produced. This is simulated using the string melting version of AMPT. This model follows a quark coalescence. This algorithm combines the two nearest quark-antiquark pair into a meson and the three nearest quarks (antiquarks) into a baryon (anti-baryon). Before coalescence the partons are essentially free from each other and hence it forms a good candidate for simulating scenario 2.

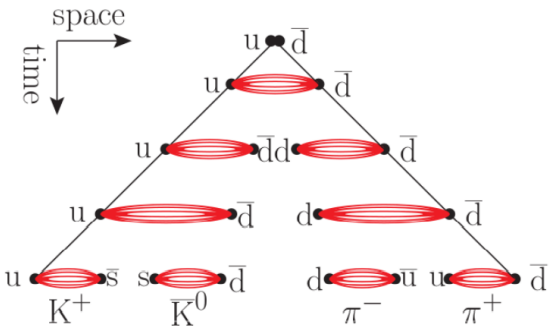

(a) Lund String Fragmentation (From Aranya's thesis)

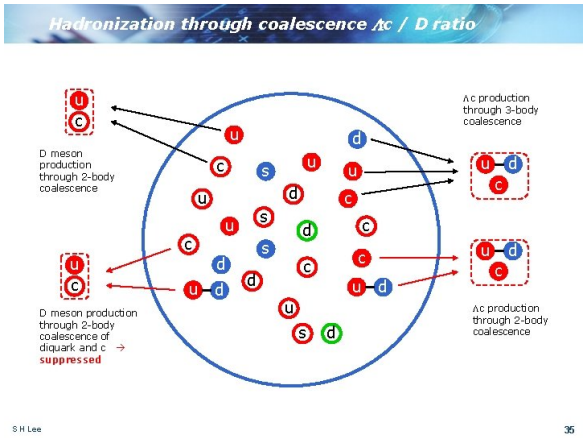

(b) Quark Coalescence (YONSEI UNIVERSITY)

Figure 43: Schematics for hadronization algorithms

11.1.1 A Preliminary Check

Before we dive into the results, let us do a preliminary check to see if momentum anisotropy is indeed dominated by elliptic flow. To do this, we plot the distribution of azimuthal angle in the momentum space for various produced particles (pion,kaons,protons,lambda and phi). The resulting histogram is then fitted using the fit equation:

$$N(\phi) = A + Bcos(2(\phi - \phi_R)) \tag{11.1.1}$$

Here A, B and ϕ_R are fit parameters. The ratio B/A quantifies elliptic flow and ϕ_R is the reaction plane angle.

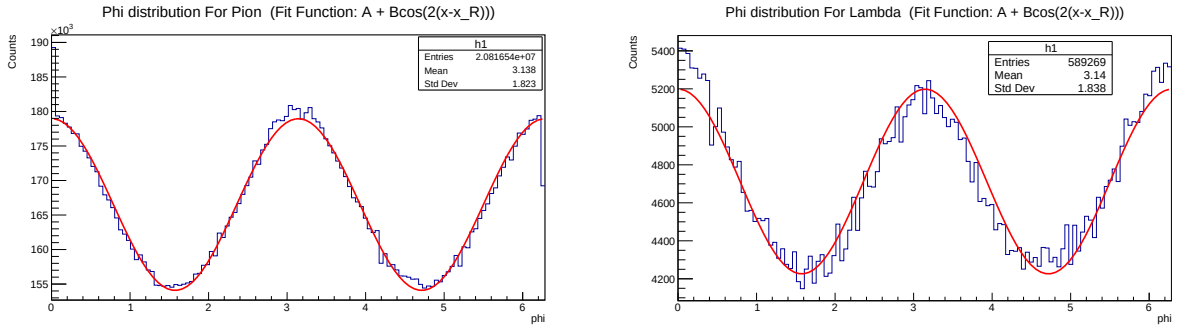

(a) For $\pi^{[\pm]}$ (b) For Λ^0

Figure 44: Azimuthal Distribution (In Momentum Space) For Some particles

As one can see from the above figure, the azimuthal distribution (In Momentum Space) for fits incredibly well to a Fourier decomposition containing only the second flow harmonic. This indeed suggests that momentum space anisotropy is dominated by elliptic flow. This also true for other produced particles which have not been shown here. The above distribution of particles have been simulated from the string melting version. To see the same for the equivalent results for default version visit Appendix J1.

Table 4: Optimum Parameters For Fit Function For Various Particles

Particle	Pid	A	ΔA	B	ΔB	ϕ_R	$\Delta\phi_R$	v_2	Δv_2
K^0_S	310	10790.9	9.29124	1114.48	13.1421	-0.00325	0.005878	0.1032796	0.0013068
Proton	2212	35278.2	16.7996	3415.07	23.757	-0.01606	0.00347	0.0968040	0.0007195
Lambda	3122	4712.26	6.13987	486.29	8.69565	0.004659	0.008891	0.1031968	0.0019798
Pion	211	166519	36.4987	12436.9	51.6395	0.002274	0.002071	0.0746876	0.0003265
Kaon	321	21574.7	13.1376	2223.62	18.5857	-0.00181	0.004165	0.1030661	0.0009242
Phi	333	2106.16	4.10479	235.48	5.80907	-0.00882	0.012279	0.1118054	0.0029760
Pi0	111	102638	28.6549	7683.84	40.5434	0.001937	0.002632	0.0748635	0.0004159

Table 4, suggests that the reaction plane angle is essentially 0 for all the particles which is to be expected. The elliptic flow coefficient is around 0.1 which is the correct order of magnitude (for string

melting version) as we shall see in the next subsection. Please note that this is not an exact analysis but a coarse graining of the problem at hand.

11.1.2 Number Of Constituent Quark (NCQ) Scaling:

For v_2:
Consider the following graphs of $\frac{\langle v_2 \rangle}{n_q}$ vs $\frac{m_T - m_0}{n_q}$. Here m_T stands for the transverse mass, m_0 goes for rest mass, $\langle v_2 \rangle$ stands for the event average of the elliptic flow and n_q refers to the number of quarks in the hadron. All v_2 computations have been done at minimum bias. The elliptic flow coefficient

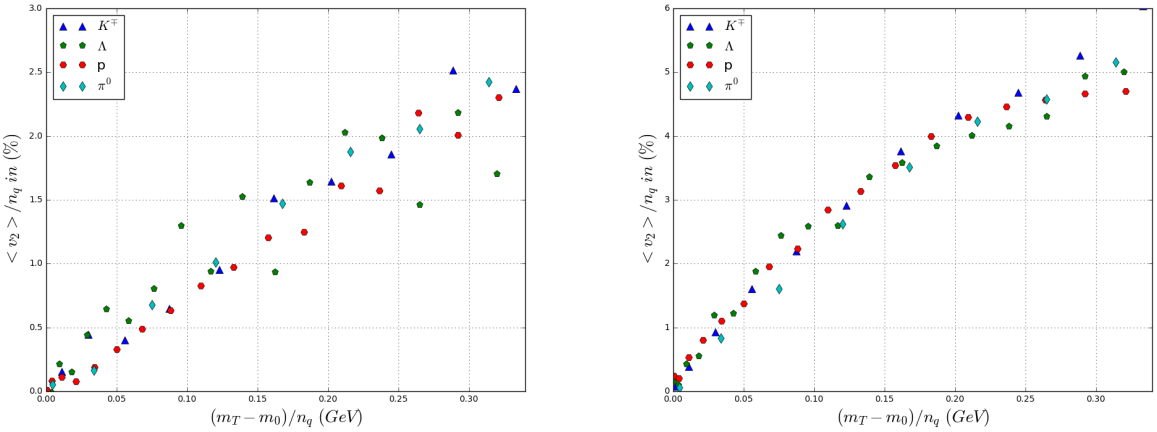

(a) For Default Version

(b) For SM version

Figure 45: Graph Of $\frac{\langle v_2 \rangle}{n_q}$ vs $\frac{m_T - m_0}{n_q}$

v_2 for an event has been calculated using the formula obtained in 10.3.5 by substituting n=2. Since, in the AMPT model the impact parameter axis is along the x-axis and the beam direction is along the z-axis, the reaction plane angle for every event is 0. This was also confirmed for many produced particles (in SM version) in the previous subsection.
One can see that for the SM version $\frac{\langle v_2 \rangle}{n_q}$ vs $\frac{m_T - m_0}{n_q}$ falls impressively on a universal curve. The graph above has been plotted for $K^{\pm}$,π^0 (which are mesons) and proton and Λ^0 (which are baryons). Hence, NCQ scaling seems to be a universal behavior (irrespective of hadron type) in the SM version. Clearly, no NCQ scaling is observed for the default version.
The presence of NCQ scaling is proof of the presence of partonic degrees of freedom at some time in the evolution of system formed from high energy collisions. The argument for this is quite simple. The $\frac{v_2}{n_q}$ scaling shows that elliptic flow of any sea-parton is independent of it's parent hadron. This implies that it doesn't matter whether an up quark comes from a proton, a pion or a Kaon. Once we have adjusted for finite mass effects of hadron. This is exactly why the scaling behavior is much prominent when plotted against $\frac{m_T - m_0}{n_q}$ rather than $\frac{p_T}{n_q}$. Since, the flow of parton is independent of the parent hadron, this suggests that at some time during the evolution of system partonic degrees were the fundamental degrees of freedom flowing collectively with the medium. Hence the presence of

NCQ scaling in the elliptic flow of produced particles is a good signature of QGP.

For v_3:
The calculation of v_3 is a bit different than that of v_2. It cannot be simply calculated by keeping n=3 in 10.3.5. This is due to the fact that the minor axis of triangular deformation has no correlation with the minor axis of eccentricity of elliptic deformation and the reaction plane angle in Glauber Monte Carlo calculations. This implies that the average triangularity calculated with respect to the reaction plane is zero. This can be explicitly seen in the figure below.

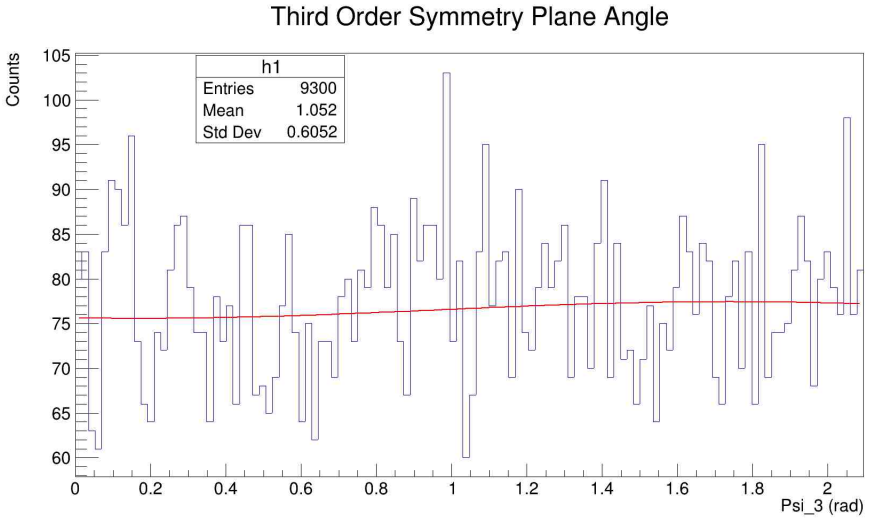

Figure 46: Distribution of third order symmetry plane wrt the reaction plane in AMPT

Each event has a different orientation for the third order symmetry plane. Since the distribution is non-uniform (but constantly fluctuates about the constant red line), one can expect a very small non-zero triangular flow (sometimes positive sometimes negative based on your luck). This is indeed what I obtained when I did this incorrectly, with v_3 *vs* p_T graph fluctuating about the mean value of 0.
The third order symmetry plane in the AMPT is calculated using the position of participant nucleons when the coordinate system is set at the center of mass of the participating nucleons. The third order symmetry plane angle is given by[18]:

$$\psi_3 = \frac{\operatorname{atan2}\left(\left\langle r^2 \sin\left(3\phi_{\text{part}}\right)\right\rangle, \left\langle r^2 \cos\left(3\phi_{\text{part}}\right)\right\rangle\right) + \pi}{3} \tag{11.1.2}$$

where (r, ϕ_{part}) are the polar coordinate positions of participating nucleons. Here ψ_3 is the minor axis of participant triangularity. It is wrt this plane that triangular harmonic flow of produced particles will be calculated as:

$$v_3 = \langle cos(3(\phi - \psi_3)) \tag{11.1.3}$$

In 11.1.2, the atan2(y,x) is a special function which makes sure that the coordinate transformation from cartesian to polar system happens correctly. It is given by:

$$\operatorname{atan}2(y,x) = \begin{cases} \arctan\left(\frac{y}{x}\right) & \text{if } x > 0, \\ \arctan\left(\frac{y}{x}\right) + \pi & \text{if } x < 0 \text{ and } y \geq 0, \\ \arctan\left(\frac{y}{x}\right) - \pi & \text{if } x < 0 \text{ and } y < 0, \\ +\frac{\pi}{2} & \text{if } x = 0 \text{ and } y > 0, \\ -\frac{\pi}{2} & \text{if } x = 0 \text{ and } y < 0, \\ \text{undefined} & \text{if } x = 0 \text{ and } y = 0. \end{cases}$$

Now we are finally ready to see NCQ in the triangular flow. The scaling function is a bit modified for triangular flow. Consider the following graphs of $\frac{\langle v_3 \rangle}{n_q^{3/2}}$ vs $\frac{m_T - m_0}{n_q}$. Here m_T stands for the transverse mass, m_0 goes for rest mass, $\langle v_3 \rangle$ stands for the event average of the triangular flow and n_q refers to the number of quarks in the hadron. All v_3 computations have been done at minimum bias.

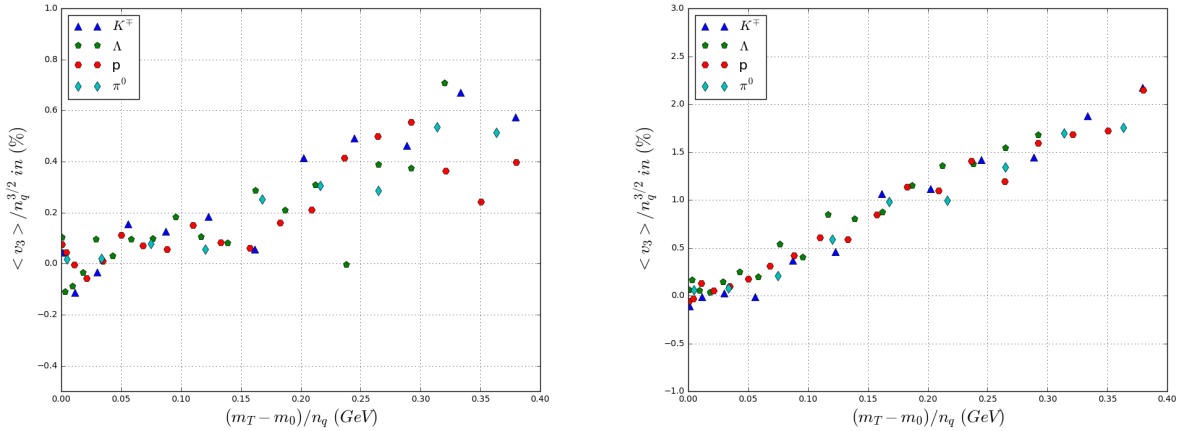

(a) For Default Version

(b) For SM version

Figure 47: Graph Of $\frac{\langle v_3 \rangle}{n_q}$ vs $\frac{m_T - m_0}{n_q}$

One can see that for the SM version $\frac{\langle v_3 \rangle}{n_q}$ vs $\frac{m_T - m_0}{n_q}$ falls impressively on a universal curve. The graph above has been plotted for $K^{\pm}$,π^0 (which are mesons) and proton and Λ^0 (which are baryons). Hence, NCQ scaling seems to be a universal behavior (irrespective of hadron type) in the SM version. Clearly, no NCQ scaling is observed for the default version. This is again a good signature for arguing that a QGP like medium is formed.

Finally, one can also observe that the elliptic and triangular flow obtained for the particles simulated from the SM version is roughly double than that for the particles simulated from the default version. As the flow is dominated by elliptic flow in both the versions, the elliptic flow coefficients for each version is much higher when compared to the triangular flow coefficients for the corresponding version. Hence a large momentum anisotropic flow can also be considered as a good signature for the production of a qgp like medium. This observation will get stronger in the coming subsections.

11.1.3 $v_{n=2,3}$ vs $\langle p_T \rangle$ Histograms

Another key observable to check is the $v_{n=2,3}$-$\langle p_T \rangle$ correlation. These variables are expected to be correlated due to equation 10.3.4. Here $\langle p_T \rangle$ is the mean transverse momenta computed for the event for which $v_{n=2,3}$ has been calculated.
This correlation will be quantified using the Pearson correlation coefficient (PCC). PCC quantifies the amount of linear correlation between two sets of data. Given a pair of random variables (X,Y), the PCC ρ_{XY} is given as:

$$\rho_{X,Y} = \frac{\mathrm{cov}(X,Y)}{\sigma_X \sigma_Y}$$
$$\rho_{X,Y} = \frac{\mathbb{E}\left[(X-\mu_X)(Y-\mu_Y)\right]}{\sigma_X \sigma_Y}$$

where: $\mu_X = \mathbb{E}[X]$
$\mu_Y = \mathbb{E}[Y]$
$\sigma_X^2 = \mathbb{E}\left[(X-\mathbb{E}[X])^2\right] = \mathbb{E}\left[X^2\right] - (\mathbb{E}[X])^2$
$\sigma_Y^2 = \mathbb{E}\left[(Y-\mathbb{E}[Y])^2\right] = \mathbb{E}\left[Y^2\right] - (\mathbb{E}[Y])^2$
$\mathbb{E}\left[(X-\mu_X)(Y-\mu_Y)\right] = \mathbb{E}[(X-\mathbb{E}[X])(Y-\mathbb{E}[Y])] = \mathbb{E}[XY] - \mathbb{E}[X]\mathbb{E}[Y]$

Here $\mathbb{E}$ is the expectation value.Substituting everything back, we finally have the working formula for PCC as:

$$\rho_{X,Y} = \frac{\mathbb{E}[XY] - \mathbb{E}[X]\mathbb{E}[Y]}{\sqrt{\mathbb{E}\left[X^2\right] - (\mathbb{E}[X])^2}\sqrt{\mathbb{E}\left[Y^2\right] - (\mathbb{E}[Y])^2}} \tag{11.1.4}$$

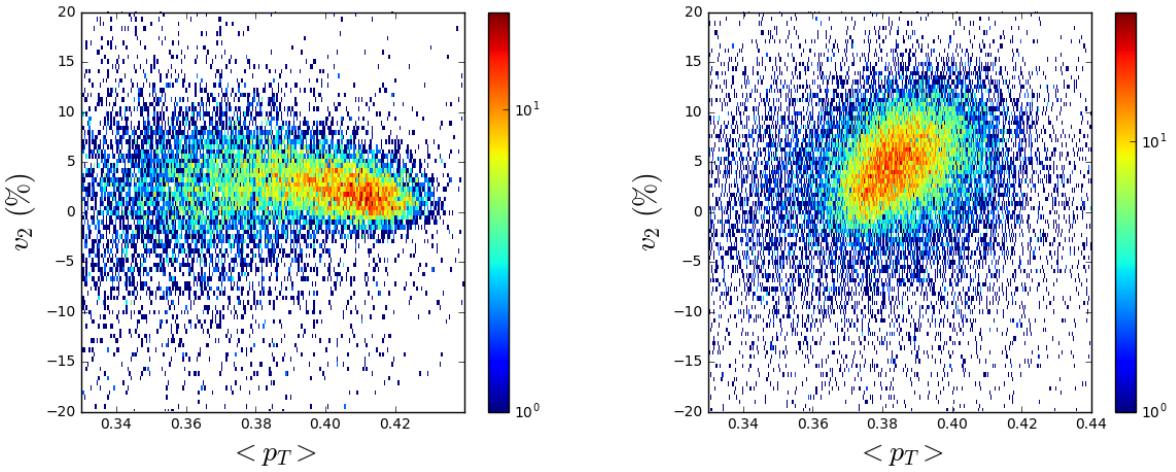

(a) For Default Version

(b) For SM version

Figure 48: v_2 vs $\langle p_T \rangle$ histograms

The final thing left to do is to interpret the value of $\rho_{X,Y}$. From equation 11.1.4, one observes that the range of correlation coefficient lies between -1 and 1. A value of 1/-1 implies that there a perfect

linear relationship between the random variables X and Y. Mathematically $y = m * x \ \forall$ ordered pairs $(x \in X, y \in Y)$. The value of +1 implies $m > 0$ and the variables are said to be positively correlated. The value of -1 implies $m < 0$ and the variables are said to be negatively correlated. A value of 0 implies that there is no linear correlation between the variables.

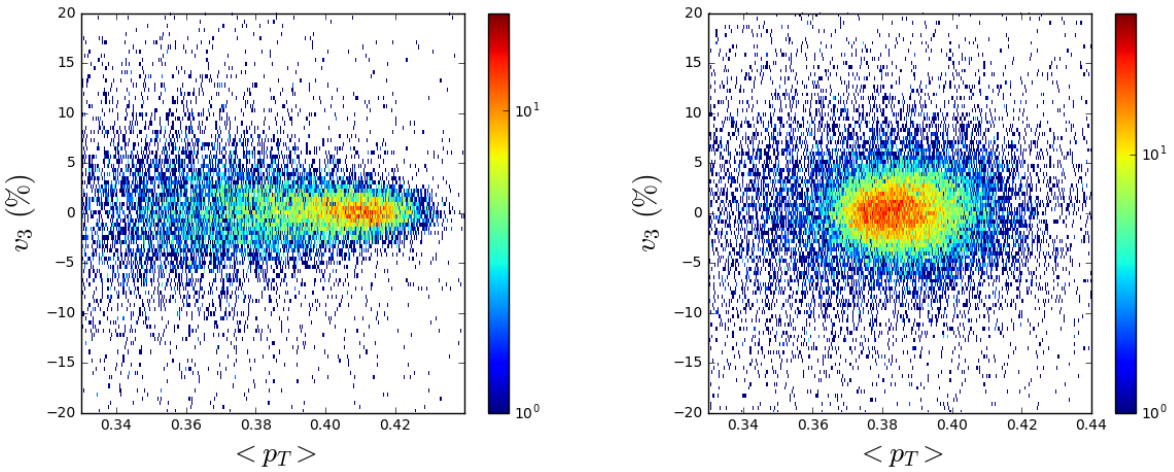

(a) For Default Version

(b) For SM version

Figure 49: v_3 vs $\langle p_T \rangle$ histograms

Just by looking at the histograms, one can say that only v_2 has some significant positive correlation with the mean p_T of the event. This can be explicitly seen from the PCC values tabulated in table 5. For v_2, there is roughly no correlation between the two observables for the default version while there is a small (yet significant) positive correlation in the SM version. For v_3, there is roughly no correlation between the two observables for the default version while there is an extremely weak positive correlation in the SM version.

Table 5: Data For Pearson correlation coefficient

Model \ Flow	Elliptic Flow	Triangular Flow
• Default	0.01	0.02
• SM	0.14	0.06

11.1.4 Collective Flow in ϕ Mesons

The ϕ meson has a quark content of $s\bar{s}$. The study of collective flow in ϕ mesons can help us directly probe the properties of the medium produced in HIC. The reason for this is that the interaction cross section for ϕ meson is less when compared to the interaction cross section for other hadrons. This can explicitly be seen from the cross section values detailed below[18]

$$\begin{aligned} \sigma_{\phi N} &\sim 10mb & \sigma_{KN} &\sim 2.1\sigma_{\phi N} \\ \sigma_{\rho N} &\sim 3\sigma_{\phi N} & \sigma_{\Lambda N} &\sim 3.5\sigma_{\phi N} \\ \sigma_{\pi N} &\sim 2.6\sigma_{\phi N} & \sigma_{NN} &\sim 4\sigma_{\phi N} \end{aligned}$$

This implies that ϕ meson decouples early. In simple words, once hadronization takes place to form the ϕ meson, it simply ignores any interaction with other particles of the medium before getting detected by the detector. This completes a qualitative argument to prove our initial claim. Consider the following graph for elliptic flow of ϕ meson as a function of $\sqrt{s_{NN}}$ (center of mass energy for a pair of nucleons) of the Au-Au colliding system.

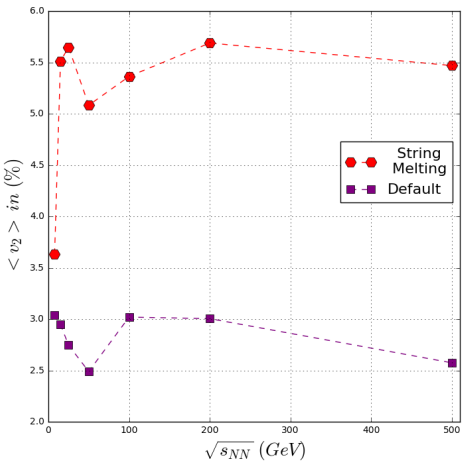

Figure 50: Elliptic Flow In ϕ meson as a function of $\sqrt{s_{NN}}$

In the above graph $\langle v_2 \rangle$ is the event average elliptic flow at corresponding $\sqrt{s_{NN}}$. This is further done at minimum bias which means that within an event the average is taken over all produced ϕ meson. One observes from the graph that that the trend followed by the default and the SM versions are roughly the same. The difference between the two versions lies primarily in the magnitude of elliptic flow produced. On an average, given $\sqrt{s_{NN}}$ the elliptic flow produced in a QGP like scenario is almost double when compared to the non-QGP like scenario. Hence, an usually large elliptic is a good indication that a QGP like medium was formed during the evolution of the collision system.

11.2 Analysis Using The Hydrodynamic Simulation

The basics of hydrodynamic framework has already been explained in section 10. As with the AMPT model, we first need to create two scenario between which we can compare to see if elliptic flow can

be effectively used as a signature of QGP.

11.2.1 Setting Up The Scenarios

The hydrodynamics simulated here will correspond to ideal hydrodynamic framework. In this framework, we don't have much freedom other than choosing the equation of state of the evolving system. This is what will differentiate between the two scenarios:

- Scenario 1 - NO QGP like medium is produced. This scenario is encoded into the simulation by using the equation of state for a massless ideal hadron resonance gas at 0 chemical potential. The parameterization in terms of energy density is given as (Appendix J2):

$$\begin{aligned} P &= \tfrac{1}{3}\epsilon \\ s &= 1.17\epsilon^{0.75} \\ T &= \tfrac{\epsilon+P}{s} = 1.14\epsilon^{0.25} \end{aligned} \tag{11.2.1}$$

- Scenario 2 - QGP like medium IS produced. This scenario is encoded into the simulation by using the equation of state from lattice QCD. A parameterization in terms in energy density can be found in arXiv:0912.2541.

11.2.2 Elliptic Flow From Ideal Hydrodynamic Framework

Consider the following $< v_2 >$ vs p_T graph for pions as recovered from the hydrodynamic simulations. Here p_T is the transverse momentum of the pions.

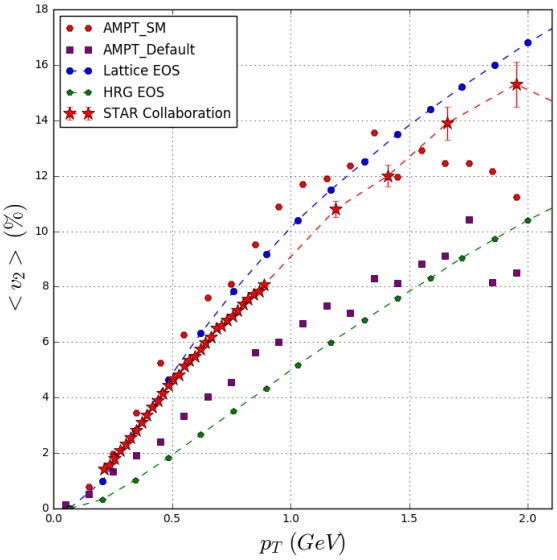

Figure 51: Elliptic Flow From Hydrodynamic Framework

One observes, that the elliptic flow obtained for Lattice EOS is almost double to what is obtained for the ideal HRG EOS. This is nothing new and was already seen in collective flow for ϕ meson that the elliptic flow is much larger for the scenario where QGP like medium is produced when compared to the non-QGP scenario. AMPT is a model that microscopically evolves the dynamics of the system while the same in the hydrodynamic system is done macroscopically. Hence, it is very satisfying to see that we obtain same results from two very different types of simulations. Further, we also see that elliptic flow obtained from lattice EOS is quite to close that of SM version of AMPT and is in good agreement from data of the STAR Collaboration. Similarly, elliptic flow obtained from AMPT default version and ideal HRG EOS are quite close to each other. In both the scenarios, elliptic flow obtained from AMPT model is just a bit higher when compared to corresponding scenarios in the hydro-simulation.

11.3 Results

- For v_2 (Elliptic Flow):
  - NCQ scaling is observed only for the scenario where the model was encoded to have a QGP medium.
  - Elliptic flow is almost double for the QGP scenario when compared to the non-QGP scenario.
  - Elliptic flow has weak positive correlation and roughly no correlation with $\langle p_T \rangle$ for SM and Default versions respectively.
  - The results for elliptic flow in both the scenarios are consistent for both the AMPT and hydrodynamic models. They are also in good agreement with the data from STAR collaboration.
- For v_3 (Triangular Flow):
  - The momentum anisotropy is dominated by elliptic flow for both the Default and SM versions.
  - A modified NCQ scaling is observed only for the scenario where the model was encoded to have a QGP medium.
  - Triangular flow is almost double for the QGP scenario when compared to the non-QGP scenario.
  - Triangular flow has an extremely weak correlation and roughly no correlation with $\langle p_T \rangle$ for SM and Default versions respectively.
- Presence of NCQ scaling for v_2 and a modified NCQ scaling for v_3 is a definite characteristic of formation of QGP like medium.
- Large elliptic flow in produced particles is a good signature of QGP like behavior.

Chapter 9: Brief Summary Of The Thesis

12 Final Conclusions

In this initial part of this thesis work, we have seen that simple statistical mechanics formulation has been incredibly efficient in explaining the physics of non-relativistic realm. When applied to photons it gives the famous Stephan-Boltzmann and Wien Displacement Laws, applied to phonons gives sigmoidal type curve for specific heat and when applied to massive bosons, it explains the phenomenon of Bose-Einstein condensation. This success has motivated us to apply statistical mechanics to the system formed due to high energy collisions in the form of Hadron Resonance Gas.

In this thesis, three different versions of HRG are considered. First is ideal HRG where constituent particles have point size, second is VDWEV HRG (Van-der waals' excluded volume) where constituent particles have finite size and finally attractive VDWEV HRG where attractive interactions between constituent particles is introduced in addition to their finite size. When compared to data of lattice QCD from Wuppertal-Budapest, it is observed that ideal gas model for HRG at 0 chemical potential is in quite good agreement. Significant deviations start appearing for $T > 150$ MeV which is close to the phase transition temperature to QGP. The attractive interacting HRG (with hard sphere radius of 0.59fm and an interacting strength corresponding to 329Mevfm^3) is a slightly better fit to lattice QCD data. This however works under the assumption that mesons and baryons are part of different subsystems. Further mesons are considered to be behaving ideally while only baryons are treated with the interacting HRG formalism.

Another thermal model called THERMUS is applied is extract chemical freeze out parameters from the invariant yields of the produced particles ($\pi^{\pm}, K^{\pm}, p(\bar{p}), \Lambda(\bar{\Lambda}), K^0_S, \Xi^-(\bar{\Xi}^+)$) to Au-Au collisions at $\sqrt{s_{NN}}$ = 7.7,11.5,15,27 and 39 GeV. The advantage of using THERMUS model is that it takes finite life-time of resonances and their decays into account which was previously absent in the HRG model. The fit parameters obtained from THERMUS are in quite good agreement with that obtained from STAR collaboration. It is observed that inclusion of strange baryons increases the freeze-out temperature as expected. The success of thermal models in describing the thermodynamics of high energy collisions suggests that indeed a thermal equilibrated medium is formed during the evolution of the medium formed due to HIC. Further AMPT model is used to constrain particle production in Au-Au collisions at $\sqrt{s_{NN}}$=7.7 GeV. AMPT model reproduces the particle spectra for hadrons containing only light quarks (pions and protons) while it fails to do so for hadron containing strange quark (kaon).

Finally, simulations from the AMPT model and hydrodynamic framework are used to see if elliptic flow can be used as a valid QGP signature. In AMPT, default model and string melting (SM) versions simulate the non-QGP and QGP like scenarios respectively. In hydro, similar scenarios are reproduced using the ideal massless HRG EOS and lattice EOS respectively. It is observed in AMPT that the presence of NCQ scaling for elliptic flow and a modified NCQ scaling for triangular is a definite characteristic of formation of QGP like medium. It is also observed that elliptic flow is almost double for the QGP scenario when compared to the non-QGP scenario. The latter observation has also been supported from elliptic flow obtained from hydro-simulations which is quite wonderful. Hence it is quite safe to say large elliptic flow in produced particles is a good and reliable signature of QGP like behavior.

Appendices And Data Tables

13 Appendix

13.1 Appendix A1: Calculation for internal energy and specific heat for Photons

The formula for energy density as 4.3.14 and 4.3.15 is:

$$\frac{U}{V} = \int_0^\infty d\omega \ \frac{\hbar}{\pi^2 c^3} \frac{\omega^3}{e^{\beta\hbar\omega} - 1}$$

Consider the integral:

$$\begin{aligned} I = \int_0^\infty d\omega \ \frac{\omega^3}{e^{\beta\hbar\omega} - 1} &= \int_0^\infty d\omega \ \frac{\omega^3 e^{-\beta\hbar\omega}}{1 - e^{-\beta\hbar\omega}} \\ &= \int_0^\infty d\omega \ \omega^3 \left[\sum_{n=0}^\infty (e^{-\beta\hbar\omega})^n \right] \\ &= \sum_{n=0}^\infty \int_0^\infty d\omega \ \omega^3 e^{-\beta\hbar n\omega} \end{aligned} \tag{13.1.1}$$

Now make the substitution $\beta\hbar\omega = t$ and $\beta\hbar d\omega = dt$ to get:

$$\begin{aligned} I &= \sum_{n=0}^\infty \frac{1}{(\hbar\beta)^4} \frac{1}{n^4} \int_0^\infty t^3 e^{-t} \ dt \\ &= \frac{\Gamma(4)}{(\hbar\beta)^4} \sum_{n=0}^\infty \frac{1}{n^4} = \frac{\Gamma(4)}{(\hbar\beta)^4} \zeta(4) \end{aligned} \tag{13.1.2}$$

Here Γ, ζ are the generalized factorial function and the Reimann zeta function respectively. Both their values are known standards and can be substituted to get:

$$I = \frac{\pi^4}{15(\beta\hbar)^4} \tag{13.1.3}$$

$$\frac{U}{V} = \frac{\pi^2}{15} \frac{(kT)^4}{(\hbar c)^3} \tag{13.1.4}$$

$$C_V = \frac{\partial U}{\partial T} = \frac{4\pi^2 V k^4 T^3}{15(\hbar c)^3} \tag{13.1.5}$$

13.2 Appendix A2: Solving Equation 4.3.21

Equation 4.3.21 are quite the special equations and require the use of Lambert W function or the product log function to solve exactly. These equations have infinitely many solutions in the complex domain, however we are lucky to solve only for the real solution. The equation has a form:

$$\begin{aligned} e^x(x-3) + 3 &= 0 \\ \implies (x-3)e^{(x-3)} &= -3e^{-3} \end{aligned} \tag{13.2.1}$$

Now apply the lambert W function on both sides. The left sides reduces simply to x due to the defining properties of the function. Hence:

$$\begin{aligned} \implies W_n\left[(x-3)e^{(x-3)}\right] &= W_n\left[-3e^{-3}\right] \\ \implies x-3 &= W_n\left[-3e^{-3}\right] \\ \implies x &= 3+W_n\left[-3e^{-3}\right] \quad n\in\mathbb{Z} \end{aligned} \tag{13.2.2}$$

Since lambert W function is inverse of a multi-valued function branch cuts are required to be defined in the complex domain to return a valid value. Each of those branch cuts are index by an integer which is the significance of 'n'. Since we only need real solutions, equation 5.2.2 need to be solved for n=0,-1. One can use Wolfram Mathematica to get the particular values to get:

$$n=0 \implies x=0 \tag{13.2.3}$$

$$n=-1 \implies x=2.82144 \tag{13.2.4}$$

Both are valid solutions to 5.2.1 (however x=0 is not a physical solution to our system).

13.3 Appendix B1: Solving For Internal Energy Of Phonons

The internal energy as given by 4.4.12 is:

$$U=\sum_{i=1}^{3N}\frac{\hbar\omega_i}{e^{\beta\hbar\omega_i}-1}$$

Using 4.4.4 and 4.4.5 to go to the continuous version to get:

$$U=\frac{3V}{2\pi^2c^3}\int_0^{\omega_m}d\omega\ \omega^2\frac{\hbar\omega}{e^{\beta\hbar\omega}-1}$$

$$\frac{U}{N}=\frac{9(kT)^4}{(\hbar\omega_m)^3}\int_0^{\beta\hbar\omega_m}dt\frac{t^3}{e^t-1}$$

The second part can be obtained by making the substitution $\beta\hbar\omega=t$. Now define the special function, Debye function and the Debye temperature as follows. The Debye function is extensively studied in mathematics and I have directly picked up its expansion at the relevant points.

$$D(x)\equiv\frac{3}{x^3}\int_0^x dt\frac{t^3}{e^t-1}=\begin{cases}1-\frac{3}{8}x+\frac{1}{20}x^2+\cdots & (x\ll 1)\\ \frac{\pi^4}{5x^3}+O\left(e^{-x}\right) & (x\gg 1)\end{cases}$$

$$kT_D=\hbar\omega_m=\hbar c\left(\frac{6\pi^2N}{N}\right)^{1/3}$$

Now everything can be finally re-substituted to get:

$$\frac{U}{N}=3kTD(T_D/T)=\begin{cases}3kT\left(1-\frac{3}{8}\frac{T_D}{T}+\cdots\right) & (T\gg T_D)\\ 3kT\left[\frac{\pi^4}{5}\left(\frac{T}{T_D}\right)^3+O\left(e^{-T_D/T}\right)\right] & (T\ll T_D)\end{cases} \tag{13.3.1}$$

13.4 Appendix B2: Solving For Specific Heat Of The Phonon System

Using 11.3.1 we want to compute the specific heat. Before starting the differentiating process define $x = T_D/T$ The major steps are as follows:

$$\frac{C_V}{Nk} = 3D(x) + 3T\left[\frac{\partial D(x)}{\partial x}\frac{\partial x}{\partial T}\right]$$
$$\frac{\partial D(x)}{\partial x} = -\frac{9}{x^4}\int_0^x \frac{t^3}{e^t-1}dt + \frac{3}{e^x-1} = -\frac{3}{x}D(x) + \frac{3}{e^x-1}$$
$$\frac{\partial x}{\partial T} = -\frac{1}{T^2}T_D = -\frac{x}{T}$$
$$\frac{C_V}{Nk} = 3\left[4D(x) - \frac{3x}{e^x-1}\right]$$

Now the value of x can be re-substituted to get back the desired result:

$$C_V = \begin{cases} 3Nk\left[1 - \frac{1}{20}\left(\frac{T_D}{T}\right)^2 + \cdots\right] & (T \gg T_D) \\ \frac{12Nk\pi^4}{5}\left(\frac{T}{T_D}\right)^3 + O\left(e^{-T_D/T}\right) & (T \ll T_D) \end{cases}$$

13.5 Appendix C1: Solving The General Bose Integrals

The integral we wish to evaluate is:

$$I_\nu(\beta,\beta\mu) = \int_0^\infty d\epsilon\ \frac{\epsilon^\nu}{e^{\beta(\epsilon-\mu)}-1}$$
$$= \int_0^\infty d\epsilon\ \epsilon^\nu \sum_{k=1}^\infty (e^{-\beta(\epsilon-\mu)})^k$$
$$= \sum_{k=1}^\infty (e^{\beta\mu})^k \int_0^\infty \epsilon^\nu\ e^{-\beta\epsilon k}\ d\epsilon$$

Now make the substitution $\beta\epsilon k = t$ and $d\epsilon = \frac{1}{\beta k}dt$ to get:

$$I = \frac{1}{\beta^{\nu+1}}\left[\sum_{k=1}^\infty \frac{(e^{\beta\mu})^k}{k^{\nu+1}}\right]\left(\int_0^\infty t^\nu e^{-t}dt\right)$$

Now it's just a matter of recognizing the famous functions. The function in [] and () brackets are the Drichlet-Reimann functions and the Generalized factorial function respectively leading to the result:

$$I = \frac{\Gamma(\nu+1)}{\beta^{\nu+1}} g_{\nu+1}(e^{\beta\mu}) \tag{13.5.1}$$

This is the general trick of solving these type of integrals. Even the fermi-integrals can be reduced using this type of analysis. All hail complex numbers and analytic continuation properties which allow us to formulate continuous versions of an otherwise discrete function.

13.6 Appendix C2: The Clayperon Equation

The Clayperon equation is a way of characterizing a discontinuous phase transition between two phases of matter having the same basic constituent. As generally, phase transitions occur under atmospheric pressure, hence this equation comes in to be quite useful.
The derivation begins by considering two phases α & β currently at equilibrium with each other. At the coexistence curve we must have:

$$d\mu_\alpha = d\mu_\beta$$

Using the extensive property of internal energy, assuming V,S and N to be the extensive variables and applying the Euler's homogeneous theorem, the internal energy has the form:

$$U = -PV + TS + N\mu$$

By first Law of thermodynamics we have:

$$dU = -PdV + TdS + \mu dN$$

Differentiating the original equation and comparing with the first law gives:

$$d\mu = -sdT + vdP$$

Using the property of the coexistence curve, we have:

$$-(s_\beta - s_\alpha)dT + (v_\beta - v_\alpha)dP = 0$$
$$\frac{dP}{dT} = \frac{\Delta s}{\Delta v} = \frac{L_p}{T\Delta v}$$

The final obtained equation is the famous Clayperon-Equation.

13.7 Appendix D1: Towards Van der Waals' Equation From The Virial Equation For Dilute Gases

Dividing the equation of state with the number density and comparing the resulting equation with the Virial equation of state, we get:

$$\sum_{l=1}^{\infty} a_l \left(\sum_{n=1}^{\infty} n\bar{b}_n z^n \right)^{l-1} = \frac{\sum\limits_{l=1}^{\infty} \bar{b}_l z^l}{\sum\limits_{l=1}^{\infty} l\bar{b}_l z^l}$$

$$\left(\bar{b}_1 z + 2\bar{b}_2 z^2 + 3\bar{b}_3 z^3 + \cdots\right) \left[a_1 + a_2 \left(\sum_{n=1}^{\infty} n\bar{b}_n z^n \right) + a_3 \left(\sum_{n=1}^{\infty} n\bar{b}_n z^n \right)^2 + \cdots \right]$$

$$= \bar{b}_1 z + \bar{b}_2 z^2 + \bar{b}_3 z^3 + \cdots$$

Comparing the coefficients of powers of z on both sides we have:

$$\begin{aligned} a_1 &= \bar{b}_1 = 1 \\ a_2 &= -\bar{b}_2 \\ a_3 &= 4\bar{b}_2^2 - 2\bar{b}_3 \\ &\dots \end{aligned}$$

Hence each Virial coefficient can be written in terms of linear combination of some cluster coefficients. Further, each cluster coefficient can be computed as a sum of finite number of integrals. Hence the classical cluster problem is simply a problem where we have to solve a large but finite number of integrals, however the integrals might not be easy. Now re-writing the Virial equation of state upto second order we have:

$$P = \frac{NkT}{V}\left[1 + a_2\lambda^3\frac{N}{V}\right]$$

Now substituting, $a_2\lambda^3 = B_2$ and realizing that for a dilute gas $\rho = N/V$ is small and using the approximation $\frac{1}{1-x} \approx 1 + x$ if $|x| << 1$:

$$\begin{aligned} P &= \frac{NkT}{V\left[1 - B_2\frac{N}{V}\right]} \\ P &= \frac{NkT}{[V - NB_2]} \\ P\left[V - NB_2\right] &= NkT \end{aligned}$$

Now:

$$\begin{aligned} B_2 &= a_2\lambda^3 = -\bar{b}_2\lambda^3 \\ B_2(T) &= -\frac{1}{2V}\iint f_{12}d\vec{r}_1 d\vec{r}_2 = -\frac{1}{2V}\iint f_{12}d\vec{r}_1 d\vec{r}_{12} \\ &= -\frac{1}{2}\int_0^\infty\int_0^\pi\int_0^{2\pi} drd\theta d\phi r^2\sin\theta f_{12} = -2\pi\int_0^\infty f_{12}r^2 dr \end{aligned}$$

Here to solve the integral we gave made the following substitutions:

$$\begin{aligned} \vec{r}_1 &= \frac{1}{2}\left[\vec{r}_1 + \vec{r}_2\right] \\ \vec{r}_{12} &= \vec{r}_2 - \vec{r}_1 \\ Determinant\ Of\ the\ Jacobian\ Matrix &= |J| = 1 \\ \int d\vec{r}_1 &= V\ (Center\ Of\ Mass\ Volume) \\ f_{12} &= f_{12}(|\vec{r}_{12}|) \end{aligned}$$

13.8 Appendix D2: Proving Some Properties Of $W_N(1,2,\cdots,N)$

Proof Of property 1:

$$W_1(1) = W_1(\vec{r}_1) = \frac{\lambda^3}{V}\sum_{\vec{p}} e^{-i\vec{p}\cdot\vec{r}_1/\hbar} e^{(\beta\hbar^2/2m)\nabla^2} e^{i\vec{p}\cdot\vec{r}_1/\hbar}$$

$$= \left(\frac{\lambda}{h}\right)^3 \int d^3p e^{-\beta p^2/2m} = 1$$

Proof Of Property 2:

$$W_N(1,2,\cdots,a,\cdots,b,\cdots,N) = N!\lambda^{3N}\sum_{\alpha}\Psi^*_\alpha(1,2,\cdots,a,\cdots,b,\cdots,N)e^{-\beta\mathscr{H}}\Psi_\alpha(1,2,\cdots,a,\cdots,b,\cdots,N)$$

$$W_N(1,2,\cdots,a,\cdots,b,\cdots,N) =$$

$$\begin{cases} N!\lambda^{3N}\sum\limits_{\alpha}\Psi^*_\alpha(1,2,\cdots,b,\cdots,a,\cdots,N)e^{-\beta\mathscr{H}}\Psi_\alpha(1,2,\cdots,b,\cdots,a,\cdots,N) & \text{for Bosons} \\ N!\lambda^{3N}\sum\limits_{\alpha}-\Psi^*_\alpha(1,2,\cdots,b,\cdots,a,\cdots,N)e^{-\beta\mathscr{H}}-\Psi_\alpha(1,2,\cdots,b,\cdots,a,\cdots,N) & \text{for Fermions} \end{cases}$$

$$W_N(1,2,\cdots,a,\cdots,b,\cdots,N) = W_N(1,2,\cdots,b,\cdots,a,\cdots,N)$$

Proof Of Property 3:

$$Let\ \Psi_\alpha = \sum_\lambda S_{\alpha\lambda}\Phi_\lambda,\ where\ S_{\alpha\lambda}\ be\ a\ unitary\ matrix:$$

$$\sum_\alpha S^*_{\alpha\lambda}S_{\alpha\gamma} = \delta_{\lambda\gamma}$$

$$\sum_\alpha \left\langle \Psi_\alpha, e^{-\beta\mathscr{H}}\Psi_\alpha\right\rangle = \sum_{\alpha,\lambda} S^*_{\alpha\lambda}S_{\alpha\gamma}\left\langle \Phi_\lambda, e^{-\beta\mathscr{H}}\Phi_\gamma\right\rangle = \sum_\lambda \left\langle \Phi_\lambda, e^{-\beta\mathscr{H}}\Phi_\lambda\right\rangle$$

13.9 Appendix D3: First Order Calculation Of $b_2 - b_2^{(0)}$ For Fermions And Bosons

For the hard sphere potential, $\eta_{l=0,1} \approx -(ka)^{2l+1}/(2l+1)$ is a good approximation to start off with. This is definitely not the exact phase shift but at the lowest order of analysis this goes through. This will not give the correct numerical coefficients, however it will depict the correct relation with the hard-sphere scattering parameter 'a'. Before the starting of this calculation, we shall assume that the potential does not form any two-particle bound states.
For Bosons, we only consider l=0 term in 2.3.11:

$$\frac{\partial\eta_0(k)}{\partial k} = -a$$

$$b_2 - b_2^{(0)} = -\frac{2^{3/2}a}{\pi}\int_0^\infty dk\ e^{-\frac{\beta\hbar^2k^2}{2m}}$$

$$b_2 - b_2^{(0)} = -\frac{2a}{\lambda} \qquad \lambda \text{ is the thermal wavelength}$$

Now for fermions only l=1 term is considered as we are doing a lowest order analysis. Hence:

$$\frac{\partial \eta_0(k)}{\partial k} = -3a^3k^2$$

$$b_2 - b_2^{(0)} = -\frac{3a^3 2^{3/2} a}{\pi} \int_0^\infty dk\ k^2 e^{-\frac{\beta\hbar^2k^2}{2m}}$$

$$\text{Change Of Variables: } \frac{\beta\hbar^2k^2}{m} = t \qquad 2kdk = \frac{m}{\beta\hbar^2}dt$$

$$b_2 - b_2^{(0)} = \frac{3\sqrt{2}a^3}{\pi}\left(\frac{m}{\beta\hbar^2}\right)^{3/2} \int_0^\infty t^{1/2}e^{-t}\ dt$$

$$b_2 - b_2^{(0)} = \frac{3\sqrt{2}a^3}{\pi}\left(\frac{m}{\beta\hbar^2}\right)^{3/2} (1/2)!$$

$$b_2 - b_2^{(0)} = -6\pi\left[\frac{a}{\lambda}\right]^3 \qquad \lambda \text{ is the thermal wavelength}$$

13.10 Appendix E1: Dependence between N-body S-wave Pseudopotential And Hard-Sphere Diameter

To find the exact expression of an N-body pseudopotential one needs to solve a corresponding l-body problem with the hard sphere potential. However, finding out the dependence on the hard sphere diameter 'a' can be done easily using a simple dimensional argument. Consider an intersection of N-surfaces of type S_{ij} as defined in 3.1.3. Then we have a N-body Schrodinger equation. Recursively applying the method of pseudopotentials suggests that this N-body Hamiltonian can be expressed as a sum of 2-body pseudopotential, 3-body pseudopotential, $\cdots$, N-body pseudopotential. Here N - body pseudopotential will consist of N-1 delta functions to incorporate the effect of N-particles colliding at the same coordinates in space. Hence:

$$\left(\nabla_1^2 + \nabla_2^2 + \cdots + \nabla_N^2 + k^2\right)\Psi$$
$$= (\text{ sum of two-body pseudopotentials }) + (\text{ sum of three-body pseudopotentials })$$
$$+ \cdots + (\text{ sum of (N-1)-body pseudopotentials }) + \delta(\vec{r}_1 - \vec{r}_2)\,\delta(\vec{r}_1 - \vec{r}_3)\cdots\delta(\vec{r}_1 - \vec{r}_N)\,C_N\Psi$$

Now a simple dimensional analysis gives:

$$\nabla_1^2 = [L]^2 \qquad \delta^3(\vec{r}_1 - \vec{r}_2) = [L]^{-3}$$
$$C_N = [L]^{3(N-1)-2} = [L]^{3N-5}$$

Since the only available parameter of length in our problem is the hard-sphere diameter, 'a' we have the following relation:

$$C_N \propto a^{3N-5}$$

13.11 Appendix E2: Energy Eigenvalues For Bose Gases For Pseudopotential Part

The Hamiltonian in consideration is:

$$V = \sum_{i<j} V_{ij}^P = \sum_{i<j} \delta(\vec{r_i} - \vec{r_j})$$

Let Φ_α is the N-body wavefunction formed by symmeterizing the product $u_{\alpha_1}(1)u_{\alpha_2}(2)\cdots u_{\alpha_N}(N)$. Here $u_{\alpha_1}(1) \equiv u_{\alpha_1}(\vec{r_1})$ is a state of a single particle wave-function corresponding to particle number 1 of the N-body system. The energy of the system can be calculated using:

$$\langle \Phi_\alpha | V | \Phi_\alpha \rangle = \int d^{3N} r \Phi_\alpha^* \sum_{i<j} V_{ij}^P \Phi_\alpha = \frac{1}{2} N(N-1) \int d^{3N} r \Phi_\alpha^* v_{12} \Phi_\alpha$$

The second integral is realized by taking into account that there are ${}^N C_2$ potential terms in the sum. Further each term depends on only two independent coordinates of the system. Hence they can be suitably renamed to match the first term of the sum. Now:

$$\begin{aligned}
\langle \Phi_\alpha | V | \Phi_\alpha \rangle &= \frac{N(N-1)}{N!2} \sum_P \sum_Q \int d^{3N} r \left[u_{P\alpha_1}^*(1) \cdots u_{P\alpha_N}^*(N) \right] v_{12} \left[u_{Q\alpha_1}(1) \cdots u_{Q\alpha_N}(N) \right] \\
&= \frac{N(N-1)}{N!2} \sum_P \sum_Q \langle P\alpha_1, P\alpha_2 | v | Q\alpha_1, Q\alpha_2 \rangle \left(\delta_{P\alpha_3, Q\alpha_3} \cdots \delta_{P\alpha_N, Q\alpha_N} \right) \\
&\text{where} \qquad \langle \alpha, \beta | v | \gamma, \lambda \rangle \equiv \int d^3 r_1 d^3 r_2 u_\alpha^*(1) u_\beta^*(2) v_{12} u_\gamma(1) u_\lambda(2)
\end{aligned}$$

Here P,Q are permutations on N objects. Permutation P sends the ordered set {1,2,...,N} to the ordered set {P1,P2,...,PN}. Summing over takes care of symmeterization but not normalization. $\langle \Phi_\alpha | \Phi_\alpha \rangle = \prod_\alpha (n_\alpha!)$ with n_α being the occupation number of the single particle state α. In the inner product, the only non-zero terms have: $P\alpha_1 = Q\alpha_1$ and $P\alpha_2 = Q\alpha_2$ or $P\alpha_2 = Q\alpha_1$ and $P\alpha_1 = Q\alpha_2$ with $P\alpha_j = Q\alpha_j \; for \; all \; jneq 1, 2$. Hence:

$$\langle \Phi_\alpha | V | \Phi_\alpha \rangle = \frac{N(N-1)}{N!2} \prod_\alpha (n_\alpha!) \quad \times \sum_P \left(\langle P\alpha_1, P\alpha_2 | v | P\alpha_1, P\alpha_2 \rangle + \langle P\alpha_1, P\alpha_2 | v | P\alpha_2, P\alpha_1 \rangle \right)$$

Now, we will change the label from states of the single particle system to occupation numbers. There are (N-2)! permutations that that effect the quantum numbers $\{\alpha_3, ..., \alpha_N\}$, leaving $\{\alpha_1, \alpha_2\}$ unchanged. Further let the occupation numbers of state α be denoted by n_α. Then the number of ways in which a pair, say (α, β) can be chosen is simply:

$$\begin{aligned}
f_{\alpha\beta} &= \begin{cases} n_\alpha n_\beta & (\alpha \neq \beta) \\ \frac{1}{2} n_\alpha (n_\alpha - 1) & (\alpha = \beta) \end{cases} \\
&\text{combining} \qquad f_{\alpha\beta} = (1 - \delta_{\alpha\beta}) n_\alpha n_\beta + \tfrac{1}{2} \delta_{\alpha\beta} n_\alpha (n_\alpha - 1)
\end{aligned}$$

Hence:

$$\left\langle \Phi'_n|V|\Phi'_n \right\rangle = \frac{1}{2}N(N-1)\frac{(N-2)!}{N!}\sum_{\alpha,\beta} f_{\alpha\beta}(\langle\alpha,\beta|v|\alpha,\beta\rangle + \langle\alpha,\beta|v|\beta,\alpha\rangle)$$

$$|\Phi'_\alpha\rangle = \frac{1}{\sqrt{\prod_\alpha (n_\alpha!)}}|\Phi_\alpha\rangle \qquad \text{is now the normalized ket}$$

$$\left\langle \Phi'_n|V|\Phi'_n \right\rangle = \frac{1}{2}\sum_{\alpha,\beta}\left[(1-\delta_{\alpha\beta})\, n_\alpha n_\beta + \frac{1}{2}\delta_{\alpha\beta} n_\alpha\,(n_\alpha - 1)\right] \quad \times(\langle\alpha,\beta|v|\alpha,\beta\rangle + \langle\alpha,\beta|v|\beta,\alpha\rangle)$$

Since, we are working with the lowest order in perturbation theory, the eigenfunctions are simply the free-particle eigenfunctions of the ideal gas. Thus, each inner product simply gives out a factor of 1/V. Hence:

$$\left\langle \Phi'_n, \sum_{i<j}\delta\left(\vec{r}_i - \vec{r}_j\right)\Phi'_n \right\rangle = \frac{1}{V}\left[\sum_{\vec{p}\neq\vec{k}} n_{\vec{p}} n_{\vec{k}} + \frac{1}{2}\sum_{\vec{p}} n_{\vec{p}}\left(n_{\vec{p}} - 1\right)\right]$$

$$\sum_{\vec{p}\neq\vec{k}} n_{\vec{p}} n_{\vec{k}} = \sum_{\vec{p}} n_{\vec{p}} \sum_{\vec{k}} n_{\vec{k}} - \sum_{\vec{p}} n_{\vec{p}}^2 = N^2 - \sum_{\vec{p}} n_{\vec{p}}^2$$

$$E_n = \left\langle \Phi'_n, \sum_{i<j}\delta\left(\vec{r}_i - \vec{r}_j\right)\Phi'_n \right\rangle = \tfrac{1}{V}\left(N^2 - \tfrac{1}{2}N - \tfrac{1}{2}\sum_{\vec{p}} n_{\vec{p}}^2\right)$$

13.12 Appendix E3: Energy Eigenvalues For Spin 1/2 Fermi Gases For Pseudopotential Part

The interacting part of the Hamiltonian in consideration is:

$$V = \sum_{i<j} V_{ij}^P = \sum_{i<j}\delta(\vec{r}_i - \vec{r}_j)$$

Let Φ_α is the N-body wavefunction formed by symmeterizing the product $u_{\alpha_1}(1)u_{\alpha_2}(2)\cdots u_{\alpha_N}(N)$. Here $u_{\alpha_1}(1) \equiv u_{\alpha_1}(\vec{r}_1)$ is a state of a single particle wave-function corresponding to particle number 1 of the N-body system. The energy of the system can be calculated using:

$$\langle\Phi_\alpha|V|\Phi_\alpha\rangle = \int d^{3N}r\Phi_\alpha^* \sum_{i<j} V_{ij}^P \Phi_\alpha = \frac{1}{2}N(N-1)\int d^{3N}r\Phi_\alpha^* v_{12}\Phi_\alpha$$

The second integral is realized by taking into account that there are ${}^NC_2$ potential terms in the sum. Further each term depends on only two independent coordinates of the system. Hence they can be

suitably renamed to match the first term of the sum. Now:

$$\langle\Phi_\alpha|V|\Phi_\alpha\rangle = \frac{N(N-1)}{N!2}\sum_P\sum_Q\int d^{3N}r\left[u^*_{P\alpha_1}(1)\cdots u^*_{P\alpha_N}(N)\right]v_{12}\left[u_{Q\alpha_1}(1)\cdots u_{Q\alpha_N}(N)\right]$$

$$= \frac{N(N-1)}{N!2}\sum_P\sum_Q\langle P\alpha_1, P\alpha_2|v|Q\alpha_1, Q\alpha_2\rangle\left(\delta_{P\alpha_3,Q\alpha_3}\cdots\delta_{P\alpha_N,Q\alpha_N}\right)$$

$$\text{where}\qquad \langle\alpha,\beta|v|\gamma,\lambda\rangle \equiv \int d^3r_1d^3r_2u^*_\alpha(1)u^*_\beta(2)v_{12}u_\gamma(1)u_\lambda(2)$$

Here P,Q are permutations on N objects. Permutation P sends the ordered set {1,2,...,N} to the ordered set {P1,P2,...,PN}. Summing over takes care of symmeterization but not normalization. $\langle\Phi_\alpha|\Phi_\alpha\rangle = \prod_\alpha(n_\alpha!)$ with n_α being the occupation number of the single particle state α. In the inner product, the only non-zero terms have: $P\alpha_1 = Q\alpha_1$ and $P\alpha_2 = Q\alpha_2$ or $P\alpha_2 = Q\alpha_1$ and $P\alpha_1 = Q\alpha_2$ with $P\alpha_j = Q\alpha_j$ *for all* $j \neq 1, 2$.
Now this is where we deviate from the case of bosons. Since the fermionic wavefunctions are completely anti-symmetric, we pick up an extra minus sign to get:

$$\langle\Phi_\alpha|V|\Phi_\alpha\rangle = \frac{N(N-1)}{N!2}\prod_\alpha(n_\alpha!)\quad\times\sum_P\left(\langle P\alpha_1, P\alpha_2|v|P\alpha_1, P\alpha_2\rangle - \langle P\alpha_1, P\alpha_2|v|P\alpha_2, P\alpha_1\rangle\right)$$

Now, we will change the label from states of the single particle system to occupation numbers. There are (N-2)! permutations that that effect the quantum numbers $\{\alpha_3, ..., \alpha_N\}$, leaving $\{\alpha_1, \alpha_2\}$ unchanged. Further let the occupation numbers of state α be denoted by n_α. Then the number of ways in which a pair, say (α, β) can be chosen is simply:

$$f_{\alpha\beta} = \begin{cases} n_\alpha n_\beta & (\alpha \neq \beta) \\ 0 & (\alpha = \beta) \end{cases}$$
$$\text{combining}\qquad f_{\alpha\beta} = (1 - \delta_{\alpha\beta})\, n_\alpha n_\beta$$

Hence:

$$\left\langle\Phi'_n|V|\Phi'_n\right\rangle = \frac{1}{2}N(N-1)\frac{(N-2)!}{N!}\sum_{\alpha,\beta}f_{\alpha\beta}(\langle\alpha,\beta|v|\alpha,\beta\rangle - \langle\alpha,\beta|v|\beta,\alpha\rangle)$$

$$|\Phi'_\alpha\rangle = \frac{1}{\sqrt{\prod_\alpha(n_\alpha!)}}|\Phi_\alpha\rangle\qquad\text{is now the normalized ket}$$

Further realizing that $n_\alpha \in \{0, 1\}$ for fermions, we have:

$$(\Phi_n, \Omega\Phi_n) = \frac{1}{2}\sum_{\alpha,\beta}n_\alpha n_\beta(\langle\alpha,\beta|v|\alpha,\beta\rangle - \langle\alpha,\beta|v|\beta,\alpha\rangle)$$

Now the free particle wavefunction can be written as:

$$u_{\rm ps}(\mathrm{r},\sigma) = \frac{1}{\sqrt{V}}e^{i\mathrm{p}\cdot\mathrm{r}/\hbar}\delta(s,\sigma)$$

$$\text{where}\qquad \delta(s,\sigma) = \begin{cases} 1 & (s = \sigma) \\ 0 & (s \neq \sigma) \end{cases}$$

However our interacting potential is independent of spin coordinates. Thus, we have:

$$\langle \alpha, \beta | \delta | \alpha, \beta \rangle = \frac{1}{V}$$
$$\langle \alpha, \beta | \delta | \beta, \alpha \rangle = \frac{1}{V} \delta \left(s_\alpha, s_\beta \right)$$

Now all we need to do is re-substitute. Let n_{ks} denote the occupation number of the momentum state 'k' with spin value 's'. Then:

$$\left\langle \Phi_n, \sum_{i<j} \delta \left(\mathbf{r}_i - \mathbf{r}_j \right) \Phi_n \right\rangle = \frac{1}{2V} \sum_{s,s'} \sum_{\mathbf{p},\mathbf{k}} n_{\mathbf{p}s} n_{\mathbf{k}s'} \left[1 - \delta \left(s, s' \right) \right]$$
$$= \frac{1}{2V} \left(N^2 - \sum_s \sum_{\mathbf{p},\mathbf{k}} n_{\mathbf{p}s} n_{\mathbf{k}s} \right)$$

Now let:

$$N_+ \equiv \sum_{\mathbf{p}} n_{\mathbf{p},+1}$$
$$N_- \equiv \sum n_{\mathbf{p},-1} = N - N_+$$

Finally, we have for spin-1/2 fermionic system:

$$\left\langle \Phi_n, \sum_{i<j} \delta \left(\mathbf{r}_i - \mathbf{r}_j \right) \Phi_n \right\rangle = \frac{N_+ N_-}{V}$$

13.13 Appendix F1:Reason For $\lambda = 6$ As The Appropriate Exponent

As an electron moves in a molecule, there exists a separation of positive and negative charges within the molecule. Hence the molecule acquires a time varying dipole moment $\vec{p}_{dip}$. Assuming this molecule to be at the origin, this instantaneous dipole moment generates an electric field given by:

$$\vec{E}(\vec{r}) = \frac{1}{4\pi\epsilon_0 r^3} \times \left[3(\vec{p}_{dip}.\vec{r})\vec{r} - |\vec{r}|^2 \vec{p}_{dip} \right]$$

Here $\vec{r}$ is the displacement vector from the origin. A second molecule, located at $\vec{r}$ relative to the first one develops an induced dipole moment due to the electric field of the first molecule. Let α be the molecular polarizability. Then the induced moment is given by:

$$\vec{p}_{ind}(\vec{r}) = \alpha \vec{E}(\vec{r})$$

The potential energy for this binary system is given by:

$$u(\vec{r}) = -\vec{p}_{ind}(\vec{r}) \bullet \vec{E}(\vec{r})$$

The average energy of interaction s the average over time and all possible orientations of $\vec{p}_{ind}(\vec{r})$. This is given by:

$$\overline{u(\vec{r})} = -\left(\frac{1}{t_2 - t_2}\right)\int_{t_1}^{t_2}\left[\left(\frac{1}{2\pi}\right)\int_0^{2\pi}\alpha|\vec{E}|^2 d\theta\right]dt$$

Computing $|E|^2$:

$$\vec{E}(\vec{r},t,\theta) = \frac{1}{4\pi\varepsilon_0|\vec{r}|^5}\left[3|\vec{p}||\vec{r}|cos\theta - |\vec{r}|^2\vec{p}\right]$$

$$|E|^2 = \frac{1}{16\pi^2\varepsilon^2|\vec{r}|^{10}}\left[9(\vec{p}\cdot\vec{r})^2|\vec{r}|^2 - 3|\vec{r}|^2(\vec{p}\cdot\vec{r})^2 - 3|\vec{r}|^2(\vec{p}\cdot\vec{r})^2 + |\vec{r}|^4|\vec{p}|^2\right]$$

$$\Rightarrow \frac{1}{16\pi^2\varepsilon^2|\vec{r}|^{10}}\left[3(\vec{p}\cdot\vec{r})^2 + |\vec{r}|^4|\vec{p}|^2\right]$$

Now using the above decomposition and the fact that $\frac{1}{2\pi}\int_0^{2\pi} cos^2\theta\ d\theta = 1/2$, we have:

$$\overline{u(\vec{r})} = \frac{-1}{(t_2 - t_1)}\int_{t_1}^{t_2}\cdot\left(\frac{\alpha}{16\pi^2\varepsilon_0^2|\vec{r}|^{10}}\right)\left[\frac{5}{2}r^4|\vec{p}|^2\right]dt$$

$$\overline{u(\vec{r})} = -\frac{5\alpha}{32\pi^2\varepsilon_0^2|\vec{r}|^6}\cdot\left\langle|\vec{p}|^2\right\rangle$$

Here the $\langle\rangle$ denote the time average. Clearly one can see that:

$$\overline{u(\vec{r})} \propto \frac{1}{|\vec{r}|^6}$$

13.14 Appendix F2: Explicit Computation Of Thermodynamic Parameters In The Excluded Volume Ideal Gas Model

Let us begin with the formula for number density. We have:

$$n_{id}^{excl}(T,\mu) = \frac{\partial P^{excl}}{\partial\mu}$$

$$= \frac{\partial P(T,\tilde{\mu})}{\partial\mu}$$

$$= \frac{\partial P(T,\tilde{\mu})}{\partial\tilde{\mu}}\frac{\partial\tilde{\mu}}{\partial\mu}$$

$$= n_{id}(T,)\left[1 - v_0\frac{\partial P(T,\tilde{\mu})}{\partial\tilde{\mu}}\right]$$

$$= n_{id}(T,\tilde{\mu})\left[1 - v_0\ n_{id}(T,\tilde{\mu})\right] + O(v_0^2)$$

Ignoring higher order terms and using $1 - x \approx \frac{1}{1+x}$ if $x \ll 1$

$$n_{id}^{excl}(T,\mu) = \frac{n_{id}(T,\tilde{\mu})}{1 + v_0\ n_{id}(T,\tilde{\mu})}$$

Now for the entropy density we have:

$$
\begin{aligned}
s_{id}^{excl}(T,\mu) &= \frac{\partial P^{excl}}{\partial T} \\
&= \frac{\partial P(T,\tilde{\mu})}{\partial T} \\
&= \left[\frac{\partial P(T,\tilde{\mu})}{\partial T}\right]_{\tilde{\mu}} + \left[\frac{\partial P(T,\tilde{\mu})}{\partial \tilde{\mu}}\right]_{T} \frac{\partial \tilde{\mu}}{\partial T} \\
&= s_{id}(T,\tilde{\mu}) + n_{id}\left[-v_0 \frac{\partial P_{id}(T,\tilde{\mu})}{\partial T}\right] = s_{id}(T,\tilde{\mu})\left[1 - v_0\ n_{id}(T,\tilde{\mu})\right] + O(v_0^2)
\end{aligned}
$$

Ignoring higher order terms and using $1 - x \approx \dfrac{1}{1+x}$ if $x \ll 1$

$$
s_{id}^{excl}(T,\mu) = \frac{s_{id}(T,\tilde{\mu})}{1 + v_0\ n_{id}(T,\tilde{\mu})}
$$

Finally, for energy density we have the following trick:

$$
\begin{aligned}
\epsilon_{id}^{excl}(T,\mu) &= T s_{id}^{excl}(T,\mu) - P + \mu n_{id}^{excl}(T,\mu) \\
P &= \frac{P[1 + v_0\ n_{id}(T,\tilde{\mu})]}{1 + v_0\ n_{id}(T,\tilde{\mu})} \approx \frac{P}{1 + v_0\ n_{id}(T,\tilde{\mu})}
\end{aligned}
$$

Using: $v_0\ n_{id}(T,\tilde{\mu}) \ll 1 \implies P \gg P \times v_0\ n_{id}(T,\tilde{\mu}) \implies P[1 + v_0\ n_{id}(T,\tilde{\mu})] \approx P$

$$
\epsilon_{id}^{excl}(T,\mu) = \frac{\epsilon_{id}(T,\tilde{\mu})}{1 + v_0\ n_{id}(T,\tilde{\mu})}
$$

As one observes, all the above formulae are only valid under first order approximation in perturbation series of v_0 and face the condition $v_0\ n_{id}(T,\tilde{\mu}) \ll 1$.

13.15 Appendix G1: Some More Graphs For Ideal Hadron Resonance Gas

This section contains the non-normalized graphs of various thermodynamic parameters at 0 chemical potential. Further, it also contains graphs for ideal hadron resonance gas at various values of baryonic chemical potential μ_B or simply μ as I have only considered baryonic chemical potential in the formulation.

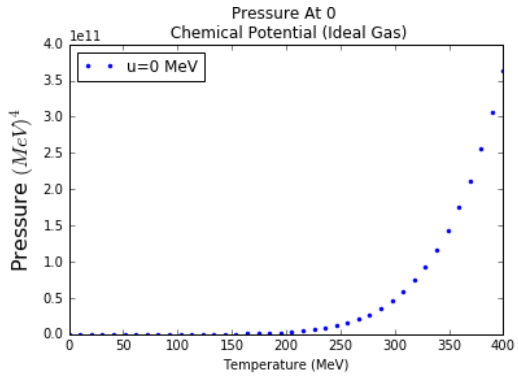

(a) Graph of Pressure vs Temperature

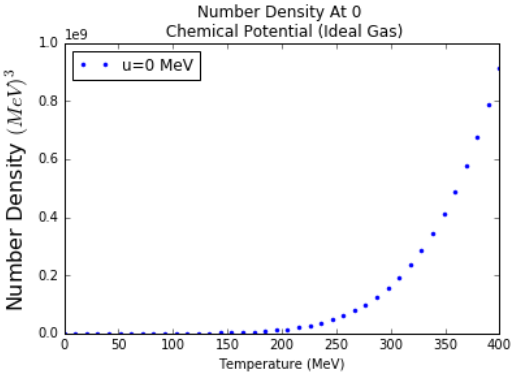

(b) Graph of Number Density vs Temperature

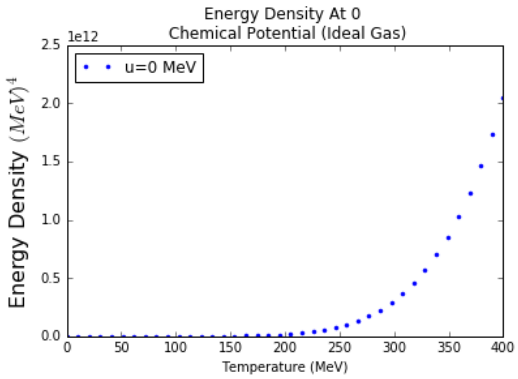

(c) Graph of Energy Density vs Temperature

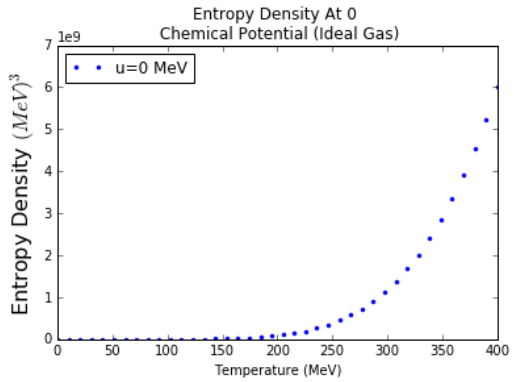

(d) Graph of Entropy Density vs Temperature

Figure 52: Graphs Of Some Important Parameters For A General Relativistic Ideal Hadron Resonance Gas At 0 Chemical Potential

The graphs shown in figure below are for a variety of values of μ. All the parameters are plotted for 7 different values of μ. The values are as follows: $['0','0.1','1','10','100','500']$

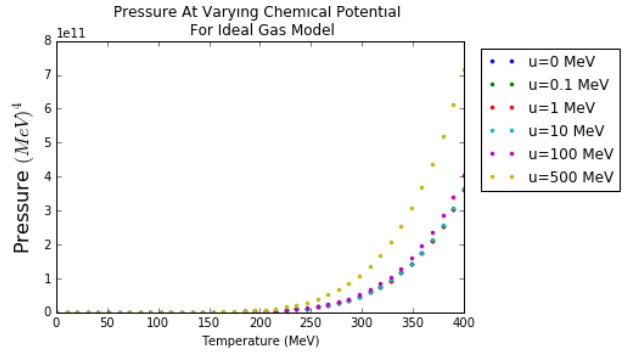

(a) Graph of Pressure vs Temperature

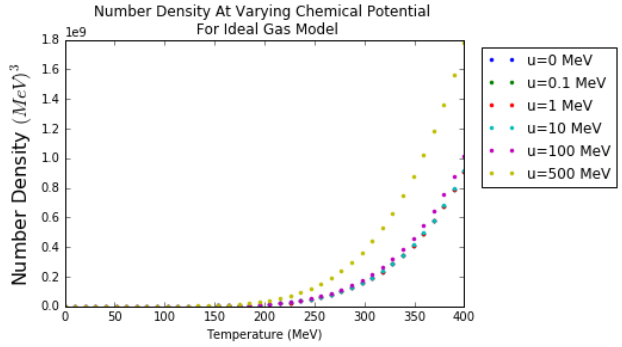

(b) Graph of Number Density vs Temperature

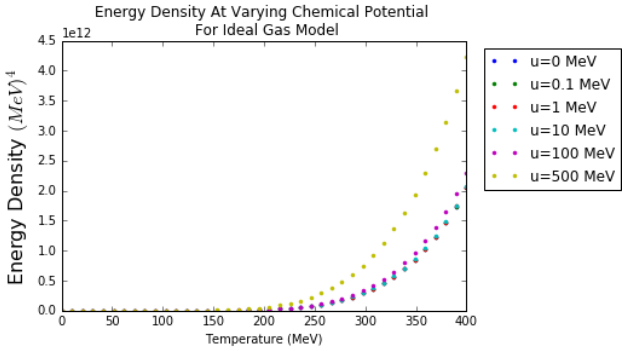

(c) Graph of Energy Density vs Temperature

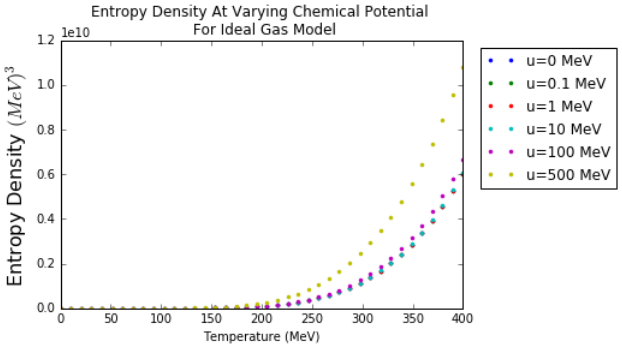

(d) Graph of Entropy Density vs Temperature

Figure 53: Graphs Of Some Important Parameters For A General Relativistic Ideal Hadron Resonance Gas At Various Chemical Potential

This completes the ideal gas analysis.

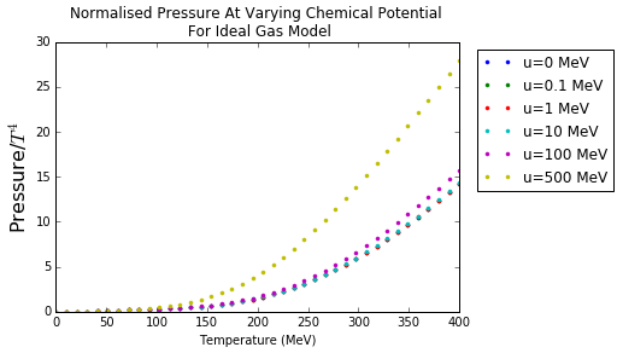

(a) Graph of Normalised Pressure vs Temperature

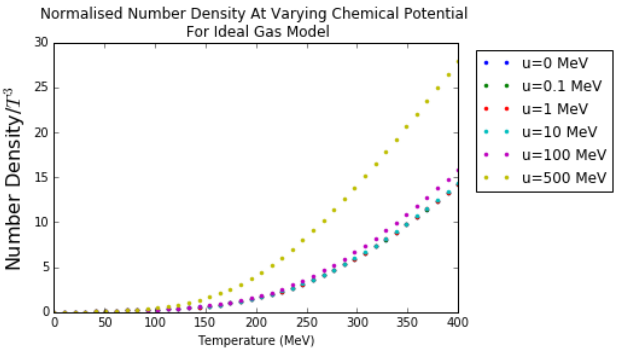

(b) Graph of Normalised Number Density vs Temperature

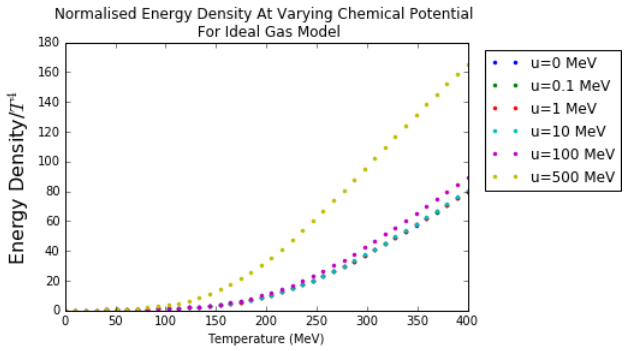

(a) Graph of Normalised Energy Density vs Temperature

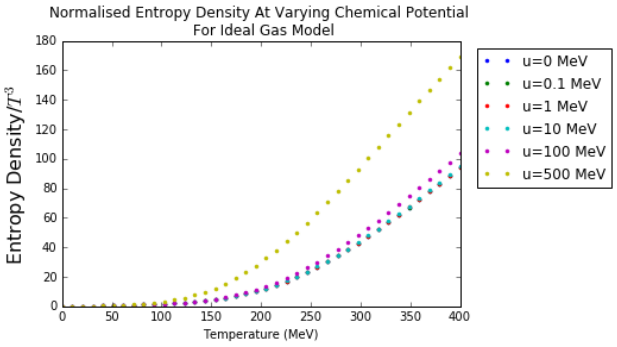

(b) Graph of Normalised Entropy Density vs Temperature

Figure 55: Normalised Graphs Of Some Important Parameters For A General Relativistic Ideal Hadron Resonance Gas At Various Chemical Potential

13.16 Appendix G2: Some More Graphs For Van der Waals' Excluded Volume Model For Hadron Resonance Gas

This section contains the non-normalized graphs of various thermodynamic parameters at 0 chemical potential. Further, it also contains graphs for Van Der Waals' excluded volume hadron resonance gas model at various values of baryonic chemical potential μ_B or simply μ as I have only considered baryonic chemical potential in the formulation. The graphs shown in figure below are for a variety of values of μ. All the parameters are plotted for 7 different values of μ. The values are as follows: $['0','0.1','1','10','100','500']$. The calculation is done for a hard sphere radius of 0.1 fm.

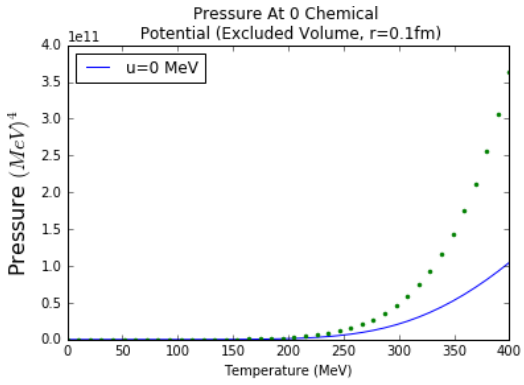

(a) Graph of Pressure vs Temperature

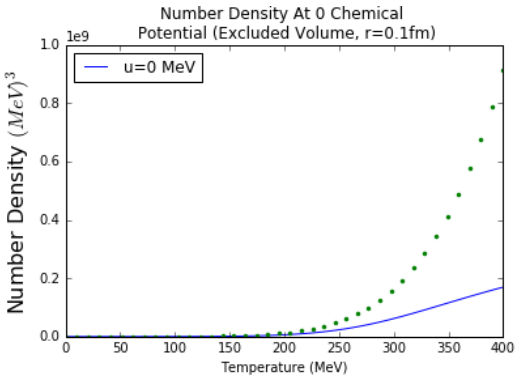

(b) Graph of Number Density vs Temperature

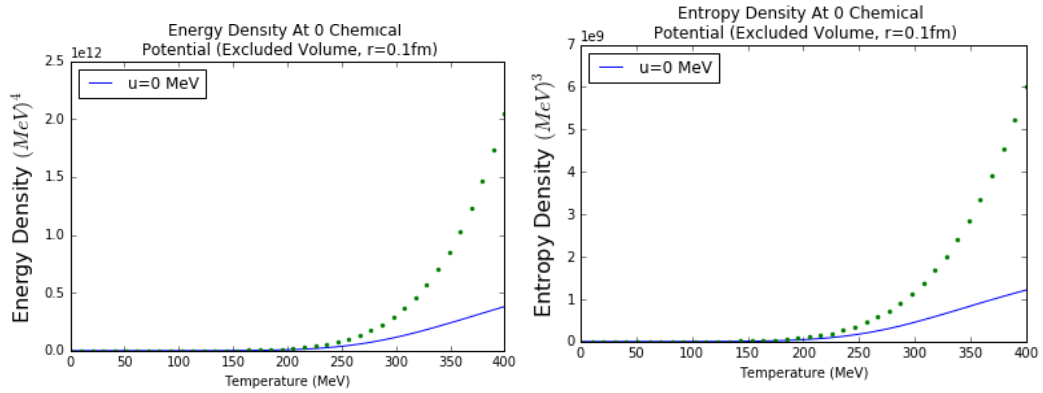

(a) Graph of Energy Density vs Temperature (b) Graph of Entropy Density vs Temperature

Figure 57: Graphs Of Some Important Parameters For A General Relativistic Van Der Waals' EV Hadron Resonance Gas At 0 Chemical Potential

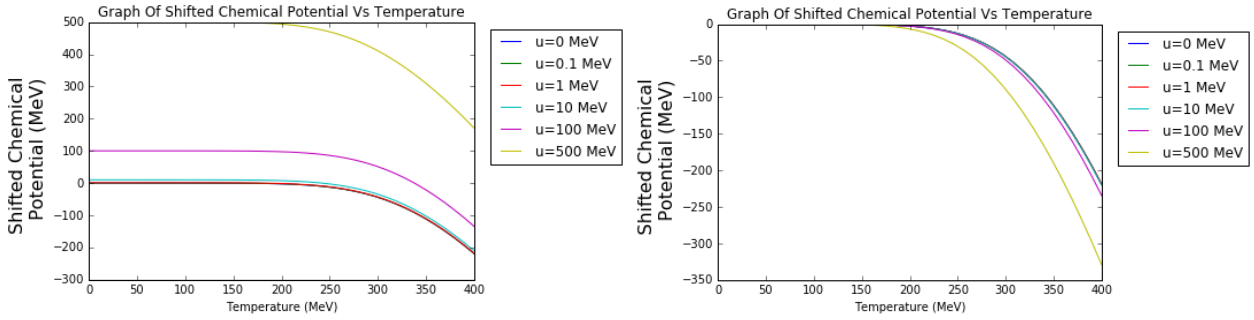

(a) For Baryons (b) For Mesons

Figure 58: Graphs Of Shifted Chemical Potential For Mesons And Baryons

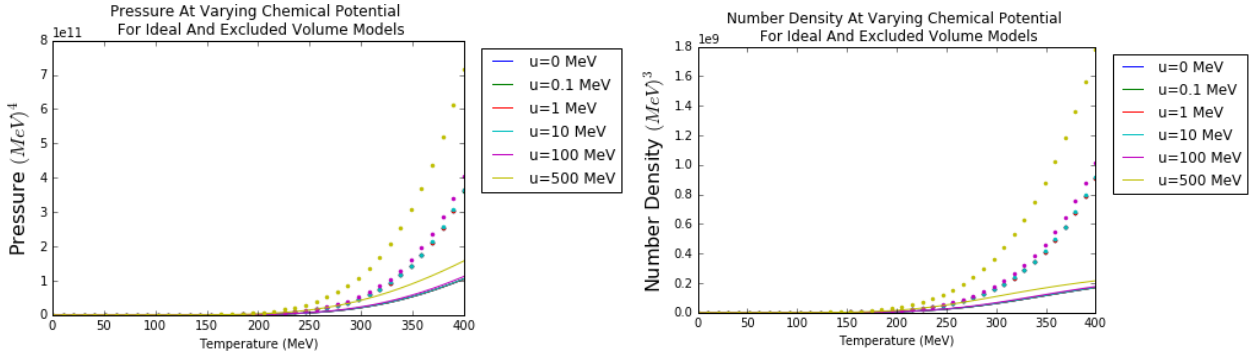

(a) Graph of Pressure vs Temperature (b) Graph of Number Density vs Temperature

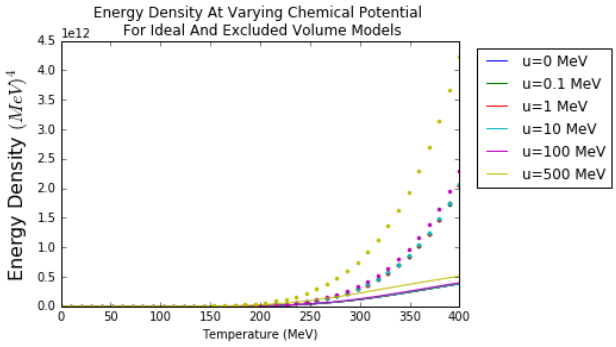

(a) Graph of Energy Density vs Temperature

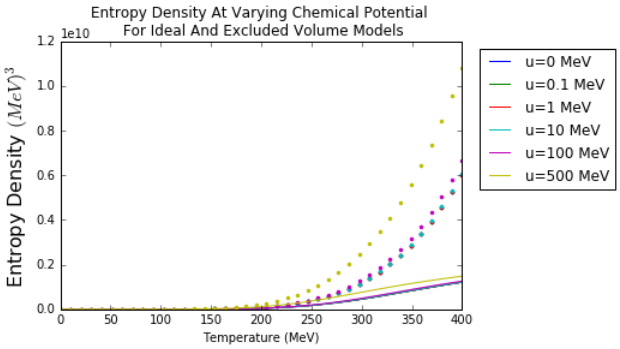

(b) Graph of Entropy Density vs Temperature

Figure 60: Graphs Of Some Important Parameters For EV Hadron Resonance Gas At Various Chemical Potentials. Ideal Gas Models are represented by dots and EV model by dashed lines

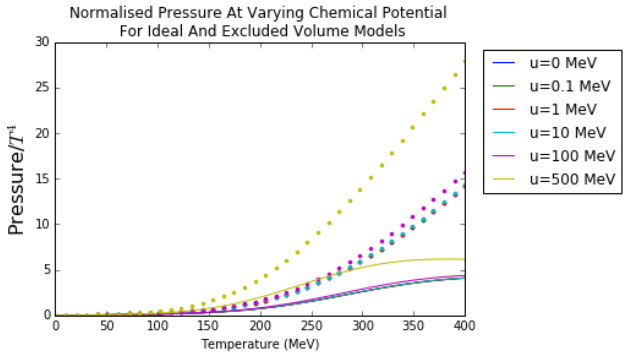

(a) Normalised Graph of Pressure vs Temperature

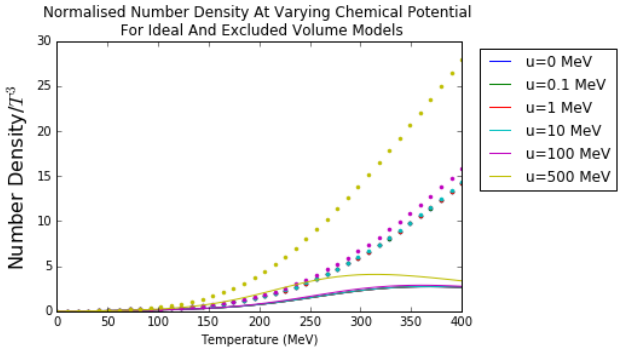

(b) Normalised Graph of Number Density vs Temperature

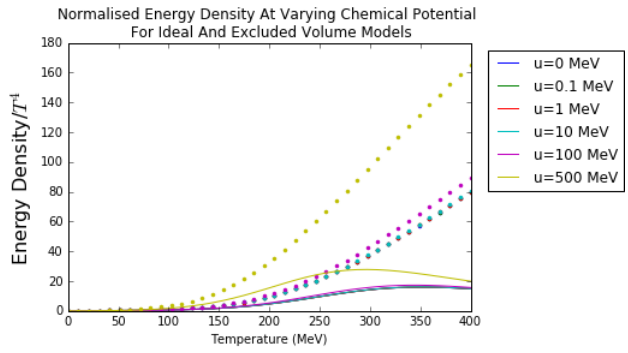

(c) Normalised Graph of Energy Density vs Temperature

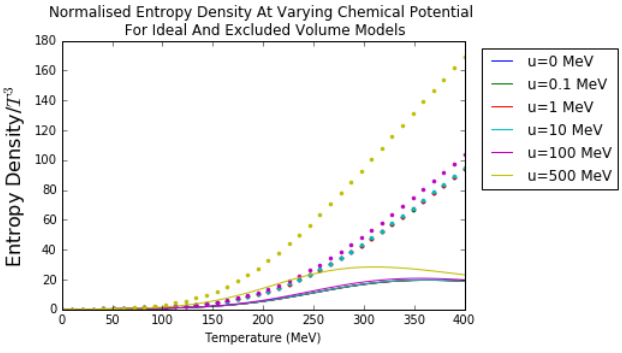

(d) Normalised Graph of Entropy Density vs Temperature

Figure 61: Normalised Graphs Of Some Important Parameters For A General Relativistic Van Der Waals' EV Hadron Resonance Gas At Various Chemical Potential. Ideal Gas Models are represented by dots and EV model by solid lines

13.17 Appendix G3: Some More Graphs For Van der Waals' Interacting Model For Hadron Resonance Gas

This section contains non-normalized graphs of various thermodynamic parameters at 0 chemical potential. Further, it also contains graphs for Interacting Van Der Waals' hadron resonance gas model at various values of baryonic chemical potential μ_B or simply μ as I have only considered baryonic chemical potential in the formulation.

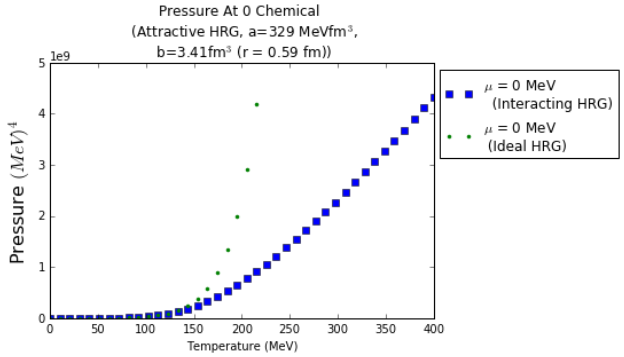

(a) Graph of Pressure vs Temperature

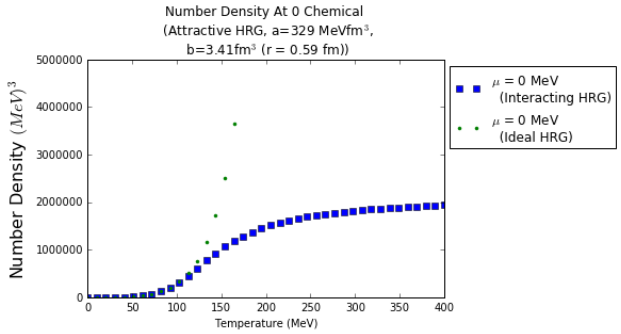

(b) Graph of Number Density vs Temperature

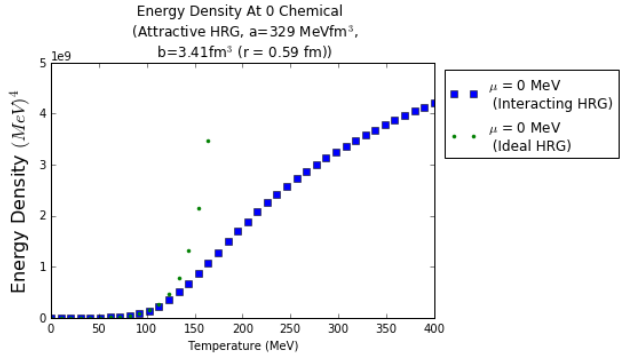

(c) Graph of Energy Density vs Temperature

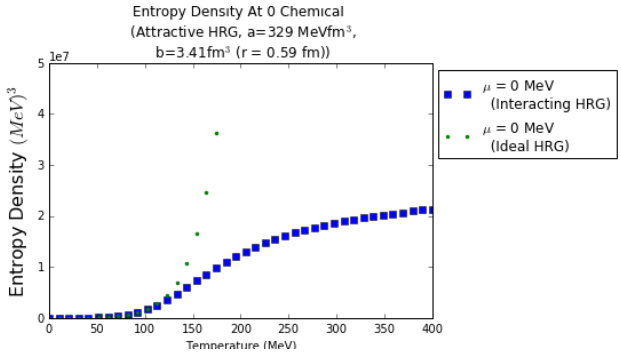

(d) Graph of Entropy Density vs Temperature

Figure 62: Graphs Of Some Important Parameters For A General Relativistic Interacting Van Der Waals' Hadron Resonance Gas At 0 Chemical Potential

As one observes from the graphs above, after T=200 MeV the thermodynamic parameters start deviating greatly form the ideal gas parameters. When appropriately normalised thermodynamic quantities are plotted, the results are quite interesting. Each normalised thermodynamic quantity when plotted against temperature has a peak near T=200 Mev for 0 chemical potential which shifts a bit towards the left as one increases the coeffcient of the baryonic chemical potential μ. This is explicitly shown on the next page.

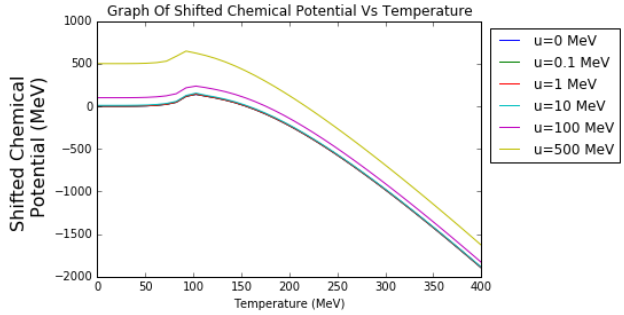

(a) For Baryons

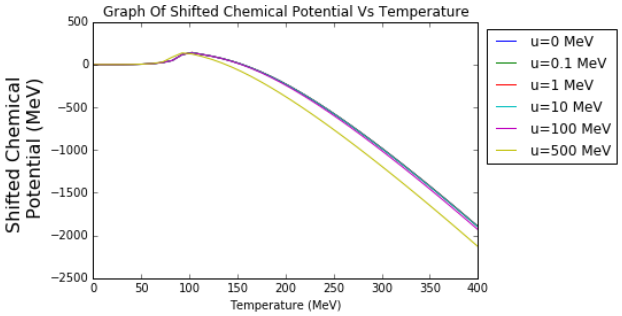

(b) For Mesons

Figure 63: Graphs Of Shifted Chemical Potential For Mesons And Baryons

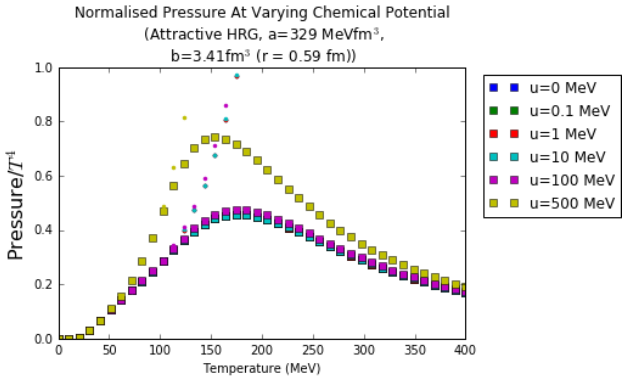

(a) Graph of Pressure vs Temperature

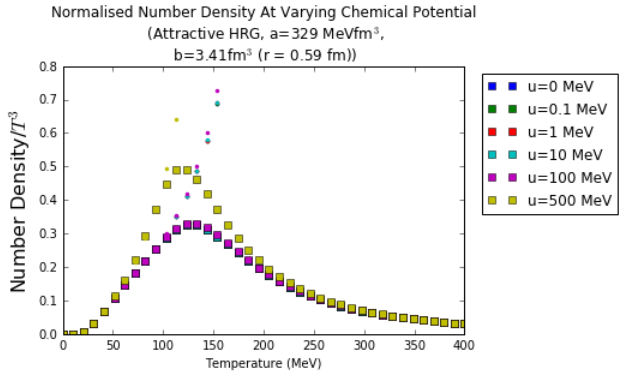

(b) Graph of Number Density vs Temperature

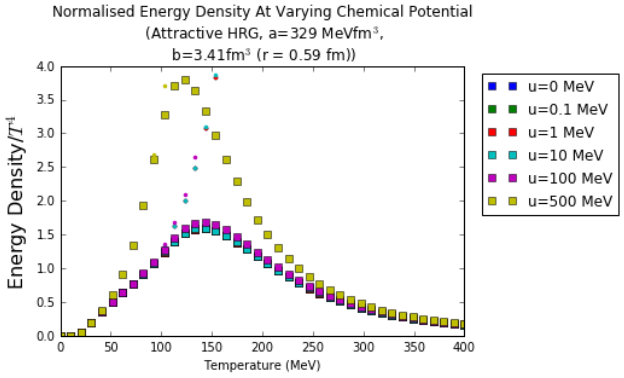

(c) Graph of Energy Density vs Temperature

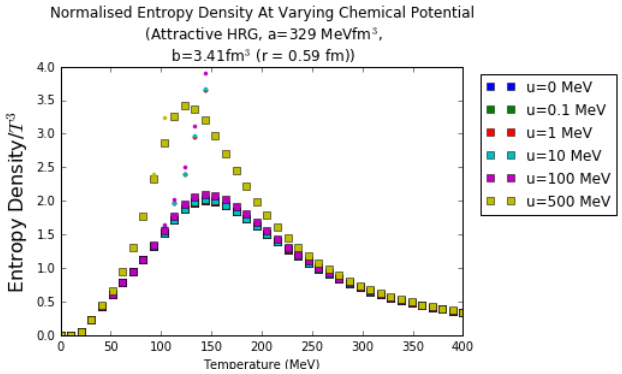

(d) Graph of Entropy Density vs Temperature

Figure 64: Normalised Graphs Of Some Important Parameters For A General Relativistic Interacting Van Der Waals' Hadron Resonance Gas At Various Chemical Potential. Squares represent interacting HRG while dots represent Ideal HRG

13.18 Appendix H1: Chemical Freeze Out Parameters After Excluding Strange Baryon Contribution

Table 6: Extracted chemical freeze-out parameters for grand canonical ensemble

$\sqrt{(s_{NN})}$	Centrality(%)	T_{ch} (MeV)	μ_B (MeV)	μ_S (MeV)	γ_S	R (fm)	χ^2/ndf
	0-5	136.4 ± 4.0	367.7 ± 19.2	79.0 ± 9.2	0.96 ± 0.10	6.76 ± 0.60	0.051
	5-10	136.4 ± 3.8	368.8 ± 18.5	79.1 ± 3.0	0.97 ± 0.09	6.32 ± 0.53	0.052
	10-20	137.0 ± 3.8	360.9 ± 18.4	77.4 ± 9.4	0.91 ± 0.09	5.77 ± 0.49	0.060
7.7 (GeV)	20-30	138.2 ± 3.9	361.1 ± 19.0	79.7 ± 10.0	0.90 ± 0.09	5.00 ± 0.43	0.056
	30-40	141.1 ± 4.5	360.6 ± 19.3	77.6 ± 11.1	0.84 ± 0.09	4.18 ± 0.39	0.079
	40-60	139.2 ± 4.1	341.3 ± 17.5	73.6 ± 9.2	0.74 ± 0.07	4.46 ± 0.38	0.064
	60-80	139.2 ± 4.2	322.0 ± 17.5	75.3 ± 10.0	0.48 ± 0.04	3.14 ± 0.27	0.402
	0-5	143.2 ± 4.3	263.0 ± 17.0	58.8 ± 11.1	0.87 ± 0.09	7.03 ± 0.60	0.022
	5-10	143.5 ± 4.7	264.5 ± 17.5	58.7 ± 11.3	0.92 ± 0.10	6.44 ± 0.58	0.027
	10-20	143.4 ± 3.9	261.9 ± 15.6	56.7 ± 10.7	0.88 ± 0.09	5.89 ± 0.46	0.020
11.5 (GeV)	20-30	146.7 ± 4.8	257.7 ± 17.3	58.0 ± 11.4	0.83 ± 0.09	4.93 ± 0.44	0.025
	30-40	147.4 ± 5.6	251.2 ± 18.0	55.9 ± 11.3	0.77 ± 0.08	4.33 ± 0.43	0.027
	40-60	149.1 ± 4.8	245.1 ± 17.1	57.7 ± 12.4	0.69 ± 0.07	4.25 ± 0.36	0.038
	60-80	147.1 ± 5.0	212.7 ± 16.8	51.9 ± 11.6	0.51 ± 0.05	3.11 ± 0.28	0.025
	0-5	146.2 ± 4.4	166.5 ± 15.6	38.1 ± 11.2	0.84 ± 0.09	7.53 ± 0.65	0.005
	5-10	147.4 ± 4.5	172.4 ± 15.8	38.4 ± 11.5	0.85 ± 0.09	6.88 ± 0.60	0.005
	10-20	150.1 ± 5.3	158.6 ± 16.4	38.2 ± 10.2	0.65 ± 0.08	6.13 ± 0.58	0.006
19.6 (GeV)	20-30	148.4 ± 5.1	164.7 ± 18.6	38.1 ± 10.5	0.83 ± 0.09	5.44 ± 0.50	0.005
	30-40	149.5 ± 5.0	152.5 ± 16.2	35.2 ± 11.5	0.80 ± 0.09	4.71 ± 0.43	0.006
	40-60	151.5 ± 5.2	144.9 ± 16.4	34.7 ± 16.0	0.74 ± 0.10	4.61 ± 0.43	0.006
	60-80	151.7 ± 5.0	128.9 ± 14.3	32.3 ± 11.0	0.60 ± 0.06	3.18 ± 0.29	0.006
	0-5	145.1 ± 4.3	164.6 ± 15.4	37.6 ± 11.1	0.81 ± 0.9	7.76 ± 0.65	0.014
	5-10	149.2 ± 5.1	133.1 ± 14.7	28.1 ± 10.4	0.86 ± 0.11	6.95 ± 0.75	0.084
	10-20	148.7 ± 4.5	126.5 ± 14.2	25.3 ± 10.2	0.86 ± 0.09	6.41 ± 0.55	0.003
27 (GeV)	20-30	149.7 ± 4.3	120.2 ± 13.4	24.1 ± 10.6	0.84 ± 0.09	5.57 ± 0.46	0.003
	30-40	152.2 ± 4.7	122.6 ± 14.3	26.2 ± 11.3	0.81 ± 0.09	4.68 ± 0.41	0.004
	40-60	153.9 ± 5.3	115.3 ± 15.4	25.8 ± 10.8	0.78 ± 0.08	4.59 ± 0.44	0.004
	60-80	154.0 ± 4.9	110.5 ± 14.1	38.9 ± 12.8	0.69 ± 0.08	3.13 ± 0.28	0.004
	0-5	149.2 ± 4.3	92.4 ± 12.9	21.2 ± 10.4	0.86 ± 0.09	7.59 ± 0.62	0.003
	5-10	150.6 ± 4.5	92.4 ± 13.3	22.0 ± 10.4	0.87 ± 0.09	6.98 ± 0.59	0.004
	10-20	149.7 ± 4.5	94.8 ± 13.4	21.2 ± 10.1	0.86 ± 0.09	6.47 ± 0.55	0.003
39 (GeV)	20-30	151.3 ± 4.6	91.9 ± 13.5	21.2 ± 11.0	0.84 ± 0.09	5.57 ± 0.48	0.004
	30-40	153.7 ± 4.7	87.0 ± 4.7	20.7 ± 10.5	0.83 ± 0.09	4.68 ± 0.41	0.003
	40-60	154.5 ± 4.5	81.6 ± 12.2	23.7 ± 11.0	0.76 ± 0.08	4.69 ± 0.40	0.025
	60-80	152.7 ± 5.1	67.2 ± 14.9	16.2 ± 10.2	0.69 ± 0.07	3.31 ± 0.30	0.007

13.19 Appendix H2:AMPT Plots For Corresponding Anti-Particles

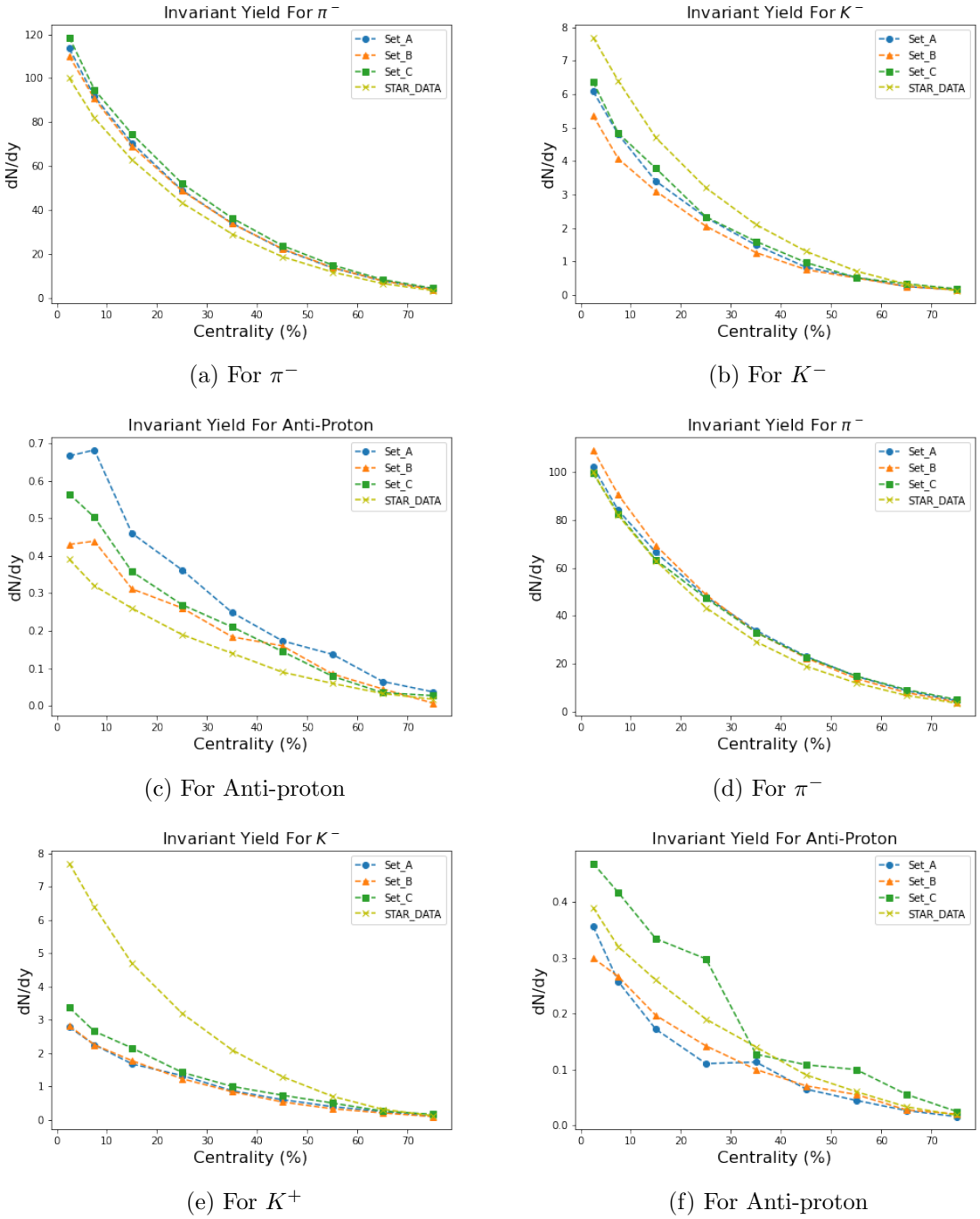

(a) For π^-

(b) For K^-

(c) For Anti-proton

(d) For π^-

(e) For K^+

(f) For Anti-proton

Figure 65: Graphs Of Particle Yields vs Collision Centrality At Mid-rapidity ($y< \mid 0.1 \mid$) from AMPT default (a-c) and string melting (d-f) models

newpage

13.20 Appendix J1:Azimuthal Distribution (In Momentum Space) For Particles In Default Version

We plot the distribution of azimuthal angle in the momentum space for various produced particles (pion,kaons,protons,lambda and phi). The resulting histogram is then fitted using the fit equation:

$$N(\phi) = A + Bcos(2(\phi - \phi_R)) \tag{13.20.1}$$

Here A, B and ϕ_R are fit parameters. The ratio B/A quantifies elliptic flow and ϕ_R is the reaction plane angle.

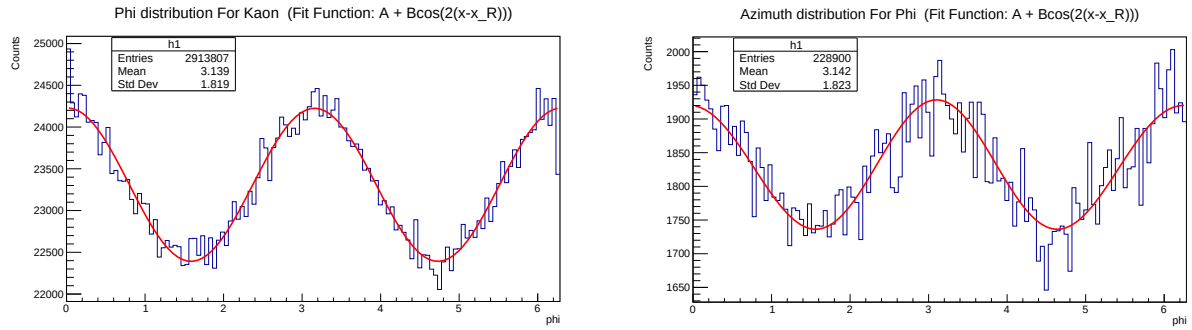

(a) For $K^{[\pm]}$

(b) For ϕ^0

Figure 66: Azimuthal Distribution (In Momentum Space) For Some particles

As one can see from the above figure, the azimuthal distribution (In Momentum Space) for fits incredibly well to a Fourier decomposition containing only the second flow harmonic. This indeed suggests that momentum space anisotropy is dominated by elliptic flow. This also true for other produced particles which have not been shown here. The above distribution of particles have been simulated from the string default version.

Table 7: Optimum Parameters For Fit Function For Various Particles

Particle	Pid	A	ΔA	B	ΔB	ϕ_R	$\Delta\phi_R$	v_2	Δv_2
K0S	310	11664.5	9.66002	491.705	13.6597	-0.0205128	0.0138813	0.0421540	0.0012060
Proton	2212	34196.1	16.5399	697.992	23.3992	-0.0138046	0.0154656	0.0204115	0.0006941
Lambda	3122	6236.31	7.06332	207.822	9.98801	-0.0226604	0.0240944	0.0333245	0.0016393
Pion	211	185961	38.5706	7162.12	54.5594	0.00225564	0.00380549	0.0385141	0.0003014
Kaon	321	23309.1	13.6555	917.557	19.316	0.0163893	0.0105343	0.0393648	0.0008518
Phi	333	1830.36	3.8266	93.9074	5.41132	-0.0408031	0.0287679	0.0513054	0.0030637
Pi0	111	106179	29.1451	4101.64	41.2252	-0.00036217	0.00502183	0.0386295	0.0003989

13.21 Appendix J2:Parameterization For Massless Ideal Hadron Gas At 0 Chemical Potential

The thermodynamics for the massless ideal hadron resonance gas at 0 chemical potential has already been discussed at length in sections 7 and 8. Our aim is to parameterize everything wrt to energy density. To do that the following fit functions are assumed:

$$p = A\epsilon + C \tag{13.21.1}$$

$$s = A\epsilon + B \tag{13.21.2}$$

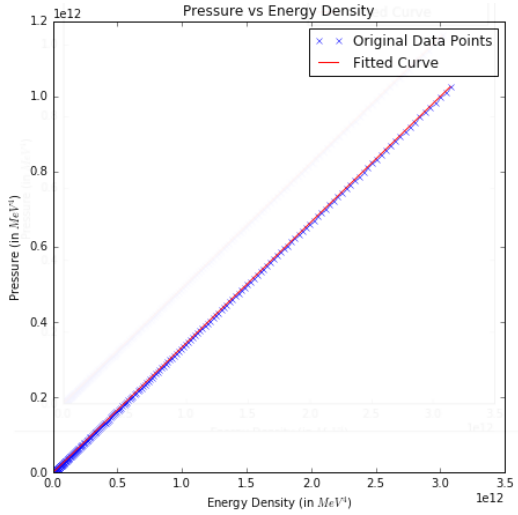

(a) Pressure vs Energy density Graph

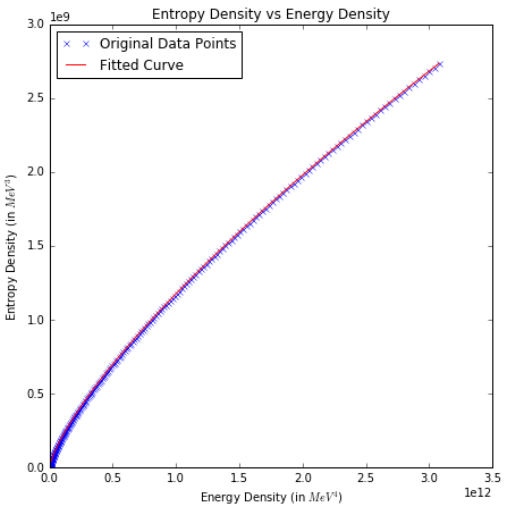

(b) Entropy Density vs Energy density

```
For A x +C, respective coefficients are:
[0.33333333 0.06673099]
The error in the fits are:
[3.18948381e-15 5.12985343e-03]
```

(c) Value Of Fit Parameters A,C in 12.21.1

```
For A x**(3/4) +  B, respective coefficients are:
[1.17733922 0.07518392]
The error in the fits are:
[7.10534607e-12 8.45466617e-03]
```

(d) Value Of Fit Parameters A,B in 12.21.2

Figure 67: Parameterization Of Pressure And Entropy Density wrt Energy Density

As one can be see that the y-intercept parameter is almost 0 and the relation can simply be expressed by the first terms of 12.21.1 and 12.21.2.

14 Data Tables From Particle Data Group (PDG)[6]

This section contains tables on leptons, quarks, baryons and mesons listing their major properties as published in the summary tables of the Particle data group. Please note that the Spin quantum number written for Baryons and Mesons is not just actually spin (S) but total angular momentum (J=L+S) in which they are found in their supposedly ground state [4]. Further the masses of the baryons and mesons are the Breight-Wigner Masses.

14.1 Leptons :

Table 8: Data For Leptons

Properties / Leptons	Mass (MeV)	Charge $\lvert e^- \rvert$	Spin ($\hbar$)	Mean Lifetime	Degrees Of Freedom
• Electron (e^-)	0.5109989461 ± 0.0000000031	-1	1/2	$> 6.6 \times 10^{28}$ yr	2
• Muon (μ^-)	105.6583745 ± 0.0000024	-1	1/2	(2.1969811 ± 0.0000022) x 10^{-6} s	2
• Tauon (τ^-)	1776.86 ± 0.12	-1	1/2	(290.3 ± 0.5) x 10^{-15} s	2

Table 9: Charge, Spin And Flavour Quantum Numbers Of Leptons

Quantum # / Leptons	Q	L	L_e	L_μ	L_τ	s
e^- (Electron)	-1	+1	+1	0	0	1/2
ν_e (Electron Neutrino)	0	+1	+1	0	0	1/2
e^+ (Positron)	+1	-1	-1	0	0	1/2
$\bar{\nu}_e$ (Electron Anti-neutrino)	0	-1	-1	0	0	1/2
μ^- (Muon)	-1	+1	0	+1	0	1/2
ν_μ (Muon Neutrino)	0	+1	0	+1	0	1/2
μ^+ (Anti-Muon)	+1	-1	0	-1	0	1/2
$\bar{\nu}_\mu$ (Muon Anti-neutrino)	0	-1	0	-1	0	1/2
τ^- (Tauon)	-1	+1	0	0	+1	1/2
ν_τ (Tau Neutrino)	0	+1	0	0	+1	1/2
τ^+ (Anti-Tauon)	+1	-1	0	0	-1	1/2
$\bar{\nu}_\tau$ (Tau Anti-neutrino)	0	-1	0	0	-1	1/2

[4] I don't understand exactly what they mean by this

14.2 Quarks

Table 10: Data For Quarks

Quark \ Properties	Mass (MeV)	Charge $\lvert e^- \rvert$	Spin ($\hbar$)	Iso-Spin I(I_z)	Degrees Of Freedom
• Up (u)	$2.16^{+0.49}_{-0.26}$	2/3	1/2	1/2 (+1/2)	6
• Down (d)	$4.67^{+0.48}_{-0.17}$	-1/3	1/2	1/2 (-1/2)	6
• Strange (s)	93^{+11}_{-5}	-1/3	1/2	0	6
• Charm (c)	1270 ± 20	2/3	1/2	0	6

Table 11: Some Important Quantum Numbers For Quarks

Quarks \ Quantum #	Q	Flavour Quantum Number				Colour Charge	Spin	Iso-Spin I(I_z)
		U	D	S	C			
Up (u)	+2/3	+1	0	0	0	YES (RGB)	1/2	1/2(1/2)
Anti-Up ($\bar{u}$)	-2/3	-1	0	0	0	YES ($\bar{R}\bar{G}\bar{B}$)	1/2	1/2(-1/2)
Down (d)	-1/3	0	-1	0	0	YES (RGB)	1/2	1/2(-1/2)
Anti-Down ($\bar{d}$)	+1/3	0	+1	0	0	YES ($\bar{R}\bar{G}\bar{B}$)	1/2	1/2(1/2)
Strange (s)	-1/3	0	0	-1	0	YES (RGB)	1/2	0
Anti- Strange ($\bar{s}$)	+1/3	0	0	+1	0	YES ($\bar{R}\bar{G}\bar{B}$)	1/2	0
Charm (c)	+2/3	0	0	0	+1	YES (RGB)	1/2	0
Anti-Charm ($\bar{c}$)	-2/3	0	0	0	-1	YES ($\bar{R}\bar{G}\bar{B}$)	1/2	0

14.3 Baryons

The Baryon tables have been grouped into various Baryon families based on the quark content and iso-spin quantum number. I have not listed those baryons whose existence is uncertain or whose quantum numbers have not been properly studied and require further experimentation. Further, this list only covers Baryons upto a mass of ~ 2600 MeV.[5]

Table 12: Data For N-Baryons

Baryons \ Properties		Quark Content	Mass (MeV)	Charge $\lvert e^- \rvert$	Spin ($\hbar$)	Iso-Spin ($\hbar$)	Degrees Of Freedom
N	p,N^+	uud	938.272081 ± 0.000006	1	1/2	1/2	6
	n,N^0	udd	939.565413 ± 0.000006	0	1/2	1/2	
N(1440) $1/2^+$****		uud,udd	1410-1470 ($\approx$ 1440)	1,0	1/2	1/2	6
N(1520) $3/2^-$****		uud,udd	1510-1520 ($\approx$ 1515)	1,0	3/2	1/2	8
N(1535) $1/2^-$****		uud,udd	1515-1545 ($\approx$ 1530)	1,0	1/2	1/2	4
N(1650) $1/2^-$****		uud,udd	1635-1665 ($\approx$ 1650)	1,0	1/2	1/2	4
N(1675) $5/2^-$****		uud,udd	1665-1680 ($\approx$ 1675)	1,0	5/2	1/2	12
N(1680) $5/2^+$****		uud,udd	1680-1690 ($\approx$ 1685)	1,0	5/2	1/2	12
N(1700) $3/2^-$***		uud,udd	1650-1800 ($\approx$ 1720)	1,0	3/2	1/2	8
N(1710) $1/2^+$****		uud,udd	1680-1740 ($\approx$ 1710)	1,0	1/2	1/2	4
N(1720) $3/2^+$****		uud,udd	1680-1750 ($\approx$ 1725)	1,0	3/2	1/2	8
N(1875) $3/2^-$***		uud,udd	1850-1920 ($\approx$ 1875)	1,0	3/2	1/2	8
N(1880) $1/2^+$***		uud,udd	1830-1930 ($\approx$ 1880)	1,0	1/2	1/2	4
N(1895) $1/2^-$****		uud,udd	1870-1920 ($\approx$ 1895)	1,0	1/2	1/2	4
N(1900) $3/2^+$****		uud,udd	1890-1950 ($\approx$ 1920)	1,0	3/2	1/2	8
N(2060) $5/2^-$***		uud,udd	2030-2200 ($\approx$ 2100)	1,0	5/2	1/2	12
N(2100) $1/2^+$***		uud,udd	2050-2150 ($\approx$ 2100)	1,0	1/2	1/2	4
N(2120) $3/2^-$***		uud,udd	2060-2160 ($\approx$ 2120)	1,0	3/2	1/2	8
N(2190) $7/2^-$****		uud,udd	2140-2220 ($\approx$ 2180)	1,0	7/2	1/2	16
N(2220) $9/2^+$***		uud,udd	2200-2300 ($\approx$ 2250)	1,0	9/2	1/2	20
N(2250) $9/2^-$****		uud,udd	2250-2320 ($\approx$ 2280)	1,0	9/2	1/2	20
N(2600) $11/2^-$***		uud,udd	2250-2750 ($\approx$ 2600)	1,0	11/2	1/2	24

[5] *** - Existence is very likely and/or quantum numbers are not well-determined
*** - Existence is certain

Table 13: Data For Δ-Baryons

Baryons \ Properties		Quark Content	Mass (MeV)	Charge $\lvert e^- \rvert$	Spin ($\hbar$)	Iso-Spin ($\hbar$)	Degrees Of Freedom
$\Delta(1232)3/2^+$	Δ^{++}	uuu	1230-1234 ($\approx$ 1232)	2	1/2	3/2 (3/2)	8
	Δ^{+}	uud		1		3/2 (1/2)	
	Δ^{0}	udd		0		3/2 (-1/2)	
	Δ^{-}	ddd		-1		3/2 (-3/2)	
$\Delta(1600)\ 3/2^{+****}$		uuu,uud udd,ddd	1500-1640 ($\approx$ 1570)	2,1,0,-1	3/2	3/2	16
$\Delta(1620)\ 1/2^{-****}$		uuu,uud udd,ddd	1590-1630 ($\approx$ 1610)	2,1,0,-1	1/2	3/2	8
$\Delta(1700)\ 3/2^{-****}$		uuu,uud udd,ddd	1690-1730 ($\approx$ 1710)	2,1,0,-1	3/2	3/2	16
$\Delta(1900)\ 1/2^{-***}$		uuu,uud udd,ddd	1840-1920 ($\approx$ 1860)	2,1,0,-1	1/2	3/2	8
$\Delta(1905)\ 5/2^{+****}$		uuu,uud udd,ddd	1855-1910 ($\approx$ 1880)	2,1,0,-1	5/2	3/2	24
$\Delta(1910)\ 1/2^{+****}$		uuu,uud udd,ddd	1850-1950 ($\approx$ 1900)	2,1,0,-1	1/2	3/2	8
$\Delta(1920)\ 3/2^{+***}$		uuu,uud udd,ddd	1870-1970 ($\approx$ 1920)	2,1,0,-1	3/2	3/2	16
$\Delta(1930)\ 5/2^{-***}$		uuu,uud udd,ddd	1900-2000 ($\approx$ 1950)	2,1,0,-1	5/2	3/2	24
$\Delta(1950)\ 7/2^{+****}$		uuu,uud udd,ddd	1915-1950 ($\approx$ 1930)	2,1,0,-1	7/2	3/2	32
$\Delta(2200)\ 7/2^{-***}$		uuu,uud udd,ddd	2150-2250 ($\approx$ 2200)	2,1,0,-1	7/2	3/2	32
$\Delta(2420)\ 11/2^{+****}$		uuu,uud udd,ddd	2300-2600 ($\approx$ 2450)	2,1,0,-1	11/2	3/2	48

Table 14: Data For Λ-Baryons

Baryons \ Properties	Quark Content	Mass (MeV)	Charge $\lvert e^- \rvert$	Spin ($\hbar$)	Iso-Spin ($\hbar$)	Degrees Of Freedom
Λ****	uds	1115.683 ± 0.006	0	1/2	0	2
$\Lambda(1405)\ 1/2^-$****	uds	$1405^{1.3}_{1.0}$	0	1/2	0	2
$\Lambda(1520)\ 3/2^-$****	uds	1518-1520 (≈ 1519)	0	3/2	0	4
$\Lambda(1600)\ 1/2^+$****	uds	1570-1630 (≈ 1600)	0	1/2	0	2
$\Lambda(1670)\ 1/2^-$****	uds	1670-1678 (≈ 1674)	0	1/2	0	2
$\Lambda(1690)\ 3/2^-$****	uds	1685-1695 (≈ 1690)	0	3/2	0	4
$\Lambda(1800)\ 1/2^-$***	uds	1750-1850 (≈ 1800)	0	1/2	0	2
$\Lambda(1810)\ 1/2^+$***	uds	1740-1840 (≈ 1790)	0	1/2	0	2
$\Lambda(1820)\ 5/2^+$****	uds	1815-1825 (≈ 1820)	0	5/2	0	6
$\Lambda(1830)\ 5/2^-$****	uds	1820-1830 (≈ 1825)	0	5/2	0	6
$\Lambda(1890)\ 3/2^+$****	uds	1870-1910 (≈ 1890)	0	3/2	0	4
$\Lambda(2100)\ 7/2^-$****	uds	2090-2110 (≈ 2100)	0	7/2	0	8
$\Lambda(2110)\ 5/2^+$***	uds	2050-2130 (≈ 2090)	0	5/2	0	6
$\Lambda(2350)\ 9/2^+$***	uds	2340-2370 (≈ 2350)	0	9/2	0	10

Table 15: Data For Singly Charmed-Baryons

Baryons \ Properties		Quark Content	Mass (MeV)	Charge $\lvert e^- \rvert$	Spin ($\hbar$)	Iso-Spin ($\hbar$)	Degrees Of Freedom
Λ_c^+****		udc	2286.46 ± 0.14	1	1/2	0	2
$\Lambda_c(2595)^+$***		udc	2592.25 ± 0.28	1	1/2	0	2
$\Lambda_c(2625)^+$***		udc	2592.25 ± 0.28	1	3/2	0	4
$\Sigma_c(2455)$****	$\Sigma_c(2455)^{++}$	uuc	2453.97 ± 0.14	2	1/2	1(1)	6
	$\Sigma_c(2455)^+$	udc	2452.9 ± 0.4	1		1(0)	
	$\Sigma_c(2455)^0$	ddc	2453.75 ± 0.14	0		1(-1)	
$\Sigma_c(2520)$***	$\Sigma_c(2455)^{++}$	uuc	$2518.41^{+0.21}_{-0.19}$	2	3/2	1(1)	12
	$\Sigma_c(2455)^+$	udc	2517.5 ± 2.3	1		1(0)	
	$\Sigma_c(2455)^0$	ddc	2518.48 ± 0.20	0		1(-1)	
Ξ_c***	Ξ_c^+	usc	$2467.94^{+0.17}_{-0.20}$	1	1/2	1/2(1/2)	4
	Ξ_c^0	dsc	$2470.90^{+0.22}_{-0.29}$	0		1/2(-1/2)	
Ξ_c'***	$\Xi_c'^+$	usc	2578.4 ± 0.5	1	1/2	1/2(1/2)	4
	$\Xi_c'^0$	dsc	2579.2 ± 0.5	0		1/2(-1/2)	
$\Xi_c(2645)$***	$\Xi_c(2645)^+$	usc	$2645.56^{+0.24}_{-0.30}$	1	3/2	1/2(1/2)	8
	$\Xi_c(2645)^0$	dsc	$2646.38^{+0.20}_{-0.23}$	0		1/2(-1/2)	

Table 16: Data For Σ-Baryons

Baryons \ Properties		Quark Content	Mass (MeV)	Charge $\lvert e^- \rvert$	Spin ($\hbar$)	Iso-Spin ($\hbar$)	Degrees Of Freedom
Σ^{****}	Σ^+	uus	1189.37 ± 0.07	1	1/2	1(1)	6
	Σ^0	uds	1192.642 ± 0.024	0		1(0)	
	Σ^-	dds	1197.449 ± 0.030	-1		1(-1)	
$\Sigma(1385)3/2^{+****}$	$\Sigma(1385)^+$	uus	1382.80 ± 0.35	1	1/2	1(1)	6
	$\Sigma(1385)^0$	uds	1383.7 ± 1.0	0		1(0)	
	$\Sigma(1385)^-$	dds	1387.2 ± 0.5	-1		1(-1)	
$\Sigma(1660)\ 1/2^{+***}$		uus,uds dds	1580-1640 (≈ 1660)	1,0,-1	1/2	1	6
$\Sigma(1670)\ 3/2^{-****}$		uus,uds dds	1665-1685 (≈ 1675)	1,0,-1	3/2	1	12
$\Sigma(1750)\ 1/2^{-***}$		uus,uds dds	1700-1800 (≈ 1750)	1,0,-1	1/2	1	6
$\Sigma(1775)\ 5/2^{-****}$		uus,uds dds	1770-1780 (≈ 1775)	1,0,-1	5/2	1	18
$\Sigma(1910)\ 3/2^{-***}$		uus,uds dds	1870-1950 (≈ 1910)	1,0,-1	3/2	1	12
$\Sigma(1915)\ 5/2^{+****}$		uus,uds dds	1900-1935 (≈ 1915)	1,0,-1	5/2	1	18
$\Sigma(2030)\ 7/2^{+****}$		uus,uds dds	2025-2040 (≈ 2030)	1,0,-1	7/2	1	24

Table 17: Data For Ξ and Ω-Baryons

Baryons \ Properties		Quark Content	Mass (MeV)	Charge $\lvert e^- \rvert$	Spin ($\hbar$)	Iso-Spin ($\hbar$)	Degrees Of Freedom
Ξ^{****}	Ξ^0	uss	1314.86 ± 0.20	0	1/2	1/2(1/2)	4
	Ξ^-	dss	1321.71 ± 0.07	-1		1/2(-1/2)	
$\Xi(1530)\ 3/2^{+****}$	$\Xi(1530)^0$	uss	1531.80 ± 0.32	0	3/2	1/2(1/2)	8
	$\Xi(1530)^-$	dss	1535.0 ± 0.6	-1		1/2(-1/2)	
$\Xi(1820)\ 3/2^{-***}$		uss,dss	1950 ± 15	0,-1	3/2	1/2	8
Ω^{-****}		sss	1672.45 ± 0.29	-1	3/2	0	4
Ω_c^{0***}		ssc	2695.2 ± 1.7	0	1/2	0	2

14.4 Mesons

Like the Baryons, Mesons have also been grouped into various families based on quark content and iso-spin adn only those whose existence is certain have been tabulated. Further, this list only contains the list of Baryons upto a mass of ~ 2400 MeV.[6]

Table 18: Data For Light Flavoured-Mesons

Mesons \ Properties		Mass (MeV)	Charge $\lvert e^- \rvert$	Spin ($\hbar$)	Iso-Spin ($\hbar$)	Degrees Of Freedom
π*	π^+	139.57039 ± 0.00018	1	0	1(1)	3
	π^0	134.9768 ± 0.0005	0		1(0)	
	π^-	139.57039 ± 0.00018	-1		1(-1)	
η*		547.862 ± 0.017	0	0	0	1
$f_0(500)$*		400-500	0	0	0	1
$\rho(770)$*		775.26 ± 0.25	1,0,-1	1	1	9
$\omega(782)$*		782.65 ± 0.12	0	1	0	3
$\eta^{prime}(958)*$		957.78 ± 0.06	0	0	0	1
$f_0(980)*$		990 ± 20	0	0	0	1
$a_0(980)$*		980 ± 20	1,0,-1	0	1	3
$\phi(1020)$*		1019.461 ± 0.016	0	1	0	3
$h_1(1170)$*		1166 ± 6	0	1	0	3
$b_1(1235)$*		1229.5 ± 3.2	1,0,-1	1	1	9
$a_1(1260)$*		1230 ± 40	1,0,-1	1	1	9
$f_2(1270)$*		1275.5 ± 0.8	0	2	0	5
$f_1(1285)$*		1281.9 ± 0.5	0	1	0	3
$\eta(1295)$*		1294 ± 4	0	0	0	1
$\pi(1300)$*		1300 ± 100	1,0,-1	0	1	3
$a_2(1320)$*		1316.9 ± 0.9	1,0,-1	2	1	15
$f_0(1370)$*		$1200 - 1500$	0	0	0	1
$\pi_1(1400)$*		1354 ± 25	1,0,-1	1	1	9
$\eta(1405)$*		1316.9 ± 0.9	0	0	0	1
$h_1(1415)$*		1416 ± 8	0	1	0	3
$f_1(1420)$*		1426.3 ± 0.9	0	1	0	3
$\omega(1420)$*		1410 ± 60	0	1	0	3
$a_0(1450)$*		1474 ± 19	1,0,-1	0	1	3
$\rho(1450)$*		1465 ± 25	1,0,-1	1	1	9

[6] *-Well Established

Mesons \ Properties	Mass (MeV)	Charge $\lvert e^- \rvert$	Spin ($\hbar$)	Iso-Spin ($\hbar$)	Degrees Of Freedom
$\eta(1475)^*$	1475 ± 4	0	0	0	1
$f_0(1500)^*$	1506 ± 6	0	0	0	1
$f_2'(1525)^*$	1517.4 ± 2.5	0	2	0	5
$\pi_1(1600)^*$	1600^{+15}_{-11}	1,0,-1	1	1	9
$a_1(1640)^*$	1655 ± 16	1,0,-1	1	1	9
$\eta_2(1645)^*$	1617 ± 5	0	2	0	5
$\omega(1650)^*$	1670 ± 30	0	1	0	3
$\omega_3(1670)^*$	1667 ± 4	0	3	0	7
$\pi_2(1670)^*$	$1670.6^{+2.9}_{-1.2}$	1,0,-1	2	1	15
$\phi(1680)^*$	1680 ± 20	0	1	0	3
$\rho_3(1690)^*$	1688.8 ± 2.1	1,0,-1	3	1	21
$\rho(1700)^*$	1720 ± 20	1,0,-1	1	1	9
$a_2(1700)^*$	1705 ± 40	1,0,-1	2	1	15
$f_0(1710)^*$	1704 ± 12	0	0	0	1
$\pi(1800)^*$	1810^{+9}_{-11}	1,0,-1	0	1	3
$\phi_3(1850)^*$	1854 ± 7	0	3	0	7
$\eta_2(1870)^*$	1842 ± 8	0	2	0	5
$\pi_2(1880)^*$	1874^{+26}_{-5}	1,0,-1	2	1	15
$f_2(1950)^*$	1936 ± 12	0	2	0	5
$a_4(1970)^*$	1967 ± 16	1,0,-1	4	1	27
$f_2(2010)^*$	2011^{+60}_{-80}	0	2	0	5
$f_4(2050)^*$	2018 ± 11	0	4	0	9
$\phi(2170)^*$	2160 ± 80	0	1	0	3
$f_2(2300)^*$	2297 ± 28	0	2	0	5
$f_2(2340)^*$	2345^{+50}_{-40}	0	2	0	5

Table 19: Quark Content For Light Flavoured-Mesons

Mesons \ Properties		Charge $\lvert e^- \rvert$	Iso-Spin ($\hbar$)	Quark Content
$M_1(\pi, b, \rho, a)$	M_1^+	1	1(1)	$u\bar{d}$
	M_1^0	0	1(0)	$(u\bar{u} - d\bar{d})/\sqrt{(2)}$
	M_1^-	-1	1(-1)	$d\bar{u}$
$M_2(\eta, \eta', h, \omega, \phi, f, f')$		0	0	$c_1(u\bar{u} - d\bar{d}) + c_2(s\bar{s})$

Table 20: Data For Strange-Mesons

Mesons \ Properties		Mass (MeV)	Charge $\lvert e^- \rvert$	Spin ($\hbar$)	Iso-Spin ($\hbar$)	Degrees Of Freedom
K	$K^{\pm}$	493.677 ± 0.016	1,-1	0	1/2	4
	$K^0, \bar{K}^0$	497.611 ± 0.013	0	0	1/2	
$K_0^*(700)$		824 ± 30	1,0,-1	0	1/2 (Two Sets)	4
K*(892)	$K^{*\pm}$	891.66 ± 0.26	1,-1	1	1/2	12
	$K^{*0}, \bar{K}^{*0}$	895.55 ± 0.20	0	1	1/2	
$K_1(1270)$		1253 ± 7	1,0,-1	1	1/2 (Two Sets)	12
$K_1(1400)$		1403 ± 7	1,0,-1	1	1/2 (Two Sets)	12
$K^*(1410)$		1414 ± 15	1,0,-1	1	1/2 (Two Sets)	12
$K_0^*(1430)$		1425 ± 50	1,0,-1	0	1/2 (Two Sets)	4
$K_2^*(1430)$	$K_2^{*\pm}$	1427.3 ± 1.5	1,-1	2	1/2	20
	$K_2^{*0}, \bar{K}_2^{*0}$	1432.4 ± 1.3	0	2	1/2	
$K^*(1680)$		1718 ± 18	1,0,-1	1	1/2 (Two Sets)	12
$K_2(1770)$		1773 ± 8	1,0,-1	2	1/2 (Two Sets)	20
$K_3^*(1780)$		1776 ± 7	1,0,-1	3	1/2 (Two Sets)	28
$K_2(1820)$		1819 ± 12	1,0,-1	2	1/2 (Two Sets)	20
$K_4^*(2045)$		2045 ± 7	1,0,-1	4	1/2 (Two Sets)	36

Table 21: Data For Charmed-Mesons

Mesons \ Properties		Mass (MeV)	Charge $\lvert e^- \rvert$	Spin ($\hbar$)	Iso-Spin ($\hbar$)	Degrees Of Freedom
D	$D^{\pm}$	1869.65 ± 0.05	1,-1	0	1/2	4
	$D^0, \bar{D}^0$	1864.83 ± 0.05	0	0	1/2	
$D^*(2010)^{\pm}$		2010.6 ± 0.05	1,0,-1	1	1/2	6
$D_0^*(2300)^0$		2300 ± 19	1,0,-1	0	1/2	2
$D_1(2420)^0$		2420.8 ± 0.5	1,0,-1	1	1/2	6
$D_S^{\pm}$		1968.34 ± 0.37	1,-1	0	0	1

Table 22: Quark Content For Charmed And Strange-Mesons

Mesons \ Properties			Charge $\lvert e^- \rvert$	Iso-Spin ($\hbar$)	Quark Content
S (Strange)	$S_1(K, K^*)$	S_1^+	1	1/2(1/2)	$u\bar{s}$
		S_1^-	-1	1/2(-1/2)	$\bar{u}s$
	$S_2(K, K^*)$	S_2^0	0	1/2(-1/2)	$d\bar{s}$
		$\bar{S}_2^0$	0	1/2(1/2)	$\bar{d}s$
C (Charmed)	$C_1(D, D^*)$	C_1^+	1	1/2(1/2)	$c\bar{d}$
		C_1^-	-1	1/2(-1/2)	$\bar{c}d$
	$C_2(D, D^*)$	C_2^0	0	1/2(-1/2)	$c\bar{u}$
		$\bar{C}_2^0$	0	1/2(1/2)	$\bar{c}u$
D_S (charmed and strange)		D_S^+	1	0	$c\bar{s}$
		D_S^-	-1	0	$\bar{c}s$

- Here are some final comments on the available degrees of freedom for Baryons and Mesons. If we look at a Baryon/Meson characterised by spin S and Iso-spin I, then:

$$Degrees\ Of\ Freedom\ -\ (2S+1)(2I+1)$$

- However, if we want to know the number of possible intrinsic quark configurations for a given baryon (for all spin configurations) then for:
  - Baryons with 3 different quarks:

$$\#(Quark\ Configurations)\ =\ ({}^4C_3)(2^3)(3!) = 192$$

  - Baryons with 2 different quarks:

$$\#(Quark\ Configurations)\ =\ ({}^4C_2)(2*3)(3) = 108$$

  - Baryons with 0 different quarks:

$$\#(Quark\ Configurations)\ =\ ({}^4C_1)(4)(1) = 16$$

  - For Mesons:

$$\#(Quark\ Configurations)\ =\ ({}^4C_1 *^4 C_1)(4)(3) = 192$$

- The first factor represents no. of ways of combining quarks (quarks-anti-quarks for mesons), the second factor is for spin and the third is the color factor for quarks as Baryons and Mesons must be a color singlet.

References

[1] https://upload.wikimedia.org/wikipedia/commons/thumb/7/7f/Particle_ overview.svg/1920px-Particle_overview.svg.png

[2] INTRODUCTION TO ELEMENTARY PARTICLES WILEY David Griffiths, Reed College,Copyright ©1987 John Wiley & Sons, Inc.

[3] https://en.wikipedia.org/wiki/Standard_Model#/media/File:Standard_Model_of_Elementary_Particles.svg

[4] New Concept of Elementary Particles Classification, Ilgaitis Prūsis, Peteris Prūsis

[5] Statistical Mechanics,Second Edition,Kerson Huang,MIT

[6] https://pdg.lbl.gov/

[7] Excluded volume effect for the nuclear matter equation of state by D.H. Rischke, M.I. Gorenstein*, H. Stocker, W. Greiner

[8] Equations of state for real gases on the nuclear scale, Volodymyr Vovchenko

[9] Criticality in a hadron resonance gas model with the van der Waals interaction Subhasis Samanta and Bedangadas Mohanty School of Physical Sciences, National Institute of Science Education and Research, HBNI, Jatni - 752050, India

[10] PHYSICAL REVIEW C 96, 044904 (2017), Bulk properties of the medium produced in relativistic heavy-ion collisions from the beam energy scan program

[11] PHYSICAL REVIEW C 102, 034909 (2020), Strange hadron production in Au + Au collisions at $\sqrt{s_{NN}}$ = 7.7, 11.5, 19.6, 27, and 39 GeV

[12] 'THERMUS ['A Thermal Model Package for ROOT'],S. Wheaton and J. Cleymans, hep-ph/0407174

[13] PHYSICAL REVIEW C 102, 024902 (2020), Constraining the particle production mechanism in Au + Au collisions at $\sqrt{s_{NN}}$ = 7.7, 27, and 200 GeV using a multiphase transport model

[14] PHYSICAL REVIEW C 72, 064901 (2005), Multiphase transport model for relativistic heavy ion collisions, Zi-Wei Lin, Che Ming Ko,Bao-An L, Bin Zhang,Subrata Pal

[15] Measurements of event-by-event fluctuation of anisotropic flow in pp, p+Pb and Pb+Pb collisions with the ATLAS detector. A Dissertation presented by Peng Huo

[16] Study of particle correlation and fluctuation from nucleus-nucleus collisions to proton-proton collisions with the ATLAS detector at the LHC A Dissertation presented by Mingliang Zhou

[17] CONCEPTS OF HEAVY-ION PHYSICS Ulrich Heinz Department of Physics, The Ohio State University, Columbus, OH 43210, USA

[18] QGP Meet 2008 : Presentation by Bedanga Mohanty